AD_____

Award Number: DAMD17-98-1-8502

TITLE: Bioactive Lipids: Role in Prostate Cancer Angiogenesis

PRINCIPAL INVESTIGATOR: Kenneth V. Honn, Ph.D.

CONTRACTING ORGANIZATION: Wayne State University
Detroit, Michigan 48201

REPORT DATE: April 2003

TYPE OF REPORT: Final

PREPARED FOR: U.S. Army Medical Research and Materiel Command
Fort Detrick, Maryland 21702-5012

REPORT DOCUMENTATION PAGE

Form Approved
OMB No. 074-0188

1. AGENCY USE ONLY (Leave blank)	2. REPORT DATE	3. REPORT TYPE AND DATES COVERED
	April 2003	Final (30 Sep 98 - 29 Mar 03)

4. TITLE AND SUBTITLE
Bioactive Lipids: Role in Prostate Cancer Angiogenesis

5. FUNDING NUMBERS
DAMD17-98-1-8502

6. AUTHOR(S)
Kenneth V. Honn, Ph.D.

7. PERFORMING ORGANIZATION NAME(S) AND ADDRESS(ES)
Wayne State University
Detroit, Michigan 48201

E-Mail: k.v.honn@wayne.edu

8. PERFORMING ORGANIZATION REPORT NUMBER

9. SPONSORING / MONITORING AGENCY NAME(S) AND ADDRESS(ES)
U.S. Army Medical Research and Materiel Command
Fort Detrick, Maryland 21702-5012

10. SPONSORING / MONITORING AGENCY REPORT NUMBER

11. SUPPLEMENTARY NOTES
Original contains color plates. All DTIC reproductions will be in black and white.

12a. DISTRIBUTION / AVAILABILITY STATEMENT
Approved for Public Release; Distribution Unlimited

12b. DISTRIBUTION CODE

13. ABSTRACT (Maximum 200 Words)

Angiogenesis is an integral part of human prostate cancer progression. In the Phase I of this grant, we have identified arachidonate 12-lipoxygenase as a promoter of angiogenesis in human prostate carcinoma by stimulating VEGF expression and via the pro-angiogenic activity of 12(S)-HETE. The first objective of phase II of this grant is to delineate the regulation of VEGF gene expression by 12-LOX in PCa cells, specifically the involvement of Sp1 and possibly AP2. The second objective of this proposal is to describe the signal transduction pathway by which 12-LOX stimulates VEGF expression. These two objectives are based upon our observations in the Phase I of this grant that that 12-LOX, when overexpressed in human PCa cells, stimulates tumor angiogenesis and growth. The third objective to evaluate the therapeutic potential of 12-LOX inhibitors for PCa treatment.

14. SUBJECT TERMS
Prostate Cancer, Bioactive Lipids

15. NUMBER OF PAGES
97

16. PRICE CODE

17. SECURITY CLASSIFICATION OF REPORT	18. SECURITY CLASSIFICATION OF THIS PAGE	19. SECURITY CLASSIFICATION OF ABSTRACT	20. LIMITATION OF ABSTRACT
Unclassified	Unclassified	Unclassified	Unlimited

Table of Contents

INTRODUCTION

The first objective of phase II of this grant is to delinate the regulation of VEGF gene expression by 12-LOX in PCa cells, specifically the involvement of Sp1 and possibly AP2. The second objective of this proposal is to describe the signal transduction pathway by which 12-LOX stimulates VEGF expression. These two objectives are based upon our observations in the Phase I of this grant that that 12-LOX, when overexpressed in human PCa cells, stimulates tumor angiogenesis and growth. The third objective to evaluate the therapeutic potential of 12-LOX inhibitors for PCa treatment.

BODY OF REPORT

KEY RESEARCH ACCOMPLISHMENT

6 research articles published
1 research article in submission
3 review articles published
A 12-lipoxygenae inhibitor developed for a potential therapeutic agent for prostate cancer

PROGRESS

Task 1. Investigate the regulation of VEGF gene expression by 12-LOX, with special focus on the *cis*-elements in VEGF promoter region and the *trans*-factors involved, Months 1 - 12:

This task has been achieved and additional findings were made as summarized as followed:

1). Transcriptional regulation of VEGF expression by 12-LOX

In Phase I of this grant, we observed an increase in VEGF production in 12-LOX transfected PC-3 cells when compared to their vector controls. Here we studied how 12-LOX regulates VEGF gene expression.

To study whether 12-LOX regulates VEGF expression at the transcriptional level, we transfected neo-control cells (neo-α) and 12-LOX transfected PC-3 cells (nL-8 or nL-12) with a VEGF promoter luciferase construct (-1176/+54), along with a lacZ control plasmid to normalize transfection efficiency. As shown in **Figure 1**, there was a more than 10-fold increase in VEGF promoter activity in 12-LOX transfected PC-3 cells as compared with their neo-controls.

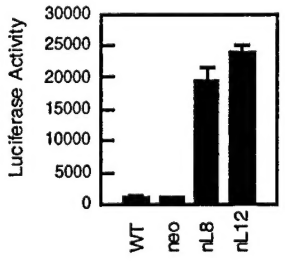

Figure 1. Increased VEGF Promoter Activities in 12-LOX Transfected PC-3 Cells.

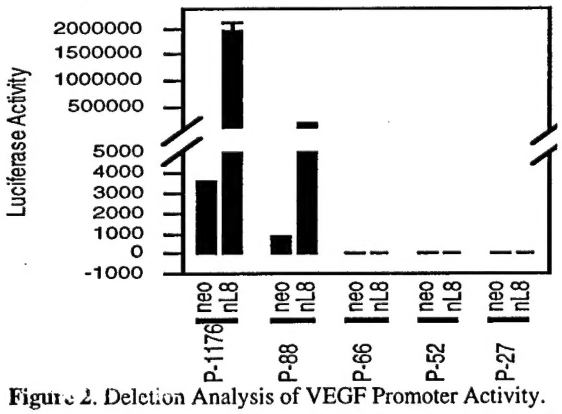

Figure 2. Deletion Analysis of VEGF Promoter Activity.

To determine which region of VEGF promoter is 12-LOX-responsive, we transfected neo-control (neo-α) and 12-LOX transfected PC-3 cells (nL8) with a series of luciferase constructs with different lengths of the VEGF promoter, along with a lacZ control plasmid. As shown in **Figure 2**, deletion of the region between -1176 and -88 significantly reduced, but did not abolish, the increased VEGF promoter activity as observed in nL8. Further deletion of the 23 bp region between -88 and -66 abolished the increased VEGF promoter activity in nL8, indicating the presence of a *cis*-element in this region responsive to 12-LOX.

Similar results were obtained with other clones of 12-LOX transfected PC-3 cells (nL2 and nL-12, data not shown).

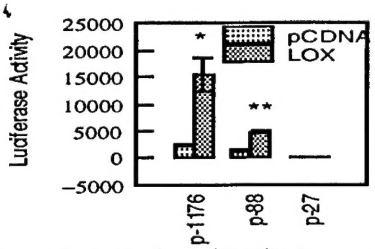

Figure 3. Activation of VEGF Promoter Activity by Co-transfection with a 12-LOX expression construct (LOX). pCDNA, vector control. *, $P < 0.05$; **, $P < 0.01$ when compared to their respective vector control.

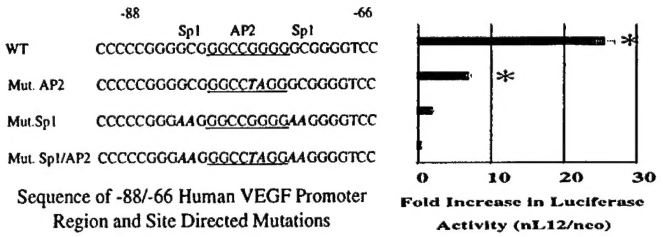

Figure 4. Site-Directed Mutation Analysis of the Role of Sp1 and AP2 Recognition Sequences in VEGF Promoter Activity. Left panel, DNA sequence between -88 and -66 of VEGF promoter. Mutated nucleotides in Sp1 recognition sequences (GC to AA) or AP2 binding site (underlined, GG to TA) are shown in italic. Right panel, fold increase of luciferase activities in nL12 when compared to those in neo-α. *, $P < 0.05$, indicating the significant difference in luciferase activities between neo-α and nL12.

Co-transfection of PC-3 parental cells with both VEGF promoter constructs and a 12-LOX expression construct demonstrated a significant increase in p-1176 and p-88, but not p-27, VEGF promoter activities, as compared with their respective pcDNA3.1 vector control (**Figure 3**). The data suggest that 12-LOX stimulates VEGF promoter activity and the observed increase in VEGF promoter activity in 12-LOX transfected PC-3 cells is not due to possible cloning artifacts associated with a particular transfectant clone. The data also demonstrate that the -88 and -27 promoter region of VEGF gene is responsive to 12-LOX, supporting our previous observation that the 23 bp DNA segment beween -88 and -66 is required for increased VEGF promoter activity in 12-LOX transfected PC-3 cells.

There are one AP2 and two Sp1 binding sites in this 23 bp region. As shown in **Figure 4**, mutation of AP2 decreased, but did not abolish, the stimulation of promoter activity by 12-LOX (from 25 fold to 8 fold increase). In contrast, mutation of two Sp1 binding sites dramatically decreased the stimulation of VEGF promoter activity by 12-LOX in which the increase of VEGF promoter activity in nL12 was no longer statistically significant. Mutation of both AP2 and Sp1 binding sites completely abolished the increased VEGF promoter activity in 12-LOX transfected PC-3 cells. The data suggest that Sp1, and to lesser extent, AP2, are involved in 12-LOX regulation of VEGF promoter activity.

2). Overexpression of the platelet-type 12-LOX in PC-3 cells increases DNA binding and transcriptional activities of NF-κB and promotes IκBα degradation.

In addition to Sp1 and AP2, NF-kB was demonstrated important for VEGF expression. Therefore we tested the effect of overexpression of platelet-type 12-LOX on the activation state of NF-κB in prostate cancer cells. For this study, we have used PC-3 prostate cancer cell line that was stably transfected with platelet-type 12-LOX. Two 12-LOX overexpressing clones (nL-8 and nL-12), a vector only transfected clone (neo), and the native PC-3 cells were used for the experiments. The effect of 12-LOX overexpression on the activation of NF-κB was studied using Electomobility Shift Assays (EMSAs), western blotting for IκBα, and transcriptional activity with luciferase reporter assay.

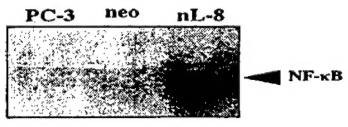

Figure 5: Effect of 12-lipoxygenase overexpression on NF-κB activity:EMSA performed on nuclear extracts of untransfected PC-3, neo, and 12-LOX transfected cells

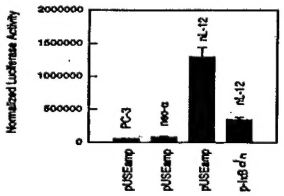

Figure 6: Effect of 12-lipoxygenase overexpression on NF-κB activity: NF-κB-luciferase reporter activities. The cells (PC-3, neo, and nL-12) were transfected with κB-luciferase and LacZ reporters (pUSEamp) and the reporter activities measured. 12-LOX transfected cells were also transiently transfected with a dominant negative mutant IκBα construct (p-IκBdn) in addition to κB-

luciferase and LacZ reporters. The normalized data shown is an average of three experiments with standard deviation. LacZ expression was used for normalization.

Nuclear protein extracts of 12-LOX transfected cells (nL-8) showed significant constitutive activation of NF-κB compared to the vector transfected control cells (neo) or the untransfected PC-3 cells (**Figure 5**). This activation was confirmed by the increased transcriptional activity of the luciferase reporter construct in nL-12 cells that were transiently transfected. (**Figure 6**). This increase in transcriptional activity observed in 12-LOX transfected cells was nearly abolished upon co-transfection of a mutant of IκBα that is resistant to proteolytic degradation (**Figure 6**). Activation of NF-κB involves phosphorylation and eventual degradation of IκB protein before NF-κB could bind to DNA. Western blots of whole cell protein extracts from neo, nL-8, and nL-12 cells showed a dramatic decrease in IκBα in nL-8 and nL-12 cells (data not shown). These results strongly suggest that overexpression of 12-LOX induces NF-κB activity by a mechanism involving proteolytic degradation of IκBα.

3). 12(S)-HETE activates NF-κB in PC-3 prostate cancer cells.

The fact that 12(S)-HETE, the stable end product of 12-LOX metabolism of arachidonic acid, mediated the activation of NF-κB was demonstrated by the increased DNA binding activity of NF-κB when native PC-3 cells were treated with 12(S)-HETE (**Figure 7**). The 12(S)-HETE driven increase in NF-κB DNA binding also paralleled the increase in transcriptional activity as determined by the NF-κB-luciferase reporter assay (**Figure 8**).

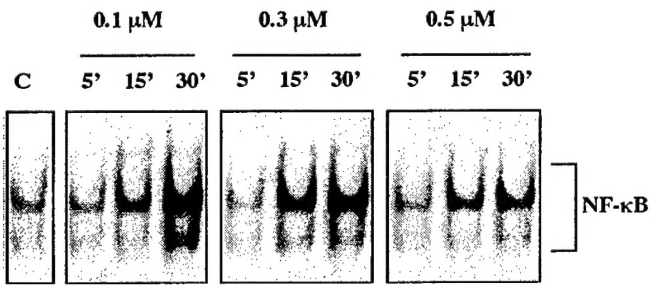

Figure 7: *Effect of 12(S)-HETE on the activation of NF-κB in PC-3 cells:* Time and dose dependent activation of NF-κB DNA binding activity by 12(S)-HETE. EMSA was performed on the nuclear extracts of the treated PC-3 cells. The cells were incubated with serum-free RPMI medium containing the amounts of 12(S)-HETE shown for the indicated time and subjected to EMSA.

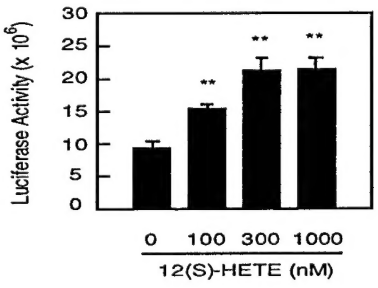

Figure 8: NF-κB-luciferase reporter activities of cells treated with 12(S)-HETE. PC-3 cells were incubated at indicated concentrations for 30 min and luciferase activities measured. **, $p < 0.01$.

Additionally, immunocytochemical analysis of the 12(S)-HETE treated PC-3 cells using antibodies against p65 subunit of NF-κB show a translocation of NF-κB from cytosol to the nucleus (**Figure 9**). Thus, the observations made with 12(S)-HETE corroborate those of 12-LOX overexpressing PC-3 prostate cancer cells.

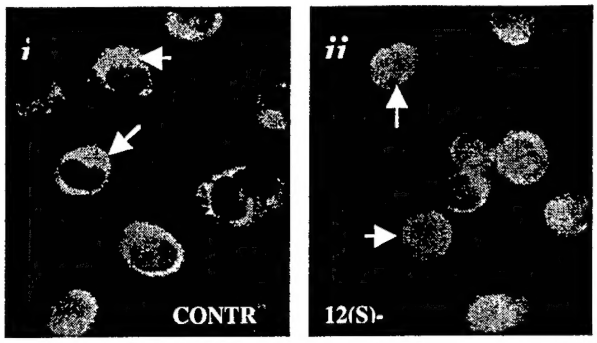

Figure 9: Immunofluorescent localization of NF-κB in PC-3 cells with and without 12(S)-HETE treatment. Cells were treated with 100 nM 12(S)-HETE or buffer for 10 min and immunostained. Staining was predominantly present in the cytoplasm of untreated control cells (*i, arrows*) and nuclear staining increased considerably in 12(S)-HETE treated cells (*ii, arrows*).

4). NF-κB activation is inhibited by 12-LOX inhibitor. It is conceivable that the observations made with the 12-LOX overexpression system and 12(S)-HETE are mutually independent and follow a different, yet unknown, mechanism. To address this possibility, we used BHPP, a specific inhibitor of 12-LOX, to study the role of the enzymatic activity of 12-LOX in NF-κB activation. DNA binding activity of NF-κB was greatly decreased upon exposure to 20 μM BHPP for 60 min (**Figure 10**). The results show the participation of the 12-LOX enzymatic activity in NF-κB activation and that it is mediated by 12(S)-HETE. Currently we are actively studying the possible involvement of this transcriptional factor in 12-LOX regulation of VEGF expression in human prostate cancer cells.

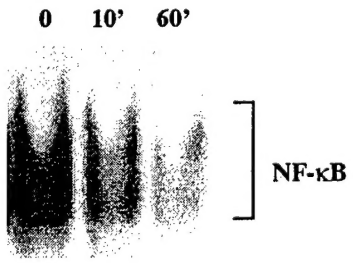

Figure 10. Inhibition of NF-kB activation in 12-LOX transfected PC-3 cells by BHPP, a select 12-LOX inhibitor.

Task 2. Study the signaling pathways involved in 12-LOX regulation of VEGF expression, Months 1-18:

•This task has been achieved. Specifically, we found an involvement of PI3 kinase and Akt signaling pathway in 12-LOX stimulated VEGF gene expression.

To study the signaling mechanism from 12-LOX leading to VEGF expression in PC-3 cells, we treated 12-LOX transfected PC-3 cells with PD98059, a Mek inhibitor, and LY294002, a PI3 kinase inhibitor, and studied VEGF expression. As shown in **Figure 11**, LY294002 (20 μM) reduced VEGF expression in both 12-LOX transfected PC-3 cells (nL-8 and nL-12) and neo-controls (neo-α and neo-σ), as well as in PC-3 parental cell line. We also found significant reduction of VEGF expression in DU145 cells by LY294002 data not shown). In contrast, we did not find any effect of PD98059 on VEGF expression in PCa cells (data not shown). The results suggest that PI3 kinase activity is required for VEGF expression in PCa cells as well as in 12-LOX transfected PC-3 cells.

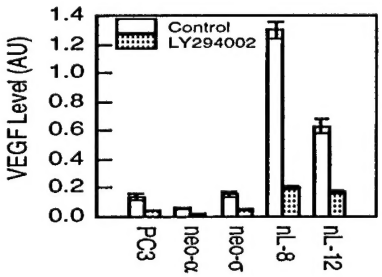

Figure 11. Down-regulation of VEGF Expression by PI3 Kinase Inhibitor LY294002.

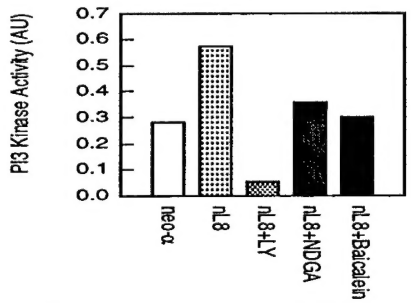

Figure 12. Increased PI3 Kinase Activity in 12-LOX Transfected PC-3 Cells. PI3 kinase activity in p85 immunoprecipitates was measured by incubating with substrate and γ-^{32}P-ATP. Phospholipids were separated by TLC, X-filmed and quantified using a NIH imaging software.

To study whether there is an increase in PI3 kinase activity in 12-LOX transfected PC-3 cells that may mediate the stimulation of VEGF expression, we measured the PI3 kinase activity. As shown in **Figure 12**, there was a 2 fold increase in PI3 kinase activity in 12-LOX transfected PC-3 cells (nL8) and this increase of PI3 kinase was inhibited by pre-treatment of nL8 cells with LOX inhibitors NDGA and baicalein. The data suggest that there is an increase in PI3 kinase activity in 12-LOX transfected PC-3 cells and inhibition of PI3 kinase activities by LY294002 reduced VEGF expression in 12-LOX transfected PC-3 cells and other PCa cells.

We investigated whether the arachidonate product of 12-LOX, 12(S)-HETE, can activate PI3 kinase. We used A431 cells, instead of PC-3 cells, in this study because there is low endogenous level of PI3 kinase activity under serum free condition but readily stimulated in A431 cells. We found 12(S)-HETE activates PI3 kinase /Akt in A431 cells and the activation of PI3 kinase is required for 12(S)-HETE activation of Erk1/2. Currently we are extending the findings obtained using A431 cells into PC-3 cells and prostate cancer cells.

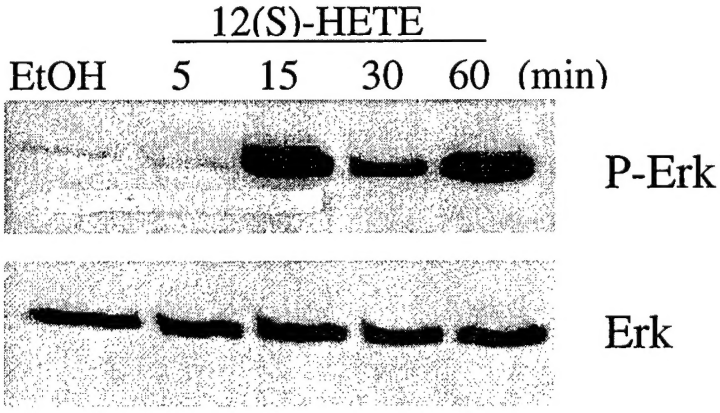

Figure 13. Activation of p42/44 MAP kinase by 12(S)-HETE in LNCaP cells. LNCaP cells were serum starved overnight and treated with 300 nM 12(S)-HETE for indicated times. Activation of p42/44 MAP kinase was indicated by the levels of phosphorylated form of Erk (upper panel), in comparison with the level of total Erk protein (bottom panel). As shown in the figure, the activation of p42/44 MAP kinase by12(S)-HETE is evident with 15 minutes of treatment.

Task 3. Evaluate the efficacy of 12-LOX inhibitors against angiogenesis induced by PCa cells using Matrigel implantation model, Months 1 -9:

This specific aim has been achieved.

In Phase I of this grant, we found that 12-LOX functions as an "angiogenic switch," governing PCa angiogenesis and growth. The findings suggest that 12-LOX may be a promising target for developing anti-angiogenesis therapy, at least for those patients whose PCa is 12-LOX positive. Previously, Dr. Honn, in collaboration with Dr. Carl Johnson (Department of Chemistry, Wayne State University) synthesized several classes of hydroxamic acid derivatives, using rational drug design for inhibition of platelet-type 12-LOX (US Patent No. 5,234,933). Compounds were initially screened for inhibition of platelet-type 12-LOX and a select group of them later tested for selectivity. The first lead compound was BMD188 which inhibits 12-LOX with IC_{50} of 3 μM. BMD188 was initially chosen for study because of its ease of synthesis in bulk, its stability and preliminary pharmacokinetic data indicates a circulating half-life in mouse of 50 hours. To demonstrate the plausibility of using 12-LOX inhibitors to reduce PCa angiogenesis and tumor growth, we first tested the effect of BMD188 on angiogenesis induced by 12-LOX transfected PC-3 cells in Matrigel plug assay. Athymic mice were injected with 2 X 10^6 12-LOX transfected PC-3 cells suspended in Matrigel. After 24, mice were injected (i.p.) with 20, 60 or 100 mg BMD188 per kg of mouse weight every other day for a total of 4 treatments. A dose dependent inhibition of angiogenesis was observed (**Figure 14**).

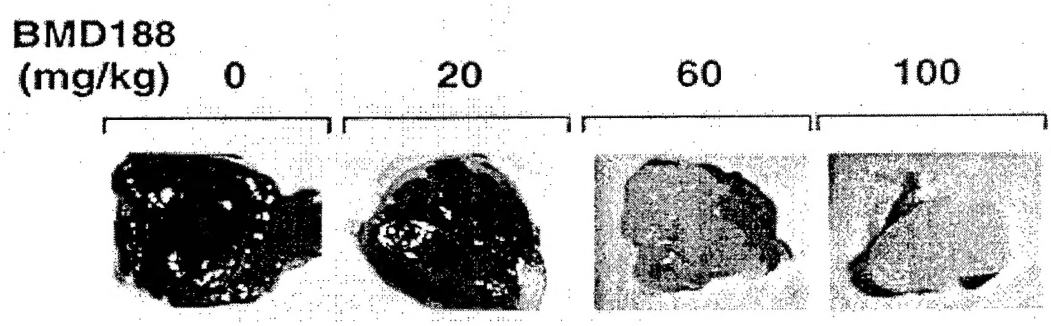

Figure 14. Inhibition of PCa cell induced angiogenesis by BMD188.

We also find WSU215 inhibit bFGF- and VEGF-induced endothelial cell migration (**Data not shown**).

Task 4. Evaluate the efficacy of 12-LOX inhibitors against s.c. tumor growth in athymic mice, Months 6 - 15:

This specific aim has been achieved.

To study the feasibility of using 12-LOXinhibitors to treat prostate tumors, a pilot toxicity experiment was performed with every other day i.p. injection of BMD188 at 0, 10, 50, and 100 mg/kg to tumor-free animals. The injection lasted 1 month. The results indicated that 100 mg/kg dose of BMD188 was toxic while doses of ≤50 mg/kg was not. Considering that tumor-bearing animals might be more sensitive to the drug treatment, a dose of 25 mg/kg was adopted for the large-scale *in vivo* efficacy experiment. As shown in Figure 3, the results also revealed the inhibitory effect of BMD188 on prostate cancer growth. Live measurement of tumor sizes (i.e., when animals were still alive), which were converted to tumor weights,

indicated that BMD188 demonstrated significant inhibitory effect in retarding the growth of Du 145 tumor *in vivo* (Figure 7A). Note that the difference in tumor weights between the control and suramin measured at the seventh week was not statistically significant (p = 0.45) due to large S.D. values (**Figure 16**). The tumor-inhibitory effect of BMD188 was also confirmed by the direct weighing of tumors isolated from surviving animals when the experiment was terminated on day 63 post the start of the treatment. As shown in Figure 6B, BMD188 demonstrated significant inhibitory effect on Du145 tumor growth (p = 0.036) while suramin was ineffective (p = 0.68).

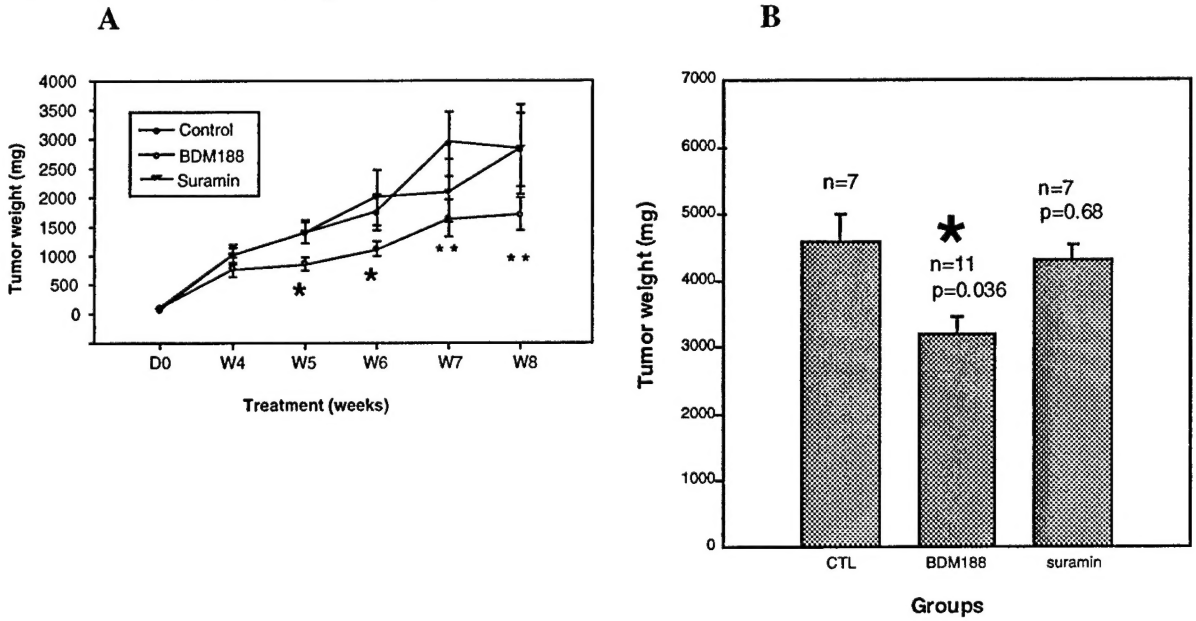

Figure 16. A, BMD188 inhibits the growth of Du145 tumors in athymic nude mice. Tumor sizes on live animals were taken on weekly basis with a caliper and converted to tumor weights. *p<0.05 between BMD188 and control; p<0.01 between BMD188 and control. B, Tumor weights at the end of the experiment. After the animals were sacrificed at the end of the night week (63 days), tumors were dissected out from surviving mice and weighed . The animal number (n) and p values compared with the control are also indicated. *Statistically significant different from the tumors in the control.

BMD188 at 25 mg/kg appeared to be very tolerable to animals since it did not demonstrate any obvious toxicity throughout the experiment. In fact, BMD188 appeared to slightly extend the survival rate of tumor-bearing animals. By the eighth week post the start of the treatment, 40% animals in the control, 52% in the BMD188 group and 32% in the suramin group survived (see Figure 4 in Appendix x). When the experiment was terminated by the end of the ninth week, 28% of the animals survived in both control and suramin groups while 44% of the tumor-bearing animals survived. Suramin demonstrated noticeable toxicity as revealed by decreased survival rated from early on. Therefore, the injection protocol was changed from every other day to once per week starting from the third week. Since tumor bearing animals died at different times, we also isolated tumor masses from each individual animal and pooled the data for each group. The pooled tumor weights were 4003.5 ± 422.2, 2902.3 ± 341.9, and 3744.3 ± 404.4 (mean ± S.E.) for the control, BMD188, and suramin group, respectively. Again, the difference between the BMD188 group and control was statistically significant (p <0.05) while the difference between the suramin group and control was not statistically significant (p = 0.66).

Task 5. Evaluate the efficacy of 12-LOX inhibitors, BMD188 and WSU-215, against the growth and progression of prostatic tumors in a SCID orthotopic model, Months 12 - 21:

This specific aim has been achieved.

To demonstrate oral efficacy of BMD188 as anti prostate cancer agent we performed a series of experiments with Du145 cells transplanted intraprostatically into SCID and the drug was administered p.o. This experiment revealed a dramatic decrease in tumor size (**Fig. 17**) indicating that BMD188 could be used orally. However, Based on the above described pharmakokinetic data (Table 1), we decided to perform most of the *in vivo* efficacy experiments by giving animals BMD188 intraperitoneally every 48 h (i.e., every other day). The rationale for i.p. administration is the following: considering that; 1) BMD188 has an approximate half life of ~50h; 2) the oral absorption of BMD188 is low and the i.p. absorption is high; 3) it is infeasible experimentally to repeatedly inject the animal tail vein. The first, small-scale, *in vivo* anti-tumor experiment was carried out using Du145 cells (androgen-independent and metastatic) orthotopically implanted into SCID mice prostates since previous studies revealed that PC3 cells did not metastasize in the SCID mice model (Appendix x). In this experiment, we performed a dose study of BMD188, i.e., 0, 1, and 10 mg/kg. Forty seven days' treatment of tumor-bearing animals by i.p. injection every other day of BMD188 did not produce apparent signs of toxicity macroscopically and microscopically by examining several internal organs (i.e., liver, kidney, lung, spleen, heart, and rectum). As shown in Table 1, BMD188 inhibited both primary growth and local invasion of Du145 tumors grown in SCID mice. The inhibitory effect on tumor growth was noticed at 1 mg/kg although the difference was not statistically significant. At 10mg/kg, BMD188 demonstrated statistically significant inhibitory effect on the growth of Du145 tumors in SCID mice (**Table 1**). Furthermore, BMD188 exhibited potent inhibitory effect on the local invasion of Du145 tumors, as revealed by the appearance of effect at 1mg/kg (**Table 1**). No distant metastasis in lung, liver, spleen, and kidney was observed in any animal during this experiment.

Inhibition by BMD188 (p.o) of Du145 intraprostatic tumor growth in SCID mice

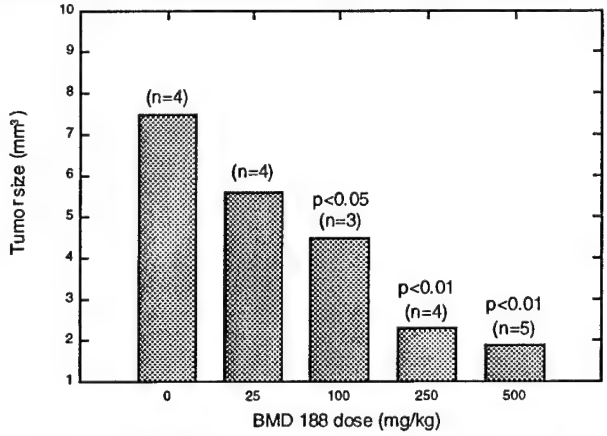

Figure 17. BMD 188 administered p.o. inhibits the primary tumor growth of Du145 prostate cancer cells orthotopically (intraprostatically) transplanted into SCID mice. Shown are mean values of each group. The S.D.s were <10%. Indicated p values obtained by comparing with the control (i.e., 0) group. Note that this experiment indicates that p.o administered BM188 is biologically active though much higher doses are required when compared to in vivo experiments described below.

Table 1. Inhibition by BMD188 (i.p.) of primary growth and local invasion of Du145 tumors orthotopically implanted into SCID mice[a].

	Control(0) (5/5)[b]	1 mg/kg (5/5)	10 mg/kg (4/5)
Primary tumor(mm^3)	291.8±90.2	216±38.7	80.8±11.3[c]
Local invasion			
prostate capsule	5/5[c]	1/5	0/4
muscle	3/5	0/5	0/4
adipose tissue	3/5	0/5	0/4
peritoneal membrane	1/5	0/5	0/4
rectal wall	2/5	0/5	0/4
lymphatic	1/5	0/5	0/4
blood vessels	2/5	0/5	0/4

[a] Refer to the Materials & Methods for experimental details.

[b] The number in the bracket indicates the informative cases of animals utilized for analysis. Specifically, 5 out of 5 animals were informative in the control (i.e. DMSO alone) and 1 mg/kg group, while only 4 out of 5 animals in the 10 mg/kg (one animal died due to experimental accident).

[c] $p<0.01$ compared with the control group (χ^2test).

[d] Local invasion involves prostate capsules or neighboring connective tissues or pelvic organs.

[e] The number refers to how many animals out of the total demonstrated evidence of local invasion/metastasis under the microscope for any individual tissue analyzed.

Task 6. Evaluate the efficacy of 12-LOX inhibitors, BMD188 and WSU-215, against the growth of PCa tumors in human bone environment, Months 12 - 24:

This specific aim has been achieved.

Using a SCID-human bone model (Nemeth et al., 1999), we studied whether BMD188 can inhibit the growth of tumors in human bone environment. As shown in **Figure 18**, at 50 or 100 mg BMD188 per kg of mouse weight, significant reduction in tumor growth was observed. Considerable reduction in angiogenesis on the surface of tumor or on the skin around tumors also was observed. The results raise the exciting possibility that inhibition of 12-LOX is a novel approach to inhibit tumor angiogenesis and curb prostate tumor growth (**Figure 19**).

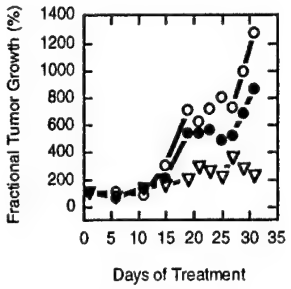

Figure 18. Inhibition of Tumor Growth in SCID-Hu Bone by BMD188. Open circle, Solvent control; Filled circle, BMD188 50mg/Kg mouse; Open triangle, BMD188, 100mg/Kg mouse.

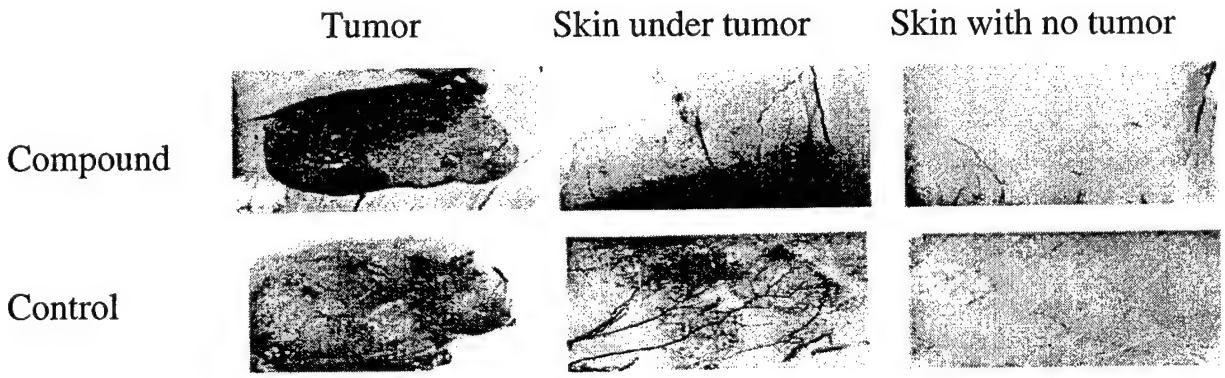

Figure 19. Inhibition of tumor angiogenesis by systematic administration of BMD188 (50 mg/Kg/day)

The ability of BMD188 to inhibit angiogenesis directly led us to study whether HA188 can inhibit the growth of tumors derived from cancer cells with little 12-LOX expression. PC3 neo-transfectants were selected for this study due to its low level of 12-LOX expression. In SCID-hu bone model, the bone enviroment greatly facilitated the tumor growth as previously described. As shown in the figure (**Figure 20**), BMD188 inhibited the growth of tumors derived from PC3 neo-transfectants. Interestingly, the inhibitory effect of BMD188 on tumor growth is more pronounced in 12-LOX transfected PC3 cells than in PC3 neo-

transfetcants, suggesting that the direct inhibition of angiogenesis by BMD188 may contribute in part, but not totally, the inhibition of the growth of tumors derived from 12-LOX transfected PC3 cells. The other part of contribution is probably due to its effect on 12-LOX activity in PC3 cells.

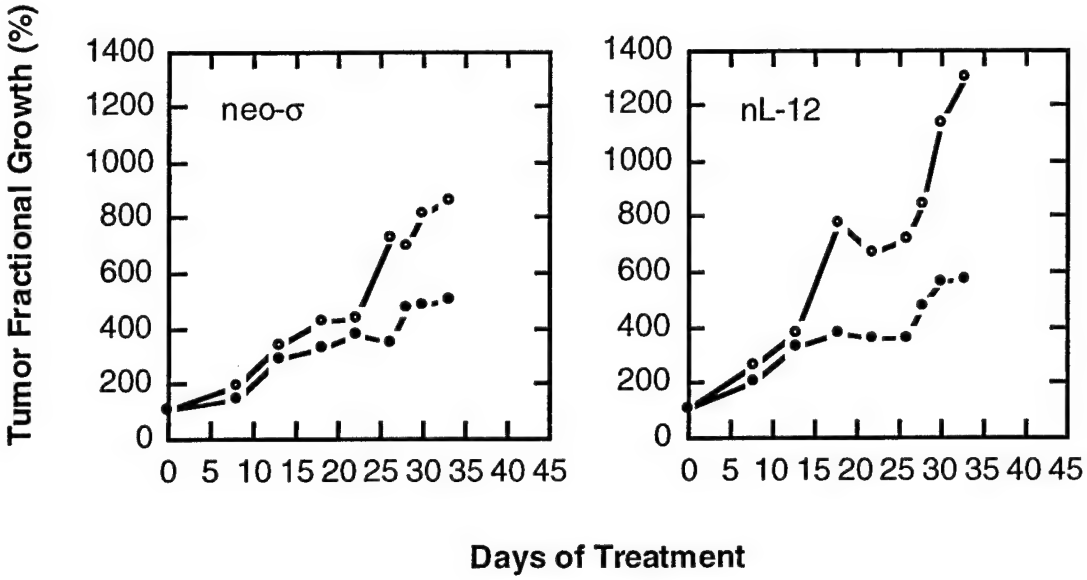

Figure 20. Growth kinetics of tumors from PC3 cells with low or high 12-LOX expression in the presence or absence of BMD188. The SCID-hu bone orthotopic model and BMD188 administration were described in "Materials and Methods." Shown here are the growth curves of tumors from neo-α and nL12, treated with vehicle (open circle) and 100 mg/kg of BMD188 (filled circle). *Data points*, mean percentage of tumor volumes, compared to their starting tumor volumes when BMD188 treatment was initiated, of four tumors for each group. The SE of each data point is within 20% of their respective mean value.

CONCLUSIONS:

The research progress made in the first year of Phase II of Award# DAMD17-98-1-8502 indicates that 12-LOX increases VEGF expression in human prostate cancer cells in a PI3 kinase/Akt dependent pathway. We also found 12-LOX and its arachidonate product, 12(S)-HETE, activate NF-κB transcriptional activity and p42/44 MAP kinase activity in human prostate cancer cells. The link between 12-LOX, a free fatty acid metabolizing enzyme, and VEGF, a putative angiogenic factor, is both novel and exciting, providing significant insights into our understanding of the regulation of VEGF expression during PCa progression. The study also found the transcriptional regulation of VEGF expression by 12-LOX and by its lipid product, 12(S)-HETE. The study also demonstrated the plausibility of using 12-LOX inhibitors such as BMD188 to inhibit prostate tumor angiogenesis and growth. The in vivo results with BMD188, a novel cyclic hydroxamic acid compound, demonstrated good absorption in lab animals when given by i.p injection. The post-absorption BMD188 demonstrated a plasma half life of ~50 h. Using this knowledge about BMD188, we performed two sets of *in vivo* efficacy experiments, both of which reveled that BMD188 could retard the growth of Du145 prostate cancers orthotopically implanted into the prostates of either SCID or athymic nude mice. The anti-tumor effect of BMD188 in stronger than that of suramin, a compound currently being attempted in humans as an anti-cancer agent. In fact, suramin hardly demonstrated any significant efficacy against Du145 tumors although it did show certain toxicities. BMD188 appears to be well-tolerated in tumor-bearing animals: no toxicities observed in range of 1-25 mg/kg using i.p injection every other day for up to 8 weeks. Our studies suggest that 12-LOX inhibitors can be used as a novel approach for treatment of prostate tumors.

REPORTABLE OUTCOMES

- Research article published.
  Szekeres, C.K., Trikha, M., Nie, D., and Honn, K.V. 2000. Eicosanoid 12(S)-HETE activates phosphatidylinostol 3-kinase. Biochem. Biophys. Res. Commun. 275: 690 – 695.
- Research article published.
  Timar, J., Raso, E., Dome, B., Li, L., Grignon, D., Nie, D., Honn, K.V., and Hagmann, W. 2000. Expression, subcellular localization and putative function of platele-type 12-lipoxygenase in human prostate cancer cell lines of different metastatic potential. Int. J. Cancer 87: 37 – 43.
- Research article published.
  Nie, D., K. Tang, C. Diglio and K. V. Honn. 2000. Eicosanoid regulation of angiogenesis: Role of endothelial arachidonate 12-lipoxygenase. Blood 95: 2304 - 2311.
- Research article published.
  Tang, K., Finley, R.L. Jr, Nie, D., and Honn, K.V. 2000. Identification of 12-lipoxygenase interaction with cellular proteins by yeast two-hybrid screening. Biochemistry 39: 3185 – 3191.
- Research article published.
  Pidgeon GP, Tang K, Cai YL, Piasentin E and Honn KV. 2003. Overexpression of platelet type 12-lipoxygenase promotes tumor cell survival by enhancing aVbeta3 and aVbeta5 integrin expression. Cancer Res. 63: 4258-4267.
- Research article published.
  Pidgeon GP, Tang K, Rice RL, Zacharek A, Li L, Taylor JD, and Honn KV. 2003. Overexpression of leukocyte type 12-lipoxygenase promotes W256 tumor cell survival by enhancing aVbeta5 expression. Intl J Cancer 105: 459-471.
- Research article submitted.
  Nie, D., Y Chen, Y Qiao, A Zacharek, K Tang, J Milanini, G Pages, D Grignon, and KV Honn. Arachidonate 12-Lipoxygenase regulates the expression of vascular endothelial growth factor in a PI3 kinase dependent pathway.
- Review article published.
  Nie, D., K. Tang, K. Szekeres, M. Trikha, and K. V. Honn. Role of eicosanoids in tumor growth and metastasis. Advances in Eicosanoid Research (C.S. Serhan, ed.). Springer, Berlin. pp. 201 - 217, 2000.
- Review article published.
  Nie, D., M. Che, D. Grignon, K. Tang, and K. V. Honn. Role of eicosanoids in prostate cancer progression. Cancer and Metastasis Review 20: 195 – 206, 2001.
- Review article published.
  Nie, D. and K.V. Honn. Cyclooxygenase, lipoxygenase, and tumor angiogenesis. Cell Mol Life Sci. 59: 799 – 807, 2002.
- Abstract published.
  Nie, D., J. A. Nemeth, M.L. Cher, Y. Chen, U. Barrosso, and K.V. Honn. 1999. Inhibition of prostate cancer cells by a novel 12-lipoxygenase inhibitor in a human orthotopic bone metastasis model. Proc. Amer. Assoc. Cancer Res. 40: 126.
- Abstract published.
  Nie, D., Y. Tang, K. and K.V. Honn. 2001. Signaling pathways in VEGF expression in human prostate cancer cells. Proc. Amer. Assoc. Cancer Res. 42: 940.
- Abstract.published.
  Nie, D., Y. Chen, K. Tang, J. Milanini, G. Pages, D. Grignon, and K.V. Honn. 2000. Arachidonate 12-lipoxygenase stimulates VEGF expression in human prostate cancer cells. Proc. Amer. Assoc. Cancer Res. 41: 792.
- Presentation.

Nie, D., Y. Chen, K. Tang, G.G. Hillman, D. Grignon, and K.V. Honn. "Arachidonate 12-lipoxygenase stimulates angiogenesis by up-regulation of vascular endothelial growth factor expression." Oral Presentation Selected by the 6th International Conference on Eicosanoids and Other Bioactive Lipids in Cancer, Inflammation and Related Diseases, Boston, MA, Sept. 12 -15, 1999.

- Presentation.
  Tang, K., Finley Jr.R.L., Nie, D., Cai, Y., Lamberti, M.P., Fridman, R., Carey, T. E., Crissman, J. D., Honn, K. V. "Physical Interaction with b4 Integrin Up-regulates Arachidonate 12-Lipoxygenase." Poster Presentation at the 6th International Conference on Eicosanoids and Other Bioactive Lipids in Cancer, Inflammation and Related Diseases, Boston, MA, Sept. 12 -15, 1999.
- Presentation.
  Tang, K., Finley Jr. R.L., Nie, D., Honn, K.V. "Interaction of 12-Lipoxygenase with Cellular Proteins." Oral Presentation at the 6th International Conference on Eicosanoids and Other Bioactive Lipids in Cancer, Inflammation and Related Diseases, Boston, MA, Sept. 12 -15, 1999.
- Presentation.
  Nie, D., Chen, Y., Tang, K., Milanini, J., Pages, G., Hillman, G.G., Grignon, D.J., Honn, K.V. "Arachidonate 12-lipoxygenase stimulates VEGF expression in human prostate cancer cells." 91th Annual Meeting (2000) of Ameican Association for Cancer Research. San Francisco, CA. April 1 - 6, 2000.
- Presentation.
  Tang, K., Finley Jr. R.L., Nie, D., Honn, K. V. "Physical interaction of b4 integrin regulates 12-lipoxygenase activity." 91th Annual Meeting (2000) of Ameican Association for Cancer Research. San Francisco, CA. April 1 - 6, 2000.
- Presentation.
  Nie, D. Tang, K., Honn, K.V. "Role of 12-lipoxygenase in prostate cancer angiogenesis and tumor growth." CapCURE Annual Research Retreat. Lake Tahoe, NV. September, 2000. (Invited presentation).
- Presentation.
  Stark, K. E., D. Nie, and K. V. Honn. "Nordihydroguaiaretic acid is an inhibitor of EGF receptor tyrosine kinase." 7th International Conference on Eicosanoids and Other Bioactive Lipids in Cancer, Inflammation and Related Diseases. Nashville, TN. October 14 – 17, 2001.
- Presentation.
  Tang, K., Y. Cai, D. Nie, M. P. Lamberti, and K. V. Honn. 12-Lipoxygenase (12-LOX) effects on androgen-stimulated prostate cancer cell growth. 93th Annual Meeting (2002) of Ameican Association for Cancer Research. San Francisco, CA. April 6 - 10, 2002.
- Grant obtained.
  Formulation of a prostate cancer drug. NCI STTR grant.
- Development of animal models: Yes.
  We developed a formula for administering BMD188 for study of inhibition of PCa cell induced angiogenesis in animal model.

[CANCER RESEARCH 63, 4258–4267, July 15, 2003]

Overexpression of Platelet-type 12-Lipoxygenase Promotes Tumor Cell Survival by Enhancing $\alpha_v\beta_3$ and $\alpha_v\beta_5$ Integrin Expression[1]

Graham P. Pidgeon, Keqin Tang, Yin Long Cai, Evano Piasentin, and Kenneth V. Honn[2]

Departments of Radiation Oncology [G. P. P., K. T., Y. L. C., K. V. H.], Pathology [K. V. H.], and Medicine [E. P.], Wayne State University, Detroit, Michigan 48202, and Karmanos Cancer Institute, Detroit, Michigan 48201 [K. V. H.]

ABSTRACT

Arachidonic acid metabolism leads to the generation of biologically active metabolites that regulate cell growth and proliferation, as well as survival and apoptosis. We have demonstrated previously that platelet-type 12-lipoxygenase (LOX) regulates the growth and survival of a number of cancer cells. In this study, we show that overexpression of platelet-type 12-LOX in prostate cancer PC3 cells or epithelial cancer A431 cells significantly extended their survival and delayed apoptosis when cultured under serum-free conditions. These effects were shown to be a result of enhanced surface integrin expression, resulting in a more spread morphology of the cells in culture. PC3 cells transfected with 12-LOX displayed increased $\alpha_v\beta_3$ and $\alpha_v\beta_5$ integrin expression, whereas other integrins were unaltered. Transfected A431 cells did not express $\alpha_v\beta_3$; however, $\alpha_v\beta_5$ integrin expression was increased. Treatment of both transfected cell lines with monoclonal antibody to $\alpha_v\beta_5$ (and in the case of PC3 cells, anti-$\alpha_v\beta_3$) resulted in significant apoptosis. In addition, treatment with 100 nM 12(*S*)-hydroxy-eicosatetraenoic acid, the end product of platelet-type 12-LOX, but not other hydroxy-eicosatetraenoic acids, enhanced the survival of wild-type PC3 and A431 cells and resulted in increased expression of $\alpha_v\beta_5$. Furthermore, Baicalein or *N*-benzyl-*N*-hydroxy-5-phenylpentamide, specific 12-LOX inhibitors, significantly decreased $\alpha_v\beta_5$-mediated adhesion and survival in 12-LOX-overexpressing cells. The results show that 12-LOX regulates cell survival and apoptosis by affecting the expression and localization of the vitronectin receptors, $\alpha_v\beta_3$ and $\alpha_v\beta_5$, in two cancer cell lines.

INTRODUCTION

LOXs[3] constitute a family of lipid-peroxidizing enzymes that metabolize AA to biologically active metabolites, including hydroperoxy-eicosatetraenoic acids and HETEs, as well as leukotrienes (1). 12-LOX is one of at least three LOXs that is expressed as two main isoforms, a platelet type cloned from human platelets (2) and a leukocyte type from porcine leukocytes, which shares 65% homology to the platelet-type cDNA (3). Several lines of evidence implicate 12-LOX as a regulator of human cancer development. It is overexpressed in a variety of tumors including breast, colorectal, and prostate tumors (4–6) and has been shown to be present in a number of cancer cell lines (7–9). In addition, we have recently shown that inhibitors to 12-LOX block cell cycle progression by regulating the expression of proteins governing the transition from G_1 to S and induce apoptosis in prostate cancer cells (10), whereas overexpression of 12-LOX increases angiogenesis and metastatic growth in mice (6).

The ability of tumors to invade beyond hemostatic boundaries and form metastatic colonies requires the complex interplay of various cell surface-associated components regulating the proteolytic disruption of the ECM and the modification of cell adhesion properties (11). These cell-ECM interactions are mediated by integrins, a family of adhesive receptors that mediate the attachment of the cell to both structural and matrix-immobilized proteins to promote cell survival, proliferation, and migration (12, 13). Integrins perform a well-documented function in cellular invasion and metastasis (14, 15). Nonligated integrins are generally spread diffusely over the cell surface with no apparent linkage to the actin cytoskeleton. However, when ligated, integrins frequently cluster into specialized structures called focal adhesion complexes, thereby providing a convergence site for multiple signaling components (15, 16), while physically linking the receptors to actin microfilaments (17, 18). Ligand binding to integrins triggers a number of signaling pathways, some of which are primarily related to cell adhesion, whereas others provide survival signals to cells. For example, prevention of cell adhesion to the ECM will trigger apoptosis in various cells [in particular, epithelial cells (19–21)], suggesting that integrin-mediated attachment relays important survival signals to the cells. Conversely, attachment or adhesion to the basement membrane or individual ECM components has been shown to promote cell differentiation and extend cell survival under various experimental conditions (22–25).

Previous studies have indicated a role for AA metabolism in cell-matrix interactions and integrin signaling. For example, inhibition of cyclooxgenase-2 by nonsteroidal anti-inflammatory drugs blocks both platelet aggregation [by suppressing activation of integrin $\alpha_{IIb}\beta_3$ (26)] and endothelial cell migration [by suppressing activation of $\alpha_v\beta_3$ integrin (27)]. Other studies have reported the role of LOXs, in particular, 12-LOX, in the regulation of surface integrin expression. For example, adhesion of B16 murine melanoma cells to microvascular endothelial cells was enhanced by pretreatment of the endothelial cells with the 12-LOX product, 12(*S*)-HETE, via up-regulation of $\alpha_v\beta_3$ integrin expression (28). In the same cell line, ligation of $\alpha_{IIb}\beta_3$ integrin induced 12(*S*)-HETE production (29), implying coregulation of integrin expression and LOX activity in these cells. Similarly, 12(*S*)-HETE treatment of human endothelial cells enhanced monocyte adhesion through increased very late-acting antigen-4 integrin expression (30). Indeed, we have recently reported the interaction of 12-LOX with a number of cellular proteins, including the integrin β_4 subunit, as determined by yeast two-hybrid screening (31). The above observations establish a potential relationship between lipid-regulated adhesive functions and cellular responses to apoptosis induction.

In this study, we examine the involvement of 12-LOX in the survival of two tumor cell lines from different histological origins under growth-restrictive conditions. The results indicate that overexpression of platelet-type 12-LOX in PC3 or A431 cells (prostate and epidermoid cancer cell lines, respectively) enhances surface expression of $\alpha_v\beta_3$ and $\alpha_v\beta_5$ integrins in PC3 cells and $\alpha_v\beta_5$ in A431 cells.

Received 5/31/02; accepted 5/8/03.

The costs of publication of this article were defrayed in part by the payment of page charges. This article must therefore be hereby marked *advertisement* in accordance with 18 U.S.C. Section 1734 solely to indicate this fact.

[1] Supported by NIH Grant, CA-29997, United States Army Prostate Cancer Research Program DAMD 17-98-1-8502, and a fellowship from the American Cancer Research Foundation (to G. P. P.).

[2] To whom requests for reprints should be addressed, at Department of Radiation Oncology, Wayne State University, 431 Chemistry Building, Detroit, MI 48202. Phone: (313) 577-1018; Fax: (313) 577-0798; E-mail: k.v.honn@wayne.edu.

[3] The abbreviations used are: LOX, lipoxygenase; AA, arachidonic acid; HETE, hydroxy-eicosatetraenoic acid; ECM, extracellular matrix; BrdUrd, bromodeoxyuridine; FBS, fetal bovine serum; TUNEL, terminal deoxynucleotidyl transferase-mediated nick end labeling; BHPP, *N*-benzyl-*N*-hydroxy-5-phenylpentamide; TBST, 10 mM Tris-HCl (pH 7.5), 100 mM NaCl, and 0.1% Tween 20; Tdt, terminal deoxynucleotidyltransferase; HODE, hydroxyoctadeca-98, 11E-dienoic acid.

This increased integrin expression prolongs cell survival, delaying the induction of apoptosis in the absence of serum.

MATERIALS AND METHODS

Cell Lines. Two carcinoma cell lines, prostate carcinoma PC3 and epidermoid carcinoma A431, were obtained from the American Type Culture Collection (Manassas, VA) and maintained in a humidified atmosphere of 5% CO_2 in air at 37°C. The cells were routinely cultured in RPMI 1640 or DMEN supplemented with 10% FBS (Life Technologies, Inc., Grand Island, NY), 2 mM L-glutamine, and 100 μg/ml penicillin-streptomycin. Experiments were performed when cells were approximately 80% confluent.

PC3 or A431 cells were transfected with the full-length cDNA encoding human platelet-type 12-LOX from pCMV-12-LOX (provided by Dr. Colin Funk, University of Pennsylvania) or empty vector and characterized as described in detail previously (6, 31). Transfected cells were taken from early passages and maintained in RPMI 1640 or DMEN containing 300 mg/ml Geneticin (G418; Life Technologies, Inc.) to prevent outgrowth of revertant cells.

Cell Proliferation/Survival Assay. Wild-type, mock-transfected, or 12-LOX-transfected PC3 or A431 cells were cultured in 96-well plates at a concentration of 5×10^3 cells/ml under serum-free medium (RPMI 1640 with 0.1% FBS) for 0–7 days. Assessment of cell survival/proliferation was carried out by means of a specific nonradioactive cell proliferation ELISA, based on the measurement of BrdUrd incorporation during DNA synthesis according to the manufacturer's instructions (Roche Diagnostics, Mannheim, Germany).

Apoptosis Assays. Wild-type, mock-transfected, or 12-LOX-transfected PC3 or A431 cells were cultured in 75-cm^3 flasks at a concentration of 3×10^6 in serum-free medium (RPMI 1640 with 0.1% FBS) over time (0–7 days) to induce apoptosis. Apoptosis was quantitated on an Epics II flow cytometer (Coulter, Hialeah, FL), using the terminal incorporation of fluorescein-12-dUTP by Tdt into fragmented DNA according to the manufacturer's instructions (Roche Diagnostics), as reported previously (10).

In addition, fragmented DNA was extracted using the NP40/RNase/SDS/proteinase K method as described previously (32) and analyzed on a 1.2% agarose gel.

Western Blot Analysis of Integrin Expression. Total cell lysates were prepared for each of the wild-type, neo-transfected, or 12-LOX-transfected cell lines. Protein (30 μg) was fractionated on precast SDS-PAGE gels and then transferred to nitrocellulose membranes. After incubation for 1 h in blocking solution containing 5% skimmed milk dissolved in TBST, blots were probed overnight with primary antibodies against $\alpha_2\beta_1$, $\alpha_3\beta_1$, $\alpha_v\beta3$, $\alpha_v\beta_5$, or α_v integrin (1:1500 dilution in 5% milk). After this, samples were washed three times in TBST, incubated for 1 h with horseradish peroxidase-conjugated goat antimouse IgG (1:1000 in TBST; Amersham Biosciences, Piscataway, NJ), and washed three times in TBST, and bound antibody complex was visualized using enhanced chemiluminescence (Pierce Chemical Co.). Equal loading of samples was illustrated by Western blotting for β-actin, a constitutively expressed protein.

For Western analysis of membrane-associated proteins, cells were taken at 80% confluence and suspended in homogenization buffer [25 mM Tris-HCl (pH 7.6) and 1 mM EGTA containing 5 mg/ml aprotinin, 10 mg/ml leupeptin, and 1 mM phenylmethylsulfonyl fluoride]. Cells were then homogenized by sonication (15 s, ×3 on ice; Vibracell-Microtip) with intervals of 3 min. Homogenates were centrifuged at 10,000 × g for 1 h at 4°C. The 10,000 × g supernatant was regarded as cytosol, and this, along with the 10,000 × g pellet, was rinsed once with homogenization buffer. Thereafter, the reconstituted pellet was centrifuged at 100,000 × g (1 h, 4°C), and the pellet, termed the membrane fraction, was suspended in lysis buffer and used immediately for electrophoresis. Protein in each fraction was determined by the Bradford method using BSA as standard.

Flow Cytometric Analysis of Adhesion Molecule Expression. Flow cytometry was performed for the analysis of integrin receptors as described previously (33). Briefly, cultured PC3 or A431 cells (1×10^6) were dissociated with 0.2 mM EDTA, washed with PBS, and then fixed in 3.7% paraformaldehyde in PBS (pH 7.4). Cells were then incubated in 20% normal goat serum to block nonspecific binding. Subsequently, cells were incubated with primary antibodies [0.1 μg/ml mouse monoclonal antibody to $\alpha_2\beta_1$, $\alpha_3\beta_1$, β_1, $\alpha_v\beta_5$, $\alpha_v\beta_3$, or $\alpha_v\beta_6$ (Chemicon, Temecula, CA) or 1.0 μg/ml polyclonal antibody to α_v or $\alpha_5\beta_1$ (Chemicon)] followed by a 1:1000 dilution of FITC-labeled secondary antibodies (Invitrogen, Carlsbad, CA). Finally, cell surface fluorescence for individual integrin receptors was analyzed on an Epics Profile II flow cytometer.

$\alpha_v\beta_5$-Mediated Adhesion Assay. To support the results obtained by flow cytometric analysis, the expression of $\alpha_v\beta_5$ integrin on the surface of cells was determined using the integrin-mediated cell adhesion kit according to manufacturers instructions (Chemicon). Briefly, a single cell suspension was prepared nonenzymatically by incubating the cells in 5 mM EDTA in PBS for 15 min. Thereafter, cells were counted on a Coulter counter, and the concentration was adjusted to 3×10^5 cells/ml. The integrin-coated and control strips were rehydrated with 200 μl PBS/well, and 100 μl of the cell suspension were added to the strips. After 2 h of incubation at 37°C in a CO_2 incubator, the cell solution was discarded, and the plates were gently washed three times with PBS. Cell stain solution (100 μl) was added for 5 min, washed, and then extracted using 100 μl of extraction buffer. The concentration of bound cells was relative to the level of surface $\alpha_v\beta_5$ expression and was determined as absorbance at 570 nm by a spectrophotometer.

Antibody Blocking Studies. To establish a functional role for individual integrin receptors in 12-LOX-mediated apoptosis resistance, 12-LOX-transfected cells were serum-starved in the presence of various antibodies to integrin receptors (outlined in the Western blot section). Cell survival and apoptosis 48–72 h after starvation were evaluated by the BrdUrd cell proliferation assay and TUNEL staining, respectively. Morphological alterations were recorded on a phase-contrast microscope.

Treatment with 12(*S*)-HETE or 12-LOX Inhibitors. To prove that 12-LOX is responsible for the increase in survival and $\alpha_v\beta_5$ surface expression in both cell lines, wild-type cells were treated with 100 nM 5(*S*)-HETE, 12(*S*)-

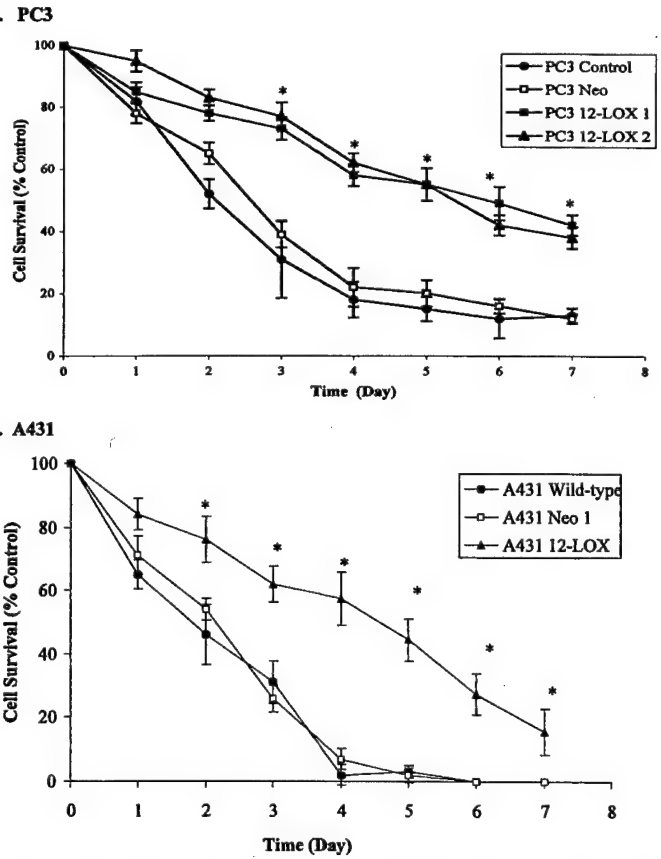

Fig. 1. Quantitation of the survival of PC3 (*A*) or A431 (*B*) transfected sublines cultured after serum withdrawl, as determined by BrdUrd incorporation assay. The values are expressed as the percentage of cell survival compared with day 0 (at which time the survival was considered to be 100%), and the *bars* represent the SE derived from three independent experiments. 12-LOX-transfected PC3 (*12-LOX 1* and *12-LOX 2*) and A431 cells (*12-LOX*) all survived significantly longer, under serum-starved conditions, compared with either wild-type or mock-transfected (*Neo 1*) controls, in each cell line. *, $P < 0.05$.

HETE, 15(*S*)-HETE, or 13(*S*)-HODE (Cayman Chemicals, Ann Arbor, MI) in serum-free conditions (0.1% FBS), and survival was assessed after 48 and 96 h by BrdUrd assay. In addition, 12-LOX-transfected cell lines were incubated with 10 μM Baicalein (Biomol, Plymouth, PA) or BHPP (Biomide Corp., Grosse Pointe Farms, MI), both of which are specific 12-LOX inhibitors, or the 5-LOX inhibitor Rev-5901 (Cayman Chemicals) for 48 h in serum-free conditions.

After treatment, cells were also assessed for their surface $\alpha_v\beta_5$ expression, using the integrin-mediated cell adhesion kit described previously. Wild-type PC3 or A431 cells were treated with 5(*S*)-HETE, 12(*S*)-HETE, 15(*S*)-HETE, or 13(*S*)-HODE 24 h before the adhesion assay.

RESULTS

Overexpression of Platelet-type 12-LOX in PC3 and A431 Cells Extends Their Survival and Delays Apoptosis in the Absence of Serum. Both of the cell lines used in this study demonstrated serum dependence for their continued growth. Several independent experiments revealed that the survival of both wild-type and neo-transfected PC3 cells declined steadily after 24 h of serum starvation (Fig. 1*A*). Within 3 days of serum withdrawal, only 35–40% of wild-type or neo-transfected cells were viable, compared with 75–80% of 12-LOX-transfected cells. Whereas 12-LOX-transfected PC3 cells cell did display a gradual decrease in cell viability over time, this decrease was much slower than that observed in either wild-type or neo-transfected cells. At all points after 3 days, there was a significantly extended survivability of 12-LOX-transfected PC3 cells ($P < 0.05$).

A431 cells were more sensitive to serum deprivation, with cell survival reduced dramatically after only 24 h of serum starvation (Fig. 1*B*). Within 4 days of serum starvation, all wild-type and mock-transfected cells were dead. A431 cells overexpressing platelet-type 12-LOX demonstrated a significantly extended overall survival ($P < 0.05$) compared with either the wild-type or mock-transfected A431 cells. Cell numbers declined steadily after 2 days of serum starvation, and by day 7, approximately 20% of cells were viable. The slope of decline was much less than that of the wild-type cells. By day 9, all of the cells were dead (data not shown).

Consistent with these observations, apoptosis was significantly ($P < 0.05$) reduced in the 12-LOX-overexpressing clones (Fig. 2, *A* and *B*). Whereas wild-type and mock-transfected PC3 cells showed a rapid and steady induction of apoptosis after serum withdrawal, the 12-LOX-transfected cells displayed a delayed apoptotic response. Quantitation of apoptotic nuclei in both wild-type and neo-PC3 cells demonstrated that approximately 65% were apoptotic by day 4, 80% were apoptotic by day 6, and essentially 100% were apoptotic by day 8 after serum removal. Representative histograms showing the percentage of Tdt-FITC-positive PC3 cells at day 0 (2.67%) and day 8 (98.7%) are shown in Fig. 2, *C* and *D*, respectively. In sharp contrast, 12-LOX clones exhibited only 15% apoptosis by day 2, maintaining this low level until day 6, at which point a steady increase in apoptosis was observed (Fig. 2*A*). A431 cells displayed a similar response, with rapid induction of apoptosis after serum starvation in both wild-type and mock-transfected cells (60% and 50%, respectively, by day 2), whereas 12-LOX-transfected cells were significantly more resistant to apoptosis (14% by day 2). These results were confirmed by DNA fragmentation assays. 12-LOX-transfected PC3 (Fig. 2*E*) or A431

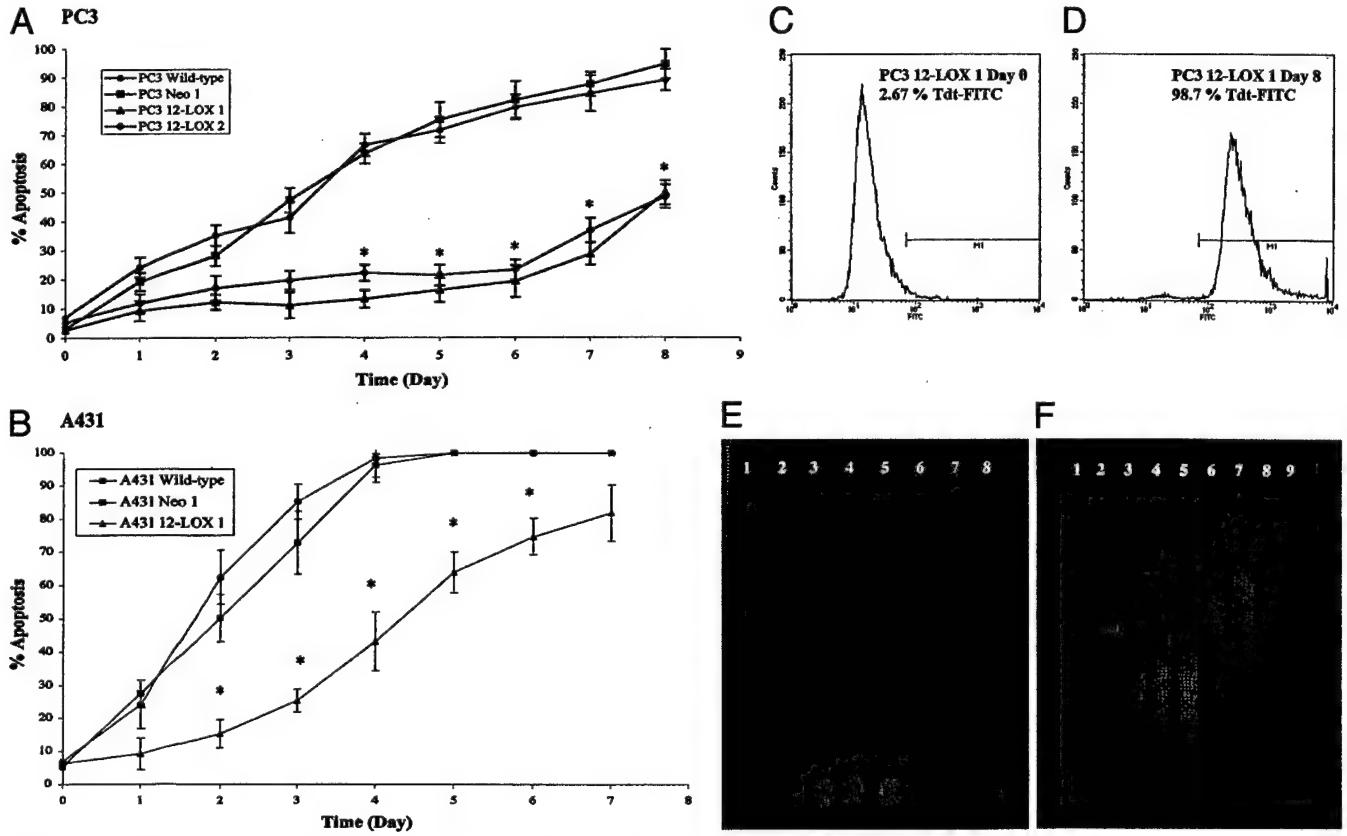

Fig. 2. 12-LOX-overexpressing cells demonstrated a delayed apoptotic response to serum starvation. Apoptosis was quantitated by TUNEL staining in PC3 (*A*) or A431 (*B*) cells serum-starved for 0–7 days. Significant apoptosis was observed after serum starvation in wild-type or mock transfectants (*Neo 1*) in both cell lines, compared with 12-LOX clones (*12-LOX 1* or *12-LOX-2*; *, $P < 0.05$). Representative Tdt-FITC% histograms are shown for PC3 wild-type cells at day 0 (*C*) and day 8 (*D*). Apoptosis was confirmed by DNA fragmentation assays in PC3 cells at day 4 after serum withdrawal (*E*) and in A431 cells at 2 days after serum withdrawal (*F*). *Lanes 1* and *9*, 1-kb ladder; *Lanes 2*, 100-kb ladder; *Lanes 3–5*, mock-transfected cells (*Neo 1*); *Lanes 6–8*, 12-LOX-transfected cells (*12-LOX 1*). It is obvious that the 12-LOX-transfected cells contain less fragmented DNA.

(Fig. 2*F*) cells displayed less fragmentation of DNA compared with mock-transfected controls after serum starvation for 2 (A431 cells) or 4 days (PC3).

Expression of Integrins in Tumor Cell Lines Determined by Flow Cytometry. Overexpression of platelet-type 12-LOX resulted in a more spread morphology under normal culture conditions compared with neo-transfected and wild-type cells, as observed after light microscopy (data not shown). Cell anchorage to the substratum is mediated by cell adhesion to the ECM proteins through integrin receptors; therefore, it is possible that 12-LOX overexpression may modulate the expression/function of integrin receptors to enhance cell spreading. We examined several potential integrins and adhesion molecules in wild-type PC3 and A431 cells to determine which ones are expressed endogenously. Wild-type PC3 cells were found to express high levels of $\alpha_2\beta_1$, $\alpha_3\beta_1$, β_1, and α_v on their surface (Fig. 3, *E, F, D,* and *H,* respectively), as indicated by a shift in the mean fluorescence relative to controls. A lower level of $\alpha_5\beta_1$, $\alpha_v\beta_3$, $\alpha_v\beta_5$, and $\alpha_v\beta_6$ integrin expression was observed (Fig. 3, *G, I, J,* and *K,* respectively).

A431 cells expressed high levels of $\alpha_2\beta_1$, $\alpha_3\beta_1$, $\alpha_5\beta_1$, and β_1 on their surface (Fig. 4, *E, F, G,* and *D,* respectively), with lower levels of α_v, $\alpha_v\beta_5$, and $\alpha_v\beta_6$ integrins (Fig. 4, *H, J,* and *K,* respectively). A431 cells did not express integrin $\alpha_v\beta_3$ at all on their surface (Fig. 4*I*), as indicated by no shift in the mean log fluorescence compared with cells alone (Fig. 4*B*) or cells with secondary antibody only (Fig. 4*C*).

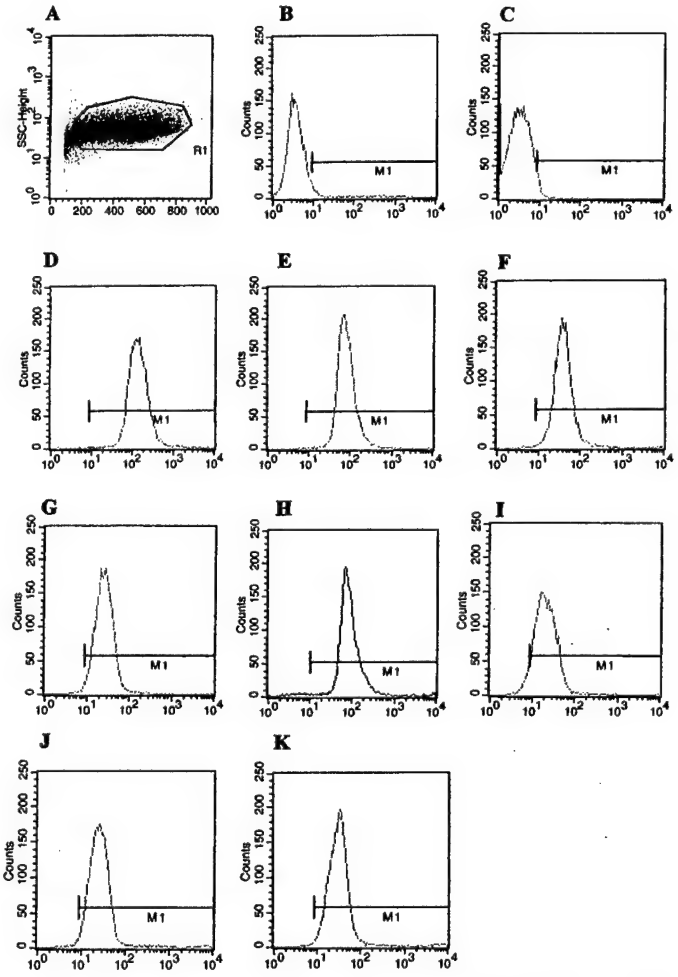

Fig. 3. Endogenous expression of integrins in PC3 carcinoma cells as determined by flow cytometry. Wild-type PC3 cells (*A*) were incubated with control (*B*; PBS) or rabbit IgG (*C*; 1.0 mg/ml) or various primary antibodies: β_1 (*D*; 0.1 mg/ml); $\alpha_2\beta_1$ (*E*; 1.0 mg/ml); $\alpha_3\beta_1$ (*F*; 0.1 mg/ml); $\alpha_5\beta_1$ (*G*; 0.1 mg/ml); α_v (*H*; 0.1 mg/ml); $\alpha_v\beta_3$ (*I*; 1.0 mg/ml); $\alpha_v\beta_5$ (*J*; 0.1 mg/ml); or $\alpha_v\beta_6$ (*K*; 0.1 mg/ml). Cells were then treated with FITC-labeled secondary antibodies, and analysis of cell surface fluorescence was performed by flow cytometry. PC3 cells express moderate levels of $\alpha_v\beta_3$, $\alpha_v\beta_5$, $\alpha_v\beta_6$, and $\alpha_5\beta_1$ integrin receptors and high levels of α_v, $\alpha_2\beta_1$, $\alpha_3\beta_1$, and β_1, indicated by a prominent shift in the mean log fluorescence intensity compared with controls.

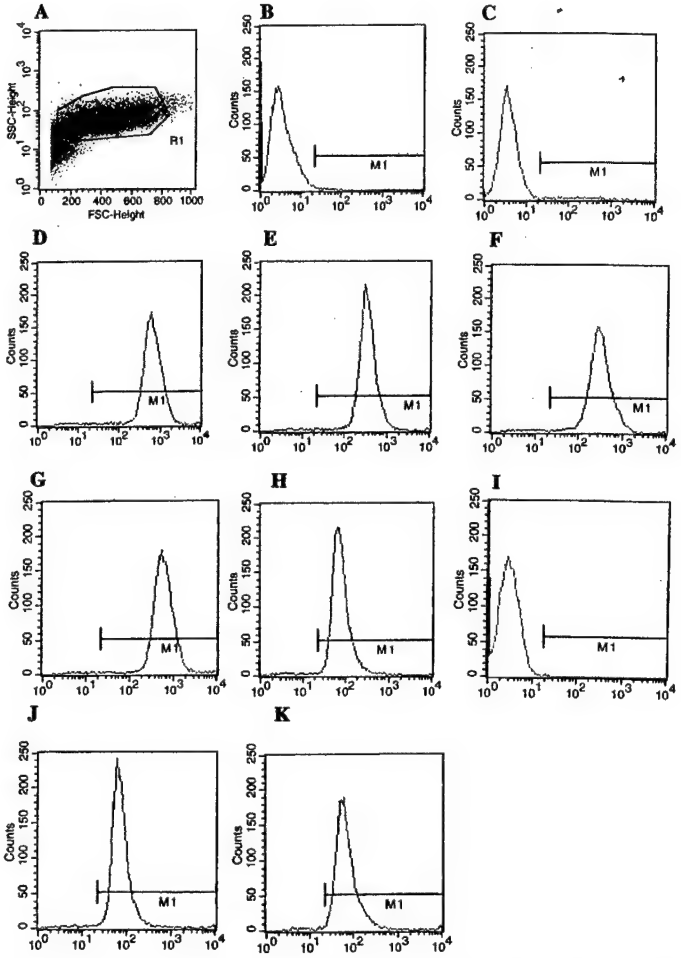

Fig. 4. Endogenous expression of integrins in A431 cells as determined by flow cytometry. Wild-type A431 cells (*A*) were incubated with control (*B*; PBS) or rabbit IgG (*C*; 1.0 mg/ml) or various primary antibodies: β_1 (*D*; 0.1 mg/ml); $\alpha_2\beta_1$ (*E*; 1.0 mg/ml); $\alpha_3\beta_1$ (*F*; 0.1 mg/ml); $\alpha_5\beta_1$ (*G*; 0.1 mg/ml); α_v (*H*; 0.1 mg/ml); $\alpha_v\beta_3$ (*I*; 1.0 mg/ml); $\alpha_v\beta_5$ (*J*; 0.1 mg/ml); or $\alpha_v\beta_6$ (*K*; 0.1 mg/ml). A431 cells did not express $\alpha_v\beta_3$ at all but expressed moderate levels of α_v, $\alpha_v\beta_5$, and $\alpha_v\beta_6$ integrin receptors. A431 cells highly expressed $\alpha_2\beta_1$, $\alpha_3\beta_1$, $\alpha_5\beta_1$, and β_1, indicated by a prominent shift in the mean log fluorescence intensity compared with controls.

Increased Surface Expression of $\alpha_v\beta_3$ and $\alpha_v\beta_5$ Integrins in PC3 and $\alpha_v\beta_5$ in A431 12-LOX-transfected Tumor Cells. Under the same experimental conditions, flow cytometric studies demonstrated relatively consistent expression levels of several integrin receptors such as $\alpha_2\beta_1$, $\alpha_3\beta_1$, β_1, α_v, and $\alpha_v\beta_6$ between PC3 wild-type and 12-LOX-transfected cells (Table 1). However, 12-LOX-transfected cells demonstrated a consistent increase in the expression of $\alpha_v\beta_5$ (3.2-fold) and $\alpha_v\beta_3$ (3.0-fold) as compared with the wild-type cells. This increase is easily observed as a shift in the mean log fluorescence to the right in 12-LOX-transfected cells relative to wild-type cells.

A431 wild-type and 12-LOX-overexpressing cells displayed similar relative levels of $\alpha_2\beta_1$, $\alpha_3\beta_1$, β_1, α_v, and $\alpha_v\beta_6$ on their surface (Table 2). A431 cells did not express $\alpha_v\beta_3$ integrin; however, 12-LOX-transfected cells had increased surface $\alpha_v\beta_5$ integrin (1.8-fold) relative to wild-type or neo-transfected controls. Interestingly, there was a slight drop in the expression of both β_1 and $\alpha_2\beta_1$ integrins

Table 1 *Integrin expression between PC3 wild-type and 12-LOX-transfected cells*

Integrin	PC3 WT[a]	PC3 Neo	PC3 12-LOX C1	PC3 12-LOX C2	Fold increase 12-LOX *vs.* WT
β_1	148.08 ± 10.38	132.08 ± 20.11	245.9 ± 16.11	219.4 ± 18.16	2.1
$\alpha_2\beta_1$	83.78 ± 3.64	72.50 ± 3.35	172.5 ± 8.29		1.93
α_v	26.69 ± 2.02	29.02 ± 5.21	44.72 ± 8.21		1.62
$\alpha_v\beta_3$	25.09 ± 4.11	22.57 ± 2.15	**78.64 ± 4.03**[b]	**71.61 ± 2.06**[b]	**2.98**
$\alpha_v\beta_5$	41.71 ± 5.3	37.56 ± 4.15	**134.23 ± 6.03**[b]	**145.63 ± 7.16**[b]	**3.22**
$\alpha_v\beta_6$	50.97 ± 4.7	62.62 ± 8.3	87.60 ± 12.7	74.10 ± 16.4	1.64

[a] WT, wild-type.
[b] Integrins most significantly overexpressed.

Table 2 *Integrin expression between A431 wild-type and 12-LOX-transfected cells*

Integrin	A431 WT[a]	A431 Neo	A431 12-LOX C1	Fold increase 12-LOX *vs.* WT
β_1	118.45 ± 1.4	123.15 ± 2.43	106.23 ± 4.21	0.86
$\alpha_2\beta_1$	103.24 ± 2.23	108.97 ± 8.45	73.36 ± 10.29	0.87
$\alpha_3\beta_1$	78.45 ± 5.42	79.02 ± 3.21	74.72 ± 5.2	0.95
$\alpha_5\beta_1$	44.67 ± 3.76	44.97 ± 5.06	49.08 ± 2.49	1.09
α_v	58.2 ± 5.28	56.73 ± 5.15	63.08 ± 3.03	1.11
$\alpha_v\beta_5$	17.46 ± 3.93	18.86 ± 2.25	**32.09 ± 3.24**[b]	**1.70**
$\alpha_v\beta_6$	51.25 ± 6.41	48.17 ± 5.8	61.93 ± 7.6	1.28

[a] WT, wild-type.
[b] Integrin most significantly overexpressed.

(0.84- and 0.68-fold, respectively), suggesting that the expression of subsets of integrins may be lost in favor of other integrins.

Overexpression of $\alpha_v\beta_5$ in PC3 and A431 cells transfected with 12-LOX was confirmed by means of an integrin-mediated adhesion assay specific for $\alpha_v\beta_5$ (as outlined in "Materials and Methods"). Wild-type, neo-transfected, or 12-LOX-transfected clones were examined, and overexpression of 12-LOX resulted in significantly more adhesion to the plates as indicated by absorbance (Fig. 5). These results prove that overexpression of 12-LOX results in increased surface expression of $\alpha_v\beta_5$ in both PC3 and A431 cells.

Overexpression of 12-LOX in PC3 or A431 Tumor Increases Membrane Localization of Integrins $\alpha_v\beta_3$ and $\alpha_v\beta_5$ in PC3 Cells and $\alpha_v\beta_5$ in A431 Cells. Having illustrated that overexpression of 12-LOX increases surface expression of $\alpha_v\beta_3$ or $\alpha_v\beta_5$ in each cell line, we next evaluated the protein expression of a variety of integrins by Western blot. $\alpha_2\beta_1$, α_v, and $\alpha_v\beta_5$ expression was examined in wild-type, neo-transfected, and 12-LOX-transfected cells, and no difference in expression was observed in either cell line (Fig. 6, *A* and *B*). This indicated that overexpression of 12-LOX did not alter translation of the protein but rather the distribution of the protein from intracellular stores to the membrane. This was confirmed by Western analysis of the membrane fractions of wild-type and 12-LOX-transfected PC3 cells for $\alpha_v\beta_3$ or $\alpha_v\beta_5$. 12-LOX-transfected PC3 cells expressed increased membrane levels of $\alpha_v\beta_3$ compared with either wild-type or neo-transfected cells (Fig. 6*C*). Similarly, membrane expression of $\alpha_v\beta_5$ was clearly increased in 12-LOX-transfected cells compared with either wild-type or neo-transfected cells (Fig. 6*D*). Clustering of integrins at the membrane and focal adhesion contacts provides a convergence site for multiple signaling components (15, 16), which could affect the survival of the cells. These studies suggest that 12-LOX-transfected PC3 cells may rely on the up-regulation of $\alpha_v\beta_3$ or $\alpha_v\beta_5$ integrin or both to maintain their adherence to the substratum to sustain their cell survival. Similar results were observed in 12-LOX-transfected A431 cells compared with wild-type cells, where membrane expression of $\alpha_v\beta_5$ was increased (Fig. 6*E*).

Integrins $\alpha_v\beta_3$ and $\alpha_v\beta_5$ Are Important Factors for 12-LOX-transfected Tumor Cell Survival in the Absence of Serum. Having examined the expression of a number of integrins on both PC3 and A431 cells and shown that overexpression of 12-LOX increased surface expression of $\alpha_v\beta_3$ (PC3) and $\alpha_v\beta_5$ (A431 and PC3), we next examined which one(s) plays a causal role in sustaining cell survival during serum deprivation. 12-LOX-transfected cells were serum-starved in the presence of PBS (as control) or an antibody to $\alpha_2\beta_1$, $\alpha_3\beta_1$, $\alpha_5\beta_1$, α_v, $\alpha_v\beta_3$, $\alpha_v\beta_5$, or $\alpha_v\beta_6$. After 2 days of serum withdrawal, control 12-LOX-transfected PC3 cells demonstrated typical spread morphology. In sharp contrast, the survival of 12-LOX-transfected PC3 cells was significantly reduced when cells were serum-starved in the presence of monoclonal anti-$\alpha_v\beta_3$ or anti-$\alpha_v\beta_5$ antibody, and a combination of both antibodies had an additive effect (Fig. 7*A*). In the presence of 0.01 μg/ml anti-$\alpha_v\beta_3$ or anti-$\alpha_v\beta_5$, pCMV-12-LOX PC3 cells underwent remarkable morphological changes consistent with apoptosis and were significantly ($P < 0.05$) more apoptotic than controls, as determined by TUNEL staining and fluorescence-activated cell-sorting analysis. In contrast, 12-LOX PC3 cells did not appear to be dependent on integrins $\alpha_2\beta_1$, $\alpha_3\beta_1$, $\alpha_5\beta_1$, α_v, or $\alpha_v\beta_6$ for maintaining survival under serum-free conditions because pretreatment with the respective antibodies did not affect either the survival or apoptosis of the cells (Fig. 7*A*).

Similar results were observed in A431 cells overexpressing 12-LOX, with anti-$\alpha_v\beta_5$ dramatically reducing the survival of 12-LOX-transfected cells (Fig. 7*B*) and resulting in significant apoptosis of these cells relative to untreated controls, an effect that was not observed when any of the other integrins were blocked. These data indicate that integrin $\alpha_v\beta_5$ and, in the case of PC3 cells, integrin $\alpha_v\beta_3$ play a critical and functional role in supporting the survival of 12-LOX-transfected cells in the absence of serum.

12(*S*)-HETE Increases the Survival and Expression of $\alpha_v\beta_5$ in PC3 and A431 Cells. In a final subset of experiments, having shown that overexpression of 12-LOX in two different cell lines prolonged survival and enhanced surface $\alpha_v\beta_5$ integrin expression, we investigated whether the end product of 12-LOX metabolism, 12(*S*)-HETE, would have similar effects in wild-type cells. Wild-type PC3 or A431

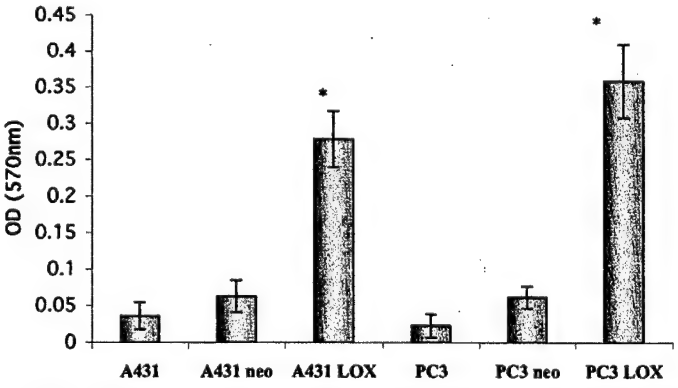

Fig. 5. 12-LOX-transfected A431 and PC3 cells exhibit increased $\alpha_v\beta_5$-mediated adhesion. PC3 or A431 wild-type, neo-transfected, or 12-LOX-transfected cells were seeded on $\alpha_v\beta_5$-specific adhesion plates as outlined in "Materials and Methods." In both PC3 and A431 cells, 12-LOX-transfected cells had significantly increased adhesion to the plates, confirming increased surface expression of the $\alpha_v\beta_5$ integrin. *, $P < 0.01$.

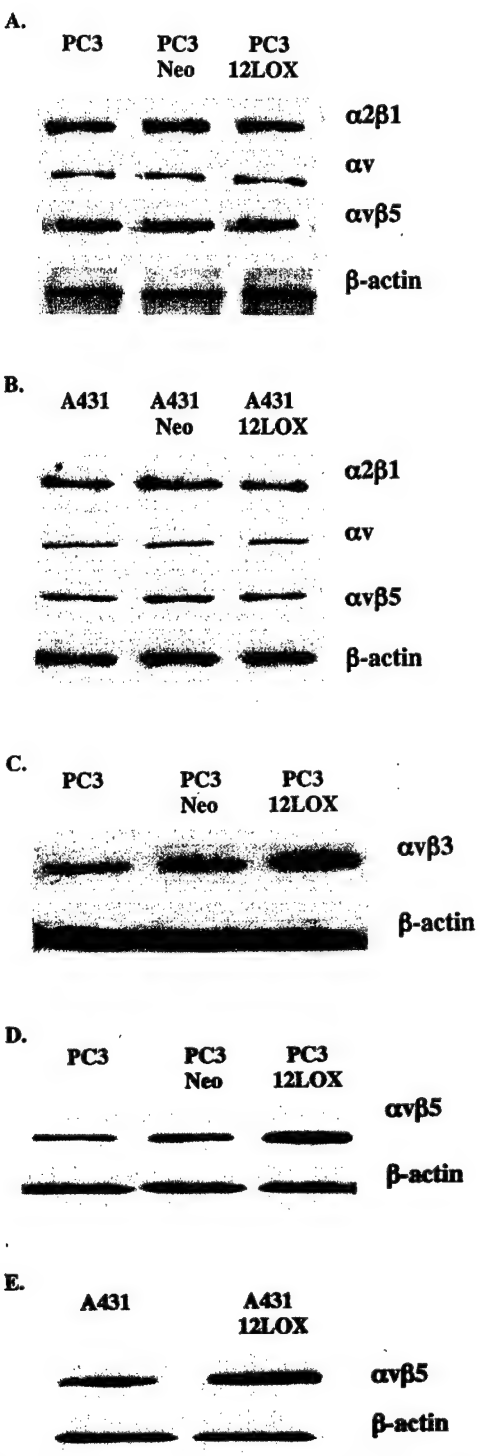

Fig. 6. Western blot analysis of integrin expression in PC3 (*A*) or A431 cells (*B*). Total cell lysates were prepared from wild-type, neo-transfected (*Neo*), and 12-LOX-transfected clones. Expression of $\alpha_2\beta_1$, α_v, and $\alpha_v\beta_5$ was determined in both PC3 and A431 cell lines. Expression of β-actin was determined as a control on cellular loading. There was no difference in the expression of any of the analyzed integrins, indicating that 12-LOX did not alter integrin expression at the translational level. *C*, increased membrane expression of $\alpha_v\beta_3$ integrin in 12-LOX-transfected PC3 cells. Membrane fractions were isolated and examined by Western analysis. *D*, increased membrane expression of $\alpha_v\beta_5$ in PC3 cells after transfection with 12-LOX. *E*, increased membrane expression of $\alpha_v\beta_5$ in A431 cells after transfection with 12-LOX.

cells were grown in 96-well plates in the absence of serum treated with 100 nM 5(*S*)-HETE, 12(*S*)-HETE, 15(*S*)-HETE, or 13(*S*)-HODE every 12 h for 48 h. Treatment with 12(*S*)-HETE resulted in significantly greater survival of both PC3 (85% compared to 58%; Fig. 8*A*) and A431 cells (60% compared with 41%; Fig. 8*B*) under serum-starved conditions. At similar concentrations, 5(*S*)-HETE, 15(*S*)-HETE, or 13(*S*)-HODE had no effect on the survival of either cell line. Separately, PC3 and A431 cells overexpressing 12-LOX were treated with 10 μM of the specific 12-LOX inhibitors Baicalein or BHPP or a specific 5-LOX inhibitor, Rev-5901, for 48 h. Inhibition of 12-LOX with either inhibitor resulted in a significant decrease in the survival of both PC3 (Fig. 8*C*) and A431 (Fig. 8*D*) cells overexpressing 12-LOX. Most importantly, inhibition of 5-LOX did not alter the survival of either cell line. The two 12-LOX inhibitors used were structurally different, and the same results were observed with either inhibitor, eliminating the possibility of separate effects unrelated to 12-LOX inhibition.

In a separate experiment, we examined the effect of each treatment on surface $\alpha_v\beta_5$ expression by examining the attachment of wild-type PC3 or A431 on $\alpha_v\beta_5$-mediated adhesion kits after treatment. 12(*S*)-HETE (100 nM) resulted in a significant increase in the number of cells attached to the plates in both PC3 (Fig. 9*A*) and A431 cells (Fig. 9*B*). In contrast, treatment with 5(*S*)-HETE had no effect, and 15(*S*)-HETE or 13(*S*)-HODE appeared to slightly reduce attachment to the plates, although this was not significant. These results confirm conclusively that the end product of 12-LOX metabolism, 12(*S*)-HETE, regulates both the survival and surface expression of $\alpha_v\beta_5$ integrin on PC3 and A431 cells.

DISCUSSION

The AA-metabolizing enzyme 12-LOX is a key regulator of tumor growth. This pathway has been implicated in tumor cell proliferation and motility, the regulation of apoptosis, and tumor angiogenesis (7–10). Platelet-type 12-LOX is actively expressed in the prostate cancer PC3 cell line (34) and is actively expressed at higher levels in the epidermoid A431 cell line (31). In this study, we report that overexpression of platelet-type 12-LOX decreases cell apoptosis induced by serum starvation and extends the survival of these two characterized tumor cell lines. The prolonged survival of the cells was not a result of increased cell proliferation (data not shown) but was due to an intrinsic property, which rendered them less susceptible to apoptosis. Transfection with 12-LOX in either cell line resulted in a more spread morphology compared with either wild-type or mock-transfected cells, even under normal culture conditions.

As late as 4 days after serum withdrawal, when 70% of wild-type and mock-transfected PC3 cells were apoptotic, the majority (80%) of the pCMV-12-LOX-transfected PC3 cells were still adherent and viable. Similar results were observed in A431 cells, with significant apoptosis as early as 2 days after serum deprivation compared with 12-LOX-transfected cells. Decreased apoptosis in PC3 and A431 cells overexpressing 12-LOX relative to mock-transfected controls was confirmed by DNA laddering. Invariably, cells would first round up and detach from the substratum (*i.e.*, culture flasks) before becoming morphologically and biochemically apoptotic. Indeed, even under normal growth conditions, 12-LOX-transfected PC3 and A431 cells exhibited a more spread morphology in culture, an effect that could be seen to a greater extent when the cells were serum-starved for 4 days. In each case, whereas the majority of wild-type or mock-transfected cells would detach from the substratum, the 12-LOX-transfected cells remained attached and more extended in shape. This observation suggests that in both cell lines examined, the more spread 12-LOX-transfected cells may possess a stronger adherence to the ECM, which would allow them to survive longer in the absence of trophic factors. This would be consistent with previous studies proposing that cells which extend themselves over a large surface area survive better and proliferate faster than cells with a more rounded shape (35).

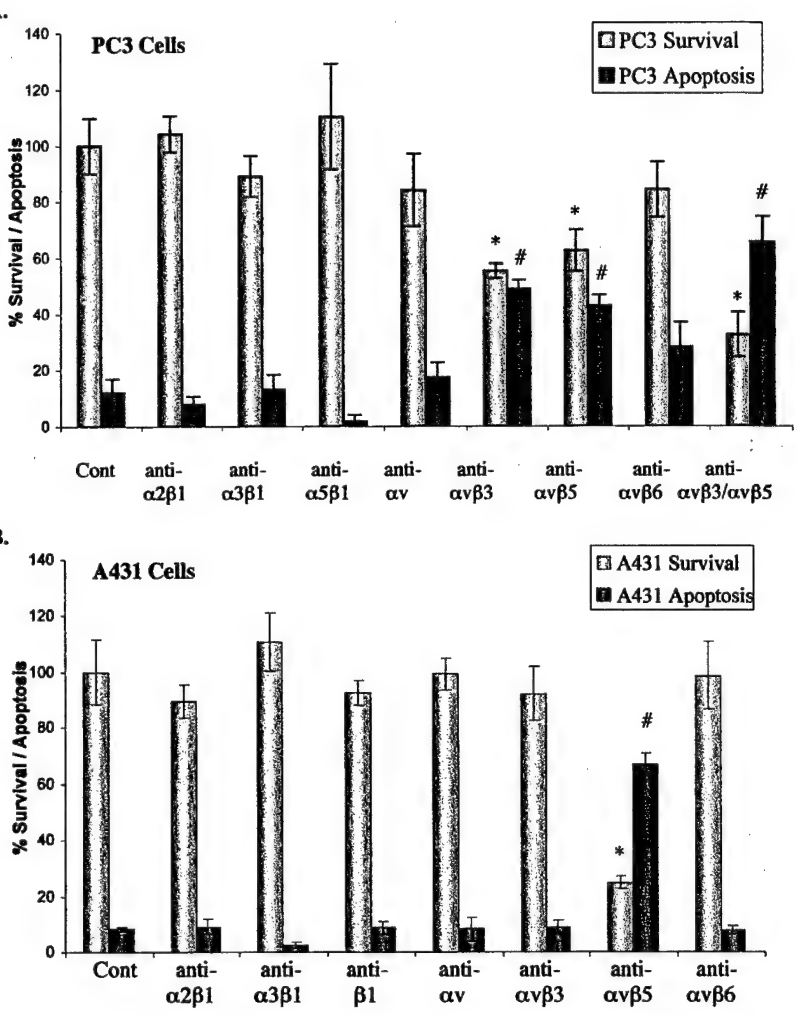

Fig. 7. Integrins $\alpha_v\beta_3$ and $\alpha_v\beta_5$ are important for the survival of 12-LOX-transfected cancer cells in the absence of serum. Survival of 12-LOX-transfected PC3 or A431 cells was examined by BrdUrd incorporation, and apoptosis was determined by TUNEL staining. 12-LOX-transfected PC3 (*A*) or A431 cells (*B*) were serum-starved for 2 days in the presence of various antibodies directed against different integrins. Results are expressed as the percentage of cell survival or apoptosis, and the mean ± SD was derived from three independent experiments. Treatment with anti-$\alpha_v\beta_3$ or anti-$\alpha_v\beta_5$ resulted in a significant decrease in PC3 (12-LOX) cell survival (*, $P < 0.05$) and increased apoptosis (#, $P < 0.05$) compared with controls, and this effect was greater when a combination of the two antibodies was used ($P < 0.02$; $P < 0.01$). Anti-$\alpha_v\beta_5$ significantly decreased survival (*, $P < 0.02$) and increased apoptosis (#, $P < 0.02$) of A431 (12-LOX) cells compared with untreated controls.

Cell shape is maintained mostly by cell-cell and cell-matrix interactions, as well as by intracellular cytoskeletal structures that are physically linked to cell-matrix interaction sites at subcellular structures termed focal adhesions. Integrins are the major cell surface receptors mediating cell-substrate adhesions. The disruption of the integrin-mediated adhesion has consistently been shown to induce anoikis (apoptosis as a result of loss of anchorage), and various integrin molecules play an important role in supporting cell survival. Integrin $\alpha_v\beta_3$ is one of the most studied and has been implicated in the survival of human vascular endothelial (36) and embryonic kidney cells (21), as well as in the survival of melanoma (37) and lymphoid tumor cells (38). Similarly, several β_1 integrins (*e.g.*, $\alpha_2\beta_1$, $\alpha_5\beta_1$, and $\alpha_6\beta_1$) have been shown to mediate the survival of a variety of cell types (19, 39–41), whereas the integrin α_5 subunit has been shown to suppress apoptosis of colon carcinoma cells induced by serum deprivation (42).

Wild-type PC3 cells expressed α_v, $\alpha_2\beta_1$, $\alpha_3\beta_1$, or β_1 as their predominant integrin receptors. These cells also expressed lower levels of integrin $\alpha_5\beta_1$, $\alpha_v\beta_3$, $\alpha_v\beta_5$, and $\alpha_v\beta_6$ on their surface. PC3 cells overexpressing 12-LOX demonstrated a significant increase in their surface expression of integrins $\alpha_v\beta_3$ and $\alpha_v\beta_5$, whereas the expression of other integrin receptors examined by flow cytometry was unaltered. These observations were confirmed by immunofluorescence staining and by means of integrin-specific adhesion assays. These results suggested that $\alpha_v\beta_3$ and $\alpha_v\beta_5$ are potential survival factors for pCMV-12-LOX PC3 cells cultured in the absence of serum. Two subsequent lines of experimental evidence support this hypothesis. First, in the 12-LOX-overexpressing PC3 cells, membrane expression of $\alpha_v\beta_3$ and $\alpha_v\beta_5$ was increased relative to that in wild-type or neo-transfected cells. This increased expression at the cell surface would presumably mediate tighter cell-matrix adhesions and contribute to a more spread morphology in culture. Second, and more importantly, a definite cause and effect relationship was established between the increased surface integrin expression and survival. 12-LOX-transfected PC3 cells, when serum-starved in the presence of a monoclonal antibody to $\alpha_v\beta_3$ or $\alpha_v\beta_5$, demonstrated a significantly reduced survivability, which was similar to that of wild-type and mock-transfected PC3 cells. Dramatically, the 12-LOX-overexpressing PC3 cells treated with anti-$\alpha_v\beta_5$ antibody formed large clusters and aggregates, in which the majority of cells rounded up and underwent apoptosis by day 2. This effect was greater when a combination of anti-$\alpha_v\beta_3$ and anti-$\alpha_v\beta_5$ was used. In addition the effect was shown to be receptor specific because antibodies to several other integrin receptors were ineffective in altering survival. Our results suggest a common characteristic of these integrins, *i.e.*, regulating the survival of PC3 cells under serum-deprived conditions.

In the epidermoid A431 tumor cell line, a high basal expression of β_1-associated integrins (namely, β_1, $\alpha_2\beta_1$, $\alpha_3\beta_1$, and $\alpha_5\beta_1$) was observed. Lower expression of α_v, $\alpha_v\beta_5$, and $\alpha_v\beta_6$ was observed. This cell line did not express the $\alpha_v\beta_3$ integrin. Overexpression of 12-LOX resulted in increased surface expression of $\alpha_v\beta_5$ integrin, with little effect on any of the other integrins examined. Interestingly, we did

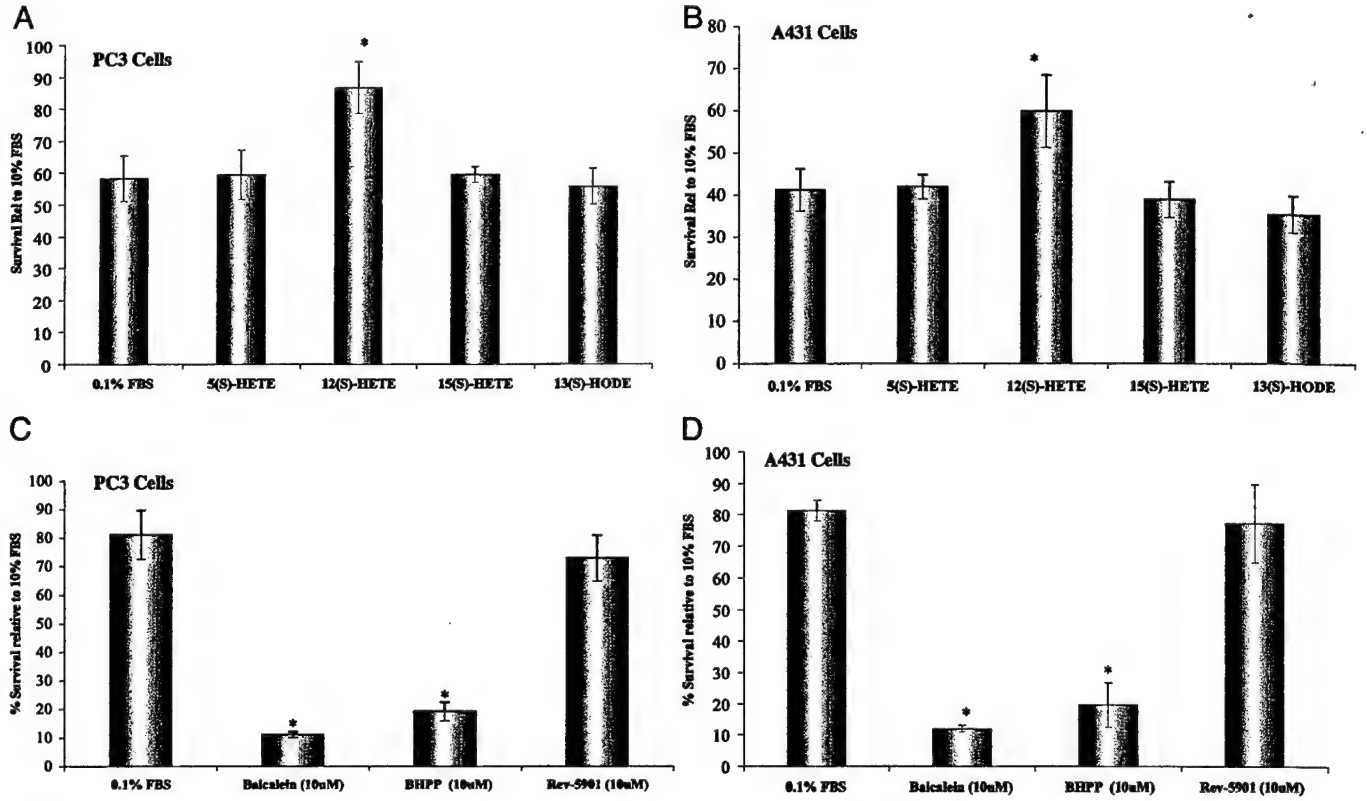

Fig. 8. The end product of 12-LOX metabolism, 12(*S*)-HETE, increased the survival of wild-type PC3 (*A*) or A431 (*B*) cells under serum-starved conditions. Wild-type cells were grown for 48 h in the absence of serum and treated with 100 nM 5(*S*)-HETE, 12(*S*)-HETE, 15(*S*)-HETE, or 13(*S*)-HODE at 12-h intervals. Survival was assessed by BrdUrd assay ("Materials and Methods"). Treatment with 12(*S*)-HETE significantly increased the survival of either PC3 or A431 cells, whereas other treatments did not. *, $P < 0.05$. In addition, 12-LOX-transfected PC3 (*C*) or A431 (*D*) cells were grown for 48 h under serum-starved conditions and treated separately with 10 μM Baicalein or BHPP, two specific 12-LOX inhibitors, or with a specific 5-LOX inhibitor, Rev-5901. Both 12-LOX inhibitors dramatically reduced the survival of 12-LOX-transfected cells, whereas the 5-LOX inhibitor had no effect. *, $P < 0.05$.

observe a slight drop in the expression of both β_1 and $\alpha_2\beta_1$ integrins in A431 cells, which suggests that the expression of subsets of integrins may be lost in favor of other integrins. This has been reported previously in the case of breast cancer, where $\alpha_2\beta_1$ and $\alpha_6\beta_1$ expression was lost in favor of α_v and $\alpha_v\beta_3$ expression in neoplastic tissue compared with normal epithelium (43).

Consistent with the previous results observed in PC3 cells, treatment of A431 cells overexpressing 12-LOX with neutralizing antibody to $\alpha_v\beta_5$ resulted in significant apoptosis and dramatically reduced survival of these cells under serum-starved conditions. Neutralizing antibodies to other integrins did not affect the survival of the 12-LOX-transfected cells. Interestingly, an antibody to $\alpha_5\beta_1$, which was abundantly expressed on A431 cells, also did not reduce the survival of pCMV-12-LOX A431 cells, although this receptor has frequently been implicated in the survival of many other cell types (19, 44–46). It is possible that $\alpha_5\beta_1$ mediates basal cell adhesion instead of providing a survival signal in that cell system. In either case, the fact that overexpression of platelet-type 12-LOX in two tumor cell lines of different histological origin results in enhanced expression of the same integrin implies a general phenomenon of 12-LOX regulating a specific subset of integrins. Integrins $\alpha_v\beta_3$ and $\alpha_v\beta_5$ have been shown to regulate cell migration; however, unlike $\alpha_v\beta_3$, $\alpha_v\beta_5$-mediated cell spreading and migration require activation of protein kinase C (46).

The stable end product of platelet-type 12-LOX metabolism, 12(*S*)-HETE, is a well-established protein kinase C activator (47) and, more importantly, has been shown to increase the surface expression of $\alpha_v\beta_3$ integrin on CD clone 3 endothelial cells (28). Interestingly, we have demonstrated previously (48) that 12(*S*)-HETE extended the survival of rat Walker W256 cells cultured in the absence of serum. In this study, we confirmed the effects of 12-LOX overexpression in both cell lines by treating wild-type PC3 or A431 cells with 12(*S*)-HETE to examine whether this provided a survival advantage in both cell lines. As expected, treatment with 12(*S*)-HETE, and not other LOX metabolites, *i.e.*, 5(*S*)-HETE, 15(*S*)-HETE, or 13(*S*)-HODE, resulted in significantly more viable cells compared with controls. In addition, 12(*S*)-HETE increased the surface expression of $\alpha_v\beta_5$ in wild-type cells, as illustrated by an integrin-mediated adhesion assay, an effect that was not observed when cells were treated with the other LOX metabolites. Also, treatment of PC3 or A431 cells overexpressing platelet-type 12-LOX with inhibitors of 12-LOX (Baicalein or BHPP) resulted in a significant reduction in the survival of either cell line, whereas the selective 5-LOX inhibitor Rev-5901 had no effect. We have demonstrated previously (10) that inhibition of 12-LOX with either of these structurally different inhibitors induces cell cycle arrest and apoptosis in two prostate cancer cell lines. Our results suggest that a more general phenomenon may be observed because survival and apoptosis of an epidermal tumor cell line, A431, was also regulated by 12-LOX and its end product, 12(*S*)-HETE.

In summary, these results demonstrate that the 12-LOX pathway of AA metabolism is a critical regulator of cell survival and apoptosis in both prostate PC3 and epidermal A431 tumor cell lines. Enforced expression of this enzyme specifically increased the expression and membrane localization of $\alpha_v\beta_3$ and $\alpha_v\beta_5$ integrin in PC3 cells and $\alpha_v\beta_5$ in A431 cells. Enhanced expression of these integrins was shown to confer a survival advantage on these cells, delaying apoptosis as a result of serum deprivation. Therefore, the inhibition of 12-LOX is a potential therapeutic approach in the treatment of met-

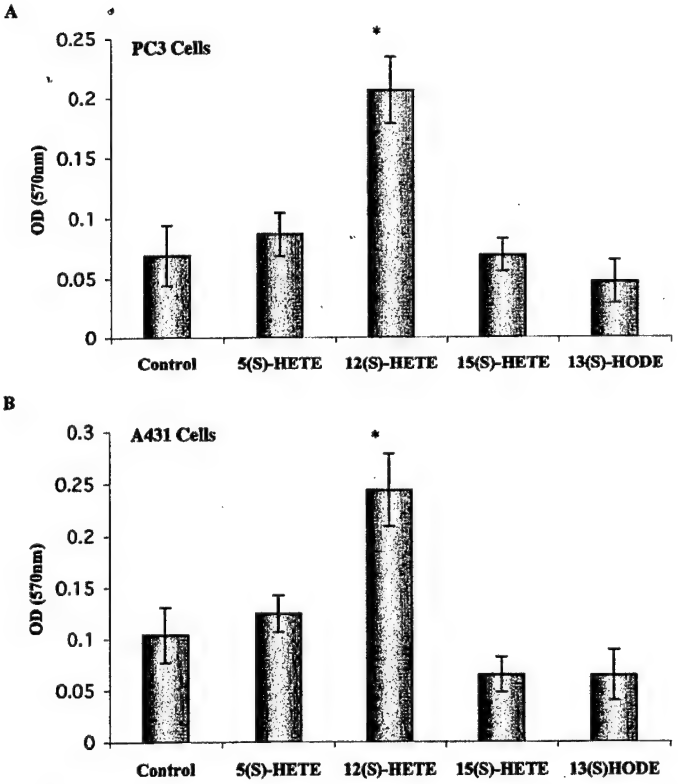

Fig. 9. 12(*S*)-HETE increases the $\alpha_v\beta_5$-mediated adhesion of wild-type PC3 (*A*) or A431 (*B*) cells. Wild-type cells were treated with 100 nM 5(*S*)-HETE, 12(*S*)-HETE, 15(*S*)-HETE, or 13(*S*)-HODE for 24 h (at 12-h intervals). Adhesion via $\alpha_v\beta_5$ was assessed by means of a commercial adhesion assay ("Materials and Methods"), and results were expressed as absorbance. Treatment with 12(*S*)-HETE significantly increased the adhesion of either PC3 or A431 cells to the plates, whereas other treatments did not. *, $P < 0.05$.

astatic disease. It is likely that treatments aimed at inhibiting 12-LOX activity should improve the efficacy of conventional treatments aimed at inducing tumor cell apoptosis, such as chemotherapy and/or radiation therapy.

ACKNOWLEDGMENTS

We are grateful to Dr. Dotai Nie, Dr. Khrisna Rao Maddipati, Dr. Mohit Trikha, and Alex Zacharek for expert technical assistance and helpful discussion.

REFERENCES

1. Funk, C. D. Molecular biology in the eicosanoid field. Prog. Nucleic Acid Res. Mol. Biol., *45:* 67–98, 1993.
2. Funk, C. D., Furci, L., and Fitzgerald, G. A. Molecular cloning, primary structure, and expression of the human platelet/erythroleukemia cell 12-lipoxygenase. Proc. Natl. Acad. Sci. USA, *87:* 5638–5642, 1990.
3. Yoshimoto, T., Suzuki, H., Yamamoto, S., Takai, T., Yokoyama, C., and Tanabe, T. Cloning and sequence analysis of the cDNA for arachidonate 12-lipoxygenase of porcine leukocytes. Proc. Natl. Acad. Sci. USA, *87:* 2142–2146, 1990.
4. Natarajan, R., Esworthy, R., Bai, W., Gu, J. L., Wilczynski, S., and Nadler, J. L. Increase 12-lipoxygenase expression in breast cancer cells and tissues. Regulation by epidermal growth factor. J. Clin. Endocrinol. Metab., *82:* 1790–1798, 1997.
5. Kamitani, H., Geller, M., and Eling, T. The possible involvement of 15-lipoxygenase/leukocyte type 12-lipoxygenase in colorectal carcinogenesis. Adv. Exp. Med. Biol., *469:* 593–598, 1991.
6. Nie, D., Hillman, G. G., Geddes, T., Tang, K., Pierson, C., Grignon, D. J., and Honn, K. V. Platelet-type 12-lipoxygenase in a human prostate carcinoma stimulates angiogenesis and tumor growth. Cancer Res., *58:* 4047–4051, 1998.
7. Timar, J., Rasa, E., Honn, K. V., and Hagmann, W. 12-Lipoxygenase expression in human melanoma cell lines. Adv. Exp. Med. Biol., *469:* 617–622, 1999.
8. Ding, X. Z., Kuszynski, C. A., El-Metwally, T. H., and Adrian, T. E. Lipoxygenase inhibition induced apoptosis, morphological changes, and carbonic anhydrase expression in human pancreatic cancer cells. Biochem. Biophys. Res. Commun., *266:* 392–399, 1999.
9. Nappez, C., Liagre, B., and Beneytout, J. L. Changes in lipoxygenase activities in human erythroleukemia (HEL) cells during diosgenin-induced differentiation. Cancer Lett., *96:* 133–140, 1995.
10. Pidgeon, G. P., Kandouz, M., Meram, A., and Honn, K. V. Mechanisms controlling cell cycle arrest and induction of apoptosis after 12-lipoxygenase inhibition in prostate cancer cells. Cancer Res., *62:* 2721–2727, 2002.
11. Woodhouse, E. C., Chuaqui, R. F., and Liotta, L. A. General mechanism of metastasis. Cancer (Phila.), *80:* 1529–1537, 1997.
12. Giancotti, F. G., and Ruoslahti, E. Integrin signalling. Science (Wash. DC), *285:* 1028–1032, 1999.
13. Bissell, M. J., Weaver, V. M., Lelievre, S. A., Wang, F., Petersen, O. W., and Schmeicel, K. L. Tissue structure, nuclear organization, and gene expression in normal and malignant breast. Cancer Res., *59* (Suppl.)*:* 1757s–1763s, discussion 1763s–1764s, 1999.
14. Clarke, E. A., and Brugge, J. S. Integrins and signal transduction pathways: the road taken. Science (Wash. DC), *268:* 233–239, 1995.
15. Howe, A., Aplin, A. E., Alahari, S. K., and Juliano, R. L. Integrin signaling and cell growth control. Curr. Opin. Cell Biol., *10:* 220–231, 1998.
16. Gilmore, A. P., and Burridge, K. Molecular mechanisms for focal adhesion assembly through regulation of protein-protein interactions. Structure, *4:* 647–651, 1996.
17. Felsenfeld, D. P., Choquet, D., and Sheetz, M. P. Ligand binding regulates the directed movement of β_1 integrins on fibroblasts. Nature (Lond.), *383:* 438–440, 1996.
18. Sheetz, M. P., Felsenfeld, D. P., and Galbraith, C. G. Cell migration: regulation of force on extracellular-matrix-integrin complexes. Trends Cell Biol., *8:* 51–54, 1998.
19. Noti, J. D., and Johnson, A. K. Integrin $\alpha_5\beta_1$ suppresses apoptosis triggered by serum starvation but not phorbol ester in MCF-7 breast cancer cells that overexpress protein kinase C-α. Int. J. Oncol., *18:* 195–201, 2001.
20. Erdreich-Epstein, A., Shimada, H., Groshen, S., Liu, M., Metelitsa, L. S., Kim, K. S., Stins, M. F., Seeger, R. C., and Durden, D. L. Integrins $\alpha_v\beta_3$ and $\alpha_v\beta_5$ are expressed by endothelium of high risk neuroblastoma, and their inhibition is associated with increased endogenous ceramide. Cancer Res., *60:* 712–721, 2000.
21. Brassard, D. L., Maxwell, E., Malkowski, M., Nagabhushan, T. L., Kumar, C. C., and Armstrong, L. Integrin $\alpha_v\beta_3$-mediated activation of apoptosis. Exp. Cell Res., *251:* 33–45, 1999.
22. Khwaja, A., Rodriguez-Viciana, P., Wennstrom, S., Warne, P. H., and Downward, J. Matrix adhesion and Ras transformation both activate a phosphoinositide 3-OH kinase and protein kinase B/Akt cellular survival pathway. EMBO J., *16:* 2783–2793, 1997.
23. Wu, C., Keightley, S. Y., Leung-Hagesteijn, C., Radeva, G., Coppolino, M., Goicoechea, S., McDonald, J. A., and Dedhar, S. Integrin-linked protein kinase regulates fibronectin matrix assembly, E-cadherin expression, and tumorigenicity. J. Biol. Chem., *273:* 528–536, 1998.
24. Uhm, J. H., Dooley, N. P., Kyritsis, A. P., Rao, J. S., and Gladson, C. L. Vitronectin, a glioma-derived extracellular matrix protein, protects tumor cells from apoptotic death. Clin. Cancer Res., *5:* 1587–1594, 1999.
25. Pouliot, N., Connolly, L. M., Moritz, R. L., Simpson, R. J., and Burgess, A. W. Colon cancer cells adhesion and spreading on autocrine laminin-10 is mediated by multiple integrin receptors and modulated by EGF receptor stimulation. Exp. Cell Res., *261:* 360–371, 2000.
26. Domingüez-Jimenez, C., Diaz-Gonzalez, F., Gonzalez-Alvaro, I., Cesar, J. M., and Sanchez-Madrid, F. Prevention of $\alpha_{II(b)}\beta_3$ activation by non-steroidal anti-inflammatory drugs. FEBS Lett., *446:* 318–322, 1999.
27. Dormond, O., Foletti, A., Paroz, C., and Ruegg, C. NSAIDs inhibit $\alpha_V\beta_3$ integrin-mediated and Cdc42/Rac-dependent endothelial-cell spreading, migration and angiogenesis. Nat. Med., *7:* 1041–1047, 2000.
28. Tang, D. T., Grossi, I. M., Chen, Y. Q., Diglio, C. A., and Honn, K. V. 12(*S*)-HETE promotes tumor-cell adhesion by increasing surface expression of $\alpha_v\beta_3$ integrins on endothelial cells. Int. J. Cancer, *54:* 102–111, 1993.
29. Raso, E., Tovari, J., Toth, K., Paku, S., Trikha, M., Honn, K. V., and Timar, J. Ectopic $\alpha_{IIb}\beta_3$ integrin signaling involves 12-lipoxygenase- and PKC-mediated serine phosphorylation events in melanoma cells. Thromb. Haemostasis, *85:* 1037–1042, 2001.
30. Patricia, M. K., Kim, J. A., Harper, C. M., Shih, P. T., Berliner, J. A., Natarajan, R., Nadler, J. L., and Hedrick, C. C. Lipoxygenase products increase monocyte adhesion to human aortic endothelial cells. Arterioscler. Thromb. Vasc. Biol., *19:* 2615–2622, 1999.
31. Tang, K., Finley, R. L., Jr., Nie, D., and Honn, K. V. Identification of 12-lipoxygenase interaction with cellular proteins by yeast two-hybrid screening. Biochemistry, *39:* 3185–3191, 2000.
32. Tang, D. G., Chen, Y. Q., and Honn, K. V. Arachidonate lipoxygenases as essential regulators of cell survival and apoptosis. Proc. Natl. Acad. Sci. USA, *93:* 5241–5246, 1996.
33. Rice, R. L., Tang, D. G., Haddad, M., Honn, K. V., and Taylor, J. D. 12(*S*)-Hydroxyeicosatetraenoic acid increases the actin microfilament content in B16a melanoma cells: a protein kinase-dependent process. Int. J. Cancer, *77:* 271–278, 1998.
34. Timar, J., Raso, E., Dome, B., Li, L., Grignon, D., Nie, D., Honn, K. V., and Hagmann, W. Expression, subcellular localization and putative function of platelet-type 12-lipoxygenase in human prostate cancer cell lines of different metastatic potential. Int. J. Cancer, *87:* 37–43, 2000.
35. Ruoslahti, E. Stretching is good for a cell. Science (Wash. DC), *276:* 1345–1346, 1997.
36. Scatena, M., and Giachelli, C. The $\alpha_v\beta_3$ integrin, NF-κB, osteoprotegerin endothelial cell survival pathway. Potential role in angiogenesis. Trends Cardiovasc. Med., *12:* 83–88, 2002.

37. Petitclerc, E., Stromblad, S., von Schalscha, T. L., Mitjans, F., Piulats, J., Montgomery, A. M., Cheresh, D. A., and Brooks, P. C. Integrin $\alpha_v\beta_3$ promotes M21 melanoma growth in human skin by regulating rumor cell survival. Cancer Res., *59:* 2724–2730, 1999.
38. Vacca, A., Ria, R., Presta, M., Ribatti, D., Iurlaro, M., Merchionne, F., Tanghetti, E., and Dammacco, F. $\alpha_v\beta_3$ Integrin engagement modulates cell adhesion, proliferation, and protease secretion in human lymphoid tumor cells. Exp. Hematol., *8:* 993–1003, 2001.
39. Smida Rezgui, S., Honore, S., Rognoni, J. B., Martin, P. M., and Penel, C. Up-regulation of $\alpha_2\beta_1$ integrin cell-surface expression protects A431 cells from epidermal growth factor-induced apoptosis. Int. J. Cancer, *87:* 360–367, 2000.
40. Freyer, A. M., Johnson, S. R., and Hall, I. P. Effects of growth factors and extracellular matrix on survival of human airway smooth muscle cells. Am. J. Respir. Cell Mol. Biol., *25:* 569–576, 2001.
41. Le Bellego, F., Pisselet, C., Huet, C., Monget, P., and Monniaux, D. Laminin-$\alpha_6\beta_1$ integrin interaction enhances survival and proliferation and modulates steroidogenesis of ovine granulosa cells. J. Endocrinol., *172:* 45–59, 2002.
42. O'Brien, V., Frisch, S. M., and Juliano, R. L. Expression of the integrin α_5 subunit, in HT29 colon carcinoma cells, suppresses apoptosis triggered by serum deprivation. Exp. Cell Res., *224:* 208–213, 1996.
43. Pignatelli, M., Cardillo, M. R., Hanby, A., and Stamp, G. W. Integrins and their accessory adhesion molecules in mammary carcinomas: loss of polarization in poorly differentiated tumors. Hum. Pathol., *23:* 1159–1166, 1992.
44. Hoyt, D. G., Rusnak, J. M., Mannix, R. J., Modzelewski, R. A., Johnson, C. S., and Lazo, J. S. Integrin activation suppresses etoposide-induced DNA strand breakage in cultured murine tumor-derived endothelial cells. Cancer Res., *56:* 4146–4149, 1996.
45. Zhang, Z., Vuori, K., Reed, J. C., and Ruoslahti, E. The $\alpha_5\beta_1$ integrin supports survival of cells on fibronectin and up-regulates Bcl-2 expression. Proc. Natl. Acad. Sci. USA, *92:* 6161–6165, 1995.
46. Lewis, J. M., Cheresh, D. A., and Schwartz, M. Z. Protein kinase C regulates $\alpha_v\beta_5$-dependent cytoskeletal associations and focal adhesion kinase phosphorylation. J. Cell Biol., *134:* 1323–1332, 1994.
47. Tang, D. G., Clement, A. D., Bazaz, R., and Honn, K. V. Transcriptional activation of endothelial cell integrin α_v by protein kinase C activator 12(*S*)-HETE. J. Cell Sci., *108:* 2629–2644, 1995.
48. Tang, D. G., and Honn, K. V. Apoptosis of W256 carcinosarcoma cells of the monocytoid origin induced by NDGA involves lipid peroxidation and deletion of GSH: role of 12-lipoxygenase in regulating tumor cell survival. J. Cell. Physiol., *172:* 155–170, 1997.

Int. J. Cancer: **105,** 459–471 (2003)

Publication of the International Union Against Cancer

OVEREXPRESSION OF LEUKOCYTE-TYPE 12-LIPOXYGENASE PROMOTES W256 TUMOR CELL SURVIVAL BY ENHANCING αvβ5 EXPRESSION

Graham P. PIDGEON[1], Keqin TANG[1], Renee L. RICE[3], Alex ZACHAREK[1], Li LI[5], John D. TAYLOR[3,4] and Kenneth V. HONN[1,2,4]*

[1]*Department of Radiation Oncology, Wayne State University, Detroit, MI, USA*
[2]*Department of Pathology, Wayne State University, Detroit, MI, USA*
[3]*Department of Biological Sciences, Wayne State University, Detroit, MI, USA*
[4]*Karmanos Cancer Institute, Detroit, MI, USA*
[5]*Biomide Corporation, Grosse Pointe Farms, MI, USA*

The metabolism of arachidonic acid (AA) leads to the generation of biologically active metabolites that have been implicated in cell growth and proliferation, as well as survival and apoptosis. We have previously demonstrated that rat Walker 256 (W256) carcinosarcoma cells express the platelet-type 12-lipoxygenase (12-LOX) and synthesize 12(S)- and 15(S)-HETE as their major LOX metabolites. Here we show that Walker 256 cells also express leukocyte-type 12-LOX and that its overexpression in these cells significantly extends their survival and delays apoptosis when cells are cultured under serum-free conditions. Under serum-free conditions, the expression of leukocyte-type 12-LOX is upregulated. 12-LOX-transfected W256 cells had a more spread morphology in culture compared with wild-type or mock-transfected cells. Examination of W256 cells showed that the cells expressed a number of integrins on their surface. Overexpression of 12-LOX enhanced the surface expression and focal adhesion localization of integrin αvβ5, while not affecting other integrins. Also, the 12-LOX-transfected W256 cells exhibited higher levels of microfilament content. Treatment of cells with monoclonal antibody to αvβ5 or cytochalasin B (a microfilament-disrupting agent), but not antibodies to other integrin receptors, resulted in significant apoptosis, characterized by rapid rounding up and detachment from the substratum. These results show that the 12-LOX pathway is a regulator of cell survival and apoptosis, by affecting the expression and localization of the αvβ5 integrin and actin microfilaments in Walker 256 cells.

Key words: *lipoxygenase; apoptosis; integrin; adhesion; Walker carcinoma*

Lipoxygenases constitute a family of lipid-peroxidizing enzymes that metabolize arachidonic acid (AA) to biologically active metabolites, including hydroxyeicosatetraenoic acids (HETEs).[1] 12-Lipoxygenase (12-LOX) is 1 of at least 3 lipoxygenases that is expressed as 2 main isoforms, a platelet-type cloned from human platelets[2] and a leukocyte-type from porcine leukocytes, which shares 65% homology with the platelet-type cDNA.[3] Several lines of evidence implicate platelet-type 12-LOX as a regulator of human cancer development. It is overexpressed in a variety of tumors including breast,[4] colorectal[5] and prostate cancer[6] and has been shown to be present in a number of cancer cell lines.[7–9] In addition, we have previously described the involvement of 12-LOX in tumor metastasis, as pretreatment of prostate cancer cells *in vitro* with inhibitors to 12-LOX blocked their ability to form lung colonies after tail-vein injection,[10] whereas overexpression of 12-LOX increased angiogenesis and metastatic growth in mice.[6] However, whether these observations are specific to the platelet form of the enzyme or constitute a more general phenomenon is unknown.

The ability of tumors to invade beyond hemostatic boundaries and form metastatic colonies requires the complex interplay of various cell surface-associated components regulating the proteolytic disruption of the extracellular matrix (ECM) and the modification of cell adhesion properties.[11] These cell-ECM interactions are mediated by integrins, a family of adhesive receptors that mediate the attachment of the cell to both structural and matrix-immobilized proteins to promote cell survival, proliferation and migration.[12,13] Integrins perform a well-documented function in cellular invasion and metastasis.[14,15] Nonligated integrins are generally spread diffusely over the cell surface with no apparent linkage to the actin cytoskeleton. However, when ligated, integrins frequently cluster into specialized structures called focal adhesion complexes (FACs), thereby providing a convergence site for multiple signaling components,[15,16] while physically linking the receptors to the actin filaments.[17,18] Ligand binding to integrins triggers a number of signaling pathways, some of which are primarily related to cell adhesion, whereas others are providing survival signals to cells. For example, prevention of cell adhesion to the ECM will trigger apoptosis in various cells, in particular epithelial cells,[19–21] suggesting that integrin-mediated cell adhesion relays important survival signals to the cells. Conversely, attachment or adhesion to the basement membrane or individual ECM components has been shown to promote cell differentiation and extend cell survival under various experimental conditions.[22–25]

Previous studies have indicated a role for arachidonic acid metabolism in cell-matrix interactions and integrin signaling. For example, inhibition of cyclooxgenase-2 (COX-2), by nonsteroidal antiinflammatory drugs (NSAIDs), blocks both platelet aggregation by suppressing activation of integrin αIIβ3[26] and endothelial cell migration by suppressing activation of αvβ3 integrin.[27] Other studies have reported the role of lipoxygenases, in particular 12-LOX, in the regulation of surface integrin expression. For example, adhesion of B16 murine melanoma cells to microvascular endothelial cells was enhanced by pretreatment of the endothelial cells with the 12-LOX product 12(S)-HETE, via upregulation of αvβ3 integrin expression.[28] In the same cell line, ligation of αIIbβ3 integrin induced 12(S)-HETE production,[29] implying co-regulation of integrin expression and lipoxygenase activity in these cells. Similarly, 12(S)-HETE treatment of human endothelial cells enhanced monocyte adhesion through increased very late-acting antigen-4 (VLA-4) integrin expression.[30] Indeed, recently we have reported the interaction of platelet-type 12-LOX with a number of cellular proteins, including the integrin β4 subunit, determined by yeast 2-hybrid screening.[31] The above observations establish a

Grant sponsor: the National Institutes of Health; Grant number: CA-29997; Grant sponsor: Biomide Corporation; Grant sponsor: the Cancer Research Foundation of America.

*Correspondence to: Department of Radiation Oncology, Wayne State University, 431 Chemistry Building, Detroit, MI 48202, USA. Fax: +313-5770798. E-mail: k.v.honn@wayne.edu

Received 16 May 2002; Revised 20 January 2003; Accepted 27 January 2003

DOI 10.1002/ijc.11134
Published online 25 March 2003 in Wiley InterScience (www.interscience.wiley.com).

potential relationship between lipid-regulated adhesive functions and cellular responses to apoptosis induction.

Here we examine the effect of leukocyte-type 12-LOX in W256 tumor cell survival. The results show that W256 cells express leukocyte-type 12-LOX and that its overexpression enhances the surface expression as well as the focal adhesion localization of integrin receptor αvβ5. Also, 12-LOX-overexpressing W256 cells exhibit higher levels of microfilament content. Together, these alterations, through a calphostin-C-sensitive mechanism, led to a more spread morphology of the cells and extended their survival in the absence of serum.

MATERIAL AND METHODS

Examination of W256 cells expressing leukocyte-type 12-lipoxygenase by RT-PCR and sequencing

Total RNA was isolated from W256 cells and using the 3′ Race Kit from Gibco (Rockville, MD) according to the manufacturer's instructions. cDNA was prepared by standard reverse transcription using 2 and 4 μg RNA per reaction. Then, using 2 μl of the resulting cDNA a PCR reaction was performed using the following primers: ML-12LOX 5 (TTTGACAAGGTGATGAGCACA) and ML-12LOX 6 (ACTGATTAGGATTGGGCAGCG) at 0.25 μg/reaction. The PCR conditions were as follows: 94°C for 5 min and then 94°C for 45 sec, 56°C for 1 min, 72°C for 1.5 min ×35 cycles, followed by extension at 72°C for 5 min. After these first 35 cycles, we took 1 μl of this reaction and used it as the template for an additional 35 cycles using the same PCR program. The resulting samples were run on a 2% agarose gel, the band was excised and DNA was isolated using a Quiagen (Chatsworth, CA) Gel Extraction Kit. The resulting DNA was then sent for sequencing to the Wayne State University Biological Science core facility.

Transfection of W256 cells overexpressing the leukocyte-type 12-LOX

Approximately 1×10^6 W256 cells were cultured in MEM supplemented with 10% FBS (Life Technologies, Bethesda, MD). Cells were cotransfected with either 4 μg of PEG-purified pCMV-12-LOX [pcDNA-MS/L, driven by a CMV promotor (mouse leukocyte 12-LOX expression vector), kindly provided by Dr. C. Funk, University of Pennsylvania, Philadelphia, PA][32] and 2 μg of pCMV-neo, or control vector (pCMV-neo) alone in serum-free media (Opti-MEM, Gibco) containing 10 μg/ml Lipofectin (Life Technologies). After 4 hr, the transfection medium was removed and the flasks were replenished with MEM containing 10% FBS for an additional 48 hr. Subsequently, 800 μg/ml G418 (Life Technologies) was added and individual resistant cells were selected and propagated with the limiting dilution method in 96-well culture plates. The resistant clones were then cultured in MEM with 10% FBS supplemented with 400 μg/ml G418.

Characterization of W256 cells overexpressing the leukocyte-type 12-LOX

Clones overexpressing 12-LOX were characterized by Western blotting, flow cytometry and immunofluorescent microscopy, using a previously characterized rabbit polyclonal anti-leukocyte-type 12-LOX antibody (Cayman, Ann Arbor, MI).[33] The Western blot protocol was previously described in detail.[34] In brief, total cell lysates were prepared and 30 μg was fractionated on precast SDS-polyacrylamide gels and transferred to nitrocellulose membranes. Purified leukocyte-type 12-LOX was generously provided by Dr. C. Funk (University of Pennsylvania) and was used as a positive control. After incubation for 1 hr in blocking buffer containing 5% skimmed milk dissolved in 10 mM Tris-HCl, pH 7.5, 100 mM NaCl and 0.1% Tween-20, blots were probed overnight with 1:1,000 dilution of the rabbit anti-12-LOX (murine leukocyte) polyclonal antibody. The membrane was then washed (3×) in Tris-buffered saline containing 0.05% Tween 20 (TBST) and incubated for 1 hr with horseradish peroxidase-conjugated goat anti-rabbit IgG (Bio-Rad, Hercules, CA; 1:1,500 in TBST). Bound antibody complexes were visualized using enhanced chemiluminescence (Pierce, Rockford, IL).

For immunofluorescent labeling of 12-LOX, cells were fixed with 3.7% paraformaldehyde in PBS (pH 7.4) and then permeabilized using 20 mM HEPES, 300 mM sucrose, 50 μM NaCl, 3 mM $CaCl_2$ and 0.5% Triton X-100 for 10 min. Cells were blocked with 20% normal goat serum (Sigma, St. Louis, MO) at 37°C for 30 min and then incubated with 1:500 dilution of rabbit anti-leukocyte type 12-LOX polyclonal antibody and subsequently with fluorescein isothiocyanate (FITC)-conjugated goat anti-mouse IgG (1:1,000) for 45 min at 37°C. The cells were washed with PBS and then mounted in Citifluor (Amersham Pharmacia Biotech, Piscataway, NJ) on glass slides.

For flow cytometry, W256 cells (2×10^6) were fixed in 3.7% paraformaldehyde in PBS (pH 7.4) for 15 min, washed with PBS (3×), permeabilized in PBS containing 0.1% Triton X-100 and blocked in 20% normal goat serum/PBS for 30 min at 37°C. Cells were then incubated with the rabbit anti-leukocyte-type 12-LOX polyclonal (1:1,000) antibody for 2 hr. Cells were washed (2×) and incubated with FITC-conjugated goat anti-rabbit IgG (1:2,000) for 30 min at 37°C in the dark. Cells were washed with PBS (2×) and measured on an Epics II flow cytometer (Coulter, Hialeah, FL) for fluorescence intensity. The data were analyzed using the mean log fluorescence, as previously described.[35]

Examination of cell survival and apoptosis after LOX inhibition or serum withdrawal

Cells were cultured in serum-free MEM with 0.1% FBS over time (0–7 days) to induce apoptosis. The expression of leukocyte-type 12-LOX was examined by Western blotting as previously described after serum starvation for 0–4 days. Assessment of cell survival and quantification of apoptosis were carried out using trypan blue dye exclusion assays, the Cell Titre MTS cell proliferation kit (Promega, Madison, WI) according to the manufacturer's instructions, or DAPI staining as previously described.[36]

Examination of integrin expression by immunofluorescence

Cells were plated on glass coverslips and subsequent immunofluorescent labeling of actin and αvβ5 surface integrin was performed essentially as described previously. For labeling of αvβ5 integrin, cells were fixed, permeabilized and blocked as described above. Cells were then incubated with monoclonal anti-αvβ5 (0.1 μg/ml) and subsequently with FITC-conjugated goat anti-mouse IgG (1:1,000) for 45 min at 37°C.

For labeling of actin, cells were fixed and permeabilized with ice-cold methanol: acetone (1:1) at −20°C for 10 min followed by washing 3× in Ca^{2+}/Mg^{2+}-free PBS (pH 7.4). Then the coverslips were incubated with rhodamine-phalloidin (1:200 in PBS, 30 min; Molecular Probes, Eugene, OR) at room temperature. In each case the cells were washed with PBS and then mounted in Citifluor (Amersham Pharmacia Biotech) on glass slides.

Flow cytometric analysis of adhesion molecule expression and cell cycle analysis

Flow cytometry was performed for the analysis of integrin receptors as previously described.[34] Briefly, cultured W256 cells (1×10^6) were dissociated with 0.2 mM EDTA, washed with PBS and then fixed in 3.7% paraformaldehyde in PBS (pH 7.4). Cells were then incubated in 20% normal goat serum to block nonspecific binding. Subsequently, cells were incubated with primary antibodies [0.1 μg/ml mouse monoclonal antibody to α2β1, β3, αvβ5, αIIbβ3 (Chemicon, Temecula, CA), β1, α4, αv (Invitrogen, Carlsbad, CA), and P-selectin (Santa Cruz Biotechnology, Santa Cruz, CA) or 1.0 μg/ml polyclonal antibody to α5β1 and αvβ3 (Invitrogen, Carlsbad, CA)] followed by 1:1,000 dilution of FITC-labeled secondary antibodies (Invitrogen). Finally, cell surface fluorescence for individual integrin receptors was analyzed on an Epics Profile II flow cytometer.

For cell cycle analysis, W256 cells were prepared as detailed previously.36+ Briefly, cells were fixed in ice-cold 70% ethanol/PBS for 20 min, rinsed in PBS containing 0.1% Triton X-100, 0.1

M EDTA and washed 3× with PBS (pH 7.4). Subsequently cells were incubated in staining buffer (50 μg/ml propidium iodide, 200 μg/ml RNase, 0.1 M EDTA, 0.1% Triton X-100) at 37°C in the dark for 30 min followed by direct analysis on the flow cytometer.

Antibody blocking studies

To establish a functional role for individual integrin receptors in 12-LOX-mediated apoptosis resistance, pCMV-12-LOX W256 cells were serum starved in the presence of various antibodies to integrin receptors (outlined in the last section). Cell survival 72 hr after serum starvation was evaluated by MTS assay. Morphological alterations were also examined using a phase contrast microscope.

Effect of cytochalasin B on W256 cell survival

W256 monolayers were subjected to serum withdrawal in the presence of various doses of cytochalasin B (1–10 μM, 15 min, 37°C) to disrupt the actin microfilaments. The effects of these agents were assessed by examining the morphology of cells. Survival was determined by the MTS assay.

Statistical analysis

Statistical comparison between study groups was carried out using ANOVA with Scheffé post hoc correction in DataDesk 4.1. Results are expressed as mean ± SD. Data were taken as significant where $p < 0.05$.

RESULTS

Examination of W256 cells expressing leukocyte-type 12-LOX

Expression of the leukocyte-type 12-LOX in W256 cells was shown using RT-PCR and subsequent sequencing of DNA products. Using specific primers for mouse leukocyte-type 12-LOX (ML-12LOX 5/6), the predicted 517 bp product was amplified when 4 μg DNA template was used (Fig. 1). This 517 bp fragment was excised from the gel and sequenced at the Wayne State University Biological Science core facility. The sequence results are as follows: 12-LOX PCR product produced with primers 5/6 and sequenced with ML-12LOX 5: GGGGGAGGCCCCTGGATCTTCTCAGCAAGCTGGAGCCTTTCTGACCTATTGCTCATTGTGTCCCCCCGATGACTTGGCTGAGCGAGGACTCTTGGATATCGAGACTTGCTTCTATGCTAAAGACGCCCTGCGACTCTGGCAGATCATGAATCGGTACGTGGTGGGAATGTTCAATCTCCACTACAAGACCGACAAAGCTGTGCAAGACGACTATGAACTGCAGAGCTGGTGTCGAGAGATCACTGACATTGGTCTTCAAGGGGCCCAGGACAGAGGCTTCCCTACCTCTCTTCAGTCCCGGGCTCAGGCTTGCTACTTCATCACCATGTGCATCTTCACGTGCACCGCACAGCACTCTTCCGTCCATCTTGGCCAGCTGGATTGGTTCTACTGGGTTCCTAATGCACCCTGCACCATGCGGCTGCCACCACCCACCACCAAGGAAGCAACAATGGAGAAGCTGATGGCTACGCTGCCCATCCCTNAATCAGTAANNNNNN. 12-LOX PCR product produced with primers 5/6 and sequenced with ML-12LOX 6: TCCATNGCTTCTCNTTGTTGCTTCCTTGGTGGTGGGTGGTGGCAGCCGCATGGTGCAGGGTGCATTAGGAACCCAGTAGAACCAATCCAGCTGGCCAAGATGGACGGAAGAGTGCTGTGCGGTGCACGTGAAGATGCACATGGTGATGAAGTAGCAAGCCTGAGCCCGGGACTGAAGAGAGGTAGGGAAGCCTCTGTCCTGGGCCCCTTGAAGACCAATGTCAGTGATCTCTCGACACCAGCTCTGCAGTTCATAGTCGTCTTGCACAGCTTTGTCGGTCTTGTAGTGGAGATTGAACATTCCCACCACGTACCGATTCATGATCTGCCAGAGTCGCAGGGCGTCTTTAGCATAGAAGCAAGTCTCGATATCCAAGAGTCCTCGCTCANCCCAGTCATCCGGGGGGACACNATGAGCAATAGGTCCANAAAGGCTCCACNTTGCTTGANAANATCCAGGGNGCCTCCCCCCNCTGNGCNCCTCNCCCTTTNTTCNAAAAANNNNNN

The sequence of the PCR product was matched with rat leukocyte-type 12-LOX by BLAST search.

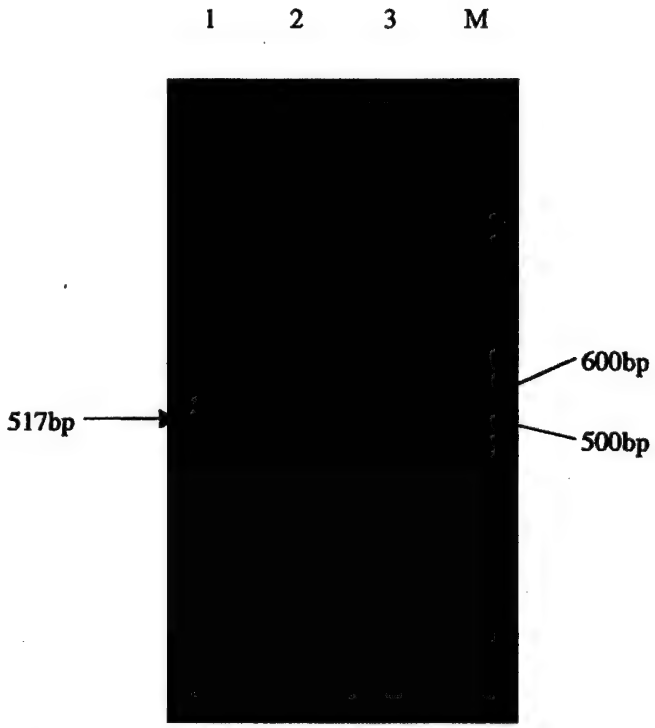

FIGURE 1 – Examination of leukocyte-type 12-lipoxygenase expression in W256 cells determined by RT-PCR and sequence analysis. Lane M, 200bp DNA marker; lane 1, 2 μg RNA; lane 2, 4 μg RNA; lane 3, without RNA control. The predicted 517 bp product was amplified when 4 μg DNA template was used and is indicated by the arrow. This product was excised from the gel, sequenced and matched with rat leukocyte-type 12-LOX by BLAST search.

Characterization of leukocyte-type 12-LOX overexpression in transfected W256 cells

Overexpression of the leukocyte-type 12-LOX in several clones of transfected cells, was confirmed using several different molecular approaches. Flow cytometric analysis revealed that pCMV-12LOX W256 cells had a significantly higher level of leukocyte-type 12-LOX (*i.e.*, enhanced fluorescence) compared with the wild-type and pCMV-neo W256 cells (Fig. 2*a–c*). These studies indicated an approximate 4–5-log-fold increase in pCMV-12LOX-transfected W256 cells compared with controls (Fig. 2*d*). To characterize further the overexpression of leukocyte-type 12-LOX, Western blotting experiments of W256 whole cell lysates were performed. As shown in Figure 2*e*, a prominent band migrating at approximately 72 kD was detected in wild-type W256 cells when they were probed with a rabbit polyclonal anti-12-LOX (leukocyte-type) antibody. This band was shown to be specific for leukocyte-type 12-LOX, as the positive control migrated at exactly the same size, demonstrating for the first time that W256 cells constitutively express the isozyme, leukocyte type 12-LOX. Transfection of W256 cells with the control empty vector (*i.e.*, pCMV-neo) did not significantly alter the expression levels of the leukocyte-type 12-LOX. In contrast, the pCMV-12LOX-transfected W256 cells, as expected, demonstrated higher levels of the protein, as quantified by densitometric scanning after normalizing to the actin protein levels (Fig. 2*e*). Immunofluorescence microscopic studies using the same antibody confirmed the flow cytometry and Western blot observations (data not shown).

W256 cells grown under serum-starved conditions upregulate leukocyte-type 12-LOX expression

Expression of leukocyte-type 12-LOX was increased after serum starvation for either 24 or 48 hr as indicated by Western blot

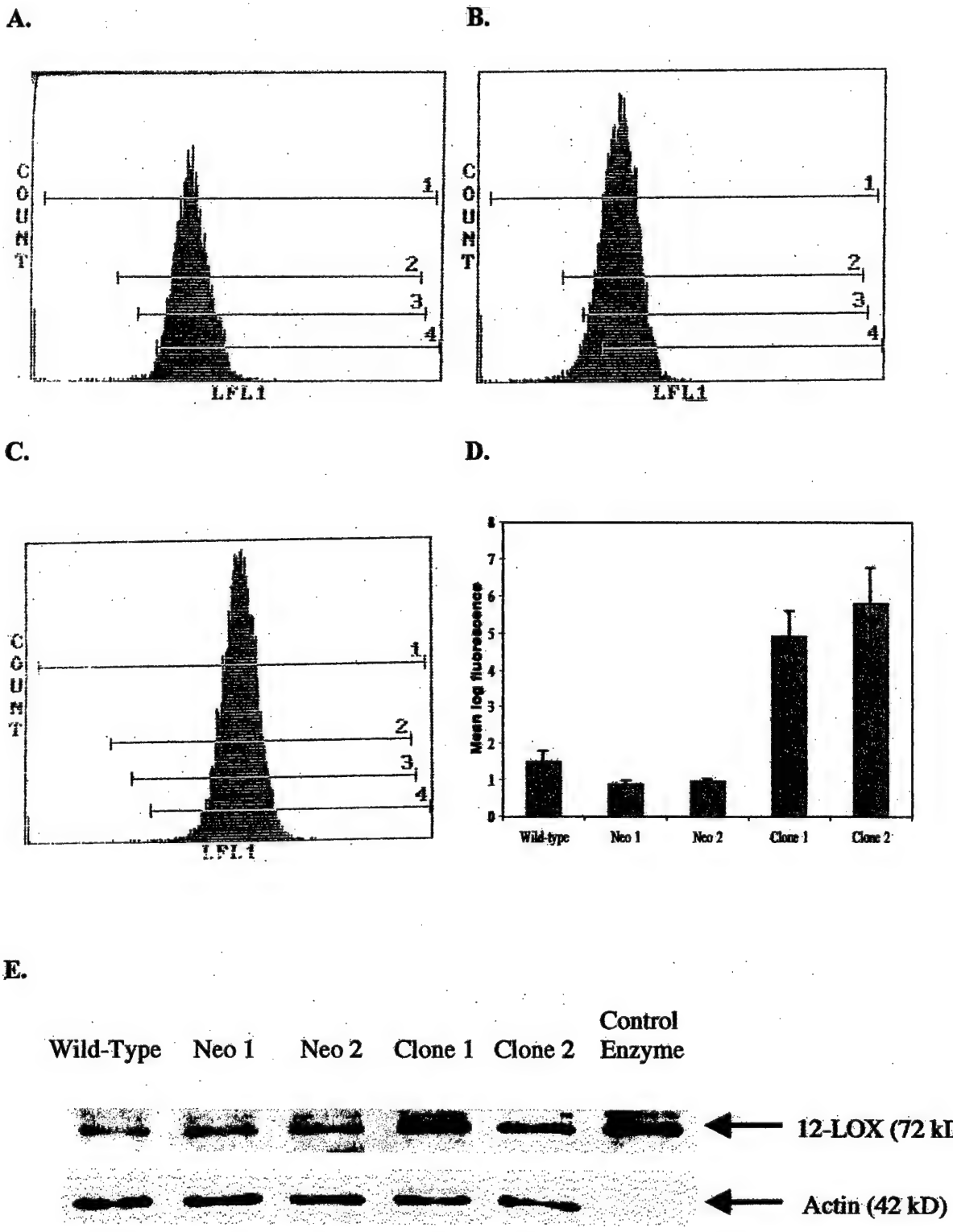

FIGURE 2 – Characterization of the overexpression of leukocyte-type 12-LOX in transfected W256 cells. (*a–c*) Histograms showing the fluorescence intensity of staining with polyclonal anti-leukocyte 12-LOX. (*a*) Wild-type W256 cells. (*b*) W256 cells transfected with empty vector (*i.e.*, pCMV-neo). (*c*) W256 cells transfected with the leukocyte-type 12-LOX pCMV (pCMV-12-LOX clone). (*d*) Quantification by flow cytometry of 12-LOX protein expression. Shown are the mean log fluorescence intensities derived from 2 independent measurements. (*e*) Western blotting of leukocyte-type 12-LOX using W256 whole cell lysates. The 72 kDa 12-LOX protein is indicated on the right with an arrow. The same blot was stripped and reprobed with a monoclonal anti-actin antibody to normalize the protein loading.

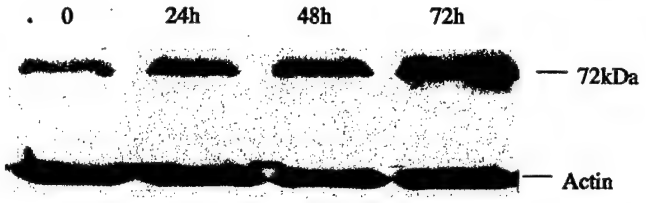

FIGURE 3 – Expression of leukocyte-type 12-LOX was increased after serum starvation for 24–72 hr. Whole cell lysates were prepared and leukocyte-type 12-LOX expression was examined by Western analysis. 12-LOX expression was upregulated relative to β-actin (lower panel).

(Fig. 3). No further increase in leukocyte-type 12-LOX expression was observed after prolonged serum depletion for 72 hr. These results show that there is an upregulation of native leukocyte-type 12-LOX after serum starvation in W256 cells, indicating a possible survival mechanism in these cells. We therefore examined the survival of W256 cells after transfection with leukocyte-type 12-LOX and their rate of apoptosis in response to serum depletion.

Overexpression of the leukocyte-type 12-LOX extends survival and delays apoptosis of W256 cells cultured in the absence of trophic factors (i.e., *serum)*

It has previously been shown that wild-type W256 cells exhibit serum dependence for their growth.[36] This observation was confirmed in the present study. Several independent experiments revealed that the survival of both wild-type and pCMV-neo W256 cells declined dramatically after 2 days of serum starvation (Fig. 4*a*). Interestingly, the mock transfectants (pCMV-neo) were slightly more sensitive to serum deprivation than wild-type W256 cells (Fig. 4*a*). Consistent with this observation, as early as 1 day post serum depletion, the mock transfected cells exhibited higher levels of apoptosis (Fig. 4*b*). In contrast, leukocyte-type 12-LOX overexpressing W256 cells (*i.e.*, clone 1 and clone 2 cells) demonstrated a significantly extended overall survivability ($p < 0.05$) compared with either the wild-type or mock transfected W256 cells. During the first 24 hr, the 12-LOX-overexpressing cells, like the wild-type and mock transfectants, demonstrated a decrease in cell viability (~25%; Fig. 4*a*). However, in contrast to the wild-type and pCMV-neo cells, 12-LOX clones did not demonstrate increased cell death in the subsequent 3 days post serum starvation, but rather exhibited a relatively constant rate of cell survival (Fig. 4*a*). Cell numbers began to decline at day 5, and by day 7 approximately 40% of cells were viable. By day 9, all the cells were dead (data not shown).

Consistent with these observations, apoptosis was significantly ($p < 0.05$) reduced in the 12-LOX overexpressing clones (Fig. 4*b*). Although wild-type and mock transfected W256 cells exhibited a rapid induction of apoptosis after serum withdrawal, the 12-LOX-transfected cells displayed a delayed apoptotic response. Quantitation of apoptotic nuclei in both wild-type and pCMV-neo W256 cells demonstrated that approximately 60% were apoptotic by day 2, 80% by day 3 and essentially 100% by day 4 post serum removal. In sharp contrast, pCMV-12-LOX clones exhibited only 20% apoptosis by day 2, 35% by day 3 and 45% by day 4 post serum withdrawal (Fig. 4*b*).

W256 cells overexpressing the leukocyte-type 12-LOX exhibit a more spread morphology

Light microscopy studies provided substantial evidence for extended survival of W256 cells overexpressing the leukocyte-type 12-LOX. As shown in Figure 5, wild-type (Fig. 5*a,b*) and pCMV-neo (Fig. 5*c,d*) W256 cells demonstrated significant cell death (*i.e.*, cell rounding with some exhibiting features reminiscent of apoptosis) 4 days after serum withdrawal (Fig. 5*b,d*). The 12-LOX-transfected W256 cells demonstrated a more spread morphology under normal culture conditions (Fig. 5*e*). There was only scattered cell death 4 days after removal of serum, with the majority of cells still spread and alive (Fig. 5*f*).

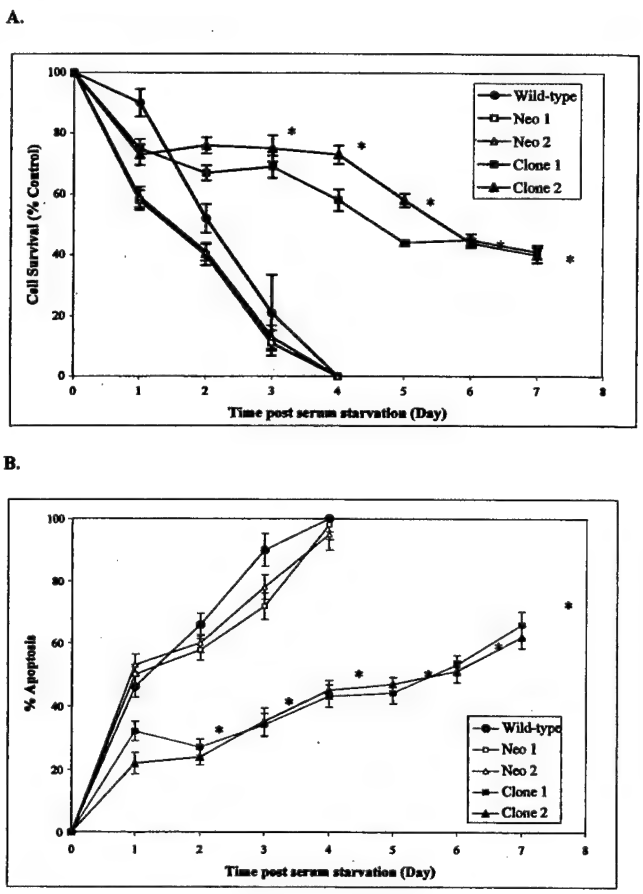

FIGURE 4 – Quantitation of the survival and apoptosis of various W256 cell sublines cultured under serum-starved conditions. (*a*) Survival was determined by MTS assay. The values are expressd as the % cell survival compared with day 0 (at which time the survival was considered to be 100%) and the bars represent standard error of the mean (SEM) derived from 3 independent experiments. pCMV-12-LOX transfected W256 cells survived significantly longer, under serum-starved conditions, compared with either wild-type or mock-transfected controls. *, $p < 0.05$. (*b*) 12-LOX-overexpressing cells demonstrated a delayed apoptotic response to serum starvation. Apoptosis was quantitated by DAPI staining in W256 cells serum-starved for 0–7 days. Apoptosis was also confirmed by microscopy and DNA fragmentation assays (data not shown). Significant apoptosis was observed after serum starvation in wild-type or mock transfectants, compared with pCMV-12-LOX clones. *, $p < 0.05$.

Expression of integrins in W256 carcinoma cells determined by flow cytometry

W256 cells overexpressing the leukocyte-type 12-LOX exhibited a more spread morphology under normal culture conditions compared with pCMV-neo and wild-type cells, remaining adherent and alive for up to day 5. These observations suggest that 12-LOX overexpression may extend cell survival by promoting cell adhesion to and spreading on the substrata [*i.e.*, extracellular matrix (ECM)]. Cell anchorage to the substratum is mediated by cell adhesion to the ECM proteins through integrin receptors; therefore it is possible that 12-LOX overexpression may modulate the expression/function of integrin receptors to enhance cell spreading. We examined several potential integrins and adhesion molecules in wild-type W256 cells to determine which ones are expressed endogenously. To this end, wild-type W256 cells were surface

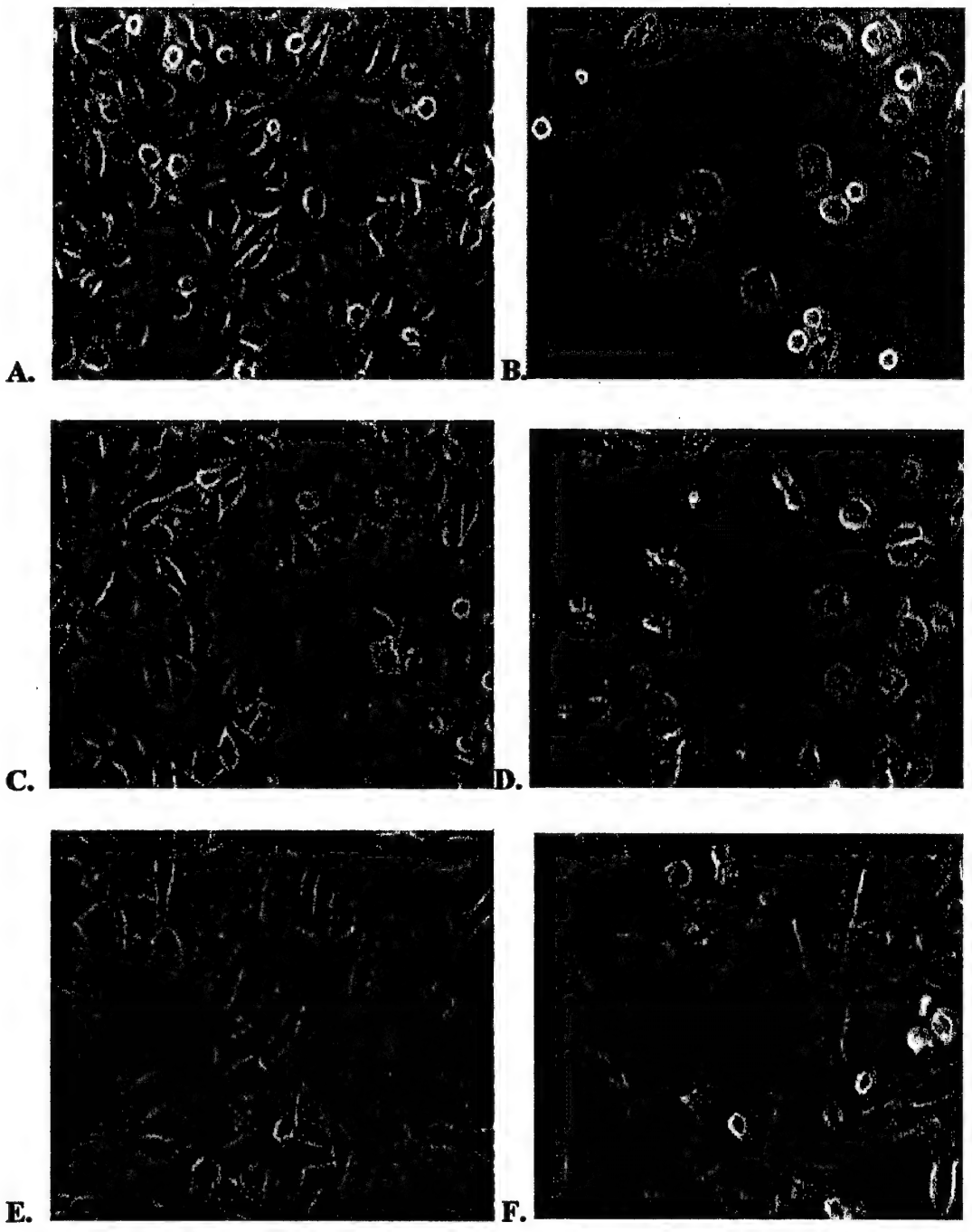

FIGURE 5 – 12-LOX overexpressing W256 cells demonstrated a more spread morphology in response to serum starvation. Light microscopy was used to examine the morphology of different W256 clones after serum starvation. Even under normal serum conditions (time 0), wild-type and neo-transfected cells (*a* and *c*, respectively) displayed a rounder morphology compared with pCMV-12-LOX-transfected cells (*e*). 4 days post serum starvation, both wild-type (*b*) and neo-transfected (*d*) cells demonstrated morphologic signs of significant cell death (*i.e.*, rounding up and detachment from the substratum). In contrast, by day 4 of serum starvation, a significant number of W256 cells remained spread and alive (*f*).

labeled with antibody to β1, α2β1, β3, αvβ5, αIIbβ3, α4, αv, α5β1, αvβ3 or P-selectin. Flow cytometric analysis demonstrated that W256 cells did not express detectable levels of α4 or α2β1 (Fig. 6*b* and *c*, respectively) or P-selectin (data not shown). Consistent with previous reports from our laboratory, W256 cells did not express integrin αv or αvβ3 on their surface (Fig. 6*e* and *g*, respectively) but did express detectable, but low, levels of αIIbβ3 and β3 integrin receptors (Fig. 6*i* and *h*, respectively).[37] Most dramatically, W256 cells predominantly expressed integrins α5β1 (Fig. 6*d*) and αvβ5 (Fig. 6*j*), as indicated by the prominent shift in the mean log fluorescence intensity compared with control.

Under the same experimental conditions, flow cytometric studies demonstrated relatively consistent expression levels of several integrin receptors such as β1, β3 and αIIbβ3 between W256 sublines (Fig. 7). However, pCMV-12-LOX W256 cells demonstrated a consistent increase (*i.e.*, ~2 log fold) in the expression of αvβ5 compared with the wild-type cells. Interestingly, the trans-

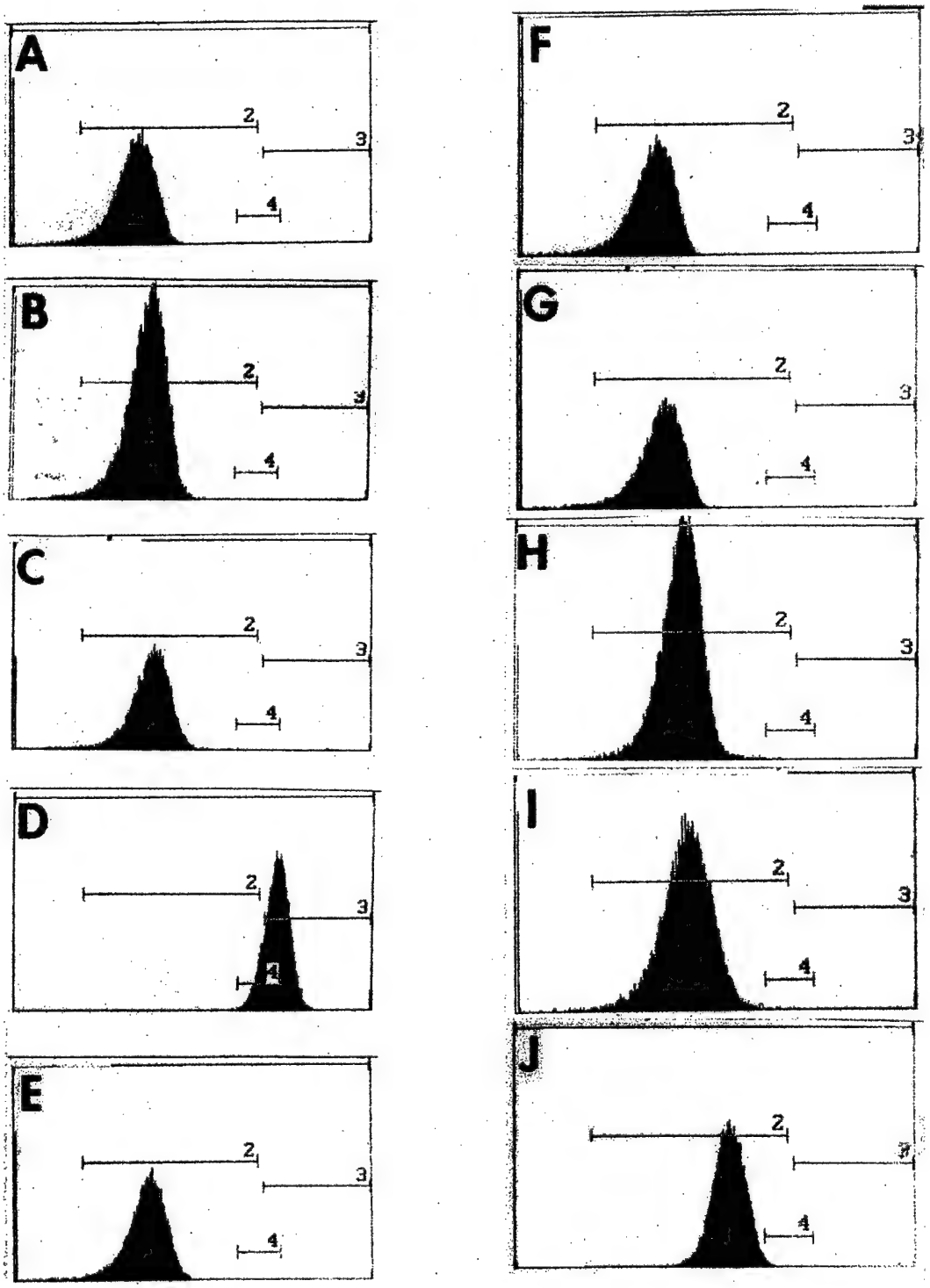

FIGURE 6 – Endogenous expression of integrins in W256 carcinoma cells determined by flow cytometry. Wild-type W256 cells were incubated with control antibodies, *i.e.* MOPC (*a*, 0.1 mg/ml) or rabbit IgG (*f*, 1.0 mg/ml), or various primary antibodies: anti-α4 (*b*, 0.1 mg/ml), -α2β1 (*c*, 0.1 mg/ml), -α5β1 (*d*, 1.0 mg/ml), -αv (*e*, 0.1 mg/ml), -αvβ3 (*g*, 1.0 mg/ml), -β3 (*h*, 0.1 mg/ml), -αIIbβ3 (*i*, 0.1 mg/ml) or –αvβ5 (*j*, 0.1 mg/ml). Cells were then treated with FITC-labeled secondary antibodies and analysis of cell surface fluorescence was performed by flow cytometry. W256 cells express low levels of αIIbβ3 and β3 integrin receptors and high levels of α5β1 and αvβ5, as revealed by a prominent shift in the mean log fluorescence intensity compared with controls.

fected cells (*i.e.*, the mock and 12-LOX overexpressors) expressed slightly higher levels of α5β1 on their surface compared with the wild-type cells (Fig. 7). This most likely represents an artifact related to the transfection procedure itself.

Increased localization of integrin αvβ5 to focal adhesions in 12-LOX W256 carcinoma cells

We next evaluated the αvβ5 expression in W256 sublines at the morphologic level. To this end, W256 cells were permeabilized

A.

Integrin	Wild-type	Neo 1	Neo 2	Clone 1	Clone 2
β1	2.089±0.38	2.404±0.11	2.900±0.34	2.816±0.11	2.194±0.16
α5β1	8.443±0.64	9.403±0.35	9.437±0.01	9.699±0.29	9.976±0.23
β3	1.271±0.01	1.825±0.29	2.238±0.01	1.554±0.01	———
αIIbβ3	1.650±0.01	2.557±0.15	2.741±0.15	2.164±0.03	2.161±0.06
αvβ5	2.278±0.10	2.625±0.01	2.773±0.21	**4.006±0.07**	**4.100±0.03**

B.

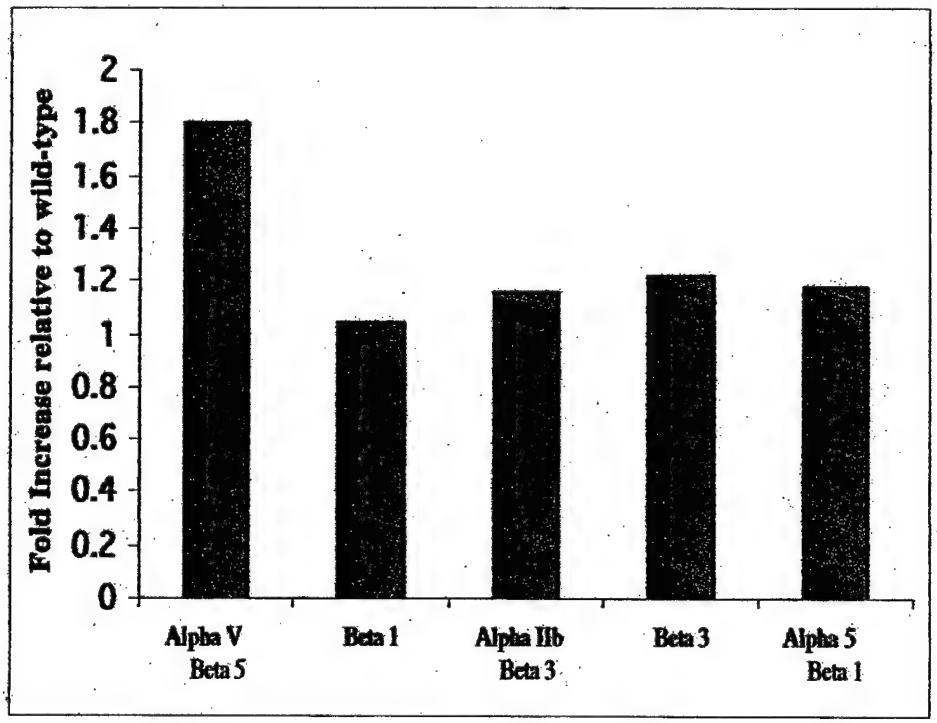

FIGURE 7 – Flow cytometric analysis of the surface expression of integrin receptors on wild-type and transfected W256 cells. An equal amount of wild-type, neo- and 12-LOX-transfected cells were surface labeled for various integrins, as described in Material and Methods, and cell surface fluorescence was analyzed by flow cytometry. (*a*) The values are expressed as mean log fluorescence intensity (mean ± SE) derived from 2 independent experiments. (*b*) The log-fold increase in surface expression was calculated for W256 12-LOX transfected cells relative to wild-type cells.

and processed for immunofluorescence microscopy. As shown in Figure 8*a* and *b*, both wild-type and pCMV-neo W256 cells exhibited a bipolar round morphology and expressed αvβ5 throughout the cytoplasm. In contrast, most W256 cells overexpressing 12-LOX demonstrated a more spread morphology (*i.e.*, a larger surface area) along with an increased distribution of αvβ5 concentrated at the cell borders/edges and focal adhesion plaques (Fig. 8*c*, arrowheads). These studies indicate that pCMV-12-LOX W256 cells may rely on the upregulation of αvβ5 integrin to maintain their adherence to the substratum in order to sustain their cell survival.

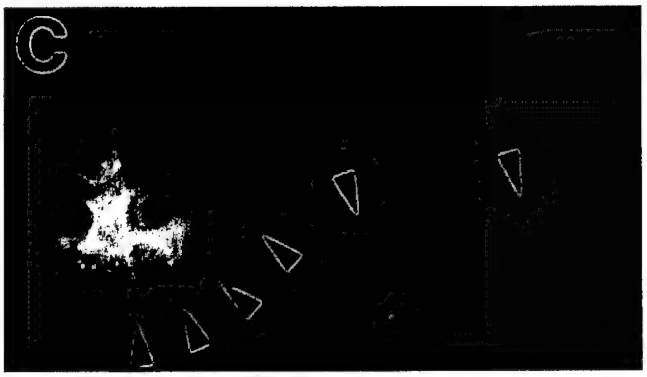

FIGURE 8 – Increased localization of integrin αvβ5 to focal adhesions in 12-LOX-transfected W256 cells. W256 cells were fixed and incubated with anti-αvβ5 (0.1 mg.ml) followed by FITC-labeled secondary antibody– and processed for fluorescence microscopy. (*a*) Wild-type cells. (*b*) pCMV-neo cells. (*c*) pCMV-12-LOX W256 cells. Arrowheads indicate focal adhesion plaques enriched in αvβ5. Original magnification: ×200.

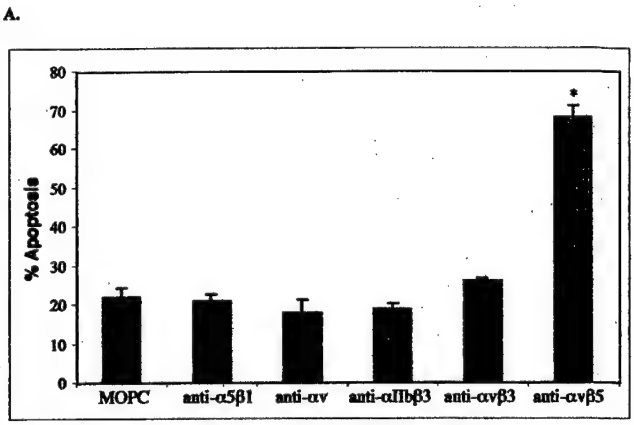

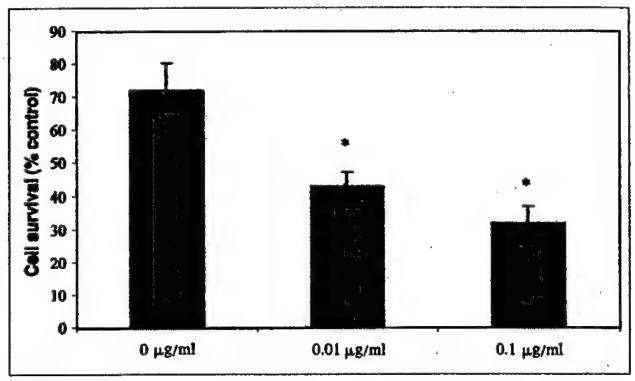

FIGURE 9 – Integrin αvβ5 is important for the survival of 12-LOX-transfected W256 carcinosarcoma cells in the absence of serum. (*a*) Apoptosis of 12-LOX-transfected W256 cells was examined by DAPI staining after serum starvation for 3 days in the presence of various antibodies directed against specific integrins or MOPC as control. The values are expressed as % apoptosis; the mean ± standard error was derived from 3 independent experiments. Antibody to αvβ5 induced significant apoptosis in 12-LOX-transfected cells compared with MOPC treated controls. *, $p < 0.05$. (*b*) Survival of 12-LOX-transfected W256 cells was examined by the MTS assay. 12-LOX-transfected cells were serum starved for 3 days in the presence of MOPC or anti-αvβ5 (0.01 or 0.1 μg/ml, respectively). Results are expressed as % cell survival and the mean ± standard error was derived from 3 independent experiments. Treatment with anti-αvβ5 resulted in a significant, dose-dependent decrease in cell survival compared with MOPC-treated controls. *, $p < 0.05$.

Integrin αvβ5 is an important factor for 12-LOX-transfected W256 cell survival in the absence of serum

Having examined the expression of a number of integrins on W256 cells, we next examined which one(s) plays a causal role in sustaining W256 cell survival during serum deprivation. 12-LOX-transfected W256 cells were serum-starved in the presence of MOPC (as control) or with an antibody to α5β1, αv, αIIbβ3, αvβ3 or αvβ5. After 3 days of serum withdrawal, control 12-LOX-transfected W256 cells demonstrated typical spread morphology without a significant amount of cell death (~20% apoptosis; Fig. 9*a*). Similarly, pCMV-12-LOX W256 cells did not appear to be dependent on integrins α5β1, αv, αIIbβ3 or αvβ3 for maintaining their survival during serum-free conditions since pretreatment with the respective antibodies did not result in significant apoptosis (~17–25%; Fig. 9*a*). In sharp contrast, the survival of 12-LOX-transfected W256 cells was significantly reduced when they were serum starved in the presence of monoclonal anti-αvβ5. In the presence of 0.01 μg/ml of anti-αvβ5, pCMV-12-LOX W256 cells underwent remarkable morphologic changes consistent with apoptosis and were significantly ($p < 0.05$) more apoptotic than controls, as determined by DAPI staining (Fig. 9*b*). This effect was shown to be dose-dependent, as an increased concentration of anti-αvβ5 (*i.e.*, 0.1 μg/ml) induced further apoptosis, resulting in ~70% apoptotic death in pCMV-12-LOX W256 cells, compared with only 28% in MOPC-treated controls (Fig. 9*b*). These data

expressing W256 cells demonstrated well-developed actin microfilaments extending from the cell nucleus to the periphery.

More importantly, these microfilaments (*i.e.*, phalloidin-positive staining) often extend to the focal contact-like structures enriched in the integrin αvβ5 (data not shown). The increased microfilament content was also confirmed by flow cytometric analysis using FITC-tagged phalloidin. As the targeting of integrin receptors to focal contacts requires the presence of stress fiber endings, it is likely that increased actin polymerization takes place prior to the alterations in αvβ5. Regardless, similar to a crucial role of αvβ5, 12-LOX-induced actin microfilament formation appears functionally important since prevention/disruption of the microfilament network with cytochalasin B, in a dose-dependent manner, blocked the survival advantage of 12-LOX-overexpressing cells under serum-starved conditions.

Interestingly, we have previously demonstrated that the major metabolic product of 12-LOX, 12(S)-HETE, increased actin microfilament content in B16a melanoma cells.[34] In that study, 12(S)-HETE promoted actin polymerization through protein kinase C (PKC)-dependent phosphorylation of cytoskeletal components such as myosin light chain. Indeed, in support of our results outlined here, under serum-starved conditions, we have observed prolonged survival of human prostate tumor cells, PC3 and human lung epidermoid carcinoma A431 cells, after overexpression of platelet-type 12-LOX, which also produces the 12(S)-HETE metabolite (unpublished observations). In both PC3 and A431cells overexpressing platelet-type 12-LOX, we also observed increased actin polymerization similar to that observed in our study with leukocyte-type 12-LOX overexpression (unpublished observations). Exogenous 12(S)-HETE has also been shown to extend the survival of W256 cells cultured in the absence of serum.[36] It is highly likely that the survival advantage conferred on 12-LOX-overexpressing W256 cells occurs via the same pathway. In summary, we have demonstrated for the first time that the leukocyte-type 12-LOX pathway is a regulator of cell survival and apoptosis in rat W256 carcinosarcoma cells. Enforced expression of this enzyme specifically increased the expression and localization of the αvβ5 integrin and microfilament assembly in these cells. Therefore, the inhibition of 12-LOX is a potential therapeutic approach in the treatment of metastatic disease.

ACKNOWLEDGEMENTS

We are grateful to Dr. D. Tang for his excellent technical assistance and to Dr. C. Funk (University of Pennsylvania, Philadelphia, PA) for generously providing the purified leukocyte-type 12-LOX enzyme and the purified pCMV-12-LOX plasmid.

REFERENCES

1. Funk CD. Molecular biology in the eicosanoid field. Prog Nucleic Acid Res Mol Biol 1993;45:67–98.
2. Funk CD, Furci L, Fitzgerald GA. Molecular cloning, primary structure, and expression of the human platelet/erythroleukemia cell 12-lipoxygenase. Proc Natl Acad Sci USA 1990;87:5638–42.
3. Yoshimoto T, Suzuki H, Yamamoto S, Takai T, Yokoyama C, Tanabe T. Cloning and sequence analysis of the cDNA for arachidonate 12-lipoxygenase of porcine leukocytes. Proc Natl Acad Sci USA 1990;87:2142–6.
4. Natarajan R, Esworthy R, Bai W, Gu JL, Wilczynski S, Nadler JL. Increased 12-lipoxygenase expression in breast cancer cells and tissues. Regulation by epidermal growth factor. J Clin Endocrinol Metab 1997;82:1790–8.
5. Kamitani H, Geller M, Eling T. The possible involvement of 15-lipoxygenase / leukocyte type 12-lipoxygenase in colorectal carcinogenesis. Adv Exp Med Biol 1991;469:593–8.
6. Nie D, Hillman GG, Geddes T, Tang K, Pierson C, Grignon DJ, Honn KV. Platelet-type 12-lipoxygenase in a human prostate carcinoma stimulates angiogenesis and tumor growth. Cancer Res 1998;58:4047–51.
7. Timar J, Rasa E, Honn KV, Hagmann W. 12-Lipoxygenase expression in human melanoma cell lines. Adv Exp Med Biol 1999;469: 617–22.
8. Ding XZ, Kuszynski CA, El-Metwally TH, Adrian TE. Lipoxygenase inhibition induced apoptosis, morphological changes, and carbonic anhydrase expression in human pancreatic cancer cells. Biochem Biophys Res Commun 1999;266:392–9.
9. Nappez C, Liagre B, Beneytout JL. Changes in lipoxygenase activities in human erythroleukemia (HEL) cells during diosgenin-induced differentiation. Cancer Lett.1995;96:133–40.
10. Timar J, Raso E, Dome B, Li L, Grignon D, Nie D, Honn KV, Hagmann W. Expression, subcellular localization and putative function of platelet-type 12-lipoxygenase in human prostate cancer cell lines of different metastatic potential. Int J Cancer 2000;87:37–43.
11. Woodhouse EC, Chuaqui RF, Liotta LA. General mechanism of metastasis. Cancer 1997;80:1529–37.
12. Giancotti FG, Ruoslahti E. Integrin signalling. Science 1999;285: 1028–32.
13. Bissell MJ, Weaver VM, Lelievre SA, Wang F, Petersen OW, Schmeicel KL. Tissue structure, nuclear organization, and gene expression in normal and malignant breast. Cancer Res 1999;59:1757–63s; discussion 1763–4s.
14. Clarke EA, Brugge JS. Integrins and signal transduction pathways: the road taken. Science 1995;268:233–9.
15. Howe A, Aplin AE, Alahari SK, Juliano RL. Integrin signaling and cell growth control. Curr Opin Cell Biol 1998;10:220–31.
16. Gilmore AP, Burridge K. Molecular mechanisms for focal adhesion assembly through regulation of protein-protein interactions. Structure 1996;4:647–51.
17. Felsenfeld DP, Choquet D, Sheetz MP. Ligand binding regulates the directed movement of beta1 integrins on fibroblasts. Nature 1996;383: 438–40.
18. Sheetz MP, Felsenfeld DP, Galbraith CG. Cell migration: regulation of force on extracellular-matrix-integrin complexes. Trends Cell Biol 1998;8:51–4.
19. Noti JD, Johnson AK. Integrin alpha 5 beta 1 suppresses apoptosis triggered by serum starvation but not phorbol ester in MCF-7 breast cancer cells that overexpress protein kinase C-alpha. Int J Oncol 2001;18:195–201.
20. Erdreich-Epstein A, Shimada H, Groshen S, Liu M, Metelitsa LS, Kim KS, Stins MF, Seeger RC, Durden DL. Integrins alpha(v)beta3 and alpha(v)beta5 are expressed by endothelium of high risk neuroblastoma and their inhibition is associated with increased endogenous ceramide. Cancer Res 2000;60:712–21.
21. Brassard DL, Maxwell E, Malkowski M, Nagabhushan TL, Kumar CC, Armstrong L. Integrin αvβ3-mediated activation of apoptosis. Exp Cell Res 1999;251:33–45.
22. Khwaja A, Rodriguez-Viciana P, Wennstrom S, Warne PH, Downward J. Matrix adhesion and Ras transformation both activate a phosphoinositide 3-OH kinase and protein kinase B/Akt cellular survival pathway. EMBO J 1997;16:2783–93.
23. Wu C, Keightley SY, Leung-Hagesteijn C, Radeva G, Coppolino M, Goicoechea S, McDonald JA, Dedhar S. Integrin-linked protein kinase regulates fibronectin matrix assembly, E-cadherin expression, and tumorigenicity. J Biol Chem 1998;273:528–36.
24. Uhm JH, Dooley NP, Kyritsis AP, Rao JS, Gladson CL. Vitronectin, a glioma-derived extracellular matrix protein, protects tumor cells from apoptotic death. Clin Cancer Res 1999;5:1587–94.
25. Pouliot N, Connolly LM, Moritz RL, Simpson RJ, Burgess AW. Colon cancer cells adhesion and spreading on autocrine laminin-10 is mediated by multiple integrin receptors and modulated by EGF receptor stimulation. Exp Cell Res 2000;261:360–71.
26. Dominguez-Jimenez C, Diaz-Gonzalez F, Gonzalez-Alvaro I, Cesar JM, Sanchez-Madrid F. Prevention of αII(b)β3 activation by nonsteroidal anti-inflammatory drugs. FEBS Lett 1999;446:318–22.
27. Dormond O, Foletti A, Paroz C, Ruegg C. NSAIDs inhibit aVb3 integrin-mediated and Cdc42/Rac-dependent endothelial-cell spreading, migration and angiogenesis. Nat Med 2000;7:1041–7.
28. Tang DT, Grossi IM, Chen YQ, Diglio CA, Honn KV. 12(S)-HETE promotes tumor-cell adhesion by increasing surface expression of avb3 integrins on endothelial cells. Int J Cancer 1993;54:102–111.
29. Raso E, Tovari J, Toth K, Paku S, Trikha M, Honn KV, Timar J. Ectopic alphaIIbbeta3 integrin signaling involves 12-lipoxygenase- and PKC-mediated serine phosphorylation events in melanoma cells. Thromb Haemost 2001;85:1037–42.
30. Patricia MK, Kim JA, Harper CM, Shih PT, Berliner JA, Natarajan R, Nadler JL, Hedrick CC. Lipoxygenase products increase monocyte adhesion to human aortic endothelial cells. Arterioscler Thromb Vasc Biol 1999;19:2615–22.
31. Tang K, Finley RL Jr, Nie D, Honn KV. Identification of 12-lipoxy-

genase interaction with cellular proteins by yeast two-hybrid screening. Biochemistry 2000;39:3185–91.
32. Chen X-S, Kurre U, Jenkins NA, Copeland NG, Funk CD. cDNA cloning expression, mutagenesis, of C-terminal isoleucine, genomic structure, and chromosomal localizations of murine 12-lipoxygenases. J Biol Chem 1994;269:13979–87.
33. Reddy RG, Yoshimoto T, Yamamoto S, Funk CD, Marnett LJ. Expression of porcine leukocyte 12-lipoxygenase in a baculovirus/insect cell system and its characterization. Arch Biochem Biophys 1994;312:219–26.
34. Rice RL, Tang DG, Haddad M, Honn KV, Taylor JD. 12(S)-hydroxyeicosatetraenoic acid increases the actin microfilament content in B16a melanoma cells: a protein kinase-dependent process. Int J Cancer 1998;77:271–8.
35. Liu B, Marnett LJ, Caudharey A, Ji J, Blair IA, Johnson CR, Diglio CA, Honn KV. Biosynthesis of 12(S)-hydroxyeicosateateatranoic acid by B16 amelanotic melanoma cells is a determinant of their metastatic potential. Lab Invest 1994;70:314–23.
36. Tang DT, Honn KV. Apoptosis of W256 carcinosarcoma cells of the monocytooid origin induced by NDGA involves lipid peroxidation and deletion of GSH: role of 12-lipoxygenase in regulating tumor cell survival. J Cell Physiol 1997;172:155–70.
37. Chang SY, Chen YQ, Fitzgerald LA, Honn KV. Analysis of integrin mRNA in human and rodent tumor cells. Biochem Biophys Res Commun 1991;176:108–13.
38. Pidgeon GP, Kandouz M, Meram A, Honn KV. Mechanisms controlling cell cycle arrest and induction of apoptosis following 12-lipoxygenase inhibition in prostate cancer cells. Cancer Res 2002;62:2721–7.
39. Ruoslahti E. Stretching is good for a cell. Science 1997;268:233–9.
40. Scatena M, Giachelli C. The alpha(v)beta3 integrin, NF-kappaB, osteoprotegerin endothelial cell survival pathway. Potential role in angiogenesis. Trends Cardiovasc Med 2002;12:83–8.
41. Petitclerc E, Stromblad S, von Schalscha TL, Mitjans F, Piulats J, Montgomery AM, Cheresh DA, Brooks PC. Integrin αvβ3 promotes M21 melanoma growth in human skin by regulating rumor cell survival. Cancer Res 1999;59:2724–30.
42. Vacca A, Ria R, Presta M, Ribatti D, Iurlaro M, Merchionne F, Tanghetti E, Dammacco F. alpha(v)beta(3) integrin engagement modulates cell adhesion, proliferation, and protease secretion in human lymphoid tumor cells. Exp Hematol 2001;8:993–1003.
43. Smida Rezgui S, Honore S, Rognoni JB, Martin PM, Penel C. Up-regulation of alpha 2 beta 1 integrin cell-surface expression protects A431 cells from epidermal growth factor-induced apoptosis. Int J Cancer 2000;87:360–7.
44. Freyer AM, Johnson SR, Hall IP. Effects of growth factors and extracellular matrix on survival of human airway smooth muscle cells. Am J Respir Cell Mol Biol 2001;25:569–76.
45. Le Bellego F, Pisselet C, Huet C, Monget P, Monniaux D. Laminin-alpha6beta1 integrin interaction enhances survival and proliferation and modulates steroidogenesis of ovine granulosa cells. J Endocrinol 2002;172:45–59.
46. O'Brien V, Frisch SM, Juliano RL. Expression of the integrin alpha 5 subunit, in HT29 colon carcinoma cells, suppresses apoptosis triggered by serum deprivation. Exp Cell Res 1996;224:208–13.
47. Urbich C, Walter DH, Zeiher AM, Dimmeler S. Laminar shear stress upregulates integrin expression: role in endothelial cell adhesion and apoptosis. Circ Res 2000;87:683–9.
48. Hoyt DG, Rusnak JM, Mannix RJ, Modzelewski RA, Johnson CS, Lazo JS. Integrin activation suppresses etoposide-induced DNA strand breakage in cultured murine tumor-derived endothelial cells. Cancer Res. 1996;56:4146-4149.
49. Zhang Z, Vuori K, Reed JC, Ruoslahti E. The alpha 5 beta 1 integrin supports survival of cells on fibronectin and up-regulates Bcl-2 expression. Proc Natl Acad Sci USA 1995;92:6161–5.
50. Sharma CP, Ezzell RM, Arnaout MA. Direct interaction of filamin (ABP-280) with the beta 2-integrin subunit CD18. J Immunol 1995; 154:3461–70.
51. Calderwood DA, Huttenlocher A, Kiosses WB, Rose DM, Woodside DG, Schwartz MA, Ginsberg MH. Increased filamin binding to beta-integrin cytoplasmic domains inhibits cell migration. Nat Cell Biol 2001;3:1060–8.

[CANCER RESEARCH 62, 2721–2727, May 1, 2002]

Mechanisms Controlling Cell Cycle Arrest and Induction of Apoptosis after 12-Lipoxygenase Inhibition in Prostate Cancer Cells[1]

Graham. P. Pidgeon,[2] Mustapha Kandouz,[2] Anthony Meram, and Kenneth V. Honn[3]

Departments of Radiation Oncology [G. P. P., M. K., A. M., K. V. H.] and Pathology [K. V. H.], Wayne State University, Detroit, Michigan 48202, and Karmanos Cancer Institute, Detroit, Michigan 48201 [K. V. H.]

ABSTRACT

Extensive studies have implicated the role of dietary fatty acids in prostate cancer progression. Platelet-type 12-Lipoxygenase (12-LOX) has been shown to regulate growth, metastasis, and angiogenesis of prostate cancer. The effect of two 12-LOX inhibitors, Baicalein and *N*-benzyl-*N*-hydroxy-5-phenylpentamide (BHPP), on the mechanisms controlling cell cycle progression and apoptosis were examined in two prostate cancer cell lines, PC3 and DU-145. Treatment with Baicalein or BHPP resulted in a dose-dependent decrease in cell proliferation, as measured by BrdUrd incorporation. This growth arrest was shown to be because of cell cycle inhibition at G_0/G_1, and was associated with suppression of cyclin D1 and D3 protein levels. PC3 cells also showed a strong decrease in phosphorylated retinoblastoma (pRB) protein, whereas the other retinoblastoma-associated proteins, p107 and p130, were inhibited in DU-145 cells. Treatment with 12-hydroxyeicosatetraenoic acid in the presence of Baicalein blocked loss of pRB, whereas 12(S)-HETE alone induced pRB expression. Treatment with either Baicalein or BHPP resulted in significant apoptosis in both cell lines as measured by terminal deoxynucleotidyltransferase-mediated dUTP nick end labeling. DU-145 cells underwent apoptosis more rapidly than PC-3 cells. The mechanisms involved were decreased phosphorylation of Akt, loss of survivin and subsequent activation of caspase-3 and caspase-7 in each cell line, decreased Bcl-2 and Bcl-X_L expression in DU-145, and a shift in Bcl-2/Bax levels favoring apoptosis in PC-3 cells. Addition of 12(S)-HETE protected both cell lines from Baicalein-induced apoptosis, whereas other LOX metabolites, 5(S)-HETE, or 15(S)-HETE did not. These results show that the 12-LOX pathway is a critical regulator of prostate cancer progression and apoptosis, by affecting various proteins regulating these processes. Therefore, inhibition of 12-LOX is a potential therapeutic agent in the treatment of prostate cancer.

INTRODUCTION

Arachidonic acid metabolism can be catalyzed by one of two distinct enzyme pathways, cyclooxygenase or LOX.[4] Its metabolism leads to the generation of biologically active metabolites that may be potentially involved in carcinogenesis by modulating mitogenic signaling and regulating cellular proliferation (1–3). Furthermore, it has been shown that the LOXs in particular are key regulators of cell survival and apoptosis in cells (4). Mammalian LOXs constitute a heterogeneous family of lipid peroxidizing enzymes that are categorized with respect to their regional specificity of arachidonic acid oxygenation. Therefore, the LOXs have been designated as 5-, 8-, 12-, and 15-LOX isoforms, which transiently produce the end products 5(S)-, 8(S)-, 12(S)-, and 15(S)-HETEs, respectively (5, 6). 12-LOX is expressed as two main isoforms, a platelet-type cloned from human platelets (7) and a leukocyte-type from porcine leukocytes, that shares 65% homology to the platelet-type cDNA (8).

Several lines of evidence implicate 12-LOX as a regulator of human cancer development. It is overexpressed in a variety of tumors including breast, colorectal, and prostate cancer (9–11), and has been shown to be present in a number of cancer cell lines (12–14). We have extensively investigated the role of platelet-type 12-LOX and 12(S)-HETE in prostate cancer. We reported previously that 12-LOX is expressed in several prostate cancer cell lines (15). In addition, we have described its involvement in tumor metastasis, as pretreatment of DU-145 prostate cancer cells *in vitro* with the 12-LOX specific inhibitors BHPP or Baicalein significantly inhibited their ability to form lung colonies after tail-vein injection (15). Other reports from our laboratory have demonstrated that 12-LOX levels are correlated with the grade and stage of human prostate tumors (16), and that s.c. injection of PC3 cells overexpressing 12-LOX increased the amount of angiogenesis and growth of tumors in mice (11).

Deregulation in the fine balances controlling cellular proliferation and cell death is the hallmark of cancer. Many proteins are involved in the process by which cells choose between growth arrest, apoptosis, or survival. The 12-LOX inhibitor, Baicalein, has been shown previously to induce apoptosis in human gastric, colon, hepatoma, and pancreatic cancer cells (13, 17–20). In addition, an analogue of Baicalein, called baicalin, has been shown to induce apoptosis in prostate cancer cells (20). The underlying mechanism whereby 12-LOX inhibition induces and executes apoptosis is not clearly defined. In the present study we examine the effect of 12-LOX inhibition by Baicalein or BHPP on the mechanisms controlling the cell cycle and apoptosis in prostate cancer cells by examining the cell cycle-regulatory proteins that are involved in the control of the G_1-S transition.

MATERIALS AND METHODS

Cells Lines. Two prostate carcinoma cell lines, DU-145 and PC3, were obtained from the American Type Culture Collection (Rockville, MD) and maintained in a humidified atmosphere of 5% CO_2 in air at 37°C. The cells were routinely cultured in RPMI 1640 supplemented with 10% fetal bovine serum (Life Technologies, Inc.), 2 mM L-glutamine, and 100 μg/ml penicillin-streptomycin. Experiments were performed when cells were ~80% confluent.

Cell Proliferation. PC3 and DU145 prostate cancer cells were seeded into 96-well plates and incubated at 37°C. After 12 h cells were cultured in serum-free medium with or without various concentrations of the selective 12-LOX inhibitors Baicalein (Biomol, Plymouth, PA) or BHPP (Biomide Corp., Grosse Pointe Farms, MI), or a specific 5-LOX inhibitor α-pentyl-4–2-quinolinylmethoxy-benzenemethanol (Rev-5901; Cayman Chemicals, Ann Arbor, MI) for 48 h. Thereafter, cell proliferation was assessed by a specific nonradioactive cell proliferation ELISA based on the measurement of BrdUrd incorporation during DNA synthesis according to the manufacturer's instructions (Roche Diagnostics GmbH, Mannheim, Germany). Statistical comparison between treatments was carried out using ANOVA with Scheffe post-hoc correction. Data are taken as significant where $P < 0.05$. Separately, cells were examined morphologically by light microscopy.

Flow Cytometry for Cell Cycle Analysis. Prostate cancer cells grown in 25-cm^2 flasks were treated with various concentrations of Baicalein for 48 h.

Received 2/13/02; accepted 2/26/02.

The costs of publication of this article were defrayed in part by the payment of page charges. This article must therefore be hereby marked *advertisement* in accordance with 18 U.S.C. Section 1734 solely to indicate this fact.

[1] Supported by NIH Grant CA-29997, the United States Army Prostate Cancer Research Program DAMD 17-98-1-8502, and a fellowship from the American Cancer Research Foundation.

[2] These authors contributed equally to this paper.

[3] To whom requests for reprints should be addressed, at Department of Radiation Oncology, 431 Chemistry Building, Wayne State University, Detroit, Michigan 48202. E-mail: k.v.honn@wayne.edu.

[4] The abbreviations used are: LOX, lipoxygenase; BHPP, *N*-benzyl-*N*-hydroxy-5-phenylpentamide; BrdU, bromodeoxyuridine; pRB, phosphorylated retinoblastoma; TUNEL, terminal deoxynucleotidyl transferase-mediated nick end labeling; PARP, poly-(ADP-ribose) polymerase; CDK, cyclin-dependent kinase; Rb, retinoblastoma; 12(S)-HETE, 12-hydroxyeicosatetraenoic acid; FLAP, 5-LOX-activating protein.

The cells were then digested by trypsin-EDTA, washed, and resuspended in serum-free medium, counted, and then fixed overnight in 75% ethanol at 4°C. The cells were then washed and resuspended in PBS (pH 7.4) containing 0.1% Triton X-100, 0.05 mg/ml DNase-free RNase A, and 50 μg/ml propidium iodide at a concentration of 0.5 ml/10^6 cells. The cells were incubated in the dark for 30 min at room temperature. The red fluorescence of the single events was recorded using an argon ion laser at 488 nm excitation wavelength and 610 nm as emission wavelength to measure DNA index.

TUNEL Assay. Apoptosis was detected using the terminal incorporation of fluorescein-12-dUTP by terminal deoxynucleotidyl transferase into fragmented DNA in prostate cancer cells treated with Baicalein according to the manufacturer's instructions (Roche Diagnostics GmbH). Briefly, cells were grown in 75-cm^2 flasks, incubated overnight in serum-free medium, and then treated with various concentrations of Baicalein for 24, 48, or 72 h. The cells were then digested by trypsin-EDTA, washed, and fixed for 1 h in 75% ethanol at 4°C. Thereafter ice-cold permeabilization solution (0.1% Triton X-100 and 0.1% sodium citrate) was added for 3 min. After this samples were washed twice in PBS, and 50 μl of the working TUNEL reaction mix was added. Samples were incubated at 37°C for 1 h, washed, and resuspended in PBS. Laser flow cytometry was used to quantify the percentage of apoptotic cells indicated by green fluorescence of fluorescein-12-dUTP incorporated by the cell.

Western Blot Analysis. Total cell lysates were prepared following various treatments. Protein (30 μg) was fractionated by precast SDS-PAGE and then transferred to nitrocellulose membranes. After incubating for 1 h in blocking buffer containing 5% skimmed milk dissolved in 10 mM Tris-HCl (pH 7.5), 100 mM NaCl, and 0.1% Tween 20, blots were probed overnight with primary antibodies against cyclin D1, D2, D3, and cyclin E; CDKs 2, 4, and 6; CDK inhibitors p21, p27, p57, p16, p18, and p19; Rb protein; and various phospo-Rb. In addition apoptosis-related proteins BCL-2, PARP, caspases, and survivin were examined. All of the antibodies, excluding Rb and phosphorylated Rb (Ser 807/811; Cell Signaling Technology, Beverly, MA); p15, p16 and p18 (Upstate Biotechnology, Lake Placid, NY); cyclin D1 (Oncogene Research Products, Boston, MA); cyclins D2, D3, and E, p21, p27, and PARP (BD PharMingen, San Diego, CA) were obtained from Santa Cruz Biotechnology (Berkeley, CA)

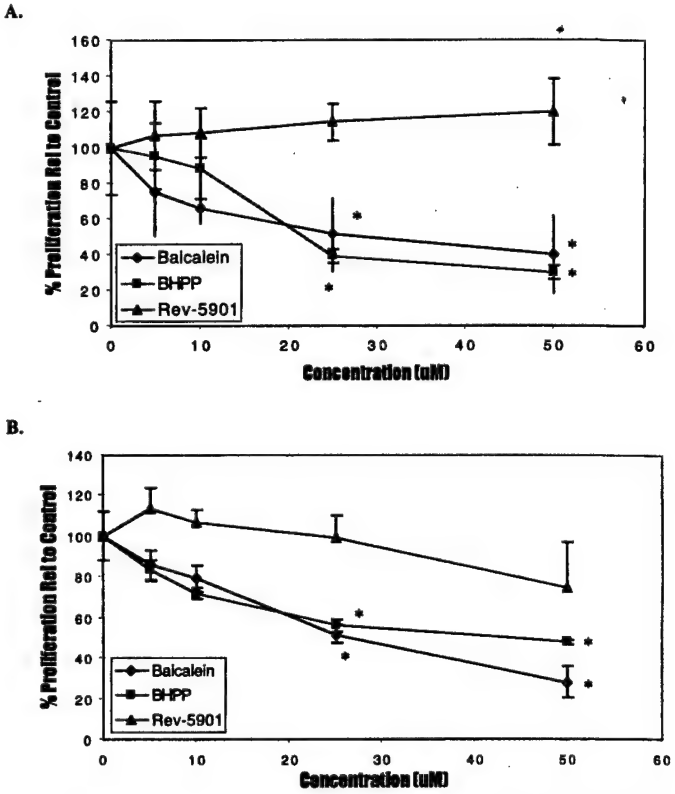

Fig. 1. Effect of LOX inhibition on the proliferation of PC-3 (*A*) and DU-145 (*B*) prostate cancer cells. The cells were treated with increasing concentrations of the 12-LOX inhibitors, Baicalein or BHPP, or the 5-LOX inhibitor Rev-5901 (5–50 μM) for 48 h. Viable cells were measured by BrdU incorporation and expressed as a percentage of the controls (n = 4); *bars*, ±SE. * indicate that levels are significantly different from the untreated controls ($P < 0.05$).

RESULTS

Effect of LOX Inhibitors on Prostate Cancer Cell Proliferation. The 12-LOX inhibitors Baicalein and BHPP both induced a significant growth inhibition in prostate cancer cells in a dose-dependent manner as measured by BrdU incorporation in both PC3 and DU145 cells at 48 h relative to control cells (Fig. 1, *A* and *B*). Treatment with 25 μM Baicalein significantly decreased proliferation of PC-3 and DU-145 cells to 51% and 52%, respectively, compared with untreated controls ($P < 0.05$). BHPP also significantly inhibited proliferation of both cell lines at similar concentrations ($P < 0.05$). After 24 h both 12-LOX inhibitors had only minor effects on cell numbers in both prostate cancer cell lines (data not shown). The specific 5-LOX inhibitor Rev-5901 had no effect on cell proliferation in either PC3 or DU145 prostate cancer cells (P = not significant; Fig. 1, *A* and *B*).

LOX Inhibition-induced Growth Arrest in Prostate Cancer Cells. To examine where in the cell cycle the growth phase arrest observed in the proliferation experiments occurred, PC3 cells were treated with the LOX inhibitors Baicalein, BHPP, or Rev-5901 for 24 h in serum-free medium. The percentage of cells in G_0/G_1 *versus* S *versus* G_2/M phases was then examined by flow cytometry after propidium iodide staining of the cellular DNA (representative DNA histograms are shown in Fig. 2*A*). Treatment of cells with 25 μM Baicalein resulted in an accumulation of cells in the G_0/G_1 phase (from 45% to 61% and from 51% to 68% in PC-3 and DU-145 cells, respectively) with a comparative drop in the S phase fraction from 36% to 23% and 32% to 24%, respectively. The G_2-M phase decreased slightly in PC-3 cells (from 19% to 16%), whereas a more dramatic decrease was observed in the DU-145 cells (from 17% to 9%; Fig. 2*B*). A similar effect was observed when both cell lines were treated with BHPP. An accumulation of cells at the G_1 phase was observed, with a proportional reduction in the S and G_2-M phase fractions (Fig. 2*B*). Therefore, it is obvious that 12-LOX inhibition induced a G_1 phase arrest in both cell lines. Conversely, treatment with the 5-LOX inhibitor Rev-5901 did not alter the growth phase fractions relative to controls in either cell line.

Effect of 12-LOX Inhibition on Proteins Regulating the G_1 to S Transition in the Cell Cycle. To determine the mechanisms involved in the cell cycle arrest caused by 12-LOX inhibition, the expression of a number of molecules that regulate passage of cells from the G_1 to the S phase of the cell cycle were examined. These include cyclins and their catalytic partners, the CDKs, inhibitors of CDKs, and the Rb family of proteins that govern exit from the G_1 phase (21).

Baicalein treatment (25 μM) resulted in a strong reduction in the expression of the D-type cyclins, D1 and D3 in both PC3 and DU-145 cells, whereas no effect was observed on cyclin E expression (Figs. 3*A* and 4*A*). Cyclin D1 levels were reduced within 3 h of Baicalein treatment and were undetectable by 14 h. Similar results were observed when the cells were treated with 25 μM BHPP (results not shown). Baicalein also resulted in a moderate reduction in CDK-2 and CDK-4 levels after 14 h, with little or no effect on CDK-6. Unexpectedly, Baicalein also resulted in a strong reduction in the CDK inhibitors p21 and p27 over time, resulting in undetectable levels by 24 h. No effect was observed on p16 (Fig. 3*B* and Fig. 4*B*), which inhibits phosphorylation of the Rb protein. The other INK4 family members, p15, p18, and p19, were also unaltered (data not shown). p21 and p27 have a dual function in the cell cycle: inhibition of CDK-cyclin formation, particularly cyclin E-cdk2, as well as facilitating the assembly of cyclinD-cdk4/6 complexes (22).

A.

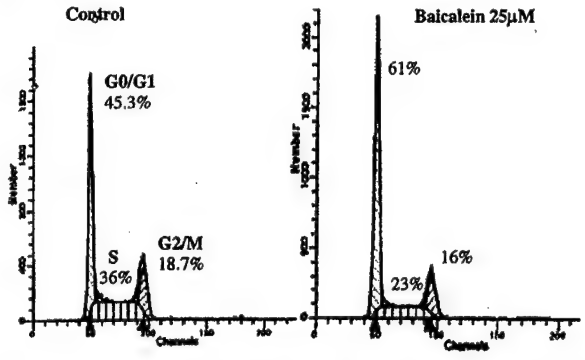

B.

Control	45.3	36.0	18.7	51.0	32.0	16.9
Baicalein 10μM	53.1	29.7	17.2	55.4	30.4	14.2
Baicalein 25μM	61.1	22.9	16.0	67.9	23.6	8.5
BHPP 10mM	49.5	32.5	18.0	56.6	31.8	13.0
BHPP 25mM	56.5	30.4	13.1	63.2	29.5	7.3
Rev-5901 10mM	46.2	30.7	23.1	51.3	32.7	16.0
Rev-5901 25mM	46.4	30.4	23.2	50.9	32.6	16.5

Fig. 2. Representative DNA histogram (*A*) and tabulated percentages (*B*) of cells after LOX inhibition and cell cycle analysis by propidium iodide staining. The 12-LOX inhibitors Baicalein and BHPP induced a specific G_0/G_1 growth phase arrest, indicated by accumulation of cells at this phase, with a corresponding decline in cells in the S (mitotic) phase. The tabulated percentages are an average calculated on the results of two separate experiments.

Effect of 12-LOX Inhibition on RB Protein Family Members. Because cyclin D and CDK-4 govern phosphorylation (inactivation) of the Rb protein during progression of the cell cycle past G_1, the above results would suggest that Rb dephosphorylation may occur in response to 12-LOX inhibition. Rb has been reported recently to be an important factor in directing the choice between permanent arrest and apoptosis in cells (23). Therefore, the phosphorylation state of the Rb protein was examined in PC3 cells. A significant reduction in the phosphorylation of the Rb protein occurred over time after treatment with 25 μM Baicalein (Fig. 3*A*), resulting in undetectable levels within 24 h of treatment. This observation is consistent with a positive contribution toward growth arrest of PC3 cells. Similar results were obtained when cells were treated with the other 12-LOX inhibitor BHPP (data not shown).

DU-145 cells that contain a mutant form of the Rb protein (24) responded in a similar manner to the PC3 cells. This would indicate that functional Rb is not required to mediate the growth arrest induced by 12-LOX inhibition. To examine if other members of the Rb family are associated with this effect, levels of p107 and p130 were examined in the cells after Baicalein treatment. Baicalein induced a decrease in the expression of both p107 and p130 in DU145 cells (Fig. 4*A*). Notably, levels of p130 were undetectable by 24 h. These results suggest that these proteins may compensate for the absence of functional Rb in DU-145 cells.

Effect of 12-LOX Inhibition on Prostate Cancer Cell Apoptosis. To investigate the fate of cells treated with 12-LOX inhibitors, PC3 and DU-145 cells were examined for levels of apoptosis using the TUNEL assay. Baicalein resulted in a dose-dependent increase in apoptosis in both cell lines, determined by FITC-dUTP staining in cells (Fig. 5, *A* and *B*). The induction of apoptosis was time dependent, with little effect occurring in either cell line after 24 h. DU145 cells were more sensitive to apoptosis than PC3 cells, with 63% of cells staining positive after 25 μM Baicalein treatment at 48 h (Fig. 5*B*) compared with 39% in PC3 cells (Fig. 5*A*). After treatment (72 h), apoptosis was significantly higher in PC3 cells (66%) relative to controls, indicating that apoptosis induction was related to length of drug exposure in PC-3 cells.

Treatment with Baicalein (25 μM) over time resulted in dramatic morphological changes in both of the cell lines examined. This was characterized by decreased cell density, elongation, and filamentous protrusions bridging many cells. By 48 h some cells visibly lost anchorage and were floating. This was more evident in the DU145 cells, which underwent apoptosis more quickly (Fig. 5*C*).

Effect of 12-LOX Inhibition on Proteins Regulating Apoptosis. To examine the mechanisms involved in propagating and executing apoptosis in prostate cancer cells, time course experiments were carried out to determine the levels of protein expressed by apoptosis-related genes. Cells were treated with 25 μM Baicalein or BHPP from 0 to 24 h.

In PC-3 cells, Baicalein treatment resulted in a decrease in the antiapoptotic protein Bcl-2 by 14 h (Fig. 6*A*). The proapoptotic protein Bax, which is known to heterodimer with Bcl-2, was increased after treatment with Baicalein as early as 6 h. DU-145 cells did not express detectable levels of Bax. However, another antiapoptotic member of the Bcl-family, Bcl-X_L, was reduced after treatment with Baicalein (Fig. 6*B*). Expression of the proapoptotic proteins Bcl-X_S or Bad, which heterodimer with Bcl-X_L, were unaltered by

A.

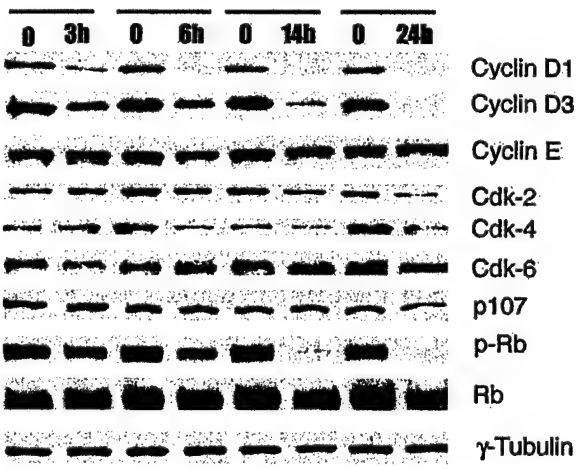

B.

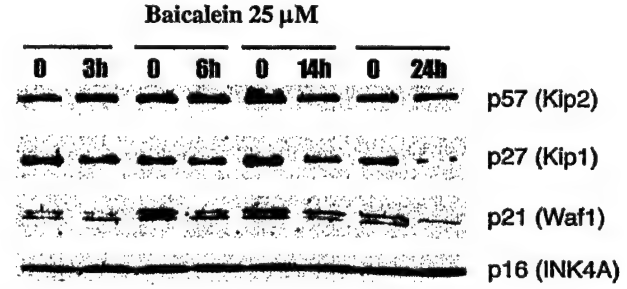

Fig. 3. *A*, protein levels of cyclin-D1, -D3, and -E; CDK-2, -4, and -6; and Rb family proteins, p107, Phos-RB, and RB in Baicalein-treated PC-3 cells. *B*, protein levels of the CDK-inhibitors p16, p21, p27, and p57 in Baicalein-treated cells. Cells were treated with 25 μM Baicalein for different time intervals (0, 3, 6, 14, and 24 h). Protein levels were detected by Western blot. Baicalein treatment resulted in decreased expression of cyclin D1 and D3, and also decreased phosphorylation of the Rb protein.

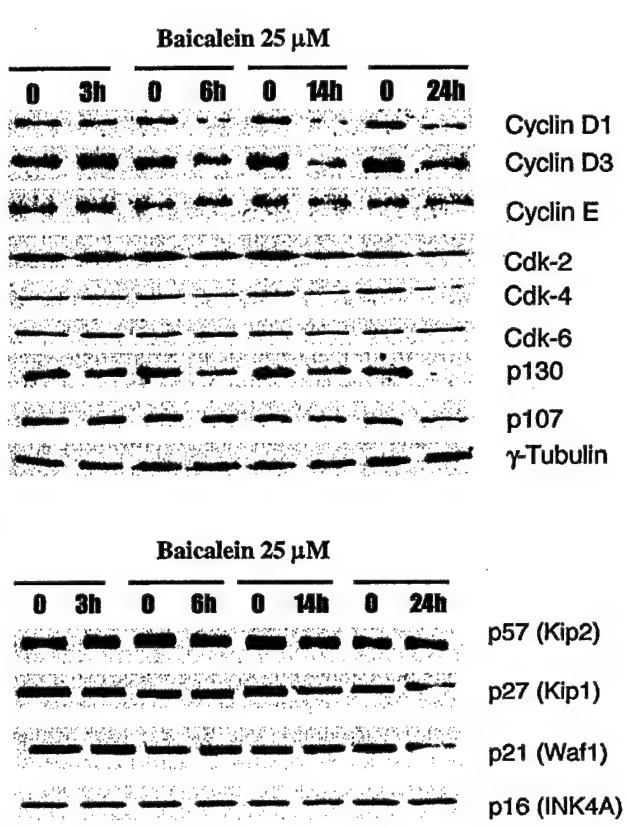

Fig. 4. *A*, protein levels of cyclin-D1, -D3, and –E; CDK-2, -4, and -6; and Rb family proteins, p130, and p107 in Baicalein-treated DU-145 cells. *B*, protein levels of the CDK inhibitors p16, p21, p27, and p57 in Baicalein-treated cells. Cells were treated with 25 μM Baicalein for different time intervals (0, 3, 6, 14, and 24 h). Protein levels were detected by Western blot. The 12-LOX inhibitor Baicalein resulted in a strong decrease in cyclin-D1 and -D3 protein levels, coupled to a decrease in the levels of pRB.

Baicalein treatment. These effects on the Bcl-family proteins would result in a dramatic shift from survival to apoptosis in both cell lines.

The inhibitor of apoptosis family member, survivin, is overexpressed in a variety of human tumors (25). Inhibition of 12-LOX by Baicalein treatment resulted in a strong decrease in survivin protein expression in both PC3 and DU-145 cell lines (Fig. 6, *A* and *B*). Survivin has been shown to inhibit apoptosis by binding to active caspase-3 and caspase-7 (26). During apoptosis active caspase-3 and -7 are formed by cleavage of the zymogens. Caspase-7 has been associated previously with Baicalein-induced apoptosis in gastric cancer cells (17). Treatment with 25 μM Baicalein in both cell lines resulted in active caspase-3 and caspase-7 fragments (Fig. 6*B*). Active caspase was induced by Baicalein at 24 h in PC-3 cells, at which time PARP expression was also reduced, which occurs downstream of caspase-3/7 cleavage. Therefore, it appears that the caspase cascade is involved in Baicalein-induced apoptosis in PC3 cells. PC3 cells did express high levels of phosphorylated-Akt that reduced over time after serum depletion (Fig. 6*A*). DU-145 cell expressed lower levels of Akt, and Baicalein treatment resulted in additional loss of phosphorylated Akt-1 in both cell lines, resulting in undetectable levels by 24 h.

Effect of 12-(S)HETE Add-Back on Apoptosis and Protein Expression Induced by 12-LOX Inhibition. To demonstrate that the effects observed in both cell lines after treatment with the 12-LOX inhibitor Baicalein are a consequence of 12-LOX inhibition, an add-back experiment was performed in which cells were treated with 25 μM Baicalein in the presence of the only product of arachidonic acid metabolization by 12-LOX, *i.e.*, 12(S)-HETE. Treatment with 12(S)-HETE (100 ng/ml) blocked Baicalein-induced apoptosis in both cell lines, reducing apoptosis to 6.6% in PC-3 and 18.6% in DU-145 cells (Fig. 7, *A* and *B*). This protective effect was maintained over time by continued treatment with 12(S)-HETE (at 12-h intervals). Treatment with either 5(S)-HETE or 15(S)-HETE did not block Baicalein-induced apoptosis, with levels of apoptosis similar to Baicalein treated cells (Fig. 7, *A* and *B*).

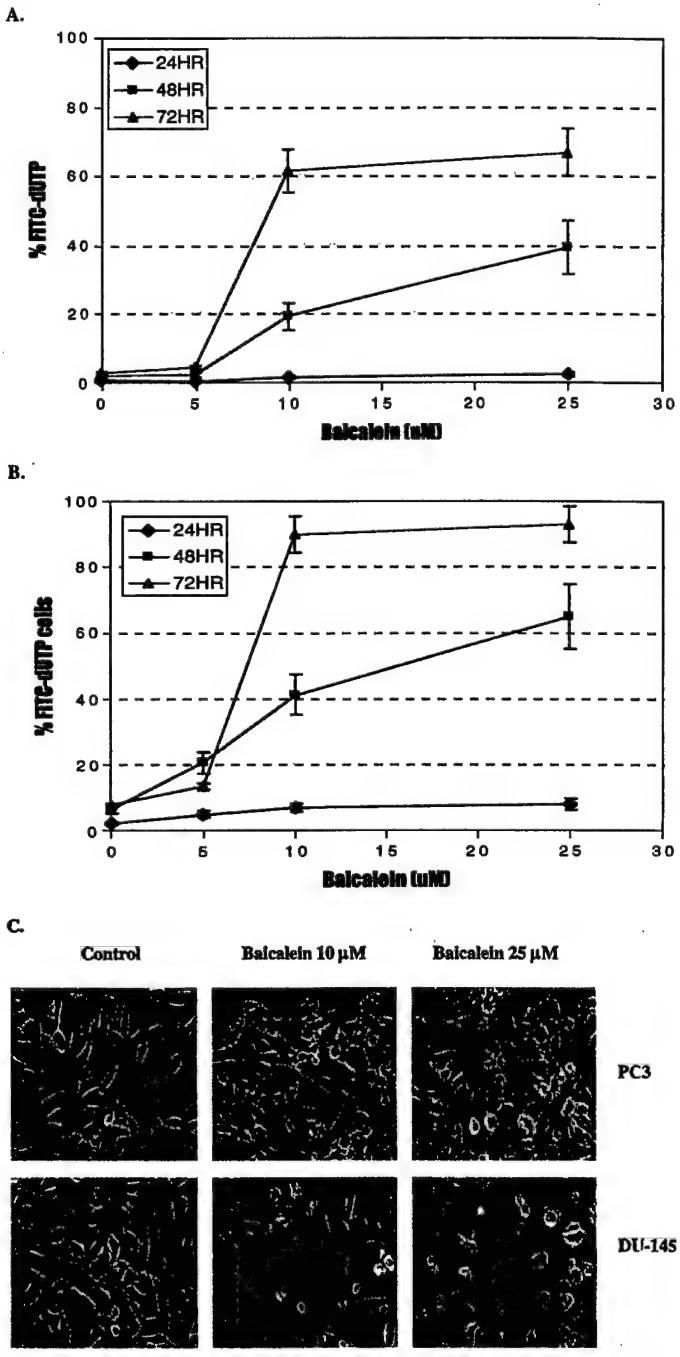

Fig. 5. Effect of Baicalein on apoptosis of PC-3 (*A*) and DU-145 (*B*) prostate cancer cells. The cells were treated with increasing concentrations of the Baicalein (5–25 μM) for 24, 48, or 72 h. DNA fragmentation was measured by FITC-dUTP staining (TUNEL) and detected by flow cytometry. Results were expressed as a percentage of the total cells. Treatment with Baicalein resulted in a dose-dependent increase in apoptosis in both cell lines. DU-145 cells were more sensitive to Baicalein than PC-3 cells, with almost all cells containing DNA fragmentation after 25 μM treatment for 48 h. The percentages are an average calculated on the results of two separate experiments; *bars*, ±SE. *C*, representative PC-3 and DU-145 cells after Baicalein treatment. DU-145 cells are more sensitive to Baicalein, indicated by cell shrinkage and loss of anchorage, characteristics of apoptosis.

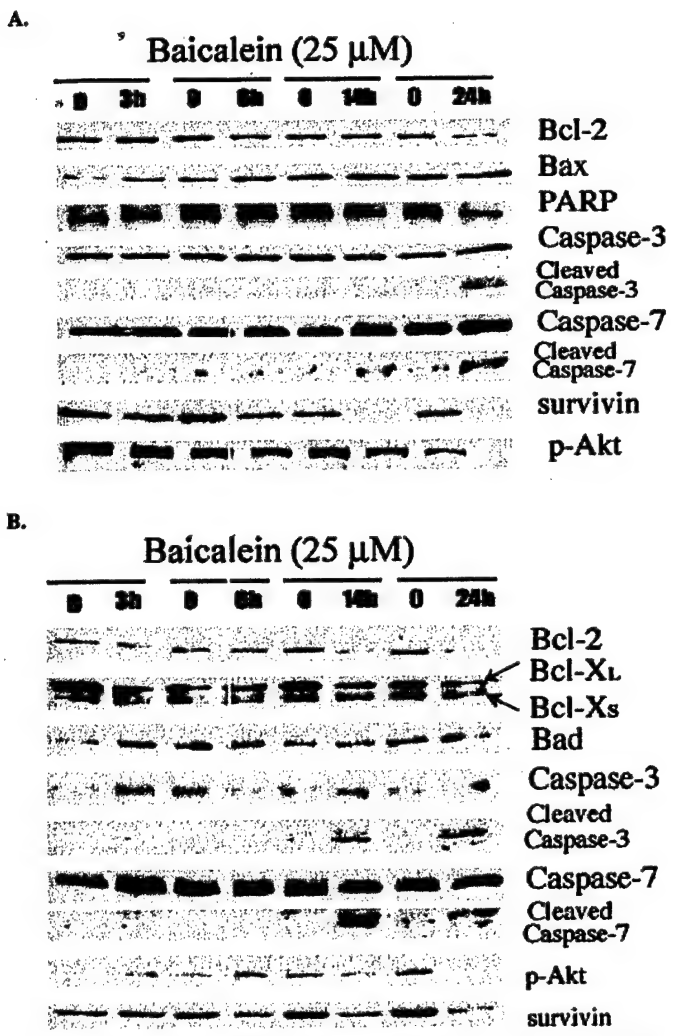

Fig. 6. *A*, protein levels of PARP, caspase-3, -7, Bcl-2, Bax, survivin, and phosphorylated-Akt in Baicalein-treated PC-3 cells. *B*, protein levels of caspase-3, -7, Bcl-X_L, Bcl-X_S, Bad, survivin, and p-Akt in Baicalein-treated DU-145 cells. Cells were treated with 25 μM Baicalein for different time intervals (0, 3, 6, 14, and 24 h). Total protein (30 μg) was probed by Western blot with different antibodies. Baicalein treatment resulted in a strong decrease over time in the survival proteins survivin and phosphorylated Akt in both cell lines. In addition a shift in the Bcl family proteins favoring apoptosis was observed, with reduced Bcl-2 and increased Bax in PC-3 cells, and decreased Bcl-X_L in DU-145 cells.

To additionally demonstrate that the effects observed after Baicalein or BHPP treatment were through inhibition of 12-LOX, PC-3 cells were treated with 12(S)-HETE for 14 h and phosphorylated RB expression examined by Western blot. The Rb protein was selected for this experiment because its levels were reduced most dramatically in response to 12-LOX inhibition, and Rb has been implicated in both cell cycle progression and apoptosis. 12(S)-HETE treatment (100 ng/ml) induced the expression of phosphorylated Rb protein in PC3 cells, whereas neither 5(S)-HETE nor 15(S)-HETE had any effect (Fig. 7*C*). In addition, continuous treatment with 12(S)-HETE blocked Baicalein-induced reductions in phosphorylated Rb at 14 h, whereas 5(S)-HETE and 15(S)-HETE had no such effect (Fig. 7*C*). Treatment with 12(S)-HETE but not 5 or 15(S)-HETE also induced the expression of phosphorylated AKT-1 in both cell lines and blocked Baicalein-induced reductions in this protein (results not shown).

DISCUSSION

The arachidonic acid-metabolizing enzyme 12-LOX and its only metabolite 12(S)-HETE are key regulators of tumor growth. This pathway has been implicated in tumor cell proliferation and motility, regulation of apoptosis, and in tumor angiogenesis (11–13). We have previously shown 12-LOX to be expressed in the prostate cancer cell lines DU-145 and PC3 (15); however, its exact role in these cells is not fully defined. The present study was aimed at investigating the effect of 12-LOX inhibition on prostate cancer cells and more importantly, examining the mechanisms governing these effects. The results from this study indicate that the 12-LOX pathway is essential for prostate cancer growth and survival. Inhibition of 12-LOX by the specific inhibitors Baicalein or BHPP resulted in a dose-dependent decrease in proliferation of both DU-145 and PC3 cells. Inhibition of 5-LOX with Rev-5901 at similar concentrations had no effect on proliferation. These results are similar to those observed in pancreatic cancer cells after 5- or 12-LOX inhibition (13). However, 5-LOX does not appear to be as critical in the two prostate cancer lines studied

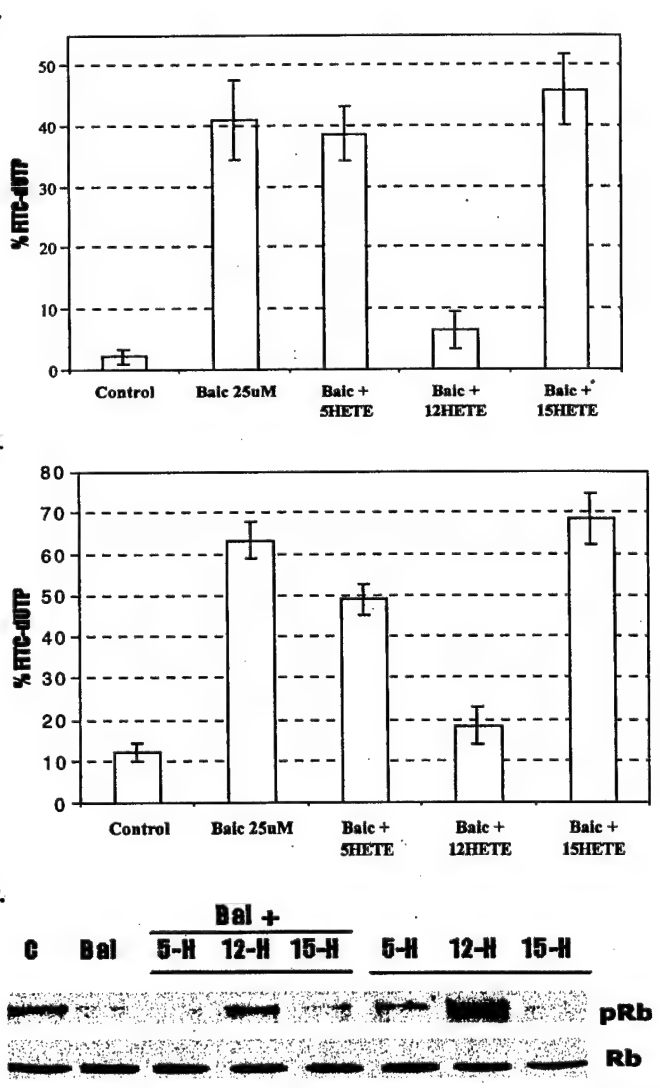

Fig. 7. Effect of 12-HETE on Baicalein-induced apoptosis in PC-3 (*A*) and DU-145 cells (*B*). PC-3 or DU-145 cells were incubated with 100 ng/ml 5(S)-HETE, 12(S)-HETE, or 15(S)-HETE and treated with 25 μM Baicalein for 48 h. HETE incubation was repeated at 12-h intervals. The percentage of apoptotic cells was calculated by FITC-dUTP labeling and flow cytometric determination. Incubation with 12(S)-HETE blocked Baicalein-induced apoptosis, whereas incubation with either 5(S)-HETE or 15(S)-HETE had no protective effect. The percentages are an average calculated on the results of two separate experiments; *bars*, ±SE. *C*, protein levels of pRB in PC-3 cells incubated with 100 ng/ml 5-, 12-, or 15(S)-HETE and treated with 25 μM 12-LOX inhibitor Baicalein for 14 h. Treatment with 12(S)-HETE alone induced the phosphorylation of RB and blocked Baicalein-induced reductions in its expression.

here. It is likely that the family of LOXs are involved in cell survival and that different isoforms are more important than others depending on the cells being studied. For example, 5-LOX has been shown recently to regulate survival of mesothelial cells (27).

To better understand the anticancer effects of 12-LOX inhibition in prostate cancer cells, we investigated which point in the cell cycle is affected by Baicalein or BHPP treatment. Treatment with either 12-LOX inhibitor resulted in a significant growth arrest in the G_0/G_1 phase of both cell lines. The G_1 arrest observed in this report is similar to that observed in response to Baicalein treatment in Hepatoma cells (19), resulting in an associated decrease in the S phase (or mitotic) and G_2-M fractions of Baicalein-treated cells. In contrast, Ding *et al.* (13) reported that Baicalein treatment in pancreatic cancer cells did not induce a specific cell phase arrest and that the inhibition of pancreatic cancer cell proliferation occurred in all phases of the cell cycle. There is substantial evidence that critical regulatory steps occur during the G_1 phase of the cell cycle, which determine whether or not the cell will synthesize DNA and divide. To examine the molecular mechanisms underlying the G_1 phase arrest observed in prostate cancer cells, we examined the levels of the regulatory proteins required for transition past the G_1 restriction point of the cell cycle. Treatment with Baicalein or BHPP resulted in a time-dependent decrease in cyclin D1 and cyclin D3 levels. Within 6 h of treatment with 12-LOX inhibitors, levels of the D-type cyclins were almost undetectable. Inhibition of 12-LOX also led to reductions in the levels of CDK-4 (the catalytic partner of cyclin D1) in both DU-145 and PC3 cells over time.

Cyclin D1 is a proto-oncogenic regulator of the G_1-S phase checkpoint that has been implicated in the pathogenesis of several cancers (28–30). Cyclin D1 functions upstream of the RB protein by binding to CDK-4 or -6 leading to RB phosphorylation. The phosphorylation of RB in mid-to-late G_1 releases the transcription factors bound by RB, resulting in their subsequent binding to the promoter regions of various genes leading to DNA synthesis (31). Within 14 h of treatment with either 12-LOX inhibitor, levels of phosphorylated RB were undetectable in PC3 cells. These results indicate the mechanism of G_1 growth arrest induced by 12-LOX inhibition in PC3 cells: reduction in D-type cyclins, which then result in decreased phosphorylation of RB, resulting in the RB protein remaining bound to the transcription factors required for DNA synthesis. Because DU-145 cells that contain a mutant form of the RB protein (24) responded in a similar manner to the PC3 cells, we examined whether other members of the RB family compensated for the loss of functional RB. We observed a strong reduction in the levels of both p107 and p130 after treatment with Baicalein in DU-145 cells. These results indicate that 12-LOX inhibition does not only result in blocking phosphorylation of functional RB protein but that it may regulate other cell pathways that compensate for mutations in certain cells. Therefore, it suggests a broader potential for Baicalein and BHPP as anticancer agents in a variety of cancers by blocking cell cycle progression. Interestingly, Baicalein treatment also reduced levels of cdk-2, which complexes with cyclin-E later in G_1, to also phosphorylate the RB protein. However, cyclin-E expression remained unchanged after treatment in either cell line. The effects of Baicalein treatment on cell cycle proteins were shown to be through 12-LOX inhibition, as addition of 100 ng/ml of the end product 12(S)-HETE partially restored phosphorylated RB levels. In contrast, addition of 5(S)-HETE or 15(S)-HETE did not restore phosphorylated RB levels after Baicalein treatment. Furthermore, treatment of PC3 cells with 12(S)-HETE alone resulted in increased expression of phosphorylated RB, an effect that was not observed when cells were treated with similar amounts of 5(S)- or 15(S)-HETE.

Because 12-LOX inhibition decreased cell proliferation and perturbed the cell cycle, we were interested in determining the effects of 12-LOX inhibition on prostate cancer cell apoptosis and the underlying mechanisms responsible for these effects. Induction of apoptosis in prostate cancer cells after treatment with an analogue of Baicalein; *i.e.,* baicalin, was reported previously (20). Our results show that Baicalein treatment in PC3 and DU-145 cells directly induces apoptosis, with DU-145 cells being more sensitive to Baicalein-induced apoptosis compared with the PC3 cells.

As illustrated in Fig. 7, we found that simultaneous addition of 12(S)-HETE to Baicalein-treated cells prevented the induction of apoptosis, lowering the apoptotic fraction to 6.6% and 18.6% in PC-3 and DU-145 cells, respectively. However, addition of other LOX products, 5(S)-HETE or 15(S)-HETE, did not protect the cells from Baicalein-induced apoptosis. These results indicate the specific requirement for the 12-LOX pathway for the survival of these cells. There are several reports suggesting that 5-LOX is the critical LOX enzyme mediating survival in prostate cancer cells (32, 33). In these reports the FLAP inhibitor MK886 was shown to induce apoptosis associated with increased oxidative stress. The differences observed in our study could be because a different 5-LOX inhibitor, Rev-5901, was used. This is supported by the fact that the FLAP inhibitor MK886 has been shown to induce apoptosis independent of FLAP inhibition, suggesting an alternate mechanism unrelated to 5-LOX inhibition (34). In addition, unlike the results observed using Baicalein and BHPP, two inhibitors of 5-LOX induced apoptosis by two morphologically distinct pathways in the same cell line, suggesting that 5-LOX inhibition is not the convergent point for apoptosis induction by these inhibitors (35).

In this study, we examined the mechanisms underlying the induction of apoptosis after 12-LOX inhibition. Results from this laboratory have reported previously that the Bcl family of proteins are involved in apoptosis induced by LOX inhibition in rat Walker-256 carcinoma cells (4). In that study LOX inhibition resulted in a down-regulation of the antiapoptotic Bcl-2 protein and a dramatic decrease in the Bcl-2:Bax ratio, which could be blocked by Bcl-2 overexpression. In this study, we found a similar decrease in Bcl-2 levels in both cell lines after 12-LOX inhibition, and this reduction was coupled to an increased expression of the proapoptotic protein Bax in the PC3 cells. DU-145 cells, on the other hand, did not express Bax; however, treatment with Baicalein resulted in decreased expression of another antiapoptotic protein of the same family, Bcl-X_L, whereas levels of its proapoptotic partner, Bcl-X_S, were unaltered. Therefore, in each cell line, Baicalein altered the expression of different Bcl-family protein members, resulting in a shift in their ratios favoring apoptosis, once again suggesting the broad applicability of these inhibitors to cancer treatment.

Survivin, a member of the inhibitor of apoptosis family, is overexpressed in the majority of human cancers, including cancer of the prostate (25, 36). Treatment with Baicalein resulted in a strong decrease in survivin expression over time, resulting in undetectable levels in both PC3 and DU-145 cells by 14 h. Survivin has been shown to inhibit apoptosis by binding to active caspase-3 and caspase-7 (26). In our study, we observed that treatment of both cells with Baicalein resulted in increased expression of active caspase-3 and caspase-7. These time points correlated with decreased levels of the survivin protein. In addition, we observed decreased PARP levels in PC3 cells after 24-h treatment with Baicalein, which occurs downstream of caspase-3/7 cleavage. These results indicate that caspase-mediated apoptosis, in response to decreases in survivin expression, is responsible for apoptosis observed after 12-LOX inhibition. A recent report has observed a strong association of survivin expression with Bcl-2 expression in cervical carcinoma tissues (37), indicating that survivin may be related to the Bcl family protein expression. Our results support this association, as we observed decreased survivin and

reduced Bcl-2 protein expression in response to 12-LOX inhibition in both cell lines. We also observed decreased levels of phosphorylated Akt-1 in both PC3 and DU-145 cells after treatment with Baicalein or BHPP. Akt activation has been shown previously to induce survival and suppress apoptosis through increased phosphorylation of Bad and subsequent liberation of antiapoptotic proteins of the Bcl family (38). Therefore, decreased expression of Bcl-2 and Bcl-X_L in the cells may also be a result of decreased levels of phosphorylated Akt after 12-LOX inhibition. Interestingly, Akt has also been shown to enhance the translation of cyclin D1 (39), and previous reports have shown that treatment with antisense cyclin D1 resulted in a strong induction of apoptosis in human squamous carcinoma (40). Our results implicate a similar mechanism may be involved in prostate cancer cells, and that Baicalein-induced decreases in phosphorylated-Akt may affect both progression through the cycle and apoptosis in prostate cancer cells. In either case, the fact that two major apoptotic pathways are stimulated simultaneously in response to 12-LOX inhibition highlight its critical role in cell survival.

In summary, we have shown that the 12-LOX pathway of arachidonic acid metabolism regulates cell growth, survival, and apoptosis of human prostate cancer cells. Inhibition of 12-LOX led to growth inhibition associated with a specific G_1 arrest, followed by induction of apoptosis through caspase and Bcl-mediated mechanisms. Therefore, the inhibition of 12-LOX is a potential therapeutic approach in the treatment of prostate cancer.

REFERENCES

1. Eling, T. E., and Glasgow, W. C. Cellular proliferation and lipid metabolism: importance of lipoxygenases in modulating epidermal growth factor dependent mitogenesis. Cancer Metastasis Rev., *3:* 397–410, 1994.
2. Honn, K. V., Tang, D. G., Gao, X., Butovich, I. A., Liu, B., Timar, J., and Hagmann, W. 12-Lipoxygenase and 12(S)-HETE: role in cancer metastasis. Cancer Metastasis Rev., *13:* 365–396, 1994.
3. Tang, D. G., Renaud, C., Stojakovic, S., Diglio, C. A., Porter, A., and Honn, K. V. 12(S)-HETE is a mitogenic factor for micro-vascular endothelial cells: its potential role in angiogenesis. Biochem. Biophys. Res. Commun., *211:* 462–468, 1995.
4. Tang, D. G., Chen, Y. Q., and Honn, K. V. Arachidonate lipoxygenases as essential regulators of cell survival and apoptosis. Proc. Natl. Acad. Sci. USA, *93:* 5241–5246, 1996.
5. Kuhn, H., and Thiele, B. J. The diversity of the lipoxygenase family. Many sequence data but little information on biological significance. FEBS Lett., *449:* 7–11, 1999.
6. Brash, A. R. Lipoxygenases: occurrence, functions, catalysis, and acquisition of substrate. J. Biol. Chem., *274:* 23679–23682, 1999.
7. Funk, C. D., Furci, L., and Fitzgerald, G. A. Molecular cloning, primary structure, and expression of the human platelet/erythroleukemia cell 12-lipoxygenase. Proc. Natl. Acad. Sci. USA, *87:* 5638–5642, 1990.
8. Yoshimoto, T., Suzuki, H., Yamamoto, S., Takai, T., Yokoyama, C., and Tanabe, T. Cloning and sequence analysis of the cDNA for arachidonate 12-lipoxygenase of porcine leukocytes. Proc. Natl. Acad. Sci. USA, *87:* 2142–2146, 1990.
9. Natarajan, R., Esworthy, R., Bai, W., Gu, J. L., Wilczynski, S., and Nadler, J. L. Increase 12-lipoxygenase expression in breast cancer cells and tissues. Regulation by epidermal growth factor. J. Clin. Endocrinol. Metab., *82:* 1790–1798, 1997.
10. Kamitani, H., Geller, M., and Eling, T. The possible involvement of 15-lipoxygenase/leukocyte type 12-lipoxygenase in colorectal carcinogenesis. Adv. Exp. Med. Biol., *469:* 593–598, 1999.
11. Nie, D., Hillman, G. G., Geddes, T., Tang, K., Pierson, C., Grignon, D. J., and Honn, K. V. Platelet-type 12-lipoxygenase in a human prostate carcinoma stimulates angiogenesis and tumor growth. Cancer Res., *58:* 4047–4051, 1998.
12. Timar, J., Rasa, E., Honn, K. V., and Hagmann, W. 12-lipoxygenase expression in human melanoma cell lines. Adv. Exp. Med. Biol., *469:* 617–622, 1999.
13. Ding, X. Z., Kuszynski, C. A., El-Metwally, T. H., and Adrian, T. E. Lipoxygenase inhibition induced apoptosis, morphological changes, and carbonic anhydrase expression in human pancreatic cancer cells. Biochem. Biophys. Res. Commun., *266:* 392–399, 1999.
14. Nappez, C., Liagre, B., and Beneytout, J. L. Changes in lipoxygenase activities in human erythroleukemia (HEL) cells during diosgenin-induced differentiation. Cancer Lett., *96:* 133–140, 1995.
15. Timar, J., Raso, E., Dome, B., Li, L., Grignon, D., Nie, D., Honn, K. V., and Hagmann, W. Expression, subcellular localization and putative function of platelet-type 12-lipoxygenase in human prostate cancer cell lines of different metastatic potential. Int. J. Cancer, *87:* 37–43, 2000.
16. Gao, X., Grignon, D. J., Chbihi, T., Zacharek, A., Chen, Y. Q., Sakr, W., Porter, A. T., Crissman, J. D., Pontes, J. E., Powell, I. J., *et al.* Elevated 12-lipoxygenase mRNA expression correlates with advanced stage and poor differentiation of human prostate cancer. Urology, *46:* 227–237, 1995.
17. Wong, B. C., Wang, W. P., Cho, C. H., Fan, X. M., Lin, M. C., Kung, H. F., and Lam, S. K. 12-Lipoxygenase inhibition induced apoptosis in human gastric cancer cells. Carcinogenesis (Lond.), *22:* 1349–1354, 2001.
18. Kuntz, S., Wenzel, U., and Daniel, H. Comparative analysis of the effects of flavonoids on proliferation, cytotoxicity, and apoptosis in human colon cancer cell lines. Eur. J. Nutr., *38:* 133–142, 1999.
19. Chen, C. H., Huang, L. L., Huang, C. C., Lin, C. C., Lee, Y., and Lu, F. J. Baicalein, a novel apoptotic agent for hepatoma cell lines: a potential medicine for hepatoma. Nutr. Cancer, *38:* 287–295, 2000.
20. Chan, F. L., Choi, H. L., Chen, Z. Y., Chan, P. S., and Huang, Y. Induction of apoptosis in prostate cancer cell lines by a flavanoid, baicalin. Cancer Lett., *160:* 219–228, 2000.
21. Collins, K., Jacks, T., and Pavletich, N. P. The cell cycle and cancer. Proc. Natl. Acad. Sci. USA, *94:* 2776–2778, 1997.
22. Sherr, C. J., and Roberts, J. M. CDK inhibitors: positive and negative regulators of G_1-phase progression. Genes Dev., *13:* 1501–1512, 1999.
23. Wang, J. Y., and Ki, S. Choosing between growth arrest and apoptosis through the retinoblastoma tumor suppressor protein, Abl and p73. Biochem. Soc. Trans., *29:* 666–673, 2001.
24. Rubin, S. J., Hallahan, D. E., Ashman, C. R., Brachman, D. G., Beckett, M. A., Virudachalam, S., Yandell, D. W., and Weichselbaum, R. R. Two prostate carcinoma cell lines demonstrate abnormalities in tumor suppressor genes. J. Surg. Oncol., *46:* 31–36, 1991.
25. Ambrosini, G., Adida, C., and Altieri, D. C. A novel anti-apoptosis gene, survivin, expressed in cancer and lymphoma. Nat. Med., *8:* 917–921, 1997.
26. LaCasse, E. C., Baird, S., Korneluk, R. G., and MacKenzie, A. E. The inhibitors of apoptosis (IAPs) and their emerging role in cancer. Oncogene, *17:* 3247–3259, 1998.
27. Romano, M., Catalano, A., Nutini, M., D'Urbano, E., Crescenzi, C., Claria, J., Libner, R., Davi, G., and Procopio, A. 5-lipoxygenase regulates malignant mesothelial cell survival: involvement of vascular endothelial growth factor. FASEB J., *15:* 2326–2336, 2001.
28. Xu, L., Davidson, B. J., Murty, V. V., Li, R. G., Sacks, P. G., Garin-Chesa, P., Schantz, P., and Chaganti, R. S. TP53 gene mutations and CCND1 gene amplification in head and neck squamous cell carcinoma cell lines. Int. J. Cancer, *59:* 383–3887, 1994.
29. Bala, S., and Peltomaki, P. Cyclin D1 as a genetic modifier in hereditary nonpolyposis colorectal cancer. Cancer Res., *61:* 6042–6045, 2001.
30. Deane, N. G., Parker, M. A., Aramandla, R., Diehl, L., Lee, W. J., Washington, M. K., Nanney, L. B., Shyr, Y., and Beauchamp, R. D. Hepatocellular carcinoma results from chronic cyclin D1 overexpression in transgenic mice. Cancer Res., *61:* 5398–5395, 2001.
31. Harbour, J. W., and Dean, D. C. Rb function in cell-cycle regulation and apoptosis. Nature Cell Biol., *2:* 65–67, 2000.
32. Ghosh, J., and Myers, C. E. Arachidonic acid stimulates prostate cancer cell growth: Critical role of 5-lipoxygenase. Biochem. Biophys. Res. Comm., *235:* 418–423, 1997.
33. Ghosh, J., and Myers, C. E. Inhibition of arachidonate 5-lipoxygenase triggers massive apoptosis in human prostate cancer cells. Proc. Natl. Acad. Sci. USA, *95:* 13182–13187, 1998.
34. Datta, K., Biswal, S. S., and Kehrer, J. P. The 5-lipoxygenase-activating protein (FLAP) inhibitor, MK886, induces apoptosis independently of FLAP. Biochem. J., *340:* 371–375, 1999.
35. Anderson, K. M., Seed, T., Vos, M., Mulshine, J., Meng, J., Alrefai, W., Ou, D., and Harris, J. E. 5-Lipoxygenase inhibitors reduce PC-3 cell proliferation and initiate non-necrotic cell death. Prostate, *37:* 161–173, 1998.
36. Xing, N., Qian, J., Bostwick, D., Bergstralh, E., and Young, C. Y. Neuroendocrine cells in human prostate over-express the anti-apoptosis protein survivin. Prostate, *48:* 7–15, 2001.
37. Wang, M., Wang, B., and Wang, X. A novel antiapoptosis gene, survivin, BCL-2, p53 expression in cervical carcinomas. Zhonghua Fu Chan Ke Za Zhi, *36:* 546–548, 2001.
38. Datta, S. R., Dudek, H., Tao, X., Masters, S., Fu, H., Gotoh, Y., and Greenberg, M. E. Akt phosphorylation of BAD couples survival signals to the cell-intrinsic death machinery. Cell, *91:* 231–241, 1997.
39. Muise-Helmericks, R. C., Grimes, H. L., Bellacosa, A., Malstrom, S. E., Tsichlis, P. N., and Rosen, N. Cyclin D expression is controlled post-transcriptionally via a phosphatidylinositol 3-kinase/Akt-dependent pathway. J. Biol. Chem., *273:* 29864–29872, 1998.
40. Sauter, E. R., Nesbit, M., Litwin, S., Klein-Szanto, A. J., Cheffetz, S., and Herlyn, M. Antisense cyclin D1 induces apoptosis and tumor shrinkage in human squamous carcinomas. Cancer Res., *59:* 4876–4881, 1999.

THE JOURNAL OF BIOLOGICAL CHEMISTRY
Vol. 275, No. 49, Issue of December 8, pp. 38831–38841, 2000
Printed in U.S.A.

Eicosanoid Activation of Extracellular Signal-regulated Kinase1/2 in Human Epidermoid Carcinoma Cells*

Received for publication, March 29, 2000, and in revised form, August 17, 2000
Published, JBC Papers in Press, August 21, 2000, DOI 10.1074/jbc.M002673200

Charles K. Szekeres‡§, Keqin Tang‡§, Mohit Trikha‡§, and Kenneth V. Honn‡§¶‖

From the ‡Department of Radiation Oncology and the ¶Departments of Pathology and Chemistry, Wayne State University, Detroit and the §Karmanos Cancer Institute, Detroit, Michigan 48202

12(*S*)-Hydroxyeicosatetraenoic acid (12(*S*)-HETE), a 12-lipoxygenase metabolite of arachidonic acid, has multiple effects on tumor and endothelial cells, including stimulation of invasion and angiogenesis. However, the signaling mechanisms controlling these physiological processes are poorly understood. In a human epidermoid carcinoma cell line (*i.e.* A431), 12(*S*)-HETE activates extracellular signal-regulated kinases 1/2 (ERK1/2), which is mediated by upstream kinases MEK and Raf. 12(*S*)-HETE stimulates phosphorylation of phospholipase Cγ1 and activity of protein kinase Cα (PKCα). In addition, independent of PKC 12(*S*)-HETE increases tyrosine phosphorylation of Shc, and Grb2, stimulates association between Shc and Src, and increases the activity of Ras, via Src family kinases. Furthermore, at low (10–100 nM) concentrations 12(*S*)-HETE counteracts epidermal growth factor-stimulated activation of ERK1/2 via stimulating protein tyrosine phosphatases. We also present evidence that 12(*S*)-HETE stimulates ERK1/2 via G proteins and that A431 cells have multiple binding sites for 12(*S*)-HETE. Finally, inhibition of 12-lipoxygenase induced apoptosis of A431 cells, which was reversed by addition of exogenous 12(*S*)-HETE. Collectively we demonstrate that the activation of ERK1/2 by 12(*S*)-HETE may be regulated by multiple receptors triggering PKC-dependent and PKC-independent pathways in A431 cells.

Tumor cell-host interactions are fundamentally influenced by bioactive lipids produced by the tumor cells themselves, as well as by the infiltrating leukocytes, monocytes, and by aggregation with platelets (1). Previous studies have demonstrated that one of the most important lipid metabolites to influence tumor progression is the lipoxygenase metabolite 12(*S*)-hydroxyeicosatetraenoic acid (12(*S*)-HETE).[1] This eicosanoid stimulates several steps of tumor invasion and motility (2–4), protects tumor cells from apoptosis (5), and promotes angiogenesis (6). Initial studies suggest that the pleiotropic effects of 12(*S*)-HETE on tumor cells are mediated by an eicosanoid receptor which activates protein kinase C (PKC) (7).

The extracellular signal-regulated kinases, ERK1 and -2, also known as p44 and p42 mitogen-activated protein kinases (p42/44 MAPK), respectively, are well characterized as convergence points of numerous signal transduction pathways. Through their diverse substrates, ERKs modulate nuclear, as well as cytoplasmic events in cells resulting in increased proliferation (8), differentiation (9), changes in cell morphology (9), and motility (10). It is well established that receptor-tyrosine kinases activate ERK via the consecutive stimulation of the guanine nucleotide exchange factor Sos, monomeric G protein Ras, and the Raf-MEK-MAPK cascade of protein kinases. In addition to growth factor receptors with tyrosine kinase activity, G protein-coupled receptors also are stimulators of ERK. G proteins can influence ERK activity via multiple mechanisms (11), which include activation of tyrosine kinases such as the EGF receptor (12) or Src (13), stimulating the early stages of the conventional cascade. Alternatively, G proteins may activate ERK by promoting the production of lipid second messengers via phospholipase C (PLC) or phosphatidylinositide 3-kinase resulting in the activation of PKC. Protein kinase C in turn can stimulate the ERK cascade through Raf and MEK.

An earlier study, reported that 12(*S*)-HETE increased the tyrosine phosphorylation of cellular proteins migrating in the 40–50-kDa range (14), which led us to hypothesize that ERK1/2 may be mediators of 12(*S*)-HETE-induced cellular responses.

In this study we identify ERK1/2 as signaling targets of exogenous 12(*S*)-HETE in A431 epidermoid carcinoma cells, and we describe the signaling mechanisms leading to this stimulation through the following: (*a*) the Src family-mediated activation of PLCγ1 and PKCα, (*b*) Src family-mediated tyrosine phosphorylation of Shc and subsequent stimulation of the Raf/MEK/ERK cascade via Ras. Furthermore, we provide evidence for the involvement of G proteins in 12(*S*)-HETE signaling.

EXPERIMENTAL PROCEDURES

Antibodies and Reagents—Anti-phospho-specific ERK, anti-phospho-specific MEK, anti-phospho-specific Elk, and phospho-specific epidermal growth factor (EGF) receptor antibodies were purchased from New England Biolabs (Beverly, MA). Anti-phospho-specific PKCα was purchased from Upstate Biotechnology, Inc. (Lake Placid, NY). Anti-pan-ERK, Ras, MEK, PY20, Shc, Grb2, anti-PKCα, and PKC sampler kit antibodies to screen PKC isotype expression were from Transduction Laboratories (Lexington, KY). Anti-actin was from ICN (Costa Mesa, CA), and horseradish peroxidase-conjugated secondary antibodies were purchased from Amersham Pharmacia Biotech. Anti-Raf-1, PLCβ2, PLCγ1, and Src (SRC 2, which recognizes Src, Yes, and Fyn) were from Santa Cruz Biotechnology (Santa Cruz, CA). 5-, 11-, 12-, and 15(*S*)-HETE were purchased from Cayman Chemicals (Ann Arbor, MI). Protein G-Sepharose 4B was from Zymed Laboratories Inc. (South San

* This work was supported by National Institutes of Health Grant CA 29997 (to K. V. H.). The costs of publication of this article were defrayed in part by the payment of page charges. This article must therefore be hereby marked "*advertisement*" in accordance with 18 U.S.C. Section 1734 solely to indicate this fact.

‖ To whom correspondence should be addressed: 431 Chemistry Bldg., Wayne State University, Detroit, MI 48202. Tel.: 313-577-1018; Fax: 313-577-0798; E-mail: k.v.honn@wayne.edu.

[1] The abbreviations used are: 12(*S*)-HETE, 12(*S*)-hydroxyeicosatetraenoic acid; ERK, extracellular signal-regulated kinase; MAPK, mitogen-activated protein kinase; PLC, phospholipase C; PKC, protein kinase C; Shc, Src homology collagen; EGF, epidermal growth factor; EGFR, epidermal growth factor receptor; Grb2, growth factor-bound protein 2; Me_2SO, dimethyl sulfoxide; DMEM, Dulbecco's modified Eagle's medium; PBS, phosphate-buffered saline; RBD, Ras binding domain; PMA, phorbol myristate acetate; PDGF, platelet-derived growth factor; FGF, fibroblast growth factor; FTase, farnesyltransferase; MEK, MAPK/ERK kinase; 12-LOX, 12-lipoxygenase; BHPP, *N*-benzyl-*N*-hydroxy-5-phenylpentanamide.

Francisco, CA). The inhibitors Go6976 (inhibitor of conventional PKC isozymes, IC_{50} 2.3 nM (15), solvent: ethanol), PP2 (inhibitor of Src family kinases (16), solvent: ethanol), PD98059 (inhibitor of MEK, IC_{50} 2 μM (17) solvent: ethanol), Tyrphostin51 (inhibitor of EGF receptor tyrosine kinase, IC_{50} 800 nM (18), solvent: Me_2SO), FTase inhibitor II (inhibitor of farnesyltransferase, IC_{50} 50 nM (19) solvent: H_2O), and suramin (inhibitor of G protein-receptor coupling (20) solvent: H_2O) were from Calbiochem. The specific peptide substrate for Src kinase assay, KVEKIGEGTYGVVYK, was purchased from Upstate Biotechnology, Inc. The 12-lipoxygenase-selective inhibitor *N*-benzyl-*N*-hydroxy-5-phenylpentanamide, BHPP (21), was a generous gift from Biomide Corp (Grosse Pointe Farms, MI). All other chemicals were obtained from Sigma.

Cell Culture—The human epidermoid carcinoma cell line A431 (American Tissue Culture Collection, Manassas, VA) was cultured in Dulbecco's modified Eagle's media (DMEM) supplemented with 10% fetal bovine serum (Life Technologies, Inc.) and 25 mg/liter gentamicin (Life Technologies, Inc.). Cells were passaged with 0.05% trypsin-EDTA.

Platelet type 12 lipoxygenase-transfected A431 cells were described earlier (22).

For drug treatments, A431 cells (1.5×10^6) were plated in 6-well plates, cultured for 1 day in DMEM supplemented with 10% fetal bovine serum, and then serum-starved overnight (20 h). Fresh serum-free DMEM was added 1 h prior to treatments. Inhibitors (at the concentrations indicated in the figure legends) or vehicle (0.1%) treatment was 15 min before stimulation with 12(*S*)-HETE or other chemicals, with the exception of farnesyltransferase inhibitor (FTase inhibitor II, 1 h) and Src family kinase inhibitor (PP2, 30 min).

Immunoblotting—Cells were rinsed twice with ice-cold phosphate-buffered saline (PBS) and lysed with 200 μl of boiling gel loading buffer (20% glycerol; 2% SDS; 2.5×10^{-2}mg/ml bromphenol blue; 125 mM Tris base, pH 6.8; 5% 2-mercaptoethanol). Cell lysates were sonicated briefly and boiled for 5 min. Aliquots (20 μl) were resolved on 10 or 4–20% SDS-polyacrylamide gels (the latter from Fisher) and electrotransferred onto nitrocellulose membrane (Bio-Rad). In gels used to detect the mobility shift of phosphorylated proteins, the acrylamide:bisacrylamide ratio was 118:1. Membranes were probed with the antibodies indicated in the text, and bands were visualized with the Supersignal system (Pierce). Blots were routinely stripped at 50 °C for 30 min in stripping buffer (0.7% 2-mercaptoethanol; 2% SDS; 62.5 mM Tris-HCl, pH 6.7) and reprobed with other antibodies. Densitometric analysis of the Western blots was performed with an LKB 2222–010 UltroScan XL laser densitometer (Bromma, Sweden).

Immunoprecipitation—Cells were serum-starved overnight, pretreated with drugs, followed by washing with ice-cold PBS. For immunoprecipitation under denaturing conditions, cells were lysed (200 μl boiling 1% SDS; 10 mM Tris, pH 7.4), boiled for 5 min, and briefly sonicated. Cell lysates were centrifuged (13,000 × *g*, 5 min), and equal amounts of debris-free supernatant was mixed with 1 ml of IP buffer (1% Triton X-100; 150 mM NaCl; 10 mM Tris, pH 7.4; 1 mM EDTA; 1 mM EGTA; 0.2 mM Na_3VO_4; 0.2 mM PMSF; 0.5% Nonidet P-40) and anti-phosphotyrosine (3 μg) or other antibodies (1 μg). In the case of non-denaturing immunoprecipitation, cells were rinsed with ice-cold PBS and scraped off into 1 ml of ice-cold IP buffer, sonicated, incubated with agitation for 30 min at 4 °C, and centrifuged (13,000 × *g*, 10 min) to remove insoluble material. Equal amounts of protein were mixed with 2 μg of antibody for 3 h and then with 50 μl of protein G-Sepharose. After overnight incubation (4 °C), beads were washed twice with dilution buffer (10 mM Tris-HCl, pH 8.0; 140 mM NaCl; 0.1% Triton X-100; 0.1% BSA; 0.025% NaN_3) and once with TSA solution (10 mM Tris-HCl; 140 mM NaCl; 0.025% NaN_3). For PLCβ2 coprecipitation with Gβ antibody anti-Gβ (2 μg) was mixed with protein G-Sepharose (50 μl) for 3 h and then washed (2 times) with IP buffer before mixing with cell lysates. Immunocomplexes were denatured by boiling in gel loading buffer.

ERK Kinase Assay—Kinase assays were performed using an MAPK assay kit from New England Biolabs according to the manufacturer's recommendations. Briefly, activated ERK was precipitated from cell lysates using anti-phospho-ERK antibody, and precipitates were incubated with a specific substrate, Elk-1, and ATP. The reaction was terminated by adding boiling gel loading buffer. ERK activity was detected by immunoblotting the products of the kinase reaction with anti-phospho-Elk antibody.

Raf Kinase Assay—Raf kinase assay was performed using the c-Raf1 immunoprecipitation kinase cascade assay kit from Upstate Biotechnology, Inc., according to the protocol provided by the manufacturer. Briefly, Raf was precipitated and incubated with GST-MEK and GST-ERK1 in [^{32}P]ATP (PerkinElmer Life Sciences) containing buffer. ERK1 was recovered on phosphocellulose paper, and the incorporated radioactivity was measured with a 1900TR Liquid Scintillation Analyzer (Packard Instrument Co.).

Src Kinase Assay—After various treatments, A431 cells were lysed, and Src was precipitated under non-denaturing conditions with anti-Src polyclonal antibody (SRC2; 3 μg/sample). Precipitates were washed (1 time) with lysis buffer and then (3 times) with 0.5 M LiCl, Tris-HCl, pH 7.5, and 1 time in 25 mM Tris-HCl, pH 7.5, then resuspended and incubated at room temperature for 30 min in 15 μl of kinase buffer (50 mM Tris-HCl, pH 7.5; 5 mM $MgCl_2$; 25 μM ATP; 1 μg/sample Src substrate; 5 μCi of [^{32}P]ATP). The reaction was terminated by adding 20 μl of 2× gel loading buffer and boiling for 5 min. Samples were run on 15% SDS-polyacrylamide, and incorporated radioactivity was quantitated with a Storm 940 PhosphorImager (Molecular Dynamics, Sunnyvale, CA).

Ras Assay—Ras activity was assessed using Raf-1 RBD (Upstate Biotechnology, Inc.) according to the manufacturer's protocol. Briefly, beads conjugated to the Ras binding domain (RBD) of Raf were used to precipitate GTP-bound Ras. The amount of precipitated Ras was determined by Western blotting, with a pan antibody that recognizes all human isoforms of Ras.

PKC Translocation—Translocation of PKC was determined as described previously (7, 23). Following 12(*S*)-HETE treatment, cells were rinsed (twice) with cold PBS, scraped off, and homogenized with 26-gauge needle in 2 ml of buffer A (25 mM Tris-HCl, pH 7.6; 1 mM EGTA; aprotinin (5 μg/ml); leupeptin (10 μg/ml) and 1 mM PMSF). Membrane and cytosolic fractions were separated by centrifugation (100,000 × *g*; 1 h, 4 °C). The membrane fraction was rinsed (twice) with buffer A and resuspended in buffer A containing 1% Nonidet P-40. Samples were applied to a 1-ml DEAE-Sepharose column (Sigma) equilibrated with buffer B (20 mM Tris-HCl, pH 7.5; 2 mM EDTA; 1 mM 2-mercaptoethanol; 0.2 mM PMSF; 0.15 mM pepstatin A). PKC was eluted with 2 ml of buffer B containing 120 mM NaCl. Samples were concentrated using a Centricon (Amicon, Beverly, MA), and the protein concentration was determined with the BCA protein assay kit (Pierce).

Inhibition of PKC Activity—PKC activity was inhibited using two approaches. First, cells were treated with PKC inhibitor as described above. Second, PKC protein level in A431 cells was down-regulated with chronic PMA treatment (22 h, 100 nM) in serum-free media (24). Phorbol ester-containing media were removed 1 h prior to initiating treatment with various drugs, and cells were washed (twice) with serum-free DMEM.

Binding Assay—2×10^5 cells were plated per well of 24-well plates (Corning Glass), cultured for 1 day under regular growth conditions, and then serum-starved overnight. Prior to performing the binding assay, cell count/well was determined, and media were changed to 12.5 mM HEPES, pH 7.4, containing 4 °C cold DMEM, and plates were placed at 4 °C for 30 min. Binding assay was initiated by adding [^{3}H]12(*S*)-HETE with or without 1000× concentration of cold 12(*S*)-HETE or other eicosanoids in DMEM/HEPES at final volume of 400 μl. The plates were kept under constant and gentle swirling at 4 °C for the times indicated in the text. Following the incubation period 50% of the binding media was set aside and the rest decanted, and plates were washed 4 times with PBS, and cells were solubilized with 300 μl of 0.1 M NaOH for 10 min at room temperature. Cell lysates or 200 μl of the binding media were mixed with Ultima Gold scintillation liquid (Packard Instrument Co.), and radioactivity was measured with a Packard 1900TR scintillation counter. Each sample was counted for 20 min to accumulate at least 500 counts. Data points under 3 nM [^{3}H]12(*S*)-HETE concentration represent the mean of triplicate determinations, and at higher concentrations duplicates were used.

Analysis of [^{3}H]12(S)-HETE Incorporation into Membrane Fraction—3×10^6 cells were incubated similar to binding assay with 3 nM [^{3}H]12(*S*)-HETE in the presence or absence of 300 nM (100 times) cold 12(*S*)-HETE for 30 min and rinsed 4 times with PBS; cells were scraped off and homogenized with brief sonication in 2 ml of buffer A (25 mM Tris-HCl, pH 7.6; 1 mM EGTA; aprotinin (5 μg/ml); leupeptin (10 μg/ml) and 1 mM PMSF). Membrane and cytosolic fractions were separated by centrifugation (100,000 × *g*; 1 h, 4 °C). The membrane fraction was rinsed (4 times) with buffer A and solubilized with sonication in 1% SDS, 10 mM Tris, pH 7.4. Lipids were extracted with 1 ml of chloroform:methanol (1:1). Lipids dissolved in the chloroform layer were loaded on Whatman silica gel 60A thin layer chromatography plates and developed with ethyl acetate:methyl chloride:glacial acetic acid (5:5:1). Plates were dried, and position of lipids was determined following treatment with iodine vapor. Ten identical areas of each lane were scraped into scintillation vials, and Ultima Gold scintillation fluid

added and radioactivity measured with a Packard 1900TR scintillation counter.

DNA Fragmentation Assay—Cells (2.5×10^6) were grown in 10-cm tissue culture dishes in DMEM until 90% confluent and serum-starved (18 h) prior to experimental use. Cells were washed with PBS (3 times) and then either treated with BHPP at different concentrations (25, 50, 100 μM) for 24 h or pretreated with 12(*S*)-HETE at 1 μM for 5 h. Equal amounts of ethanol were used as a vehicle control. Subsequently, cells were harvested with a rubber policeman, and fragmented DNA was extracted with 200 μl of the lysis buffer (50 nM Tris-HCl, pH 7.5, 20 mM EDTA, 1% Nonidet P-40) for 5 min. Samples were then centrifuged at $500 \times g$ for 5 min. The resultant supernatants were transferred to a clean set of Eppendorf tubes, and pellets were dissolved in 200 μl of lysis buffer and extracted for 2 min. Samples were centrifuged again, and the resultant supernatants were combined with previous supernatants. Subsequently, SDS and DNase-free RNase (Ambion, Austin, TX) were added to the pooled supernatants to the final concentration of 0.1% and 5 mg/ml, respectively, and samples were incubated at 56 °C for 2 h. At the end of RNase treatment, proteinase K (2.5 ml/ml) was added, and samples were further incubated for 2 h at 37 °C. Samples were extracted once with alkaline phenol:chloroform:isoamyl alcohol (25:24:1) and DNA precipitated with 0.3 M NaAc, pH 5.2. DNA from equal number of cells or equal amounts of DNA (20 μg) were run on a 1.2% agarose gel, and the DNA ladder formation was visualized by ethidium bromide staining.

RESULTS

12(S)-HETE Activates ERK1/2—Following 12(*S*)-HETE treatment both ERK1 and -2 were transiently activated, as determined by Western blot analyses with an antibody to the activated forms of ERK1/2. A single peak of activation (10-fold) was observed 10 min after stimulation with 12(*S*)-HETE (300 nM) (Fig. 1*A*). The increase in ERK1/2 phosphorylation was detected as early as 2 min, returned to basal level 30 min after stimulation, and was concentration-dependent in the 0–500 nM 12(*S*)-HETE range (Fig. 1*B*). These results were confirmed with an *in vitro* kinase assay where an increase in phosphorylation of a MAPK-specific substrate, *i.e.* Elk, paralleled the increase in ERK1/2 activity (Fig. 1, *A* and *B*).

To test whether 12(*S*)-HETE is unique or whether other eicosanoids also activate ERK1/2 in A431 cells in similar dose and time ranges, cells were treated with 5(*S*)-HETE, 11(*S*)-HETE, 12(*S*)-HETE, and 15(*S*)-HETE (300 nM, 10 min). Anti-phospho-ERK probed Western blots revealed (Fig. 1*C*) that under these conditions 12(*S*)-HETE is the most potent activator of ERK1/2, whereas 11(*S*)-HETE was 50% less potent. 5- and 15(*S*)-HETE stimulated ERK1/2 only to the extent of 5–15% of 12(*S*)-HETE, respectively. These results indicate that multiple HETEs may activate ERK1/2 in A431 cells, but 12(*S*)-HETE is the most potent, suggesting that this function is mediated by a specific response.

To investigate whether activation of ERK kinase by 12(*S*)-HETE was restricted to the A431 cell line, we tested human melanoma (WM983B and HT168), human prostate carcinoma (DU145), mouse melanoma (B16a), mouse lung carcinoma (3LL), endothelial (RVECT and HUVEC) as well as Chinese hamster ovary and African green monkey kidney (COS-1) cell lines. In these cell lines, with the exception of HT168, Chinese hamster ovary, and COS-1 cells, 12(*S*)-HETE also increased ERK1/2 activity within 10 min of treatment (data not shown). These findings indicate that 12(*S*)-HETE activation of ERK1/2 is not unique to A431 cells, but neither is it a ubiquitous phenomenon.

Other investigators (25) have reported that 12(*S*)-HETE increases the activity of another MAPK, *i.e.* c-Jun N-terminal kinase. In contrast, by using A431 cells, we found no evidence that either p38 or JNK mitogen-activated protein kinases were stimulated by this lipid mediator in a similar time and dose range as observed for ERK (data not shown).

The activity of ERK can be modulated at several levels in the evolutionarily conserved ERK cassette, *i.e.* either by enhancing GTP loading of Ras, by phosphorylation of Raf and MEK (26), or by binding non-enzymatic scaffold proteins (27). Some studies also suggest MEK-independent mechanisms for ERK activation, such as phosphatidylinositide 3-kinase-dependent or conventional PKC-dependent pathways (28). Therefore, we tested whether MEK, the immediate upstream dual specificity kinase to ERK, was involved in 12(*S*)-HETE-stimulated ERK1/2 activity.

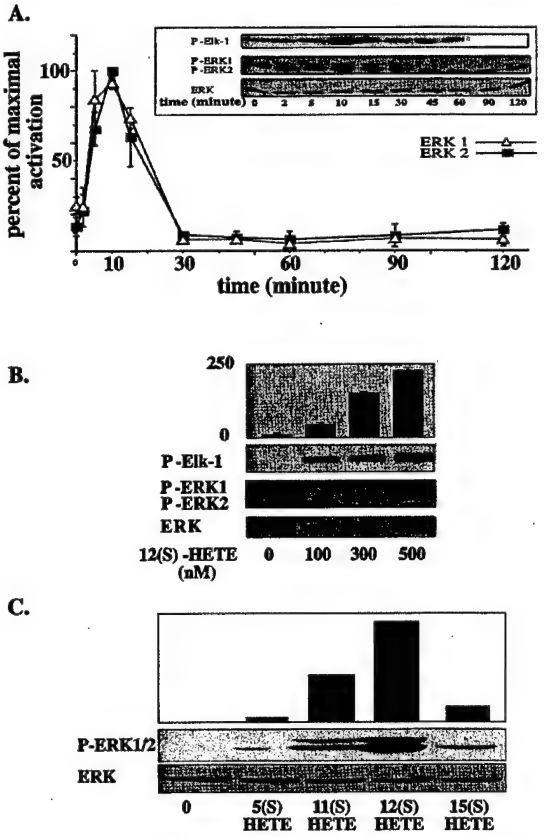

FIG. 1. **12(*S*)-HETE activates ERK1 and ERK2.** *A*, 12(*S*)-HETE activates ERK1/2 in a time-dependent manner. ERKs were precipitated at the indicated time points from 12(*S*)-HETE (300 nM)-treated A431 cells. Elk was used as a specific substrate for *in vitro* kinase assay (*inset, upper panel*). ERK activity was monitored by probing blots for phosphorylated Elk. 12(*S*)-HETE also increased the phosphorylated (activated) state of ERK1/2 as revealed by Western blots of whole cell lysates with phospho-specific ERK1/2 antibody (*inset, middle panel*). The blot was reprobed with non-phospho-specific ERK antibody to demonstrate equal loading (*inset, lower panel*). Western blots of three independent experiments probed for phospho-ERK1/2 were analyzed by densitometric scanning, and the results are represented in the graph as a percent of maximal activation. *B*, 12(*S*)-HETE activates MAPK in a dose-dependent manner. A431 cells were treated for 10 min with increasing concentration of 12(*S*)-HETE, and ERK1/2 activity was determined either by its ability to phosphorylate Elk in an *in vitro* kinase assay (*upper panel*) or by probing Western blots of whole cell lysates for activated ERK1/2 (*middle panel*). The blot was stripped and reprobed with non-phospho-specific ERK antibody for loading control (*lower panel*). The *bar graph* represents densitometric analysis of three independent anti-phospho-ERK Western blots. Results are expressed in arbitrary units. *C*, HETEs affect on ERK1/2 activity. A431 cells were treated for 10 min with 300 nM vehicle, 5(*S*)-HETE, 11(*S*)-HETE, 12(*S*)-HETE, or 15(*S*)-HETE, and ERK1/2 phosphorylation was evaluated by Western blotting (*upper panel*). Blot was stripped and reprobed with non-phospho-specific ERK antibody for loading control (*lower panel*). The *bar graph* represents densitometric analysis of the anti-phospho-ERK Western blot.

12(S)-HETE Activates MEK—12(*S*)-HETE increased (8-fold) the activity of MEK in a dose-dependent manner in the 0–600 nM range (Fig. 2*A*). Furthermore, PD98059, a specific inhibitor

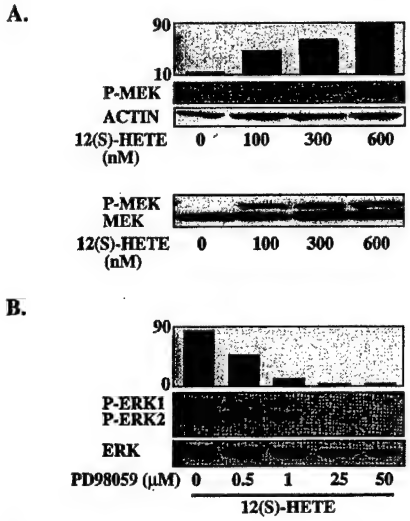

FIG. 2. **12(S)-HETE activates ERK1/2 through MEK.** *A,* MEK is activated following 10 min of 12(*S*)-HETE treatment (0–600 nM), as determined by probing Western blots of whole cell lysates for activated MEK (*upper panel*). The blot was reprobed for actin as loading control (*lower panel*). The *bar graph* represents densitometric analysis of the Western blot. Results are expressed as arbitrary units. 12(*S*)-HETE dose-dependently increases phosphorylation of MEK (*lower blot*). Phosphorylated MEK runs slower than the non-phosphorylated form in low bisacrylamide SDS-polyacrylamide gel electrophoresis. In Western blots probed for MEK after 12(*S*)-HETE treatment, the *upper band* represents the phosphorylated form of MEK and the *lower band* represents the non-phosphorylated form of MEK. *B,* a MEK inhibitor blocks 12(*S*)-HETE stimulated activation of MAPK. MEK inhibitor PD98059 (15 min, at the indicated doses)-pretreated cells were exposed to 12(*S*)-HETE for 10 min. Whole cell lysates were probed for activated ERK1/2 on a Western blot (*upper panel*), stripped, and reprobed for ERK1/2 as a loading control (*lower panel*). The *bar graph* represents densitometric analysis of the Western blot with the results expressed as arbitrary units.

of MEK1/2 dose dependently abolished MAPK activation by 12(*S*)-HETE (Fig. 2*B*), thus ruling out the possibility that 12(*S*)-HETE modulates ERK activity by a MEK-independent mechanism.

12(S)-HETE Activates Raf—Since MEK is a convergence point for several signaling pathways, we next tested for the involvement of Raf1 in 12(*S*)-HETE signaling. By utilizing an *in vitro* kinase assay, we observed that Raf kinase activity was increased (3-fold) 5 min after cells were treated with 300 nM 12(*S*)-HETE (Fig. 3) and that this activation was decreased (75%) in cells pretreated with the PKC inhibitor, Go6976 (at 10× IC_{50} dose (15)). These data suggest that PKC participates in 12(*S*)-HETE activation of Raf1.

12(S)-HETE Activates PKCα—The inhibition of 12(*S*)-HETE-stimulated Raf activity by Go6976 led us to examine the extent to which conventional PKCs were involved in the observed ERK1/2 stimulation. Treatment with 12(*S*)-HETE induced a dose-dependent translocation (5-fold at 600 nM) of PKCα from the cytosol to the membrane fraction accompanied by increased phosphorylation (5-fold at 300 nM) (Fig. 4, *A* and *B*). Enzyme activity in the subcellular fractions was confirmed with a kinase assay using myelin basic protein as a substrate for immunoprecipitated PKC (data not shown). Phosphorylation of PKCα reached a maximum at approximately 2.5 min (Fig. 4*C*). Therefore, the time course of PKC activation by 12(*S*)-HETE, in A431 human epidermoid carcinoma cells, is similar to that observed in B16a murine melanoma cells (7).

12(S)-HETE-stimulated ERK1/2 Activity Is Mediated in Part by PKCα—Western blotting of A431 cells revealed that they express seven isoforms of PKC, *i.e.* α, δ, ε, ζ, λ, μ, and ι (Fig. 5*A*). Chronic exposure to phorbol esters leads to degradation of the activated PKC species. In A431 cells PKC α, δ, and ε but not PKC ζ, μ, λ, and ι were eliminated by chronic phorbol ester exposure. To determine whether 12(*S*)-HETE activation of ERK1/2 was mediated by PKC, we tested whether PKC depletion could block ERK1/2 activation. Depletion of PKC resulted in a partial (40%) inhibition of 12(*S*)-HETE activation of ERK1/2 (Fig. 5*B*). In contrast, this treatment completely abolished ERK1/2 activation by PMA, a direct and potent acti-

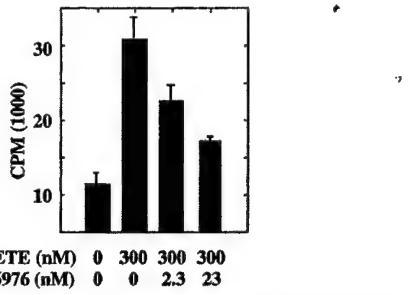

FIG. 3. **Raf is stimulated by 12(*S*)-HETE in a conventional PKC-dependent manner.** A431 cells were pretreated with the conventional PKC inhibitor Go6976 (at 1 and 10× IC_{50}, 2.3 and 23 nM, respectively) for 15 min and then with 12(*S*)-HETE (300 nM, 5 min). Raf was immunoprecipitated and used for an *in vitro* kinase assay where it activated GST-MEK which in turn phosphorylated ([^{32}P]ATP) GST-ERK2. Proteins were bound on phosphocellulose paper, and after extensive washing incorporated radioactivity was determined. Pretreatment of cells with a PKC inhibitor reduced activation of ERK2. *Error bars* represent S.D. of triplicate determinations, and the graph is a representative of three independent experiments.

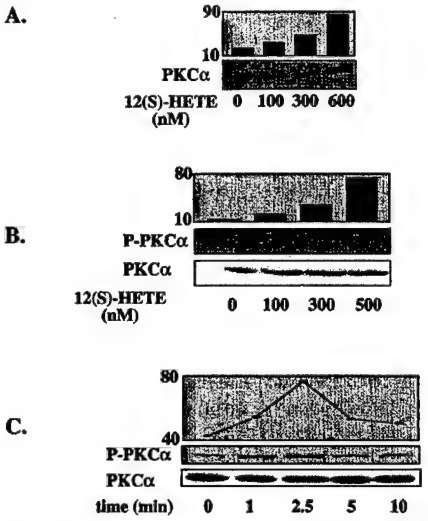

FIG. 4. **12(*S*)-HETE activates PKCα in a time- and concentration-dependent manner.** *A,* 12(*S*)-HETE dose dependently activates PKCα. After 3 min 12(*S*)-HETE treatment, cytosolic and particulate fractions were isolated from A431 cells. Proteins from the particulate fractions were analyzed by Western blotting with an antibody directed to PKCα. 12(*S*)-HETE dose dependently increased translocation of PKCα to the particulate fraction. The *bar graph* represents densitometric analysis of 3 Western blots, with the results expressed as arbitrary units. *B,* 12(*S*)-HETE dose dependently induces phosphorylation of PKCα. A431 cells were treated with the indicated doses of 12(*S*)-HETE for 3 min. Western blots of whole cell lysates were probed for the phosphorylated form of PKCα (*upper panel*). As a loading control the blot was reprobed with a non-phospho-specific PKCα antibody (*lower panel*). The *bar graph* represents densitometric analysis of the Western blot, with the results expressed as arbitrary units. *C,* PKC is transiently activated by 12(S)-HETE. Probing blots from 12(*S*)-HETE (300 nM)-stimulated whole cell lysates with anti-phospho-PKCα antibody revealed that PKCα is maximally activated at 2.5 min after stimulation (*upper panel*). As a loading control the blot was stripped and reprobed with a non-phospho-specific PKCα antibody (*lower panel*). The graph represents densitometric analysis of the Western blot, with the results expressed as arbitrary units.

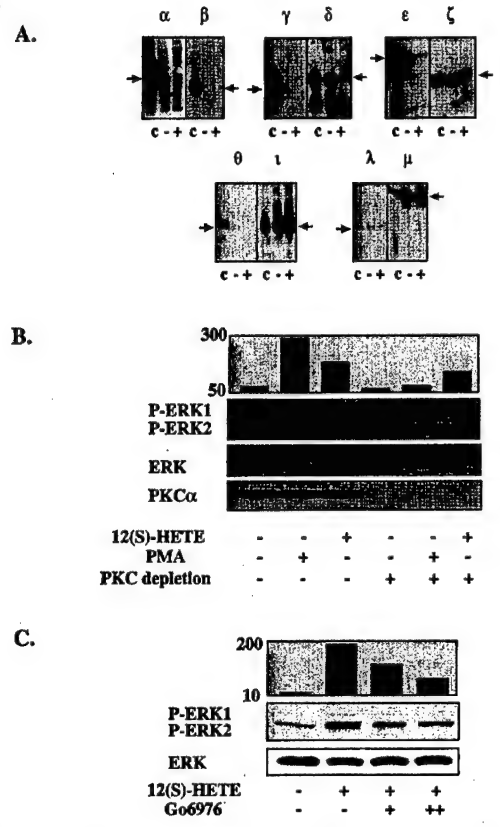

FIG. 5. **ERK1/2 activation by 12(*S*)-HETE is dependent, in part, on conventional PKC activity.** *A*, PKC α, δ, ε, ζ, ι, λ, and μ are expressed in A431 cells at a detectable level, as determined by Western blotting. Chronic PMA exposure depletes PKC α, δ, and ε. *c*, positive control, mouse brain lysate (α, β, γ, δ, ε, ζ, ι, λ) or Jurkat cell lysate (θ and μ); + and − represent PMA-depleted and non-depleted A431 cell lysates, respectively. *B*, conventional PKCs are partially responsible for 12(*S*)-HETE induced ERK1/2 activation. Chronic exposure to phorbol ester (100 nM PMA, 20 h) eliminated PKCα from A431 cells (*lower panel*). In PKCα-depleted cells, ERK1/2 activation was not induced by PMA treatment (10 min, 100 nM). 12(*S*)-HETE (10 min, 300 nM)-stimulated ERK1/2 activation is decreased when compared with that of cells in which PKC was not depleted; however, it was not eliminated completely (*upper panel*). Blot was stripped and reprobed with an antibody to ERK that recognizes these enzymes independent of their phosphorylation state (*middle panel*). The *bar graph* represents densitometric analysis of the Western blot, with the results expressed as arbitrary units. *C*, pretreatment of cells with a specific chemical inhibitor Go6976 (23 nM (+) and 115 nM (++)) for conventional PKCs dose dependently inhibited 12(*S*)-HETE-mediated activation of ERK1/2. Western blots of whole cell lysates were probed for activated ERK1/2 (*upper panel*), stripped, and reprobed with non-phospho-specific ERK antibody as a loading control (*lower panel*). The *bar graph* represents densitometric analysis of the Western blot, with the results expressed as arbitrary units.

vator of PKC (Fig. 5*B*). Chronic exposure to another, nonrelated PKC activator, bryostatin, also resulted in a partial inhibition of 12(*S*)-HETE activation of ERK1/2 (data not shown). Chemical inhibition of conventional PKC isoforms by Go6976 partially (60%) reduced 12(*S*)-HETE activation of ERK in a dose-dependent manner (Fig. 5*C*). Even at 50 times the IC_{50} concentration, Go6976 failed to completely block the 12(*S*)-HETE activation of ERK1/2. Together, these results suggest that the conventional PKC pathways are important but are not the exclusive mechanism for 12(*S*)-HETE activation of ERK.

12(S)-HETE Activates PLCγ1—Activation of PKCα by 12(*S*)-HETE in B16a murine melanoma cells can be blocked by either PLC inhibitors or by an inhibitor of G_i proteins, *i.e.* pertussis toxin (7). The PLCβ family of isoforms are activated by G

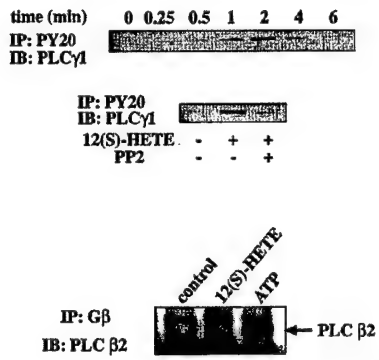

FIG. 6. **Involvement of phospholipases in 12(*S*)-HETE signaling.** *A*, PLCγ1 is rapidly phosphorylated on tyrosine residues after exposure to 12(*S*)-HETE (300 nM). Tyrosine-phosphorylated proteins were immunoprecipitated and probed for PLCγ1 by Western blot (*upper panel*). Maximal phosphorylation was observed between 0.5 and 2 min. Pretreatment with an inhibitor of Src family kinases (PP2, 5 μM, 30 min) abolished the 12(*S*)-HETE effect on tyrosine phosphorylation of PLCγ1 (*lower panel*). *B*, PLCβ2 is not involved in 12(*S*)-HETE signal transduction. PLCβ2 coprecipitated with Gβ subunits in ATP (1 μM, 30 s) but not in 12(*S*)-HETE (300 nM, 30 s)-treated cells.

proteins (29), and stimulation of PLCβ2 is sensitive to pertussis toxin treatment (30). Therefore, we tested for a role for this PLC isoform in 12(*S*)-HETE signaling. PLCβ2 co-immunoprecipitated with the Gβ subunit after a stimulus with exogenous ATP, but not after 12(*S*)-HETE, or in non-stimulated cell lysates (Fig. 6*B*), suggesting that this PLC isoform is not involved in 12(*S*)-HETE signaling events.

Members of the PLCγ family were thought to be activated by receptors with inherent tyrosine kinase activity (29). However, recent publications demonstrate that angiotensin II (31) and leukotriene B4 (32), both of which exert their effects through G protein-coupled receptors, stimulate tyrosine phosphorylation and activity of PLCγ1 as rapidly as 15 s after exposure. Therefore, we examined if PLCγ1 is involved in mediating the 12(*S*)-HETE effect (Fig. 6*A*). Tyrosine-phosphorylated proteins were immunoprecipitated, and Western blots were probed for PLCγ1. In 12(*S*)-HETE-challenged cells PLCγ1 is tyrosine-phosphorylated within 30 s and remains phosphorylated for 4 min. The time course for this phosphorylation precedes that of PKCα, thereby supporting a role for PLCγ1 in the activation of PKCα during 12(*S*)-HETE signaling.

Growth Factor Receptors Are Not Activated by 12(S)-HETE—The finding that activation of PLCγ1 is an early event after 12(*S*)-HETE exposure suggests that the putative 12(*S*)-HETE receptor may be coupled to tyrosine kinases. A number of publications illustrate that G protein-coupled receptors can trans-activate receptor-tyrosine kinases, such as the EGF-, insulin-like growth factor-, and PDGF receptors (33–35). The EGF receptor is expressed at high level in A431 cells; therefore, we tested whether this receptor was responsible for the early tyrosine phosphorylation events induced by 12(*S*)-HETE. Tyrphostin 51, a specific inhibitor of the EGF receptor kinase, did not affect 12(*S*)-HETE signaling (Fig. 7*A*). In contrast, under similar experimental conditions it blocked the EGF-induced activation of ERK1/2 (Fig. 7*A*). In addition, Western blots using an anti-active EGFR antibody could not detect EGF receptor activation by 12(*S*)-HETE (Fig. 7*B*). No increase in tyrosine phosphorylation was apparent in precipitates of the PDGFβ receptor or the FGF receptor substrate FRS2 following 12(*S*)-HETE treatment (data not shown). We conclude that the trans-activation of EGF, PDGF, or FGF receptors does not appear to play a role in 12(*S*)-HETE signaling.

12(S)-HETE Affects EGF Signaling—Since G protein-coupled receptors may activate protein tyrosine phosphatases (36),

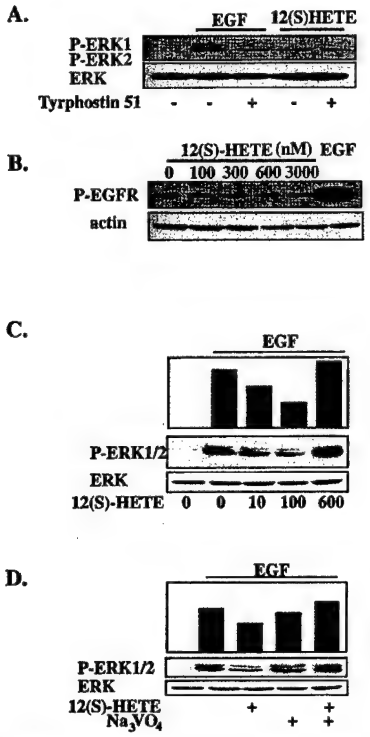

FIG. 7. **Interaction between EGF and 12(*S*)-HETE signaling.** *A*, EGF receptor (*EGFR*) is not involved in 12(*S*)-HETE signaling in A431 cells. Tyrphostin 51, a specific inhibitor of EGF receptor kinase, inhibits ERK1/2 activation by EGF but does not effect 12(*S*)-HETE activation. Cells were treated with the inhibitor (at IC_{50}, 800 nM, 20 min) and then with either EGF (1 ng/ml, 10 min) or 12(*S*)-HETE (300 nM, 10 min). Western blots of whole cell lysates were probed for active ERK1/2 (*upper panel*), stripped, and reprobed for ERK as a loading control (*lower panel*). *B*, EGF receptor is not activated by 12(*S*)-HETE. A431 cells were treated with the indicated concentrations of 12(*S*)-HETE or EGF (0.5 ng/ml for 1 min). Western blots were probed with a phospho-EGF receptor antibody to assess the receptor activation (*upper panel*) and with an actin antibody as a loading control. No activation of the EGF receptor is apparent after eicosanoid treatment. *C*, influence of 12(*S*)-HETE on EGF signaling. Cells pretreated with 12(*S*)-HETE (1 min, 0–600 nM) were challenged with EGF (50 ng/ml, 5 min). ERK1/2 activation in response to EGF was attenuated by 12(*S*)-HETE exposure in the 10–100 nM range and enhanced by 600 nM 12(*S*)-HETE (*upper panel*). Blots were stripped and reprobed with anti-ERK antibody to demonstrate even loading (*lower panel*). Results from the densitometric analysis of the *middle panel* is shown in the *bar chart* (arbitrary units). *D*, 12(*S*)-HETE affect on EGF signaling is mediated by protein tyrosine phosphatases. Cells were pretreated with protein tyrosine phosphatases inhibitor Na_3VO_4 (2 mM, 30 min), then exposed to 100 nM 12(*S*)-HETE or vehicle (1 min), and treated with EGF (50 ng/ml, 5 min). ERK1/2 activation identified with Western blotting (*upper panel*), stripping, and reprobing the membrane for ERK served as demonstration of even loading (*lower panel*). Results from the densitometric analysis are shown in the *bar chart* (arbitrary units).

next we tested whether 12(*S*)-HETE may have an opposing rather than synergistic effect on EGF signaling. Serum-starved cells were challenged with 0–600 nM 12(*S*)-HETE for 1 min and then with 50 ng/ml EGF for 5 min, and cell lysates were tested for ERK1/2 activity. We found a biphasic response. Lower concentrations of 12(*S*)-HETE (10–100 nM) reduced EGF-stimulated ERK1/2 phosphorylation, and higher (600 nM) concentrations of 12(*S*)-HETE further increased EGF-stimulated ERK1/2 activity (Fig. 7*C*).

One possibility is that at the 10–100 nM concentration 12(*S*)-HETE stimulates a phosphatase. To evaluate this, cells were pretreated with or without sodium orthovanadate (2 mM, 30 min); similar to the above described experiments, cells were treated with EGF in the presence or absence of 100 nM 12(*S*)-HETE. ERK1/2 activation was tested by Western blotting (Fig. 7*D*). In the absence of the protein tyrosine phosphatase inhibitor sodium orthovanadate, as earlier, 100 nM 12(*S*)-HETE interfered with EGF-stimulated ERK1/2 activation (35% reduction). In contrast, in the presence of the protein tyrosine phosphatase inhibitor, pretreatment with 100 nM 12(*S*)-HETE resulted in a slight (15%) increase in ERK1/2 phosphorylation. Taken together these results suggest that at lower doses 12(*S*)-HETE stimulates ERK1/2 activity, as well as stimulates a protein tyrosine phosphatase that antagonizes EGF signaling. However, at higher concentrations, 12(*S*)-HETE does not activate the protein tyrosine phosphatase, only ERK1/2, hence its effect is additive to that of EGF on ERK1/2.

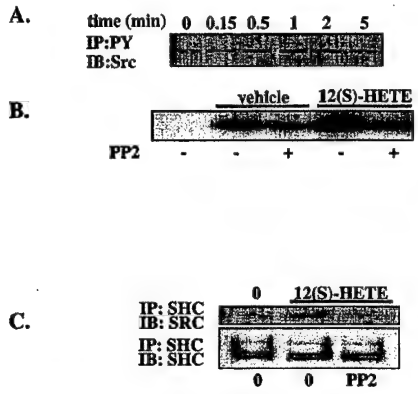

FIG. 8. **Src family kinases are involved in 12(*S*)-HETE signaling.** *A*, Src family kinases are phosphorylated in response to 12(*S*)-HETE. Tyrosine-phosphorylated proteins were precipitated 10 and 30 s or 1, 2, or 5 min after 12(*S*)-HETE treatment. Western blot (*IB*) was probed with an antibody that recognizes multiple members of Src family. *B*, Src family kinases are activated by 12(*S*)-HETE. A431 cells were pretreated with Src inhibitor PP2 (5 μM, 30 min) and with 12(*S*)-HETE (100 nM, 1 min). Immunoprecipitated (*IP*) Src family kinases were used in an *in vitro* kinase assay. Radioactivity incorporated into a specific substrate was determined by PhosphorImager analysis. *C*, Src family kinases associate with Shc adapter proteins in response of 12(*S*)-HETE treatment in an Src kinase activity dependent manner. A431 cells were pretreated with Src inhibitor PP2 (5 μM, 30 min) and then with 12(*S*)-HETE (100 nM, 1 min). Shc proteins were immunoprecipitated under non-denaturing conditions, and the associated proteins were analyzed by Western blotting.

Src Family Kinases Are Involved in Early 12(S)-HETE Signaling—The Src family of non-receptor tyrosine kinases are implicated in signaling events downstream of G proteins (13). Pretreatment of A431 cells with PP2, a specific inhibitor of Src kinases, abolished tyrosine phosphorylation of PLCγ1 stimulated by 12(*S*)-HETE (Fig. 6*A*). Therefore, we questioned whether Src family kinases are activated by 12(*S*)-HETE. Western blot analysis of proteins precipitated from 12(*S*)-HETE treated A431 cells revealed a time-dependent increase in tyrosine phosphorylation of Src family kinases (Fig. 8*A*) as rapidly as 10 s following exposure to 12(*S*)-HETE. However, tyrosine phosphorylation of these enzymes can either stimulate or inhibit their activity, depending on the site of phosphorylation (37). Therefore, we assayed for Src kinase activity in SRC2 antibody-generated precipitates and found that 12(*S*)-HETE stimulated Src activity. Pretreatment with PP2 (5 μM) was sufficient to reduce kinase activity below basal levels (Fig. 8*B*). As revealed with immunoprecipitation and Western blotting, 12(*S*)-HETE increased association of Src with Shc (Src homology and collagen) adapter proteins, which was abolished by pretreating the cells with PP2 (Fig. 8*C*). Furthermore, PP2 (5 μM) significantly inhibited, but did not entirely abolish, ERK1/2 activation by 12(*S*)-HETE (Fig. 10*B*).

12(S)-HETE Stimulates Phosphorylation of Shc—The potential involvement of Src family kinases in 12(*S*)-HETE signaling suggested an alternative pathway to the previously established

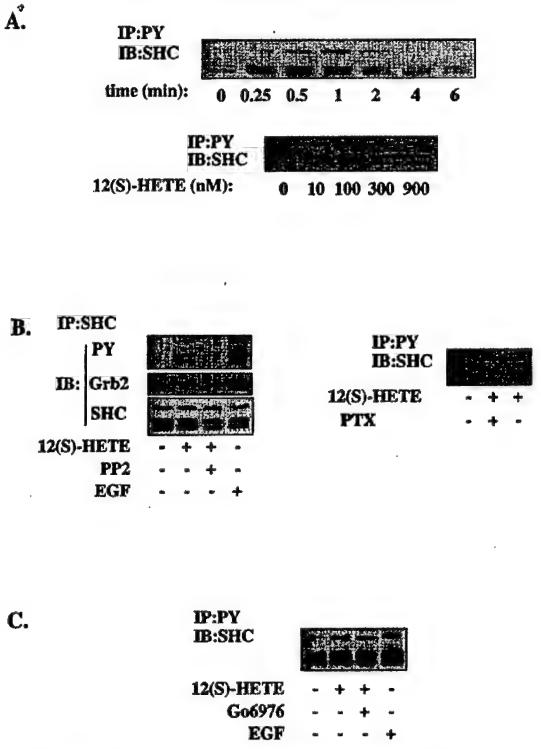

FIG. 9. **Adapter proteins are involved in 12(S)-HETE signaling.** *A*, Shc is tyrosine-phosphorylated after 12(*S*)-HETE exposure in a time- (*upper panel*) and dose (*lower panel*)-dependent manner. Tyrosine-phosphorylated proteins were immunoprecipitated (*IP*) under denaturing conditions, and Western blots (*IB*) were analyzed with anti-Shc antibody. Maximal phosphorylation was observed at approximately 1 min (*upper panel*) and at 300 nM concentration (*lower panel*). *B*, Shc phosphorylation is dependent on Src family kinase activity but not on G_i proteins. A431 cells were pretreated with an inhibitor of Src family kinases (PP2, 5 μM, 30 min) and then with 12(*S*)-HETE (300 nM, 1 min) or EGF (0.5 ng/ml, 2 min). Shc was immunoprecipitated under nondenaturing conditions, and Western blots of the precipitated proteins were probed for phosphotyrosine (*left, upper panel*), stripped, and reprobed for Grb2 (*left, middle panel*), stripped again and probed for Shc as loading control (*left, lower panel*). Inhibition of Src family kinases completely blocked Shc tyrosine phosphorylation and its association with Grb2. Inhibition of G_i proteins with pertussis toxin pretreatment (*PTX*, 100 ng/ml, overnight) did not effect Shc phosphorylation (*right panel*) after 12(*S*)-HETE exposure (300 nm, 1 min) as determined by analyzing Western blots of tyrosine-phosphorylated proteins that were precipitated under denaturing conditions. *C*, 12(*S*)-HETE-stimulated phosphorylation of Shc is independent of conventional PKC activity. Pretreatment with PKC inhibitor Go6976 (115 nM, 15 min) did not influence the 12(*S*)-HETE (300 nM, 1 min)-induced phosphorylation of Shc. Treatment with EGF (0.5 ng/ml, 2 min) served as a positive control.

PLC-PKC route of ERK1/2 activation. Adapter proteins, such as Grb2 (growth factor receptor-bound protein 2; pp24) and Shc (pp66, pp52, and pp46), are tyrosine-phosphorylated by activated growth factor receptor and oncogene-tyrosine kinases and link these kinases to the ERK cascade. Therefore, we tested whether adapter proteins are phosphorylated in response to 12(*S*)-HETE treatment. Tyrosine phosphorylation of Shc adapter proteins was detectable as early as 15 s after 12(*S*)-HETE stimulation (Fig. 9*A*) and peaks at 30–60 s. The tyrosine phosphorylation of Shc is maximal in the 100–300 nM range of 12(*S*)-HETE (3.5-fold over basal level). Another adapter protein, Grb2 (growth factor receptor-bound), also was tyrosine-phosphorylated, and it associated with Shc in response to 12(*S*)-HETE treatment (Fig. 9*B*). Pretreatment with the Src family kinase inhibitor, PP2, completely abolished activation of these adapter proteins. Shc and Grb2 are well characterized as activators of Ras through the guanine nucleotide exchange factor, Sos. Pretreatment with a PKC inhibitor

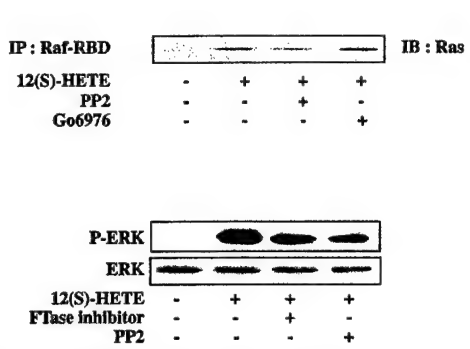

FIG. 10. **Ras is involved in 12(S)-HETE signaling.** *A*, Ras is activated by 12(*S*)-HETE in an Src-dependent but cPKC-independent manner. Cells were treated with PP2 (5 μM) or Go6976 (115 nM) for 30 min and then with 12(*S*)-HETE (300 nM) for 3 min. Cells were lysed, and activated Ras was precipitated (*IP*) with Raf-Ras binding domain (Raf-RBD)-conjugated beads. Western blots were probed for Ras. *B*, inhibitors of both Ras (FTase inhibitor I, 5 μM, 1 h) and Src family kinase (PP2, 5 μM, 30 min) reduced, but did not completely block, 12(*S*)-HETE (600 nM, 10 min)-stimulated ERK1/2 activation as revealed by probing Western blot (*IB*) for activated ERK1/2 (*upper panel*). Blot was stripped and reprobed for ERK as loading control (*lower panel*).

(Go6976) did not affect the increase in tyrosine phosphorylation of Shc (Fig. 9*C*). Therefore, Shc may represent an alternative pathway to PKC activation of ERK following 12(*S*)-HETE stimulation.

12(S)-HETE Activates Ras—To test whether Ras was stimulated in our system, we took advantage of the fact that only GTP-Ras (the activated form) binds its effector, Raf. We found that 300 nM 12(*S*)-HETE stimulated Ras binding 3 min after 12(*S*)-HETE exposure (Fig. 10*A*), which was blocked by pretreatment with Src inhibitor, PP2 (5 μM, 30 min), but not by an inhibitor of conventional PKCs, Go6976 (115 nM, 30 min). Next we questioned the contribution of Ras to 12(*S*)-HETE-induced ERK activation. Inhibitors of farnesyltransferase (FTase inhibitor II, 5 μM, 1 h) interfere with Ras function. Farnesyltransferase inhibitor pretreatment partially blocked ERK activation by 12(*S*)-HETE (Fig. 10*B*).

G Proteins Are Involved in 12(S)-HETE Signaling—Since previous reports suggested involvement of G proteins in 12(*S*)-HETE signaling (7, 38), we tested whether they were involved in activation of ERK using two inhibitors of serpentine receptor/G protein signaling. Uncoupling seven transmembrane receptors from G proteins with suramin (5 min, 150 μM) (20) abolished the 12(*S*)-HETE effect on ERK phosphorylation (Fig. 11*B*). At higher concentrations suramin may block the interaction of growth factors with their receptor, such as EGF with EGFR. However, the suramin dose applied in our experiments did not affect the ERK response to EGF (Fig. 11*B*). Previous studies suggested the involvement of $G_i\alpha$ in 12(*S*)-HETE signaling (7); therefore, we exposed A431 cells (18 h) to various doses of pertussis toxin (a specific inhibitor of $G_i\alpha$). The results demonstrated that 12(*S*)-HETE stimulates ERK1/2 in both a $G_i\alpha$-dependent and -independent manner (Fig. 11*A*). Pertussis toxin inhibition of ERK1/2 reached its maximum at 100 ng/ml and reduced 12(*S*)-HETE (300 nM) activation of ERK1/2 to 60% of the maximum at 10 min. Collectively, these results suggest that ERK1/2 activation by 12(*S*)-HETE is mediated by more than one heterotrimeric G protein.

A431 Cells Have Multiple Binding Sites for 12(S)-HETE—The inconsistency between the concentration of 12(*S*)-HETE necessary to saturate Shc phosphorylation (~100 nM, Fig. 9*A*) and ERK1/2 activation (>500 nm, Fig. 1) suggested that more than one receptor might be involved in mediating the 12(*S*)-HETE response in A431 cells. To substantiate this hypothesis A431 cell monolayers were incubated with [^{3}H]12(*S*)-HETE in

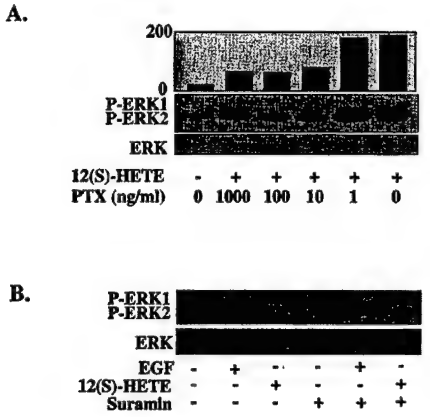

FIG. 11. **The putative 12(S)-HETE receptor is G protein-coupled.** *A*, $G_i\alpha$ proteins are involved in 12(*S*)-HETE signaling. A431 cells were incubated with the indicated concentrations of pertussis toxin (*PTX*) overnight and then challenged with 300 nM 12(*S*)-HETE for 10 min. Western blotting with anti-active ERK1/2 reveals that ADP-ribosylation of $G_i\alpha$ only partially block ERK1/2 activation (*upper panel*). Blot was stripped and reprobed for ERK as loading control (*lower control*). The *bar graph* represents densitometric analysis of the Western blot, with the results expressed as arbitrary units. *B*, suramin (5 min, 150 μM), which uncouples G proteins from receptors, reduced ERK1/2 activity to basal level after 12(*S*)-HETE stimulus (300 nM, 10 min), whereas it did not inhibit EGF (5 ng/ml) signaling (*upper panel*). Blot was stripped and reprobed for ERK as loading control (*lower panel*).

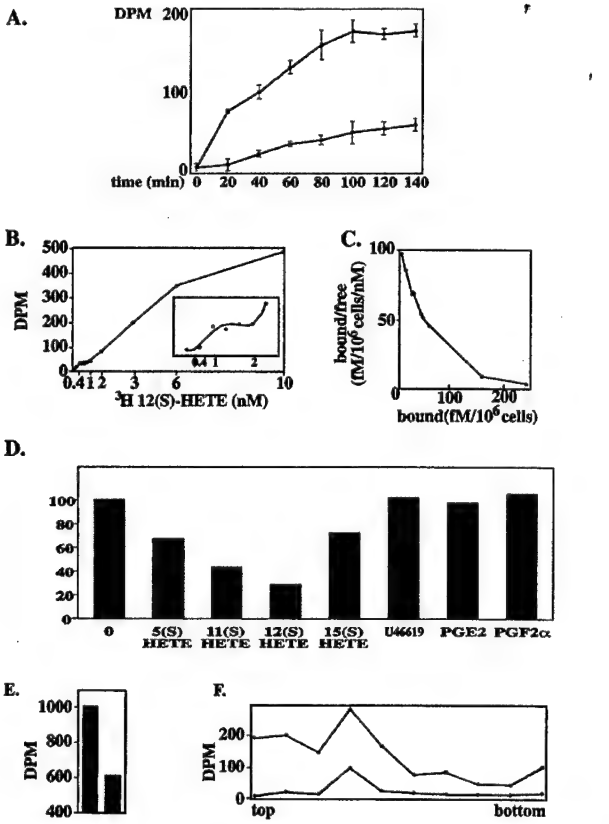

FIG. 12. **There are multiple 12(S)-HETE-binding sites on A431 cells.** *A*, time-dependent binding. Cell monolayer was incubated at 4 °C with 2 nM ^{3}[H]12(*S*)-HETE with (*lower line*) or without (*upper line*) competing 2 μM cold 12(*S*)-HETE for the indicated periods. Cell-bound radioactivity is expressed as disintegrations per min. Specific binding site is saturated at 100 min at 4 °C. The figure is representative of 3 independent experiments, and points are triplicate determinations. *B*, concentration-dependent binding. Cells were incubated for 120 min at 4 °C with 0.4–10 nM [^{3}H]12(*S*)-HETE with or without competing 1000× cold 12(*S*)-HETE. The difference between specific and nonspecific binding was charted. *Inset*, plot of the specific binding at the high affinity binding region. The figure is representative of 4 independent experiments, and points are triplicate determinations. *C*, Scatchard plot representation of data generated from the concentration-dependent binding assays. Specific binding is plotted against specific binding/concentration of free 12(*S*)-HETE. The non-linear data suggests multiple binding sites. *D*, competition for the specific binding site with eicosanoids. Cells were incubated for 120 min at 4 °C with 2 nM ^{3}[H]12(*S*)-HETE with or without competing 1000× cold eicosanoids. Results are expressed as percent of the radioactivity without competing eicosanoid (*0*). U46619, thromboxane A_2-mimetic. *E*, radioactivity (3 nM [^{3}H]12(*S*)-HETE) incorporated into plasma membrane with (*right column*) or without (*left column*) competing 100× cold 2(*S*)-HETE. *F*, thin layer chromatography analysis of membrane incorporated [^{3}H]12(*S*)-HETE. Cells were incubated with 3 nM [^{3}H]12(*S*)-HETE, and the membrane fraction was isolated. Lipids extracted from this fraction (*lower line*) or [^{3}H]12(*S*)-HETE standard (*upper line*) were separated on a TLC plate, and radioactivity in even size rectangles from top (*left side*) to bottom (*right size*) of the plate was determined. Exposure to iodine vapor revealed that the majority of membrane lipids remained in the 2nd to 4th rectangles from the bottom, whereas the majority of the radioactivity corresponded to the position of free ^{3}[H]12(*S*)-HETE.

the presence or absence of competing 1000× non-labeled 12(*S*)-HETE. As shown in Fig. 12*A*, specific association between 12(*S*)-HETE and A431 cells was maximal at 100 min. Binding was further characterized by incubating cells with 0.4–10 nM [^{3}H]12(*S*)-HETE with or without competing 1000× non-labeled 12(*S*)-HETE for 120 min. These studies reproducibly showed (Fig. 12*B*) a binding site that was saturated at approximately 0.8 nM concentration and another, which was not completely saturated by 10 nM 12(*S*)-HETE. Scatchard transformation of the binding data resulted in a curve plot rather than a linear plot (Fig. 12*C*) suggesting that 12(*S*)-HETE binds to A431 cells through multiple binding sites, with different binding affinities.

Competition between Binding of 12(S)-HETE and Other Eicosanoids—In order to evaluate the specificity of 12(*S*)-HETE binding, A431 cells were incubated with 3 nM [^{3}H]12(*S*)-HETE in the presence of various eicosanoids (Fig. 12*D*). One thousand-fold non-labeled 12(*S*)-HETE was the best competitor, decreasing incorporated radioactivity by 70% and 11(*S*)-HETE by 55%. Of the HETEs tested 5(*S*)-HETE and 15(*S*)-HETE were the least potent, reducing binding by 30%. Other eicosanoids, prostaglandin E_2 and prostaglandin $F_2\alpha$, or thromboxane A_2 analog U46619 did not affect [^{3}H]12(*S*)-HETE binding to A431 cells.

12(S)-HETE Binds to Cell Membrane—Previous experiments suggested involvement of trimeric G proteins in 12(*S*)-HETE signaling. Since G protein-coupled receptors reside in the plasma membrane, we next questioned whether there is specific 12(*S*)-HETE binding to this cell compartment. Cells were exposed to 3 nM [^{3}H]12(*S*)-HETE with or without competing 100-fold non-labeled 12(*S*)-HETE and then the membrane fraction was isolated. Radioactivity was recovered from the membrane fractions, which was displaced by excess non-labeled 12(*S*)-HETE (Fig. 12*E*). It is conceivable that the recovered 12(*S*)-HETE is in an esterified form. Therefore, following [^{3}H]12(*S*)-HETE incubation, lipids were extracted from the membrane fraction and analyzed by thin layer chromatography. The majority of the radioactivity showed an identical migration pattern on TLC as authentic standard [^{3}H]12(*S*)-HETE (Fig. 12*F*), suggesting that the 12(*S*)-HETE recovered from the membrane is non-esterified under these experimental conditions.

12(S)HETE Rescues A431 Cells from Apoptosis Induced by a 12-LOX Inhibitor—Previous studies showed that 12-LOX functions as a survival factor in several tumor cell lines and that exogenous 12(*S*)-HETE blocks apoptosis induced by 12-LOX inhibitors (5). First, we showed by DNA laddering assay that the 12-LOX-specific inhibitor, BHPP, induced apoptosis in A431 cells in dose-dependent manner (Fig. 13*A*), similar to the

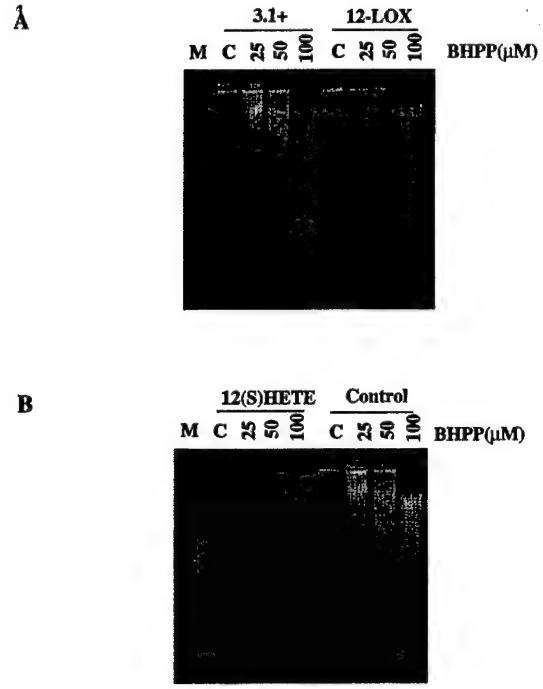

FIG. 13. **12(S)-HETE effect on BHPP-induced apoptosis in A431 cells by DNA laddering assay.** *A*, comparison of A431 12-LOX transfectants with vector control 3.1+. Cells were treated with BHPP at the concentrations indicated for 24 h and were low molecular weight DNA-extracted, run on a 1.2% agarose gel, and visualized with ethidium bromide. *B*, A431 cells were pretreated with 12(*S*)-HETE (1 μM) before incubation in DMEM in the presence of BHPP, see details under "Experimental Procedures." Aliquots of DNA extracts were subjected to 1.2% agarose gel and visualized with ethidium bromide. *M*, DNA marker; *C*, ethanol as vehicle control; *3.1+*, empty vector control; *12-LOX*, A431 cells transfected with human full-length platelet-type 12-LOX; *Control*, without 12(*S*)-HETE treatment.

effects found in an earlier study with W256 cells (5). When A431 cells, 12-LOX-transfected A431 cells, or vector control cells were treated (37 °C; 24 h) with BHPP at 25, 50, or 100 μM, the cells transfected with platelet-type 12-LOX were more resistant to apoptosis induced by BHPP than 3.1+ vector control cells as shown by the density of the DNA ladder (Fig. 13*A*). Prior to the treatment with BHPP, A431 cells were incubated with 12(*S*)-HETE for 2 h. As shown in Fig. 13*B*, 12(*S*)-HETE pretreatment completely prevented A431 cells from undergoing apoptosis triggered by BHPP at low dose and significantly reduced the response to high dose BHPP (Fig. 13*B*). The results suggest that the 12-LOX product, 12(*S*)-HETE, provides cells with resistance to apoptosis and also that 12(*S*)-HETE may play a role in an anti-apoptotic signaling pathway.

DISCUSSION

The platelet-type 12-lipoxygenase is ectopically expressed in a variety of human and rodent cancer cells, and 12-lipoxygenase expression has been correlated positively with metastatic potential in a rodent tumor model (39). More importantly, in a clinical study of 132 tumors from prostate cancer patients, the expression of 12-lipoxygenase message correlated with tumor stage, grade, and the presence of cancer cells in the surgical margins (40). The sole product of the metabolism of arachidonic acid by platelet type 12-lipoxygenase is 12(*S*)-HETE. This bioactive lipid is reported to induce a plethora of cellular responses when added exogenously to tumor cells or endothelial cells and to alter tumor growth when overexpressed endogenously. The latter effect may be due to the suppression of apoptosis and stimulation of angiogenesis (5, 6). For example, exogenously added 12(*S*)-HETE alters the metastatic phenotype by inducing alterations in the cancer cell cytoskeleton (41), thereby enhancing tumor cell motility (4), secretion of proteinases (42, 43), expression of integrins (2, 44), and increased invasion (46). In endothelial cells, 12(*S*)-HETE induces the non-destructive retraction of monolayers (47) and promotes tumor cell adhesion (46). The motility of isolated endothelial cells and tube formation is also enhanced by 12(*S*)-HETE (6). Given the numerous and varied cellular responses to 12(*S*)-HETE, we delineated in this study the signaling pathways utilized by this bioactive lipid in A431 human epidermoid carcinoma cells. Data presented in this study demonstrate that exogenous 12(*S*)-HETE induces a transient activation of ERK1/2. We report for the first time that 12(*S*)-HETE stimulates phosphorylation of PLCγ1, which in turn is responsible for activation of a conventional PKC isoform (*i.e.* PKCα). We show that PKCα plays a significant but not exclusive role in ERK1/2 activation. Furthermore, we demonstrate that the 12(*S*)-HETE-induced activation of Src family kinases and the subsequent phosphorylation of adapter proteins (*i.e.* Shc and Grb2) lead to activation of ERK1/2 via Ras. Furthermore, the data presented suggest that protein tyrosine phosphatases are involved in eicosanoid signaling and that multiple receptors might be involved in the A431 response to 12(*S*)-HETE. Finally, we show that inactivation of endogenous 12(*S*)-HETE production with 12-lipoxygenase inhibitors leads to apoptosis of A431 cells, which is counteracted by overexpression of 12-lipoxygenase or by exogenously added 12(*S*)-HETE.

Many of the above-mentioned signaling molecules are implicated in cellular functions known to be affected by 12(*S*)-HETE. For example, 12(*S*)-HETE-stimulated PKC activity may be responsible for altered cellular morphology, since 12(*S*)-HETE induces phosphorylation of cytoskeletal proteins including actin, vimentin, and myosin light chain (48) and stimulates cellular spreading (4). 12(*S*)-HETE-stimulated PKC may promote the cellular migratory phenotype (46). All of the aforementioned 12(*S*)-HETE stimulated responses can be inhibited or significantly reduced with select PKC inhibitors (42, 46).

The above results demonstrate that 12(*S*)-HETE also protects tumor cells from the induction of apoptosis, but the exact mechanism of this effect needs further investigation. However, one may speculate that since ERK can activate $p90^{rsk}$, which in turn can phosphorylate BAD and CREB (49), two proteins demonstrated to have an anti-apoptotic effect, this may be a plausible mechanism to explain the anti-apoptotic effect of 12(*S*)-HETE. Alternatively, PKCα may prevent apoptosis independent of ERK. Ruvolo *et al.* (50) suggested that mitochondrial protein kinase Cα may inhibit apoptosis through phosphorylation of Bcl2.

The findings that 12(*S*)-HETE signaling can be inhibited by suramin or pertussis toxin suggests the existence of G protein-coupled receptor(s). However, no HETE receptors have yet been cloned. Receptors for arachidonate-lipoxygenase products that have been identified to date are the lipoxin A_4 (51) and leukotriene B_4 (52) and cysteinyl leukotriene receptors (53, 54). These receptors, similar to the receptors for prostaglandins, are members of the family of G protein-coupled seven transmembrane receptors. Several attempts to identify a 12(*S*)-HETE receptor have resulted only in the identification of a cytoplasmic binding complex, which is not well characterized (55, 56). Several lines of evidence suggests that 12(*S*)-HETE might have multiple receptors on A431 cells. 1) Binding studies revealed at least two binding sites on intact cells. 2) Shc tyrosine phosphorylation is maximal around 100 nM 12(*S*)-HETE concentration, but ERK activation is not saturated even at 500 nM. 3) 12(*S*)-HETE effect on EGF-stimulated activation of ERK is bi-phasic; at 100 nM it is negative, but at 600 nM, ERK phosphorylation is

augmented. Considering these data we speculate that 12(*S*)-HETE may have a high and a low affinity receptor. The high affinity receptor stimulates a protein tyrosine phosphatase as well as a protein tyrosine kinase, *i.e.* Src. This is not necessarily conflicting, since Src family kinases are inhibited by phosphorylation of a C-terminal residue. The proposed phosphatase may remove phosphate from this residue, lifting the inhibition, which then leads to activation of Src. The observed increase in the overall tyrosine phosphorylation of Src following 12(*S*)-HETE exposure might reflect autophosphorylation of the activated Src on the two positive regulatory tyrosine residues. In this pathway Src is positioned upstream of Shc, Grb2, Ras, and ultimately of the ERK cascade. The low affinity receptor does not appear to stimulate either the protein tyrosine phosphatase, Src, or Shc. Possibly the low affinity receptor activates ERK1/2 via stimulation of PKCα (hence increased translocation of PKCα at 600 nM 12(*S*)-HETE concentration). However, that does not exclude the possibility that low dose 12(*S*)-HETE activates PKCα via the high affinity receptor coupled to phospholipases.

The notion of multiple 12(*S*)-HETE receptors is supported by the fact that high affinity (K_d 1 nM (7)) as well as low affinity (K_d 658 nM (38)) binding sites were found on different cell lines, and by our observation that human prostate carcinoma cell lines express both high and low affinity binding sites simultaneously.[2] Furthermore, the Shc phosphorylation response curve is shaped like the curve of functional responses to 12(*S*)-HETE by melanoma cells that express the high affinity binding site (7).

It is not surprising that the utilization of labeled 12(*S*)-HETE for isolation of its receptor has been unsuccessful, considering that the serpentine receptors are sensitive to solubilization and may lose binding of their ligands once extracted from the plasma membrane or dissociated from G proteins (57). Therefore, functional cloning is a method that may lead to the isolation of the 12(*S*)-HETE receptor(s). The present report identifies downstream effector molecules of 12(*S*)-HETE signaling which can be monitored and hence provide useful tools for future cloning of the 12(*S*)-HETE receptor(s).

Following activation of the putative, G protein-coupled 12(*S*)-HETE receptor, we observed activation of Src kinases and a bifurcation of the signaling pathway. The concept of a G protein-coupled signaling system utilizing parallel pathways to activate ERK is not unique to 12(*S*)-HETE. For example, angiotensin II can stimulate ERK through activation of PKC or, alternatively, by trans-activating the EGF receptor (12).

Although this study describes two novel pathways for 12(*S*)-HETE-induced activation of ERK, it raises some interesting questions. The two pathways identified in the present study emanate from the activation of Src kinases. However, inactivation of Src family kinases with PP2 completely inhibited tyrosine phosphorylation of both PLCγ1 and Shc, following 12(*S*)-HETE treatment, yet this was insufficient to suppress completely ERK1/2 stimulation, suggesting the possibility of a Src-independent pathway in 12(*S*)-HETE signaling.

Both mitogenic and motogenic cellular responses are elicited by 12(*S*)-HETE (46). The different responses to the same signaling molecule may be due to the duration of the signal stimulated by 12(*S*)-HETE and whether or not 12(*S*)-HETE stimulation results from exogenously or endogenously generated eicosanoid. The duration of ERK activation has a profound effect on the cellular response. Depending on the cell type, the short time period activation of ERK might lead to differentiation, and long term activity of ERK may result in proliferation

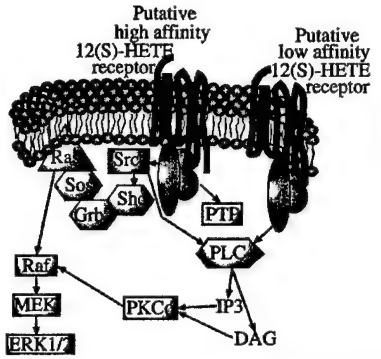

FIG. 14. **Schematic representation of the proposed 12(*S*)-HETE signal transduction pathways.** 12(*S*)-HETE binds to a putative high affinity, trimeric G protein-coupled receptor that results in activation of a protein tyrosine phosphatase and Src family kinases. These kinases phosphorylate PLCγ1 and the adapter protein Shc. PLC activation results in stimulation of PKCα, whereas Shc phosphorylation leads to recruitment of Grb2, Sos, and ultimately to increased GTP loading of Ras. Ultimately both of these pathways converge on Raf. A putative low affinity receptor also activates PKCα via PLC. *DAG*, diacylglycerol; *IP3*, inositol 1,4,5-trisphosphate; *PTP*, protein tyrosine phosphatase.

or vice versa (58). In this study, the addition of exogenous 12(*S*)-HETE to A431 cells stimulated ERK activity for approximately 30 min. However, phorbol ester or EGF can stimulate ERK activity for a period of hours. The short duration of the ERK response observed in the present study may result from esterification of exogenously added 12(*S*)-HETE into membrane lipids (59), limiting the availability of free eicosanoid, and hence, dampening the duration of the ERK response. It is possible that continuous, endogenous production of 12(*S*)-HETE could result in a constitutively elevated level of ERK activity. The addition of a single bolus of exogenous 12(*S*)-HETE to tumor cells, as utilized in this study, may mimic a situation that occurs during metastasis when tumor cells are exposed to exogenously produced 12-HETE during their aggregation with platelets, a rich source of 12(*S*)-HETE (1). However, the biological response may be different in the case of continuous, endogenous production of 12(*S*)-HETE, such as in epidermal growth factor (60) or autocrine motility factor (61)-stimulated cells.

Downstream signaling pathways activated by other lipoxygenase products are not well characterized. Nevertheless, there are similarities among the findings described in the literature and those in the present study. For example, neutrophil 5(*S*)-HETE, a positional isomer of 12(*S*)-HETE, also stimulates ERK via RAF and MEK (62). In eosinophils, leukotriene B_4 activates ERK1/2 but not JNK or p38 MAPK (63) and promotes hydrogen peroxide production in a PKC-dependent manner (64). Lipoxin A_4 increases intracellular calcium concentration in a manner inhibited by pertussis toxin (65). Leukotriene D_4 also increases calcium concentration in cells but by two pathways as follows: 1) by a pertussis toxin-sensitive pathway that results in the stimulation of extracellular calcium influx, and 2) by a pertussis toxin-insensitive pathway resulting in the mobilization of the intracellular calcium pool (45). Therefore, both leukotriene D_4 and 12(*S*)-HETE promote a simultaneous effect (*i.e.* an increase in intracellular calcium concentration or ERK activity, respectively), in a pertussis toxin-dependent and -independent manner. These examples suggest that lipoxygenase generated eicosanoids signal via pathways that are in common with other paracrine effectors.

Fig. 14 depicts a model of 12(*S*)-HETE-mediated signaling consistent with the data presented in this report. Stimulation of a putative high affinity G protein-coupled receptor leads to the activation of Src family kinases and a protein tyrosine

[2] K. V. Honn, unpublished observations.

phosphatase. The pathway bifurcates with tyrosine phosphorylation of two Src family substrates, Shc and PLCγ1. In one arm of the pathway Shc recruits Grb2 and activates Sos and Ras which in turn activates MEK and ERK. In the parallel pathway, PLCγ1 activates PKCα, leading to activation of Raf, which stimulates the downstream kinases MEK and ERK. A low affinity receptor may also stimulate PKCα and ultimately ERK1/2.

The goal of this study was to identify signaling molecules that may be responsible for the pleiotropic effects of 12(*S*)-HETE on tumor cells. We identified PKC, Ras, and ERK1/2 as targets of 12(*S*)-HETE stimulation. These molecules are at the intersections of multiple signaling pathways, activation of which can lead to diverse changes in cellular behavior. Stimulation of these signaling molecules may help to explain the many and varied effects of 12(*S*)-HETE on tumor metastasis, *i.e.* adhesion, spreading, migration, and invasion (2–4), stimulation of angiogenesis (6), and protection against the induction of apoptosis (5). Since the presence of 12-lipoxygenase has been correlated with prostate cancer progression in a clinical setting (40), it is important to identify the signaling pathways utilized by its principal arachidonate metabolite (*i.e.* 12(*S*)-HETE). Future studies are directed toward the identification of the 12(*S*)-HETE receptor(s).

Acknowledgments—We thank Yinlong Cai for excellent help with the apoptosis studies; Dr. Debra Skafar for most helpful suggestions on the binding studies; and Drs. Jozsef Timar, Daotai Nie, Clem Stanyon, and Avraham Raz for helpful discussion.

REFERENCES

1. Honn, K. V., Tang, D. G., and Crissman, J. D. (1992) *Cancer Metastasis Rev.* **11,** 325–351
2. Chopra, H., Timar, J., Chen, Y. Q., Rong, X. H., Grossi, I. M., Fitzgerald, L. A., Taylor, J. D., and Honn, K. V. (1991) *Int. J. Cancer* **49,** 774–786
3. Timar, J., Chen, Y. Q., Liu, B., Bazaz, R., Taylor, J. D., and Honn, K. V. (1992) *Int. J. Cancer* **52,** 594–603
4. Timar, J., Silletti, S., Bazaz, R., Raz, A., and Honn, K. V. (1993) *Int. J. Cancer* **55,** 1–8
5. Tang, D. G., Chen, Y. Q., and Honn, K. V. (1996) *Proc. Natl. Acad. Sci. U. S. A.* **93,** 5241–5246
6. Nie, D., Hillman, G. G., Geddes, T., Tang, K., Pierson, C., Grignon, D., and Honn, K. V. (1998) *Cancer Res.* **58,** 4047–4051
7. Liu, B., Khan, W. A., Hannun, Y. A., Timar, J., Taylor, D. J., Lundy, S. K., Butovich, I., and Honn, K. V. (1995) *Proc. Natl. Acad. Sci. U. S. A.* **92,** 9323–9327
8. Landgren, E., Schiller, P., Cao, Y., and Claesson-Welsh, L. (1998) *Oncogene* **16,** 359–367
9. Whalen, A. M., Galasinski, S. C., Shapiro, P. S., Nahreini, T. S., and Ahn, N. G. (1997) *Mol. Cell. Biol.* **17,** 1947–1958
10. Klemke, R. L., Cai, S., Giannini, A. L., Gallagher, P. J., de Lanerolle, P., and Cheresh, D. A. (1997) *J. Cell Biol.* **137,** 481–492
11. Sugden, P. H., and Clerk, A. (1999) *Cell. Signal.* **5,** 337–351
12. Li, X., Lee, J. W., Graves, L. M., and Earp, H. S. (1998) *EMBO J.* **17,** 2574–2583
13. Luttrell, L. M., Hawes, B. E., van Biesen, T., Luttrell, D. K., Lansing, T. J., and Lefkowitz, R. J. (1996) *J. Biol. Chem.* **271,** 19443–19450
14. Tang, D. G., Tarrien, M., Dobzynski, P., and Honn, K. V. (1995) *J. Cell. Physiol.* **165,** 291–306
15. Gschwendt, M., Dieterich, S., Rennecke, J., Kittstein, W., Mueller, H. J., and Johannes, F. J. (1996) *FEBS Lett.* **392,** 77–80
16. Hanke, J. H., Gardner, J. P., Dow, R. L., Changelian, P. S., Brissette, W. H., Weringer, E. J., Pollok, B. A., and Connelly, P. A., (1996) *J. Biol. Chem.* **271,** 695–701
17. Kultz, D., Madhany, S., and Burg, M. B. (1998) *J. Biol. Chem.* **273,** 13645–13651
18. Levitzki, A. (1990) *Biochem. Pharmacol.* **40,** 913–918
19. Vogt, A., Qian, Y., Blaskovich, M. A., Fossum, R. D., Hamilton, A. D., and Sebti, S. M. (1995) *J. Biol. Chem.* **270,** 660–664
20. Beindl, W., Mitterauer, T., Hohenegger, M., Ijzerman, A. P., Nanoff, C., Freissmuth, M. (1996) *Mol. Pharmacol.* **50,** 415–423
21. Chen, Y. Q., Duniec, Z. M., Liu, B., Hagmann, W., Gao, X., Shimoji, K., Johnson, C. R., and Honn, K. V. (1994) *Cancer Res.* **54,** 1574–1579
22. Tang, K., Finley, R. L., Nie, D., and Honn, K. V. (2000) *Biochemistry* **39,** 3185–3191
23. Gopalakrishina, R., and Barsky, S. H. (1988) *Proc. Natl. Acad. Sci. U. S. A.* **85,** 612–616
24. Liu, B., Timar, J., Howlett, J., Diglio, C. A., and Honn, K. V. (1991) *Cell Regul.* **2,** 1045–1055
25. Bleich, D., Chen, S., Wen, Y., and Nadler, J. L. (1997) *Biochem. Cell Biol.* **230,** 448–3451
26. Standaert, M. L., Galloway, L., Karnam, P., Bandyopadhyay, G., Moscat, J., and Farese, R. V. (1997) *J. Biol. Chem.* **272,** 30075–300082
27. Schaeffer, H. J., Catling, A. D., Ebling, S. T., Collier, L. S., Krauss, A., and Weber, M. J. (1998) *Science* **281,** 1668–1671
28. Grammer, T. C., and Blenis, J. (1997) *Oncogene* **14,** 1635–1642
29. Katan, M. (1996) *Cancer Surv.* **27,** 199–121
30. Sankaran, B., Osterhout, J., Wu, D., and Smrcka, A. V. (1998) *J. Biol. Chem.* **273,** 7148–7154
31. Venema, R. C., Ju, H., Venema, V. J., Schieffer, B., Harp, J. B., Ling, B. N., Eaton, D. C., and Marrero, M. B. (1998) *J. Biol. Chem.* **273,** 7703–7708
32. Gronroos, E., Andersson, T., Schippert, A., Zheng, L., and Sjolander, A. (1996) *Biochem. J.* **316,** 239–245
33. Rao, G. N., Delafontaine, P., and Runge, M. S. (1995) *J. Biol. Chem.* **270,** 27871–27875
34. Linseman, D. A., Benjamin, C. W., and Jones, D. A. (1995) *J. Biol. Chem.* **270,** 12563–12568
35. Daub, H., Weiss, F. U., Wallasch, C., and Ullrich, A. (1996) *Nature* **379,** 557–560
36. Graness, A., Hanke, S., Boehmer, F. D., Presek, P., and Liebmann, C. (2000) *Biochem. J.* **347,** 441–447
37. Thomas, A. M., and Brugge, J. S. (1997) *Annu. Rev. Cell Biol.* **13,** 513–609
38. Zakaroff-Girard, A., Gilbert, M., Meskini, N., Nemoz, G., Lagarde, M., and Prigent, A.-F. (1999) *Life Sci.* **64,** 2135–2148
39. Liu, B., Marnett, L. J., Chaundhary, A., Ji, C., Blair, I. A., Johnson, C. R., Diglio, C. A., and Honn, K. V. (1994) *Lab. Invest.* **70,** 314–323
40. Gao, X., Grignon, D. J., Chbihi, T., Zacharek, A. R., Chen, Y. Q., Sakr, W., Porter, A. T., Crissman, J. D., Pontes, J. D., Powell, I. J., and Honn, K. V. (1995) *Urology* **46,** 227–237
41. Tang, D. G., and Honn, K. V. (1997) *Adv. Exp. Med. Biol.* **400,** 349–361
42. Honn, K. V., Timar, J., Rozhin, J., Bazaz, R., Sameni, M., Ziegler, G., and Sloane, B. F. (1994) *Exp. Cell Res.* **214,** 120–130
43. Liu, X. H., Connolly, J. M., and Rose, D. P. (1996) *Clin. Exp. Metastasis* **14,** 145–152
44. Tang, D. G., Diglio, C. A., Bazaz, R., and Honn, K. V. (1995) *J. Cell Sci.* **108,** 2629–2644
45. Sjolander, A., and Gronroos, E. (1994) *Ann. N. Y. Acad. Sci.* **744,** 155–160
46. Honn, K. V., Tang, D. G., Gao, X., Butovich, I. A., Liu, B., Timar, J., and Hagmann, W. (1994) *Cancer Metastasis Rev.* **13,** 365–396
47. Honn, K. V., Tang, D. G., Grossi, I., Duniec, Z. M., Timar, J., Renaud, C., Leithauser, M., Blair, I., Johnson, C. R., Diglio, C. A., Kimler, V. A., Taylor, J. D., and Marnett, L. J. (1994) *Cancer Res.* **54,** 565–574
48. Rice, R. L., Tang, D. G., Haddad, M., Honn, K. V., and Taylor, J. D. (1998) *Int. J. Cancer* **77,** 271–278
49. Bonni, A., Brunet, A., West, A. E., Datta, S. R., Takasu, M. A., and Greenberg, M. E. (1999) *Science* **286,** 1358–1362
50. Ruvolo, P. P., Deng, X., Carr, B. K., and May, W. S. (1998) *J. Biol. Chem.* **273,** 25436–25442
51. Fiore, S., Maddox, J. F., Perez, H. D., and Serhan, C. N. (1994) *J. Exp. Med.* **180,** 253–260
52. Yokomizo, T., Izumi, T., Chang, K., Takuwa, Y., and Shimizu, T. (1997) *Nature* **387,** 620–624
53. Sarau, H. M., Ames, R. S., Chambers, J., Ellis, C., Elshourbagy, N., Foley, J. J., Schmidt, D. B., Muccitelli, R. M., Jenkins, O., Murdock, P. R., Herrity, N. C., Halsey, W., Sathe, G., Muir, A. I., Nuthulaganti, P., Dytko, G. M., Buckley, P. T., Wilson, S., Bergsma, D. J., and Hay, D. W. (1999) *Mol. Pharmacol.* **56,** 657–663
54. Kevin, R. Lynch, K. R., Oneill, G. P., Liu, Q., Im, D. S., Sawyer, N., Metters, K. M., Coulombe, N., Abramovitz, M., Figueroa, D. J., Zeng, Z., Connolly, G. M., Bai, C., Austin, C. P., Chateauneuf, A., Stocco, R., Greig, G. M., Kargman, S., Hooks, S. B., Hosfield, E., Williams, D. L., Ford-Hutchinson, A. W., Caskey, C. T., and Evans, J. F. (1999) *Nature* **399,** 789–793
55. Herbertsson, H., Kuhme, T., Evertsson, U., Wigren, J., and Hammarstrom, S. (1998) *J. Lipid Res.* **39,** 237–244
56. Kurahashi, Y., Herbertsson, H., Soderstrom, M., Rosenfeld, M. G., and Hammarstrom, S. (2000) *Proc. Natl. Acad. Sci. U. S. A.* **97,** 5779–5783
57. Mong, S., Sarau, H. M. (1990) *Mol. Pharmacol.* **37,** 60–64
58. Marshall, C. J. (1995) *Cell* **80,** 179–185
59. Costello, P. B., Baer, A. N., and Green, F. A. (1991) *Inflammation* **15,** 269–279
60. Hagmann, W., Gao, X., Timar, J., Chen, Y. Q., Strohmaier, A. R., Fahrenkopf, C., Kagawa, D., Lee, M., Zacharek, A., and Honn, K. V. (1996) *Exp. Cell Res.* **228,** 197–205
61. Silletti, S., Timar, J., Honn, K. V., and Raz, A. (1994) *Cancer Res.* **54,** 5752–5756
62. Capodici, C., Pillinger, M. H., Han, G., Philips, M. R., and Weissmann, G., (1998) *J. Clin. Invest.* **102,** 165–175
63. Lindsay, M. A., Haddad, E. B., Rousell, J., Teixeira, M. M., Hellewell, P. G., Barnes, P. J., and Giembycz, M. A. (1998) *J. Leukocyte Biol.* **64,** 555–562
64. Perkins, R. S., Lindsay, M. A., Barnes, P. J., and Giembycz, M. A. (1995) *Biochem. J.* **310,** 795–806
65. Maddox, J. F., Hachicha, M., Takano, T., Fokin, V. V., and Serhan, C. N. (1997) *J. Biol. Chem.* **272,** 6972–6978

Int. J. Cancer: **87**, 37–43 (2000)

Publication of the International Union Against Cancer

EXPRESSION, SUBCELLULAR LOCALIZATION AND PUTATIVE FUNCTION OF PLATELET-TYPE 12-LIPOXYGENASE IN HUMAN PROSTATE CANCER CELL LINES OF DIFFERENT METASTATIC POTENTIAL

József TIMÁR[1]*, Erzsébet RÁSÓ[1], Balázs DÖME[1], Li LI[2], David GRIGNON[3], Daotai NIE[3], Kenneth V. HONN[3,4] and Wolfgang HAGMANN[5]

[1]*Department of Tumor Progression, National Institute of Oncology, Budapest, Hungary*
[2]*Biomide Corporation, Grosse Pointe Farms, Michigan, USA*
[3]*Departments of Radiation Oncology and Pathology, Wayne State University, Detroit, Michigan, USA*
[4]*Karmanos Cancer Institute, Detroit, Michigan, USA*
[5]*Division of Tumor Biochemistry, German Cancer Research Center, Heidelberg, Germany*

The involvement of 12-lipoxygenase (12-LOX) expression and function in tumor metastasis has been demonstrated in several murine tumor cell lines. In addition, 12-LOX expression was detected in human prostatic tumors and correlated to the clinical stage of disease. Here we provide data that human prostate cancer cell lines express the platelet-type isoform of 12-LOX at both the mRNA and protein levels, and immunohistochemistry revealed 12-LOX expression in human prostate tumors. The enzyme was localized to the plasma membrane, cytoplasmic organelles and nucleus in non-metastatic cells (PC-3 nm) and to the cytoskeleton and nucleus in metastatic cells (DU-145). After orthotopic/intraprostatic injection of tumor cells into SCID mice, the metastatic prostate carcinoma cells (DU-145) expressed 12-LOX at a significantly higher level compared with the non-metastatic counterparts, PC-3nm. The functional involvement of 12-LOX in the metastatic process was demonstrated when DU-145 cells were pretreated *in vitro* with the 12-LOX inhibitors N-benzyl-N-hydroxy-5-phenylpentamide (BHPP) or baicalein, the use of which significantly inhibited lung colonization. These data suggest a potential involvement of 12-LOX in the progression of human prostate cancer. *Int. J. Cancer* 87: 37–43, 2000.
© *2000 Wiley-Liss, Inc.*

Membrane receptors regulate cellular activities by triggering a cascade of events ultimately affecting the function of various kinases. Significant components of the signaling cascade are phospholipases providing arachidonate, which is further metabolized by either cyclooxygenase (COX) or lipoxygenase (LOX) enzymes. It is known that both COX (Brinkman *et al.*, 1990; Thompson *et al.*, 1984) and LOX (Honn *et al.*, 1994*a*; Eling and Glasgow, 1994) products are able to provide mitogenic signals to cells. Further, it has been shown that LOXs are essential regulators of cell survival and apoptosis (Tang *et al.*, 1996). However, 12-LOX and its product 12-hydroxyeicosatetraenoic acid (12-HETE) have several other physiological functions including the induction of endothelial cell retraction, platelet aggregation and chemokinesis of leukocytes (Honn *et al.*, 1994*a*). 12-LOX is expressed in 3 immunologically and enzymologically distinct forms (platelet, leukocyte and epithelial) which are characterized by unique tissue distributions (Takahashi *et al.*, 1998; Hamsbrough *et al.*, 1990; Hagmann, 1997).

It was shown that various rodent and human tumor types express 12-LOX, produce 12-HETE or respond to exogenous 12-HETE. These include murine melanomas (Chen *et al.*, 1994; Silletti *et al.*, 1994) and carcinomas (Chen *et al.*, 1994; Hagmann *et al.*, 1995; Wang *et al.*, 1996), human leukemias (Hagmann *et al.*, 1993), carcinomas (Chen *et al.*, 1994; Hagmann *et al.*, 1996) and melanomas (Timar *et al.*, 1999), suggesting an important function for 12-HETE in tumor biology. Systematic studies revealed that in addition to the importance of 12-HETE as a mitogenic signaling molecule, 12-LOX and 12-HETE have important roles in tumor metastasis as generators of motogenic signals (Timar *et al.*, 1993*a*), upregulation of adhesion molecules (Chopra *et al.*, 1991) and promotion of local invasion through matrices by enhancing proteolytic enzyme release (Honn *et al.*, 1994*b*).

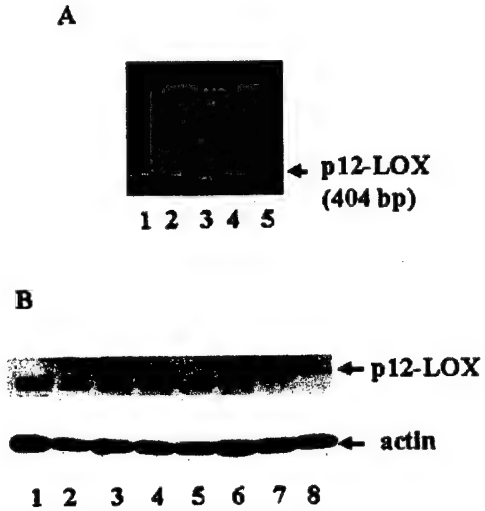

FIGURE 1 – *(a)* RT-PCR analysis of 12-LOX mRNA in human prostate cell lines. Total RNA from PC-3 nm (lane 1), DU-145 (lane 2), HEL (as positive control; lane 4) and sample without RNA (lane 5) were PCR amplified using platelet-type-specific 12-LOX primers. PCR products were separated on 2% agarose gel and visualized by ethidium bromide staining. Lane 3 is molecular size standard (plasmid digest). *(b)* Western blot analysis of cellular proteins from human prostate cancer cell lines probed for platelet-type 12-LOX. Cellular proteins were isolated, separated by SDS-PAGE, transferred to nitrocellulose membrane and probed for 12-LOX protein as described in Material and Methods. Platelet lysate was used as positive control (lane 1). Control actin blot serves as protein and loading reference. ML2 (lane 2), TSU (lane 3), DU-145 (lane 4), PC-3 (lane 5), LN (lane 6) and PPC-1 (lane 7) are human prostate cancer cell lines, whereas NHP (lane 8) is a prostate epithelial cell line. Note the double bands in ML2, TSU, DU-145, LN and PPC-1 cells.

Grant sponsor: Hungarian Science Fund; Grant numbers: OTKA T-21149; T-25155; Grant sponsor: Hungarian Ministry of Welfare; Grant number: T-542/96; Grant sponsor: NIH; Grant number: CA-29997; Grant sponsor: NATO; Grant number: LST.CLG.975184.

*Correspondence to: Department of Tumor Progression, National Institute of Oncology, Ráth Gy. u.7-9, H-1122 Budapest, Hungary. Fax: 36 1 224 8620. E-mail: jtimar@oncol.hu

Received 26 October 1999; Revised 6 January 2000

Prostate cancer has become a leading malignancy in the aging populations of the Western hemisphere, which justifies the increased interest in the biology of this disease. Previously, we demonstrated that 12-HETE promotes rodent prostate carcinoma motility and invasion (Liu *et al.,* 1994*b*), suggesting that this molecule might be an important component of the motogenic signaling pathway in prostate cancer, similar to melanoma (Timar *et al.,* 1993*a*). Therefore, the aim of our study was to establish the expression of 12-LOX in human prostate carcinoma cell lines both at the mRNA and protein levels, as well as at the protein level in human prostate tissue, and to study its subcellular localization and functional significance.

MATERIAL AND METHODS

Cell and tumor lines

PC-3, DU-145, LNCaP and HEL cells were obtained from American Type Culture Collection (Rockville, MD) and routinely cultured in RPMI 1640 supplemented with 10% fetal bovine serum, 2 mM L-glutamine and antibiotics. A non-metastatic subline of PC-3 (*i.e.,* PC-3 nm) was established. The PC-3 nm line proved to be tumorigenic but non-metastatic, whereas the DU-145 cell line was both tumorigenic and metastatic *in vivo* in SCID mice after orthotopic implantation (Timar *et al.,* 1996*b*). Normal human prostate (NHP) epithelial cells were obtained from Clonetics (San Diego, CA) and cultured in KBM basic medium with 5 μg/ml insulin, 0.5 μg/ml hydrocortisone, 10 ng/ml epidermal growth factor, 50 μg/ml bovine pituitary extract, 10 ng/ml cholera toxin and antibiotics. Primary prostate carcinoma-1 (PPC-1) cells were initially provided by Dr. A. Brothman (Eastern Virginia Medical School). The TSU cell line was provided by Dr. W.G. Nelson (Johns Hopkins Cancer Center). A PC-3 subline that preferentially metastasizes to bone (PC-3-ML2) was provided by Dr. M. Stearns (Medical College of Pennsylvania). These latter 3 cell lines were cultured in RPMI 1640 supplemented with 10% fetal bovine serum, 2 mM L-glutamine and antibiotics.

Detection of 12-LOX expression at RNA level

Total RNA was obtained using the guanidinium isothiocyanate-CsCl method as described previously (Hagmann *et al.,* 1996) and suspended at 1 mg/ml in distilled water. Three micrograms of RNA was reverse transcribed (RT) using oligo(dT)18 primers and 2 μl of the cDNA mixture was amplified by polymerase chain reaction (PCR) with sense and antisense primers. The primers span exon-intron boundaries of the 12-LOX gene thus avoiding amplification of genomic DNA during PCR. DNase was used to prevent PCR product carryover and genomic DNA contamination. The RT-PCR was performed in the GeneAmp PCR 9600 (Perkin-Elmer-Cetus, Wellesley, MA) at 94°C for 30 sec, 70°C for 30 sec and 72°C for 30 sec for 35 cycles. The sequence of the platelet-specific 12-LOX sense and antisense probes was described previously (Hagmann and Borgers, 1997). Fifteen microliters of PCR products was separated by electrophoresis on 2% agarose gels, stained by ethidium bromide and photographed. PCR products were sequenced directly or after cloning into the pCR2.1 TOPO II vector (Invitrogen, La Jolla, CA) and sequenced with T-7 and SP-6 primers as described (Trikha *et al.,* 1996, 1997). The sequence was aligned to 12-LOX cDNA (Funk *et al.,* 1990) by using the MacVector 4.1 software on a Macintosh Quadra 630 computer.

Detection of 12-LOX expression at protein level

Western blotting. Adherent tumor cells cultured *in vitro* were dislodged from the flask and washed in PBS. Aliquots of the homogenate were subjected to sodium dodecyl sulfate-polyacrylamide gel electrophoresis (SDS-PAGE) on 8% gels. Proteins were electrophoretically transferred to nitrocellulose membranes. Cells were lysed in TNC (10 mM Tris-acetate, 0.5% NP-40, and 5 μM $CaCl_2$, pH 7.4) buffer on ice. The solubilized proteins were loaded on 4–20% gradient SDS-PAGE, transferred to nitrocellulose paper (the non-specific binding sites were blocked by non-fat milk) and then probed with primary antibody anti-12-LOX (Oxford Biomedical, Oxford, UK) and secondary antibody goat anti-rabbit IgG (Bio-Rad, Munich, Germany) conjugated to horseradish peroxidase. Enhanced chemiluminescence (ECL; Amersham, Little

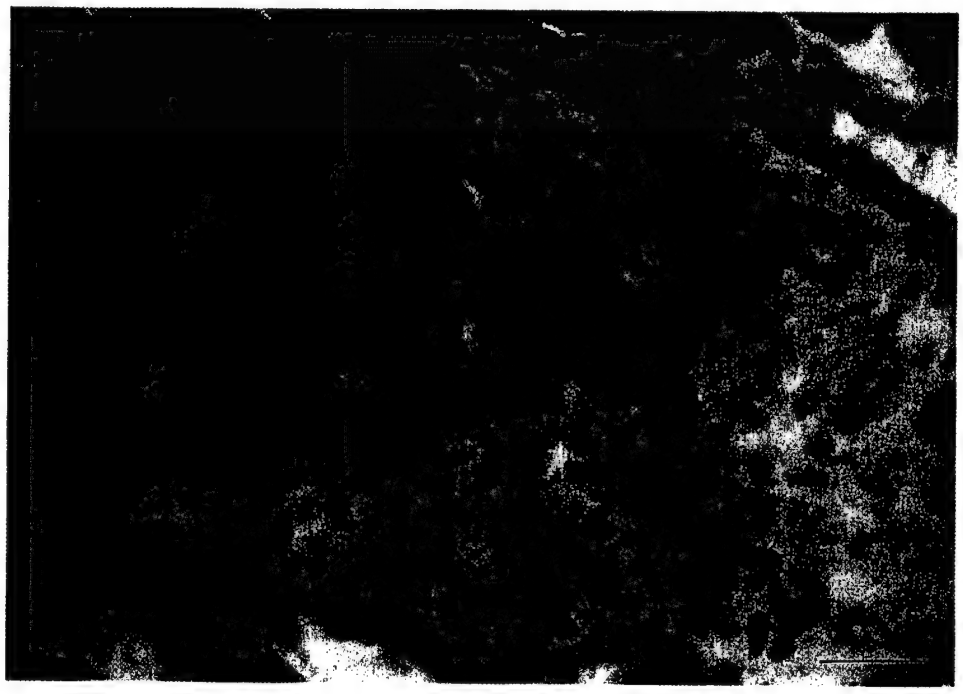

FIGURE 2 – Immunohistochemistry of 12-LOX performed on frozen prostate tumor. There is intense cytoplasmic positivity in the malignant glands of this Gleason score 6 adenocarcinoma. There is no immunoreactivity in the epithelium of the normal prostatic glands (N) or the stromal cells in the background. Scale bar = 50 μm.

Chalfont, UK) was used for detection. For positive controls we utilized either human erythroleukemia (HEL) cells, which have been demonstrated to express platelet-type 12-LOX (Funk *et al.*, 1990), or partially purified human platelet-type 12-LOX obtained from human platelet lysates (Oxford Biomedical).

Flow cytometry. Adherent cells were detached from tissue culture flasks by using low EDTA washing or isolated from solid tumors as described previously (Trikha *et al.*, 1998), centrifuged at 100*g* and fixed in absolute methanol for 10 min. After washing in PBS, cells were labeled for platelet-type 12-LOX using a rabbit polyclonal antibody, biotinylated goat anti-rabbit IgG (Amersham) and Streptavidin-FITC (Amersham). For negative controls, the primary antibody was omitted. Flow cytometry of the samples was performed as described previously (Timar *et al.*, 1993*a*), wherein 90% of the fluorescence of the negative control cell population served as the gate. Both percent of positive cells and fluorescence intensity were determined. Samples were run in triplicate.

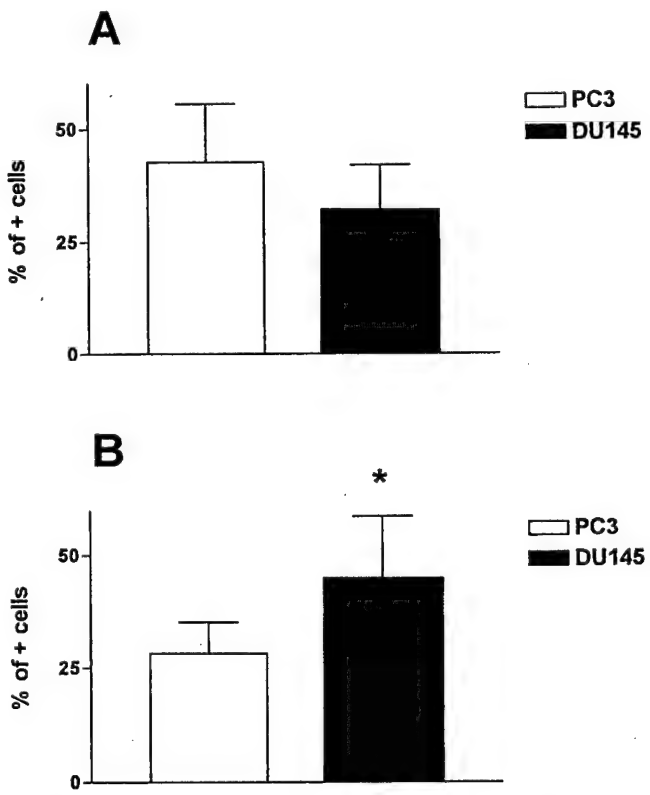

FIGURE 3 – Flow cytometric analysis of 12-LOX expression at protein level in human prostate cancer cell lines. *(a) In vitro* cultured cells. *In vitro* cultured tumor cells were detached from the plastic surface, suspended, fixed in methanol and labeled for platelet-type 12-LOX using a polyclonal anti-human 12-LOX-specific rabbit antibody. The bound antibody was revealed by a biotinylated secondary antibody and FITC-labeled Streptavidin. Cells (10^4) were analyzed by flow cytometry from each sample for the percent of positive cells. Gate was set according to the fluorescence intensity of the negative controls. Data are expressed as means ± SD (n = 3). *(b) In vivo* growing primary tumors. Tumor cells were injected orthotopically into the prostate of SCID mice, 5–10-mm-sized primary tumors were removed and tumor cells were isolated by an enzymatic method (see Material and Methods). Single cell suspensions were fixed in methanol and labeled for platelet-type 12-LOX using a polyclonal anti-human 12-LOX-specific rabbit antibody. The bound antibody was revealed by a biotinylated secondary antibody and FITC-labeled Streptavidin. Cells (10^4) were analyzed by flow cytometry from each sample for the percent of positive cells. The gate was set according to the fluorescence intensity of the negative controls. Platelets and red blood cells were gated out from the measurement by their light scatter characteristics. Data are expressed as means ± SD (n = 3). $*p < 0.05$.

Confocal laser scanning microscopy. Tumor cells were plated onto fibronectin-coated glass coverslips *in vitro* for 60 min at 37°C in serum-free RPMI medium, washed and the adherent cells were fixed in 1% paraformaldehyde (PFA)/PBS or absolute methanol for 10 min. The PFA-fixed cells were permeabilized by 0.1% Triton X-100/PBS (4 min). After washing in PBS, coverslips were blocked with 10% non-immune goat serum/PBS for 30 min at room temperature. Platelet-type 12-LOX was identified by immunocytochemistry using the polyclonal anti-12-LOX antibody as above. The primary antibody was diluted 1:100 in 3% bovine serum albumin (BSA)/PBS and the cells were incubated for 60 min at room temperature. After repeated washings in PBS, the bound antibody was detected using a biotinylated goat anti-rabbit IgG (Amersham) and Streptavidin-FITC (Amersham). Control cells were incubated with non-immune rabbit serum alone. To promote the subcellular localization of the enzyme, cells were counterstained with propidium iodine to identify the DNA-containing nucleus. Confocal microscopy was performed on a Bio-Rad MRX 1024 confocal microscope operating LaserSharp software (Bio-Rad).

Detection of 12-LOX expression in human prostate cancer

Immunohistochemistry. Sections were cut from snap-frozen human prostate cancer tissue at 4 μm thickness and placed on gelatin-coated glass slides. Prostate tissues from radical prostatectomy specimens removed from a total of 18 patients were examined. The sections were fixed in 100% cold acetone for 10 min. Primary antibody against 12-LOX (Oxford Biomedical) was diluted ×100 and incubated for 20 min. Detection was performed with an ABC kit (Vector Labs, Burlingame, CA).

Inhibition of 12-LOX in vitro

The select 12-LOX inhibitors used were N-benzyl-N-hydroxy-5-phenylpentammide (BHPP; Biomide Corp., Grosse Pointe Farms, MI; Chen *et al.*, 1994; Liu *et al.*, 1994) and baicalein (BioMol, Plymouth Meeting, PA; Kimura *et al.*, 1987). Cultured tumor cells were treated with the 12-LOX inhibitors BHPP (Chen *et al.*, 1994), or baicalein (Kimura *et al.*, 1987) dissolved in EtOH for 60 min at 37°C in serum-free RPMI at a concentration of 5 μM. This concentration was derived from previous studies (Chen *et al.*, 1994). Control cultures were treated with ethanol solvent alone.

Orthotopic injection, re-isolation of tumor cells and flow cytometry

Cultured tumor cells were detached from the plastic surface by low EDTA (Timar *et al.*, 1993*a*), resuspended in RPMI and 5×10^5 tumor cells injected into the prostate of SCID mice in 50 μl volume under anesthesia by Nembutal. On the 8th week of the experiment animals were sacrificed by Nembutal overdose, the 5–10-mm-sized primary tumors were surgically removed, sliced with crossed scalpels in RPMI and digested with collagenase type IV (Sigma, St. Louis, MO), testicular hyaluronidase (Sigma) and DNase (Sigma). A single cell suspension was prepared by repeated centrifugations and the contamination of the human tumor suspension with host mouse cells was determined by flow cytometric measurement of murine transplantation antigen H2d-expressing cells. These studies indicated that the host cell contamination was always less than 15%.

Lung colonization assay

In vitro cultured tumor cells were detached from culture dishes by using low EDTA, washed in RPMI and injected into the tail vein of SCID mice at a dose of 10^5 tumor cells/mouse. Animals were sacrificed by Nembutal overdose on the 30th day and the internal organs were analyzed for 10^5 tumor colonies. Histologic analysis was performed on the lung tissue to confirm the presence of prostate carcinoma metastases. In view of the huge tumor mass

TABLE I – INVASIVE PHENOTYPE OF HUMAN PROSTATE CANCER CELL LINES PC-3 AND DU-145 IN THE PROSTATE OF SCID MICE[1]

Type of invasion	PC-3 nm	DU-145 (%)
Prostate capsule	Not detected	100
Rectum	Not detected	50
Muscle	Not detected	60
Vascular	Not detected	40

[1]Data represent the incidence of local invasion.

in the lungs, the weight of the organ was determined in all experimental groups.

RESULTS

The expression of 12-LOX mRNA was examined in HEL cells, low metastatic PC-3 cells (*i.e.*, PC-3 nm) and high metastatic prostate cancer cells (DU-145). Total RNA was isolated from each cell line, reversed transcribed to cDNA and amplified by PCR using platelet-type 12-LOX-specific primers, as described in Material and Methods. The RNA from HEL, PC-3 nm and DU-145 cells all yielded the predicted 404 bp size fragment (Fig. 1*a*). The authenticity of this fragment was confirmed by Southern blot analysis with a human 12-LOX cDNA probe (data not shown). The fragment shared 100% homology with human platelet-type 12-LOX (Funk *et al.*, 1990) within the sequenced region (data not shown).

The presence of platelet-type 12-LOX in prostate carcinoma cells was further confirmed by Western blotting of cellular proteins using 6 *in vitro* cultured human prostatic carcinoma cell lines. The apparent size of the band (73 kDa) corresponded to partially purified human platelet-type 12-LOX isolated from platelet lysates (Fig. 1*b*). A positive band was detected in ML-2, TSU, DU-145, PC-3 (wild type), LN and PPC-1 prostate carcinoma cells. A minor amount of 12-LOX was also detected in NHP epithelial cells (Fig. 1*b*). An upper band of approximately 75 kDa was detected in TSU, DU-145, LN and PPC-1 cells. This may represent a phosphorylated form of platelet-type 12-LOX (K. Tang and K.V. Honn, unpublished observation).

The above data demonstrate that authentic platelet-type 12-LOX is expressed at both the message and protein levels in *in vitro* cultured prostate carcinoma cells. To confirm that the expression of platelet-type 12-LOX was not an artifact of *in vitro* cell culture, we performed immunohistochemical analysis of radical prostatectomy specimens. A total of 12 of 18 patient tumors stained positive for 12-LOX. A representative section is shown in Figure 2. Positive staining was observed in the tumor cells with little or no staining in normal tissue.

After we established the presence of platelet-type 12-LOX both *in vitro* and *in vivo* in prostate cancer, further studies in this report focused on the PC-3 nm and DU-145 cell lines. Immunocytochemistry and flow cytometry indicated that 30–40% of cultured tumor cells express the platelet-type 12-LOX (Fig. 3*a*). Interestingly, when tumor cells were injected into the prostate of SCID mice and the tumor cells re-isolated from the primary tumor, flow cytometry detected 12-LOX expression in DU-145 cells at a significantly higher proportion compared with the PC-3 nm cell line (Fig. 3*b*), suggesting that the local environment may differentially regulate the expression of the enzyme at the protein level in these 2 cell lines. We next compared the subcellular localization of 12-LOX in PC-3 nm and DU-145 cells. Confocal microscopy revealed that the 12-LOX protein in PC-3 nm cells can be detected at the peripheral plasma membrane of spread tumor cells, at vesicular cytoplasmic organelles and in the interchromatic space of the nucleus (Fig. 4*a*). In DU-145 cells, the 12-LOX protein was also observed at the peripheral plasma membrane and in the nucleus; however, the protein was found predominantly in the cytoplasm forming filaments which appeared to surround the nucleus (Fig. 4*b*).

In vivo PC-3 nm cells are tumorigenic but not invasive, whereas DU-145 cells are both tumorigenic and metastatic (Timar *et al.*, 1996). *In vivo* studies indicated that the 2 tumor cell lines have different invasive potential after intraprostatic injection (Table I). PC-3 nm tumor did not penetrate the prostatic capsule and never progressed beyond that border (Fig. 5*a*). In contrast, DU-145 tumors always infiltrated the prostatic capsule and in 50% of the cases it was possible to find evidence of local invasion in the muscle (Fig. 5*b*), adipose tissues or rectum (data not shown).

Since we observed that after intraprostatic growth the metastatic DU-145 cells express 12-LOX protein at a significantly higher level compared with the PC-3 nm cells (Fig. 3*b*), we postulated that this may have functional significance. Therefore, *in vitro* cultured DU-145 tumor cells were pretreated with the LOX inhibitors baicalein or BHPP *in vitro* (60 min; 5 μM) and tested for their lung colonization potential. Measurement of the tumor-bearing lungs 30 days after injection indicated that both agents reduced lung colonization and the effect of BHPP proved to be statistically significant (Fig. 6).

DISCUSSION

Expression of platelet-type 12-LOX in the human prostate cancer cell line PC-3 was demonstrated recently (Nie *et al.*, 1998). In that study, high expressor clones were produced by stable transfection with platelet-type 12-LOX. These high expressor clones exhibited an increased *in vivo* growth due to enhanced tumor-induced angiogenesis (Nie *et al.*, 1998). In this study, we provided evidence for the presence of 12-LOX message in 2 cell lines (PC-3 and DU-145), and 12-LOX protein in 6 prostate cancer cell lines. We compared the expression of 12-LOX in a metastatic human prostate cancer cell line, DU-145, with a non-metastatic counterpart, PC-3 nm, a subline of PC-3, and have provided evidence that DU-145 cells, similar to PC-3 nm, not only express the platelet-type 12-LOX gene but also contain the enzyme protein. RT-PCR indicated the presence of the same message in prostate cancer cell lines PC-3 nm and DU-145 as in the positive control HEL cells. Furthermore, Western blotting revealed a predominant protein band in both tumor lines using an anti-12-LOX antibody. However, the molecular weight of the predominant band in both prostate cancer cell lines was lower (73 kDa) than the one in HEL cells (75 kDa). Lower molecular weight 12-LOX protein bands in tumor cell lines were observed previously in 3LL murine carcinoma cells (Hagmann *et al.*, 1995). Furthermore, a 12-LOX of 68 kDa size was isolated recently from rat skin cells (Lomnitski *et al.*, 1995). Explanation for the lower molecular mass of these proteins could be various phosphorylation states, presence of splice variants or partial protein degradation. The significance of our finding of 12-LOX expression in human prostate cancer cells can be fundamental from both a prognostic and a therapeutic point of view. Endogenous production of 12-HETE was correlated to the invasive and metastatic potential of murine tumors (Chen *et al.*, 1994; Hagmann *et al.*, 1993). Further, it was also demonstrated that the enzyme which initiates 12-HETE production is actually 12-LOX (Chen *et al.*, 1994; Hagmann *et al.*, 1993, 1996). On the other hand, 12-LOX expression in tumors is not restricted to rodents, since various human tumor cell lines have been found to express 12-LOX (mostly the platelet-type isoform) including epidermoid carcinoma (Hagmann *et al.*, 1996), colorectal adenocarcinoma (Chen *et al.*, 1994), melanomas (Timar *et al.*, 1999) and erythroleukemias (Hagmann *et al.*, 1993). Transfection of platelet-type 12-LOX into PC-3 nm cells increased tumor-induced angiogenesis (Nie *et al.*, 1998), whereas *in vivo* treatment of animals with a select 12-LOX inhibitor resulted in a delayed growth of DU-145 cells in the prostate (Tang *et al.*, 1998) suggesting a role for platelet-type 12-LOX in the regulation of growth of prostate cancer. On the other hand, in contrast to several rodent tumor types, there are no data on non-hemopoietic human tumors concerning a possible function of 12-LOX in tumor metastasis. Therefore, it is

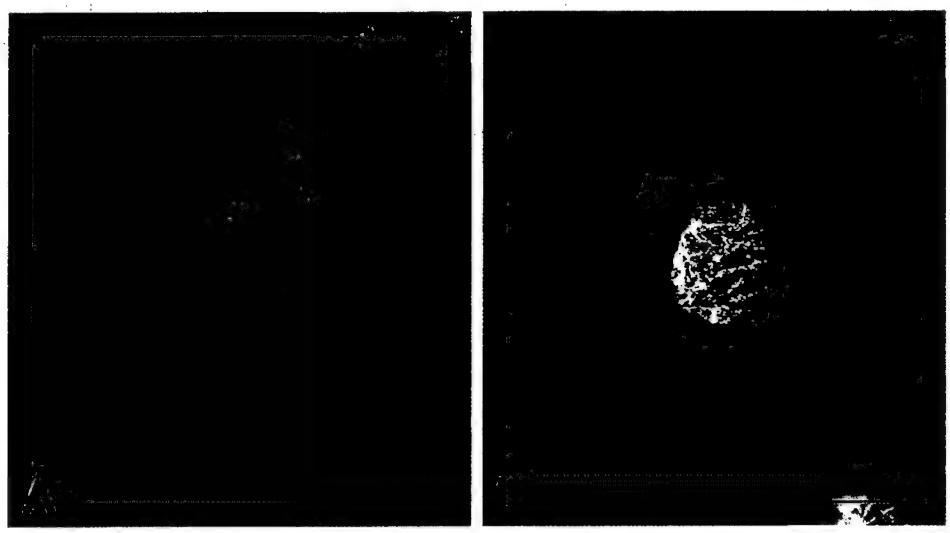

FIGURE 4 – Localization of 12-LOX in cultured prostate cancer cells by confocal laser scanning microscopy. *(a)* Informative optical section of a fibronectin-adherent PC-3 nm cell. 12-LOX protein (green fluorescence) appears in the nucleus (red fluorescence) in the interchromatic spaces, in the cytoplasm in the form of heterogeneous vesicles and at the cell membrane. *(b)* Informative optical section of a fibronectin-adherent DU-145 cell. 12-LOX protein (green fluorescence) appears in the nucleus (red fluorescence) and in the cytoplasm as filaments or individual granules. Note the accumulation at the cell center (arrow). Fibronectin-adherent ells were fixed in MetOH, blocked for non-specific binding and labeled with a polyclonal rabbit IgG produced against platelet-type 12-LOX diluted 1:100; the bound antibody was detected by a biotinylated anti-rabbit IgG and FITC-conjugated Streptavidin (dilution 1:100). Nuclei were detected by propidium iodine post-staining. Confocal images were obtained by using the merged red and green signals superimposed on the phase contrast image. Scale bar = 10 μm.

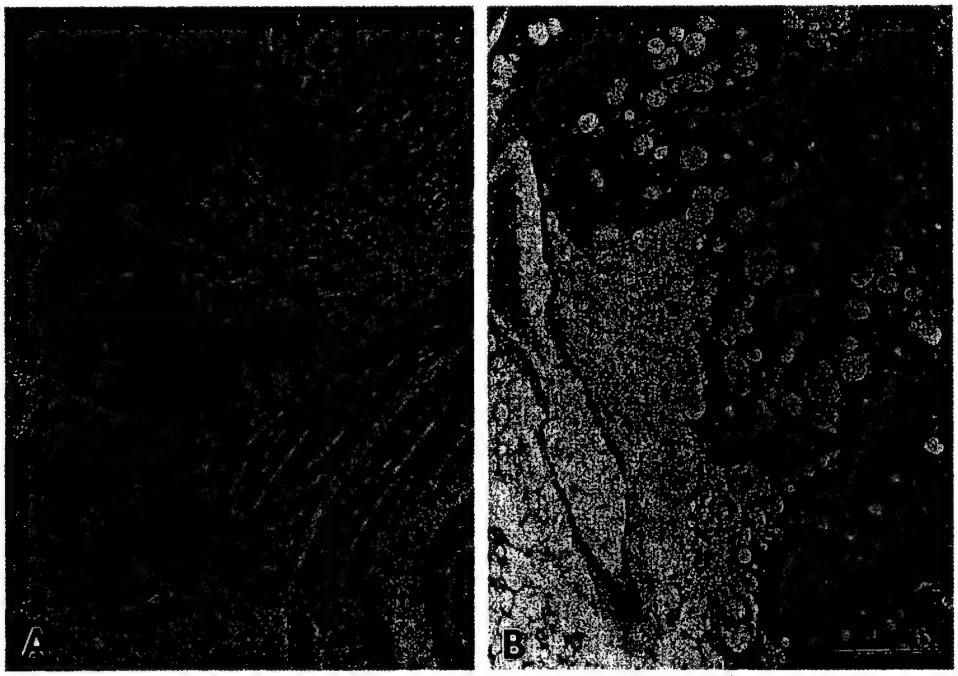

FIGURE 5 – Histology of the intraprostatic human prostate cancer xenografts. *(a)* PC-3 nm tumor. Peripheral area of the tumor in the SCID mouse prostate 4 weeks after intraprostatic injection. Note the intact fibrous capsule between the tumor (lower left area), the prostate gland (upper left area) and the muscular tissue (right). *(b)* DU-145 tumor. Peripheral area of the tumor in the SCID mouse 4 weeks after intraprostatic injection. Note the anaplastic tumor cell nests infiltrating the periprostatic muscular tissue. Hematoxylin-eosin stains. Scale bar = 25 μm.

important that we have shown in this report that a significant proportion of the human prostate cancer cells expresses 12-LOX. Furthermore, the metastatic cell line DU-145, implanted into the prostate of SCID mice, expressed 12-LOX at a significantly higher level than the non-metastatic counterpart, PC-3nm, suggesting that the enzyme might be functional in the metastatic cascade similar to what was observed previously in several rodent tumors (Honn *et al.*, 1994*a*). This assumption was further corroborated in *in vivo* experiments where we have shown that *in vitro* pretreatment of human prostate carcinoma cells with 12-LOX inhibitors dimin-

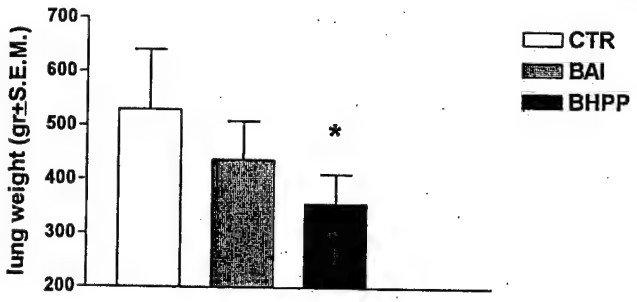

FIGURE 6 – Effect of LOX inhibitor pretreatments of DU-145 cells on lung colonization in SCID mice. Tumor cells were pretreated *in vitro* for 60 min with 5 μM baicalein (BAI), 5 mm BHPP or solvent (CTR). Pretreated tumor cells were injected into the tail vein of SCID mice at 10^6 cells/animal. The experiment was terminated on the 30th day, and lungs were removed. Due to the large amount of tumor nodules in the lungs of the control animals, the weight of the lungs was determined to quantitate the lung colonization. Data are expressed in grams and are means ± SD of 8–10 animals. $*p < 0.05$.

ished their lung colonization potential. The most effective inhibitor, BHPP, was shown previously to be antimetastatic in the case of murine melanoma at comparable *in vitro* dose ranges (*i.e.*, 5–10 μM) (Chen *et al.*, 1994).

This study also provided novel data on the subcellular distribution of 12-LOX in tumor cells. Previously, 12-LOX was localized to the apical plasma membrane, to the cytosol and to the nucleus (Hagmann, 1997; Hagmann *et al.*, 1996). Here we have demonstrated that in matrix adherent prostate carcinoma cell lines 12-LOX is also present in the plasma membrane, at cytoplasmic vesicles and at cytoskeletal filaments. The presence at the plasma membrane can be correlated to the known signaling function of 12-HETE and 12-LOX (Liu *et al.*, 1994*a*), while the presence at the nucleus may be correlated to its role in cell survival and apoptosis (Tang *et al.*, 1996; Hagmann, 1997). The novel finding that 12-LOX is also associated to cytoplasmic vesicles and cytoskeletal filaments might explain those observations that 12-HETE has regulatory effects on organelle translocation or cytoskeletal rearrangements (Timar *et al.*, 1993*b*). It is noteworthy to mention in this respect that biochemical studies suggested that almost all biological effects of 12-HETE are mediated through protein kinase C(α) (Liu *et al.*, 1995), which was also found to be associated not only to the plasma membrane but to the cytoskeleton and cytoplasmic vesicles (Timar *et al.*, 1996*a*). Collectively, these observations suggest that a 12-LOX/protein kinase C complex might serve as a translocating signal unit acting not only at the plasma membrane but at receptor-containing vesicles, the cytoskeleton or in the nucleus. Furthermore, the system may have important functions in the progression of human prostate cancer.

REFERENCES

BRINKMAN, H.J., VAN BUUL-WORTENBOER, M.F. and VAN MOURIK, J.A., Involvement of cyclo-oxygenase and lipoxygenase-mediated conversion of arachidonic acid in controlling human vascular smooth muscle cell proliferation. *Thromb. Hemost.*, **63,** 291–297 (1990).

CHEN, Y.Q., DUNIEC, Z.M., LIU, B., HAGMANN, W., GAO, X., SHIMOJI, K., MARNETT, L.J., JOHNSON, C.R. and HONN, K.V., Endogenous 12(S)-HETE production by tumor cells and its role in metastasis. *Cancer Res.*, **54,** 1574–1579 (1994).

CHOPRA, H., TIMAR, J., CHEN, Y.Q., RONG, X., GROSSI, I.M., FITZGERALD, L.A., TAYLOR, J.D. and HONN, K.V., The lipoxygenase metabolite 12-(S)-HETE induces a cytoskeleton-dependent increase in surface expression of integrin αIIbβ3 on melanoma cells. *Int. J. Cancer,* **49,** 774–786 (1991).

ELING, T.E. and GLASGOW, W.C., Cellular proliferation and lipid metabolism: importance of lipoxygenases in modulating epidermal growth factor-dependent mitogenesis. *Cancer Metast. Rev.*, **3,** 397–410 (1994).

HAGMANN, W., 12-Lipoxygenase in human tumor cells. *Pathol. oncol. Res.*, **3,** 83–88 (1997).

HAGMANN, W. and BORGERS, S., Requirement for epidermal growth factor receptor tyrosine kinase and for 12-lipoxygenase activity in the expression of 12-lipoxygenase in human epidermoid carcinoma cells. *Biochem. Pharmacol.*, **53,** 937–942 (1997).

HAGMANN, W., GAO, X., TIMAR, J., CHEN, Y.Q., STROHMAYER, A.-R., FAHRENKOPF, C., KAGAWA, D., LEE, M., ZACHAREK, A. and HONN, K.V., 12-Lipoxygenase in A431 cells: genetic identity, modulation of expression and intracellular localization. *Exp. Cell Res.*, **228,** 197–205 (1996).

HAGMANN, W., GAO, X., ZACHAREK, A., WOJCIECHOWSKI, L.A. and HONN, K.V., 12-Lipoxygenase in Lewis lung carcinoma cells: molecular identity, intracellular distribution of activity and protein, and Ca^{2+}-dependent translocation from cytosol to membranes. *Prostaglandins,* **49,** 49–62 (1995).

HAGMANN, W., KAGAWA, D., RENAUD, C. and HONN, K.V., Activity and protein distribution of 12-lipoxygenase in HEL cells: induction of membrane-association by phorbol ester TPA, modulation of activity by glutathione and 13-HPODE, and Ca^{2+}-dependent translocation to membranes. *Prostaglandins,* **46,** 471–477 (1993).

HANSBROUGH, J.R., TAKAHASHI, Y., UEDA, N., YAMAMOTO, S. and HOLTMAN, M.J., Identification of a novel arachidonate 12-lipoxygenase in bovine tracheal epithelial cells distinct from leukocyte and platelet forms of the enzyme. *J. biol. Chem.*, **265,** 1771–1776 (1990).

HONN, K.V., TANG, D.G., GAO, X., BUTOVICH, I.A., LIU, B., TIMAR, J. and HAGMANN, W., 12-Lipoxygenases and 12(S)-HETE: role in cancer metastasis. *Cancer Metast. Rev.*, **13,** 365–396 (1994*a*).

HONN, K.V., TIMAR, J., ROZHIN, J., BAZAZ, R., SAMENI, M., ZIEGLER, G. and SLOANE, B.F., A lipoxygenase metabolite, 12(S)-HETE, stimulates protein kinase C-mediated release of cathepsin B from malignant cells. *Exp. Cell Res.*, **214,** 120–130 (1994*b*).

KIMURA, Z., OKUDA, H. and ARICHI, S., Effects of baicalein on leukotriene biosynthesis and degranulation in human polymorphonuclear leukocytes. *Biochim. biophys. Acta,* **922,** 278–286 (1987).

LIU, B., KHAN, W., HANNUN, Y., TIMAR, J., TAYLOR, J., LUNDY, S., BUTOVICH, I. and HONN, K.V., 12(S)-hydroxyeicosatetraenoic acid and 13(S)-hydroxyoctadecadienoic acid regulation of protein kinase C-a in melanoma cells: role of receptor-mediated hydrolysis of inositol phospholipids. *Proc. natl. Acad. Sci. (Wash.),* **92,** 9323–9327 (1995).

LIU, B., MAHER, R.J., HANNUN, Y.A., PORTER, A.T. and HONN, K.V., 12-(S)-HETE enhancement of prostate tumor cell invasion: selective role of PKCa. *J. natl. Cancer Inst.*, **86,** 1145–1151 (1994*a*).

LIU, B., MARNETT, L.J., CHAUDHARY, A., JI, C., BLAIR, I.A., JOHNSON, C.R., DIGLIO, C.A. and HONN, K.V., Biosynthesis of 12-(S)-hydroxyeicosatetraenoic acid by B16 amelanotic melanoma cells is a determinant of their metastatic potential. *Lab. Invest.*, **70,** 314–323 (1994*b*).

LOMNITSKI, L., SKLAN, D. and GROSSMAN, S., Lipoxygenase activity in rat dermis and epidermis: partial purification and characterization. *Biochim. biophys. Acta,* **1255,** 351–359 (1995).

NIE, D., HILLMAN, G.G., GEDDES, T., TANG, K., PIERSON, C., GRIGNON, D.J. and HONN, K.V., Platelet-type 12-lipoxygenase in a human prostate carcinoma stimulates angiogenesis and tumor growth. *Cancer Res.*, **58,** 4047–4051 (1998).

SILLETTI, S., TIMAR, J., HONN, K.V. and RAZ, A., Autocrine motility factor induces differential 12-lipoxygenase expression and activity in high- and low-metastatic K1735 melanoma cell variants. *Cancer Res.*, **54,** 5752–5756 (1994).

TAKAHASHI, Y., UEDA, Y. and YAMAMOTO, S., Two immunologically and catalytically distinct arachidonate 12-lipoxygenases of bovine platelets and leukocytes. *Arch. Biochem. Biophys.*, **266,** 2613–2621 (1988).

TANG, D.G., CHEN, Y.Q. and HONN, K.V., Arachidonate lipoxygenases as essential regulators of cell survival and apoptosis. *Proc. natl. Acad. Sci. (Wash.),* **93,** 5241–5246 (1996).

TANG, D.G., LI, L., ZHU, Z., JOSHI, B., JOHNSON, C.R., MARNETT, L.J., HONN, K.V., CRISSMANN, J.D., KRAJEWSKI, S., REED, J.C., TIMAR, J. and PORTER, A.T., BMD188, a novel hydroxamic acid compound, demonstrates potent anti-prostate cancer effects *in vitro* and *in vivo* by inducing apoptosis: requirements for mitochondria, reactive oxygen species and proteases. *Pathol. oncol. Res.*, **4,** 179–191 (1998).

THOMPSON, P.A., JELINEK, D.F. and LIPSKY, P.E., Regulation of human B cell proliferation by prostaglandin E2. *J. Immunol.*, **133,** 2446–2453 (1984).

TIMAR, J., LIU, B., BAZAZ, R. and HONN, K.V., Association of protein kinase C-α with cytoplasmic vesicles in melanoma cells. *J. Histochem. Cytochem.*, **44,** 177–182 (1996*a*).

TIMAR, J., RASO, E., FAZAKAS, Z.S., SILLETTI, S., RAZ, A. and HONN, K.V., Multiple use of a signal transduction pathway in tumor cell invasion. *Anticancer Res.*, **16,** 3299–3306 (1996*b*).

TIMAR, J., RASO, E., HONN, K.V. and HAGMANN, W., 12-Lipoxygenase expression in human melanoma cell lines. *Advanc. Exp. Biol. Med.*, **469,** 616–622 (1999).

TIMAR, J., SILLETTI, S., BAZAZ, R., RAZ, A. and HONN, K.V., Regulation of melanoma cell motility by lipoxygenase metabolite 12(S)-HETE. *Int. J. Cancer*, **55,** 1003–1010 (1993*a*).

TIMAR, J., TANG, D., BAZAZ, R., HADDAD, M.M., KIMLER, V.A., TAYLOR, J.D. and HONN, K.V., PKC mediates 12(S)-HETE-induced cytoskeletal rearrangement in B16a melanoma cells. *Cell Motil. Cytoskel.*, **26,** 49–65 (1993*b*).

TRIKHA, M., TIMAR, J., LUNDY, S.K., SZEKERES, K., CAI, Y., PORTER, A.T. and HONN, K.V., The high affinity αIIbβ3 integrin is involved in invasion of human melanoma cells. *Cancer Res.*, **57,** 2522–2528 (1997).

TRIKHA, M., TIMAR, J., LUNDY, S.K., SZEKERES, K., TANG, K., GRIGNON, D., PORTER, A.T. and HONN, K.V., Human prostate carcinoma cells express functional αIIbβ3 integrin 1. *Cancer Res.*, **56,** 5071–5078 (1996).

WANG, X.Q., OTSUKA, M., TAKAGI, J., KOBAYASHI, Y., SATO, F. and SAITO, Y., Inhibition of adenyl cyclase by 12(S)-hydroxyeicosatetraenoic acid. *Biochem. Biophys. Res. Comm.*, **228,** 81–87 (1996).

Biochemical and Biophysical Research Communications 275, 690–695 (2000)
doi:10.1006/bbrc.2000.3348, available online at http://www.idealibrary.com on IDEAL®

Eicosanoid 12(S)-HETE Activates Phosphatidylinositol 3-Kinase

Charles K. Szekeres,*,† Mohit Trikha,*,† Daotai Nie,*,† and Kenneth V. Honn*,†,‡,[1]

*Department of Radiation Oncology and ‡Department of Pathology and Chemistry, Wayne State University, Detroit, Michigan 48202; and †Karmanos Cancer Institute, Detroit, Michigan 48201

Received July 17, 2000

The arachidonic acid metabolite of 12 lipoxygenase, 12(S)-hydroxyeicosatetraenoic acid (12(*S*)-HETE) promotes metastatic behavior of tumor cells. In this study we set out to identify 12(*S*)-HETE signaling pathways, and their contribution to cellular functions in A431 epidermoid carcinoma. (1) 12(*S*)-HETE stimulated phosphotyrosine associated PI3 kinase activity. (2) 12(*S*)-HETE stimulated ERK1/2 in a PI3 kinase dependent manner. (3) PI3 kinase affected the 12(*S*)-HETE stimulated Raf/MEK/ERK cascade at the level of MEK. (4) 12(*S*)-HETE stimulated ERK1/2 via PKCζ. (5) 12(*S*)-HETE stimulated cell migration on laminin, which was eliminated by PI3 kinase and cPKC inhibitors, but it was unaffected by inhibition of ERK1/2. © 2000 Academic Press

Key Words: **eicosanoid; 12(*S*)-HETE; PI3 kinase; PKC; ERK; MAPK; migration.**

Arachidonic acid is metabolized by cycloxygenases and lipoxygenases, leading to the formation of a wide variety of eicosanoids, which have potent biological activity, including promotion of tumor progression. In particular, expression of 12 lipoxygenase (12 LOX) was found to correlate with the more malignant stage of prostate cancer (1, 2). Studies on the arachidonic acid metabolite of 12 lipoxygenase, 12(*S*)-HETE, revealed that this lipid promotes multiple functions that are important for metastasis, such as adhesion (3), spreading (4), secretion of proteases (5), migration (6), endothelial cell retraction (7), as well as protection from apoptosis (8) and stimulation of angiogenesis (9). The multitude of cellular functions that are affected by 12(*S*)-HETE suggests the activation of a complex signaling network. Earlier works on melanomas demonstrated that phospholipase C, and protein kinase C (PKCα) are important factors in 12(*S*)-HETE signaling (4). Recent publications underscore the contribution of other signaling molecules in 12(*S*)-HETE signaling, such as phospholipase D (10), the extracellular-regulated kinase (ERK) cascade (11), and Src family kinases (11).

In this study we attempted to further elucidate 12(*S*)-HETE stimulated cellular signaling. We established that PI3 kinase is involved in 12(*S*)-HETE signaling in A431 epidermoid carcinoma cells. PI3 kinase enhanced MEK and in turn ERK1/2 activity via PKCζ. Conventional PKCs and PI3 kinase are essential for 12(*S*)-HETE stimulated migration of A431 cells on laminin but inhibition of ERK had no effect on this process.

Abbreviations used: ERK, extracellular regulated protein kinase; PI3K, phosphoinositide-3 kinase; PKC, protein kinase C; PLC, phospholypase C.

[1] To whom correspondence should be addressed at 431 Chemistry Building, Wayne State University, Detroit, MI 48202. Fax: (313) 577-0798. E-mail: k.v.honn@wayne.edu.

MATERIALS AND METHODS

Antibodies and reagents. Anti-phospho-specific ERK and MEK antibodies were purchased from New England Biolabs (Beverly, MA). Anti-pan ERK, PY20, MEK were from Transduction Laboratories (Lexington, KY), and horse radish peroxidase conjugated secondary antibodies were purchased from Amersham (Arlington, IL). Anti-PKCζ was from Santa Cruz Biotechnologies (Santa Cruz, CA). 12(*S*)-HETE was purchased from Cayman Chemicals (Ann Arbor, MI). Protein G-Sepharose4B was from Zymed (S. San Francisco, CA). The inhibitors Go6976 (inhibitor of conventional PKC isozymes, IC_{50} 2.3 nM, solvent: ethanol) PD98059 (inhibitor of MEK, IC_{50} 2 μM, solvent: ethanol), and Ly294002 (PI3 kinase inhibitor, IC_{50} 1.4 μM, solvent: ethanol) were from Calbiochem (La Jolla, CA). Purified ERK2, MEK2 and myelin basic proteins were from Upstate Biotechnologies. All other chemicals were obtained from Sigma (St. Louis, MO).

Cell culture. The human epidermoid carcinoma cell line A431 (American Tissue Culture Collection, Rockvell, MD) was cultured in Dulbecco's modified Eagle media (DMEM) supplemented with 10% FBS (Gibco, Gaithersburg, MD) and 25 mg/l Gentamycin (Gibco). Cells were passaged with 0.05% Trypsin–EDTA.

Plasmids that encode wild type (wt) or dominant negative(dn) PKCζ were generous gifts of Dr. Jorge Moscat [Universidad Autonoma de Madrid, Spain, (12)], the corresponding empty vector, pcDNA3.1 was purchased from Invitrogen (Carlsbad, CA). A431 cells were transfected with wt PKCζ, dn PKCζ or control plasmid using Fugene6 transfection reagent (Boehringer-Mannheim, Indianapolis, IN) according to the manufacturer's recommendations. Trans-

0006-291X/00 $35.00

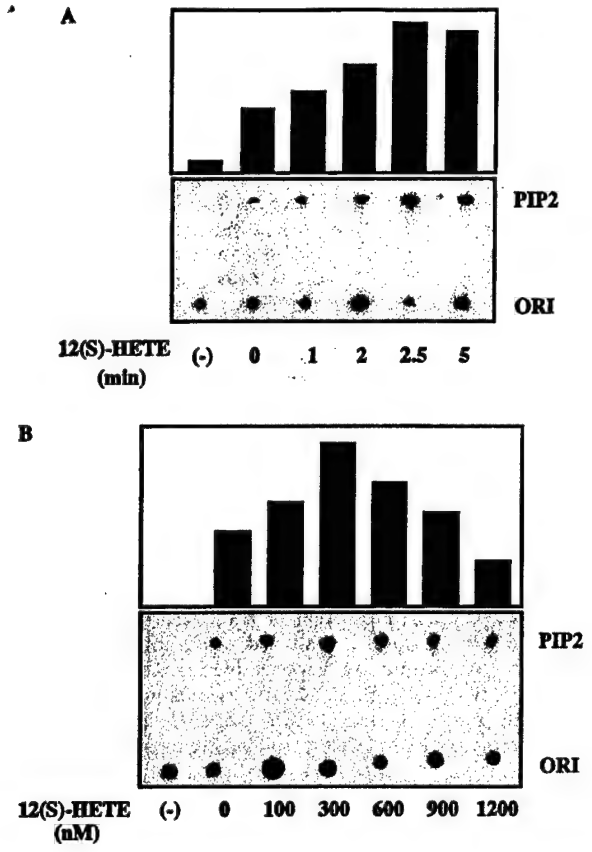

FIG. 1. 12(*S*)-HETE stimulates phosphotyrosine associated PI3 kinase activity in a time and dose dependent manner. Serum starved cells were treated with 100 nM 12(*S*)-HETE for 0–5 min (A) or with 0–1200 nM 12(*S*)-HETE for 5 min (B). Following treatment tyrosine phosphorylated proteins were immunoprecipitated, and immunucomplexes were assayed for PI3 kinase activity. Thin layer chromatography plates were visualized (lower panels) and quantitated (upper panels) with a phosphorimmager.

kinase is stimulated by 12(*S*)-HETE as early as 2 min following treatment (Fig. 1A) with maximal (2.2-fold) activation at 300 nM concentration (Fig. 1B).

12(S)-HETE stimulated ERK1/2 activity is partially dependent on PI3 kinase. To test whether PI3 kinase plays a role in ERK1/2 activation, two structurally unrelated pharmacological inhibitors of these enzymes (Ly294002 or wortmannin) were utilized. As determined by Western blotting both PI3 kinase inhibitors dose dependently reduced 12(*S*)-HETE stimulated activation of ERK1/2 (Fig. 2). It is noteworthy, that even 10× of the IC_{50} of Ly294002 or wortmannin did not completely abolish 12(*S*)-HETE stimulated phosphorylation of ERK1/2, suggesting that other, PI3 kinase independent mechanisms may also be involved (11).

PI3 kinase activity affects the Raf-MEK-ERK cascade at the level of MEK. Signaling upstream of ERK1/2 is modulated at several levels. For example receptor tyrosine kinases stimulate Raf via Ras, and conventional PKCs modulate activity of Raf kinase. To test where PI3 kinase exerts its influence on the Raf/MEK/ERK cascade, activity of upstream kinases MEK and Raf was monitored in the presence or absence of PI3 kinase inhibitor LY294002 following 12(*S*)-HETE treatment. 12(*S*)-HETE (100 nM) stimulated activity (Fig. 3A), as well as serine phosphorylation (Fig. 3B) of MEK kinase, which was reduced in the presence of LY294002. In contrast to MEK, Raf activity was not significantly different in the presence or absence of LY294002 in cells challenged with 12(*S*)-HETE (Fig. 3C), as determined by an *in vitro* kinase assay. Collectively these results suggest that PI3 kinase stimulates ERK1/2 via MEK, but not Raf in response to 12(*S*)-HETE treatment.

PKCζ is involved in 12(S)-HETE stimulation of ERK1/2. In vitro studies demonstrated that D-3 phosphoinositide lipids activate novel PKC isoforms, i.e., δ ϵ, and η as well as atypical PKCs, i.e., PKCζ (in 15), but not conventional PKCs. Of the PI3 kinase dependent enzymes, PKCζ has been shown to activate the ERK cascade. Further, PKCζ appears to directly influence MEK (12), as opposed to PKCα, which activates Raf (11). Therefore we tested whether PKCζ is activated by 12(*S*)-HETE. *In vitro* kinase assays revealed that 12(*S*)-HETE stimulates PKCζ activity with a similar time course to that of PI3 kinase activity (Fig. 4A). In order to demonstrate involvement of PKCζ in 12(*S*)-HETE simulation of ERK1/2, A431 cells were transfected with either wild type, or a dominant negative PKCζ expressing plasmid. Overexpression of wild type PKCζ slightly (by 10%) increased the responsiveness of A431 cells to 12(*S*)-HETE in terms of ERK1/2 activation, while overexpression of dominant negative form of PKCζ reduced responsiveness by 50% (Fig. 4B).

Migration of A431 cells on laminin is stimulated by 12(S)-HETE. The eicosanoid 12(*S*)-HETE is known to stimulate migration of melanoma cells (6). In order to attribute function to the signaling molecules that were

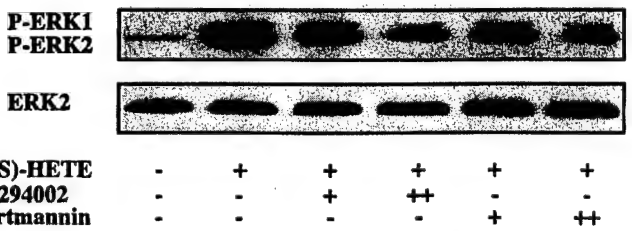

FIG. 2. PI3 kinase and ERK1/2 play a role in 12(*S*)-HETE signaling. A431 cells were pretreated with Ly294002 or wortmannin for 15 min (+, 2.3 μM, or 5 nM; ++, 23μM, or 50 nM, respectively), then challenged with 300 nM 12(*S*)-HETE for 10 min. Whole cell lysates were analyzed by Western blotting, using an antibody directed to the activated form of ERK1/2 (upper panel). To demonstrate even loading, blot was stripped and reprobed with an antibody that recognizes ERK independent of its phosphorylation status.

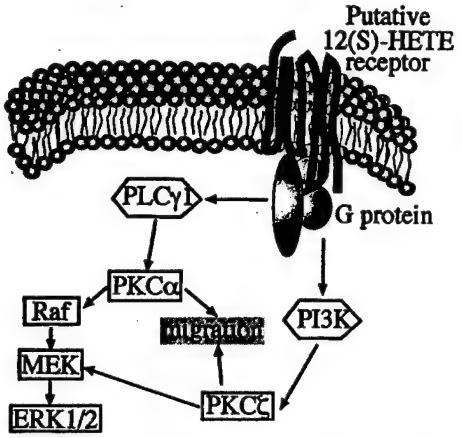

FIG. 6. Schematic representation of the signaling pathways and their effects on cell function. The putative 12(*S*)-HETE receptor activates PKCα via phospholypase C and stimulates PKCζ via inositide kinase. Both PKC isoforms contribute to phosphorylation of the Raf/MEK/ERK cascade, PKCα at the level of Raf, PKCζ via MEK. While both pathways are essential for mediating migratory phenotype, downstream kinase ERK is necessary for this function.

study and their most important implications are as follows: (1) 12(*S*)-HETE stimulates PI3 kinase activity; (2) and PI3 kinase is rate limiting for ERK1/2 activation, pointing to the possibility that PI3 kinase may be more important in mediating the effects of eicosanoids than was previously assumed; (3) Inhibiting PI3 kinase activity reduces 12(*S*)-HETE induced MEK activity, but does not affect stimulation of Raf. This finding underscores the importance of MEK as a point of regulation, rather than a simple signal relay molecule; (4) 12(*S*)-HETE activates PKCζ and in turn PKCζ contributes to ERK1/2 phosphorylation, which in concert with earlier findings demonstrates that multiple PKC isoforms may be involved in transmitting the 12(*S*)-HETE signal in a given system; (5) 12(*S*)-HETE promoted A431 cell migration on laminin is dependent on PI3 kinase and on conventional PKCs, but not on MEK, which support the concept, that individual members of the multi level signaling networks might be responsible for a particular function without the involvement of downstream elements. These findings are summarized in Fig. 6. There are some indications in the literature that PI3 kinase may participate in eicosanoid signaling. For example in vascular smooth muscle cells prostaglandin F2α activated ERK2 in a PI3 kinase-dependent and -independent pathway (19), and leukotriene B4 induced leukocyte migration was blocked by a PI3 kinase inhibitor, i.e., wortmannin (20). The overlap between eicosanoid and PI3 kinase mediated functions suggest that inositide kinases might be involved in eicosanoid signaling to a much larger extent than currently appreciated, therefore demonstration of PI3 kinase activity and function in response to an eicosanoid [12(*S*)-HETE] is a significant step toward uncovering the mechanism of action of bioactive lipids. Further work is required to evaluate whether PI3 kinase is involved in other 12(*S*)-HETE functions, such as in stimulation of cell survival (8), since both PI3 kinase and PKCζ are implicated in mediating anti-apoptotic signals.

Our results demonstrating that PI3 kinase stimulated the ERK cascade via MEK, complement Berra *et al.* (12), who found that the dominant negative mutant of PKCζ dramatically impairs activation of ERK and MEK by serum and tumor necrosis factor, and Schonwasser *et al.* (21), who demonstrated that in contrast to conventional and novel PKCs, which are potent activators of c-Raf1, atypical PKCs do not stimulate c-Raf1, but rather activate MEK through an independent mechanism.

The role of signaling molecules in migration is complex, and it is system dependent. For example ERK antisense nucleotides block FG carcinoma cell migration, and the motility of COS-7 cells transfected with the constitutively active ERK is stimulated because ERK phosphorylates myosine light chain kinase (22). While there are only a limited number of examples whereby ERK modulate migration, the role of various PKC isotypes in organizing the cytoskeleton, and therefore affecting cell shape and motility is well documented (reviewed in 23). However, it is an intriguing concept, that one function (in this case motility) requires activity of multiple independent (i.e., cPKC and PI3 kinase) signaling pathways.

In conclusion, this study links eicosanoid signaling to PI3 kinase, a potent mediator of cytoskeletal alterations and anti-apoptotic effects.

ACKNOWLEDGMENTS

The authors thank Dr. Jorge Moscat for generously providing the wild type and dominant negative PKCζ containing constructs. This study was supported by NIH Grant CA 29997 to K.V.H.

REFERENCES

1. Gao, X., Grignon, D. J., Chbihi, T., Zacharek, A. R., Chen, Y. Q., Sakr, W., Porter, A. T., Crissman, J. D., Pontes, J. D., Powell, I. J., and Honn, K. V. (1995) Elevated 12-lipoxygenase mRNA expression correlates with advanced stage and poor differentiation of human prostate cancer. *Urology* **46,** 227–237.
2. Nie, D., Hillman, G. G., Geddes, T., Tang, K., Pierson, C., Grignon, D. J., and Honn, K. V. (1998) Platelet-type 12-lipoxygenase in a human prostate carcinoma stimulates angiogenesis and tumor growth. *Cancer Res.* **58,** 4047–4051.
3. Chen, Y. Q., Duniec, Z. M., Liu, B., Hagmann, W., Gao, X., Shimoji, K., Marnett, L. J., Johnson, C. R., and Honn, K. V. (1994) Endogenous 12(S)-HETE production by tumor cells and its role in metastasis. *Cancer Res.* **54,** 1574–1579.
4. Timar, J., Chen, Y. Q., Liu, B., Bazaz, R., Taylor, J. D., and Honn, K. V. (1992) The lipoxygenase metabolite 12(S)-HETE promotes alpha IIb beta 3 integrin-mediated tumor-cell spreading on fibronectin. *Int. J. Cancer* **52,** 594–603.
5. Honn, K. V., Timar, J., Rozhin, J., Bazaz, R., Sameni, M., Ziegler, G., and Sloane, B. F. (1994) A lipoxygenase metabolite, 12-(S)-

Identification of 12-Lipoxygenase Interaction with Cellular Proteins by Yeast Two-Hybrid Screening

Keqin Tang, Russell L. Finley, Jr., Daotai Nie, and Kenneth V. Honn

From the Department of Radiation Oncology and Pathology, Center for Molecular Medicine and Genetics, Wayne State University School of Medicine, and Karmanos Cancer Institute, Detroit, Michigan 48202

Biochemistry®

Reprinted from
Volume 39, Number 12, Pages 3185–3191

Biochemistry

 Volume 39, Number 12 March 28, 2000

Accelerated Publications

Identification of 12-Lipoxygenase Interaction with Cellular Proteins by Yeast Two-Hybrid Screening†

Keqin Tang,‡ Russell L. Finley, Jr.,§ Daotai Nie,‡ and Kenneth V. Honn*,‡,||

From the Department of Radiation Oncology and Pathology, Center for Molecular Medicine and Genetics, Wayne State University School of Medicine, and Karmanos Cancer Institute, Detroit, Michigan 48202

Received November 18, 1999; Revised Manuscript Received January 20, 2000

ABSTRACT: The platelet isoform of 12-lipoxygenase (12-LOX) is expressed in a variety of human tumors. 12-LOX metabolizes arachidonic acid to 12(*S*)-hydroxyeicosateraenoic acid (12(*S*)-HETE), which induces a number of cellular responses associated with tumor progression and metastasis. Little is known about 12-LOX regulation and no direct regulators of 12-LOX activity have been identified. To identify potential regulators of 12-LOX, we isolated cDNAs encoding 12-LOX interacting proteins using the yeast two-hybrid system. We screened a yeast two-hybrid interaction library from human epidermoid carcinoma A431 cells and identified four cellular proteins that interact specifically with 12-LOX. We identified type II keratin 5, lamin A, the cytoplasmic domain of integrin $\beta 4$ subunit and a phosphoprotein C8FW as 12-LOX interacting proteins. Here, we demonstrated that keratin 5, a 58 kD protein required for formation of 8 nm intermediate filaments, binds to 12-LOX in human tumor cells and may contribute to the regulated trafficking of 12-LOX. We also showed that lamin A binds 12-LOX in human tumor cells. These proteins provide the first candidate regulators of 12-LOX.

12-lipoxygenase (EC 1.13.11.31), one of at least three lipoxygenases, metabolizes arachidonic acid (AA) to 12-hydroperoxyeicosatetraenoic acid (12-HPETE),[1] which is subsequently converted to 12(S)-HETE and hepoxilins (*1*). Enzymological, immunological, and molecular biological evidence indicates that the 12-LOX proteins expressed in leukocytes, platelets, and tracheal epithelium are three distinctly different enzymes (*2*−*3*). Platelet-type 12-LOX is expressed normally in platelets, megakaryocytes, umbilical vein endothelial cells, and a wide variety of human and rodent tumor cells including HEL (human erythroleukemia) cells and A431 cells (human epidermoid carcinoma) (*4*). Platelet 12-lipoxygenase is a dual-function enzyme that posseses both oxygenase and lipoxin synthase activity (*5*). Platelet 12-LOX metabolizes only AA (but not c-18 fatty acids, such as linoleic acid) to form exclusively 12(S)-HETE (*6*) and utilizes leukotriene A_4 to generate lipoxin A_4 and B_4 during platelet−leukocyte interactions (*5*). 12(S)-HETE induces a plethora of responses in tumor cells and is linked to tumor progression and metastasis (*7*). For example, 12-(S)-HETE has been reported to stimulate integrin expression and secretion of proteinases, enhance tumor cell motility and invasion, and induce angiogenesis (*7*−*8*). Leukotrienes and

† This work was supported by National Institute of Health Grants CA-29997 (K.V.H.) and NIH R29HG01536 (R.L.F.).

* To whom correspondence should be addressed: Dr. Kenneth V. Honn, Department of Radiation Oncology, 431 Chemistry Bldg., Wayne State University, Detroit, MI 48202. Telephone: (313) 577-1018. Fax: (313) 577-0798. E-mail: k.v.honn@wayne.edu.

‡ Department of Radiation Oncology.

|| Department of Pathology.

§ Center for Molecular Medicine and Genetics.

[1] Abbreviations: A431 cell, human epidermoid carcinoma; 12-LOX, 12-lipoxygenase; 12(*S*)-HETE, 12(*S*)-hydroxyeicosateraenoic acid; AA, arachidonic acid; HEL, human erythroleukemia; Cdk, cyclin-dependent kinase; FLAP, 5-lipoxygenase activating protein.

10.1021/bi992664v CCC: $19.00
Published on Web 02/29/2000

lipoxins participate in multicellular events including thrombosis, inflammation, immunity, and atherosclerosis. For instance, lipoxin A_4 down-regulates leukocyte responses and trafficking and neutrophil−endothelial interaction (*9*−*10*), while lipoxin B_4 regulates human neutrophil adherence and motility (*11*).

Human platelet-type 12-LOX is believed to play a role in cancer and other pathological conditions, such as psoriasis, atherosclerosis, and arthritis. In a clinical study of 137 prostate cancer patients, platelet-type 12-LOX expression levels were determined in cancer tissue and compared with the levels in matching normal tissue from each patient. Approximately 38% of the patients studied exhibited elevated levels of platelet-type 12-LOX in the cancer tissues. This elevated 12-LOX correlated positively with tumor stage and grade and positivity for prostate cancer cells in the surgical margins (*12*). In addition 12-LOX activity is up regulated in tumor cells following γ radiation (*13*). Clearly, understanding how the 12-LOX enzyme is regulated will be an important step in elucidating the role of this enzyme in a variety of human cancers.

The enzyme activity of 12-LOX and 5-LOX is regulated by a translocation process following cell stimulation. It has been shown that Ca^{2+} and thrombin increase 12-LOX activity and 12(S)-HETE production by the translocation of 12-LOX from cytosol to membrane in human platelets, HEL cells, and A431 cells (*14*−*15, 33, 41*). A recent report demonstrates that an anti-platelet agent inhibits the 12-LOX activity and 12(S)-HETE production by blocking the translocation of 12-LOX (*15*). However, to date there is no diret evidence for protein(s) that could mediate 12-LOX translocation, and no direct regulator/interacting protein of 12-LOX has been found. In constrast, for leukocyte 5-LOX, there is evidence of complex protein−protein interactions in its nuclear membrane translocation, activation, and substrate acquisition in intact cells (*27*). For example, FLAP (5-lipoxygenase-activating protein) assocation with 5-LOX after its translocation acts as an arachidonic acid transfer/docking protein that "presents" the substrate to 5-LOX on the leukocyte nuclear membrane (*16*). This finding was the first indication that a protein directly associates with and regulates the activity of a member of the lipoxygenase family. Recently, three additional 5-LOX-interacting proteins that may be involved in regulation and/or nuclear localization were identified using the yeast two-hybrid system (*17*).

In this study, we used a yeast two-hybrid approach to identify proteins that interact with 12-LOX and that may regulate its activity. We constructed a two-hybrid library from A431 cells and identified from it four distinct cellular proteins that interacted specifically with 12-LOX. They are human type II keratin K5, nuclear envelope protein lamin A, integrin β4 cytoplasmic domain, and human C8FW phosphoprotein. The identification of these 12-LOX-interacting proteins may help us to understand the complex ways in which 12-LOX is involved in tumor progression and metastasis.

MATERIALS AND METHODS

Yeast Strains and Manipulation. Saccharomyces cerevisiae yeast strains used were RFY231 (MATa *his*3 *ura*3-1 *trp*1Δ::*his*G *leu*2::3Lexop-*LEU*2) (*19*) and RFY206 (MATa *his*3Δ200 *leu*2-3 *lys*2Δ201 *ura*3-52 *trp*1Δ::*his*G) (*21*). Yeast were grown using standard microbiological techiques and media (*22*−*23*). Media designations are as follows: YPD is YP (yeast extract plus peptone) medium with 2% glucose. Minimal dropout media are designated by the component that is left out (e.g., -ura -his -trp -leu medium lacks uracil, histidine, tryptophan, and leucine). Minimal media contained either 2% glucose (Glu) or 2% galactose plus 1% raffinose (Gal). X-Gal minimal dropout plates contained 40 mg/mL X-Gal and phosphate buffer at pH 7.0. DNA was introduced into yeast by LiOAc-mediated transformation as described (*24*).

Human A431 Cell cDNA Library Construction. RNA was isolated from human epidermoid carcinoma A431 cells, and mRNA was purified using Oligo-tex Beads mRNA kit (QIAGEN Inc, Valencia, CA). cDNA was synthesized with the Stratagene cDNA synthesis kit, essentially according to the manufacturer's instructions. Briefly, poly(A)+ mRNA derived from human epidermoid carcinoma A431 cells was used to direct the synthesis of first-strand cDNA by reverse transcriptase with an XhoI-oligo d(T) primer. Following second-strand synthesis, the cDNA was ligated to an EcoRI adaptor, digested with XhoI, and subsequently size selected over cDNA Size Fractionation Columns from Gibco BRL. Fractions containing cDNAs ranging from 500 bp to > 3 kb in length were pooled and subcloned into the yeast library plasmid pJG4-5 (*25*). The average insert size was evaluated by purifying plasmid DNA from 48 random clones and digesting with EcoRI+XhoI. The size of each product was determined by gel electrophoresis. The A431 cDNA had 3.0×10^6 independent clones, and 90% of the plasmids had cDNA inserts of 0.3−3.8 kb (average size, 1.2 kb). The resultant cDNA library contains 3.0×10^6 primary recombinant clones.

Plasmids. Bait plasmids expressing LexA fusion proteins were derivatives of the *HIS*3 2 μm plasmid, pEG202 (*20*). The full-length cDNA encoding human platelet-type 12-LOX was provided by Dr. Colin Funk (University of Pennsylvania). The entire coding region of the cDNA was amplified by the polymerase chain reaction (PCR) with a 5′ *Bam*HI site introduced in the upper primer (CCGGGGATCCG-T*ATG*GGCCGCTACCGCATC) and the lower primer corresponding to an *Xho*I site from the original cDNA downstream of the stop codon (GCCGGCGAGCTCAGTCTACCA-CTGTGACAA). The PCR product was digested with *Bam*HI and *Xho*I and inserted into the *Bam*HI/*Xho*I sites of pEG202 (*20*) to generate the bait plasmid pLexA-12-LOX; the plasmid encodes the entire 663 amino acid human platelet 12-LOX protein. Additional bait plasmids used in the specificity test are described elsewhere (*21, 25*−*26*).

Yeast Two-Hybrid Screen. The yeast two-hybrid procedures were conducted as described (*28*−*29*). Strain RFY231 containing pSH18-34 and pLexA-12-LOX was transformed with A431 interaction library DNA and a total of 6.5×10^6 independent colonies were collected. The selection for interacting clones was performed in media containing galactose and lacking leucine. 400 Leu+ yeast colonies were further tested for lacZ expression by plating them on medium containing galactose and X-Gal. 40 of the Leu+ positive clones demonstrated galactose-dependent activation of both reporters, suggesting interaction between the galactose-inducible cDNA protein and 12-LOX. Library plasmids from yeast colonies, expressing the putative 12-LOX-interacting proteins, were rescued by transformation of yeast plasmid

DNA into KC8 *E. coli* followed by selection on minimal medium lacking tryptophan (*29*). To determine which clones were unique, PCR products generated with primers flanking the cDNA insertion site in pJG4-5 (BC01 and BC01, ref *29*) were digested with *Alu*I and *Hae*III and analyzed on a 2% agarose gel. The specificity of the unique interactors was tested using the interaction mating assay as described (*21*). Briefly, rescued library plasmids were introduced into RFY231 and the transformants were mated with various derivatives of RFY206 that each contained pSH18-34 and a bait plasmid expressing a LexA fusion. 12 library plasmids encoded proteins that interacted with the 12-LOX bait but not unrelated baits. These 12 cDNAs were sequenced and evaluated by the Basic Local Alignment Search Tool (BLAST) through the National Center for Biotechnology Information Internet site (www.ncbi.nlm.nih.gov).

Immunoprecipitation. Cells were lysed in a cold lysis buffer consisting of 1% Triton X-100, 150 mM NaCl, 10 mM Tris, pH 7.4, 1 mM EDTA, 1 mM EGTA, pH 8.0, 0.2 mM sodium ortho-vanadate, 0.2 mM PMSF, 0.5% NP-40, 0.1% SDS. The lysate was clarified by centrifugation at 10000g for 10 min. Isolation of nuclear extracts was according to the standard protocol (*30*). The supernatants and soluble nuclear extracts were immunoprecipitated with 4−6 μL (1−2 μg)antibody against human platelet-type 12-LOX or anti-5LOX and anti-15-LOX antibodies (Oxford Biomedical Research, Oxford, MI) or the anti-keratin (Chemicon International INC., Temecula, CA) or anti-lamin A (Santa Cruz Biotechnology, Inc., Santa Cruz, CA) for 2 h, followed by 40 μL Sepharose 4B-conjugated protein G at 4 °C overnight. Immune complexes were washed three times in the lysis buffer, and the pellets were suspended in SDS sample buffer for SDS-PAGE electrophoresis. Aliquots of total cell lysate were mixed with 1 vol of SDS sample buffer (85 mM Tris-HCl, pH 6.8, containing 1.4 (w/v) SDS, 14% (v/v) glycerol, 5% (v/v) mercaptoethanol and a trace of bromophenol blue, boiled for 5 min and subjected to SDS-PAGE on 4−20% acrylamide gel. Proteins were electrophoretically transferred to nitrocellulose membranes. After transfer, nonspecific sites were blocked with 5% (w/v) nonfat-dry milk in TTBS (0.1% Tween-20, 20 mM Tris base, 137 mM NaCl, 3.8 mM HCl, pH 7.6) for 2 h at 25 °C followed by probing primary antibody. After the blot was washed three times in TTBS, the membranes were incubated for 1 h at 25 °C with horseradish peroxidase-conjugated secondary anti- IgG (dilution: 1:4500. Amersham, Arlington Heights, IL). The blot was washed again in TTBS, then developed using ECL according to the manufacture's instructions (Amersham, Arlington Heights, IL).

Immunofluorescent Staining. Intracellular 12-LOX and keratin were localized using a modification (*49*) of the general immunocytochemical methodologies described by Willingham (*50*). 2×10^4 Cells were grown in 4-well Lab-Tek chamber (Nalge Nunc Intl, Naperville, IL) in 0.5 mL media to 60−80% confluence and the media changed to serum free media the night before the experiment. Cells were washed with PBS 3× and then fixed with 3.7% formaldehyde in phosphate-buffer saline, pH 7.4 for 10 min. Fixation and subsequent steps were performed at 25 °C for intracellular labeling. After the sample was washed with PBS, the cells were blocked with 2 mg/mL BSA in PBS. All subsequent antibody and wash solution contained 0.1% saponin. Cells were incubated with primary antibody (rabbit anti-human 12-LOX, mouse anti-human keratin) for 2 h and washed. In controls, preimmune serum (rabbit or mouse) was substituted for the primary antibody (1:100 dilution). Cells were incubated in secondary antibody (FITC-conjugated AffiniPure Goat anti-mouse IgG or Rhodamine Red-X-conjugated AffiniPure-Goat anti-Rabbit IgG) and secondary blocking reagent for 1 h. Secondary antibody was diluted in PBS-0.1% saponin (1:100 dilution) and 5% normal goat serum was added to this solution. After the resultant was washed, the coverslips were mounted upside-down on slides with SlowFade anti-fade reagent and observed with a Zeiss LSM 310 laser confocal microscope.

Transfection. The full-length cDNA encoding human platelet-type 12-LOX from pCMV-12-LOX (provided by Dr. Colin Funk, University of Pennsylvania) was cloned into the *Eco*RI/*Xba*I sites of pcDNA3.1 (Invitrogen), which uses the neomycin-resistance gene as the selectable marker. Cells grown in 6-well plates were transfected with 3−12 μg of pcDNA-12-LOX by the FuGENE 6 Transfection Reagent (Boehringer Mannheim Co., Indianapolis, IN) following the manufacture's instructions. Neomycin-resistant cells were selected in 300 μg/mL Geneticin (G418; LifeTechnologies, Inc., Grand Island, NY). The cells were passaged and tested by immunoprecipitation and Western Blotting assays for enhanced 12-LOX protein expression. Cells transfected with vector alone were selected and analyzed in parallel. While in culture, cells were fed with a G418-containing medium to prevent outgrowth of revertant cells. All of the cells were frozen at early passage for subsequent study.

RESULTS AND DISCUSSION

A431 Interaction Library. To identify proteins that may interact with 12-lipoxygenase, we constructed a yeast two-hybrid interaction library from A431 cells. This cell line has been widely used to study 12-LOX in tumor cells, since it expresses enzymatically active platelet-type 12-LOX protein, but not the leukocyte-type isoform (*33*−*35*). In A431 cells, the predominant amount of 12-LOX protein resides in the cytosol (*33, 36*). In contrast, 12-LOX enzyme activity is mainly localized in the membrane fraction (*33, 37*). EGF (TPA, Ca^{2+}) increases total cellular 12-LOX protein and enhances the association of 12-LOX protein with perinuclear or cytoplasmic membrane (*33, 37*−*41*). In addition, EGF stimulates 12-LOX activity and generation of 12(S)-HETE from cellular arachidonate (*33, 36*−*37, 41*). These features make A431 cells an ideal model to study the regulation of 12-LOX activity.

To construct the cDNA library from A431 cells, we isolated poly(A)+ mRNA from 80% confluent cultured A431 cells, used it to synthesize unidirectional cDNA, and inserted the cDNA into the yeast two-hybrid vector pJG4-5 (see Materials and Methods). This vector allows conditional expression (induced by galactose and repressed by glucose) of cDNA-encoded proteins with a transcription activation domain at their amino termini. The resulting library had 3.0×10^6 independent clones, of which 90% had inserts with sizes ranging from 0.3 to 3.8 kb (average size 1.2 kb).

12-Lipoxygenase Interacting Proteins. To identify potential regulators of 12-LOX, we screened the A431 library for clones that encoded 12-LOX-interacting proteins (see Ma-

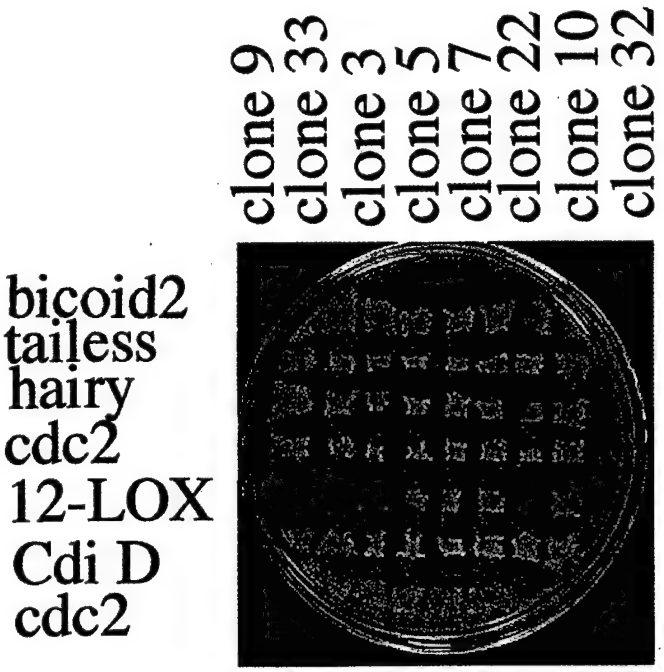

FIGURE 1: Specificity of 12-LOX interactors in the yeast two-hybrid assay. Representative plate of a mating assay to test the specificity of 12-LOX interactors. This plate demonstrates the interactions between seven bait proteins (horizontal lines of yeast) and eight prey proteins (vertical lines) on a Gal/Raf X-Gal plate (urp-his-trp- drop out). The strength of the interaction is suggested by the level of activation of lacZ reporter as indicated by blue color, as summaried in Table 1.

terials and Methods). Yeast expressing the full-length platelet isoform of 12-LOX fused to the LexA DNA-binding domain were transformed with the A431 interaction library. From 6.5×10^6 yeast transformants, we identified 12 independent clones in which the LexA-driven reporters were active only in galactose, indicating that they contained cDNA-encoded proteins that interacted with LexA-12-LOX. We isolated the library plasmids from these clones and determined that they represented four different cDNAs. Six identical clones encoded the carboxy-terminal 330 amino acid residues of type II keratin K5. Two clones encoded the carboxy-terminal 202 residues of the nuclear envelope protein lamin A. Another two clones encoded the cytoplasmic domain of integrin β4. The final two clones encoded a phosphoprotein, C8FW, with some similarity to protein kinases. To further determine the specificity of the four 12-LOX interactors, we conducted a two-hybrid mating assay to test for interactions with LexA-12-LOX and with other unrelated LexA fused proteins. As shown in Figure 1 and Table 1, all four clones interacted specifically with 12-LOX, but not with several other proteins including *Drosophila* cyclin D, Cdk1, hairy, tailess, or bicoid.

Human Keratin K5 Interacts with 12-LOX in A431 Cells. Keratins are major components of intermediate filaments. In epithelial cells, cytoskeletal intermediate filaments contain type I and type II keratins. The 58 kD K5 protein is essential for formation of 8-nm intermediate filaments, disruption of which may reduce tumor invasion and metastasis (*42*−*43*). For example, disruption of intermediate filaments has been shown to inhibit the expression of integrins on the surface of tumor cells (*44*), decrease their interaction with platelets and endothelial cells (*45*), and reduce lung colonization in

Table 1: Specific 12-LOX Interactors[a]

		bait panel					
clone	sequence	12-LOX	biciod2	tailess	hairy	cdc2	Cdi D
1	keratin K5	++++	−	−	−	−	−
2	β4 integrin	+++	−	−	−	−	−
3	C8FW	++	−	−	−	−	−
9	β4 integrin	+++	−	−	−	−	−
10	lamin A	+++	±	−	−	−	−
12	C8FW	++	±	−	−	−	−
15	keratin K5	++++	−	−	−	−	−
33	keratin K5	++++	−	−	−	−	−
34	keratin K5	++++	−	−	−	−	−
35	lamin A	+++	±	−	−	−	−
37	keratin K5	++++	−	−	−	−	−
38	keratin K5	++++	−	−	−	−	−

[a] Summary of 12-LOX interactions with the panel of baits. Interaction mating was performed as described in Materials and Methods and shown in Figure 1. Level of interaction lac Z (reporter gene activation) as determined by blue color on X-Gal indicator plates: ++++ indicates dark blue, +++ blue, ++ light blue, + very light blue, ± almost white, and − white.

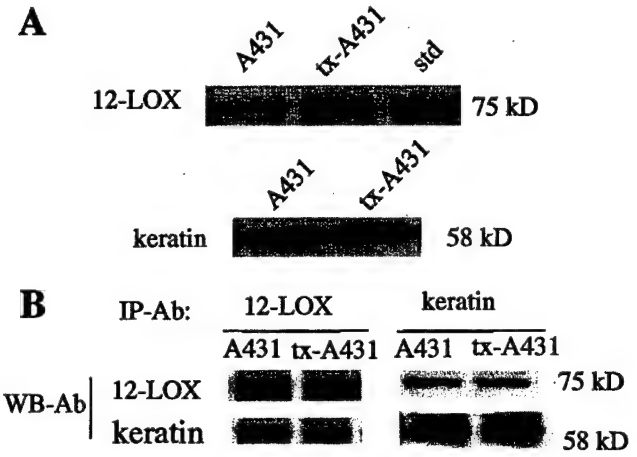

FIGURE 2: Interaction of 12-lipoxygenase and keratin in vitro. (A) Western blotting: 12-LOX (upper panel) and keratin (lower panel) protein in untransfected A431 cells (A431) and 12-LOX transfectants (tx-A431). Human recombinant platelet-type 12-LOX was used as standard (std). (B) Immunoprecipitation: 12-LOX and keratin coimmunoprecipitated from untransfected A431 cells (A431) and 12-LOX transfectant (tx-A431). Aliquots of cell lysates from either cell type were immunoprecipitated either with anti-12-LOX or anti-keratin 5 antibodies. After the samples were washed, precipitated pellets were resolved by SDS-PAGE, and proteins were detected by immunoblotting with anti-keratin 5 or anti-12-LOX antibodies. Positions of 12-LOX and keratin are indicated. The experiment was repeated three times. For each experiment, mouse, or rabbit IgG and Sepharose 4B-conjugated protein G beads alone were used as controls.

an experimental metastasis assay (*46*). Interestingly, treatment of tumor cells with a selective 12-LOX inhibitor (e.g., BHPP; see ref *47*) also has been demonstrated to inhibit integrin expression, tumor cell platelet, and tumor cell endothelial cell interactions (*48*) and experimental metastasis in vivo (*49*). To confirm the interaction of 12-LOX with keratin in human cells, we conducted immunoprecipitation assays and confocal immunofluorescent staining in A431 cells. Meanwhile, A431 cells were transfected with a pcDNA 3.1 expression construct, containing human platelet-type 12-lipoxygenase cDNA. The overexpression of 12-LOX in A431 cells was confirmed by Western Blotting (Figure 2A). 12-LOX antibody co-immunoprecipitated keratin with 12-LOX in A431 cells and transfectants. Similarly, keratin antibody

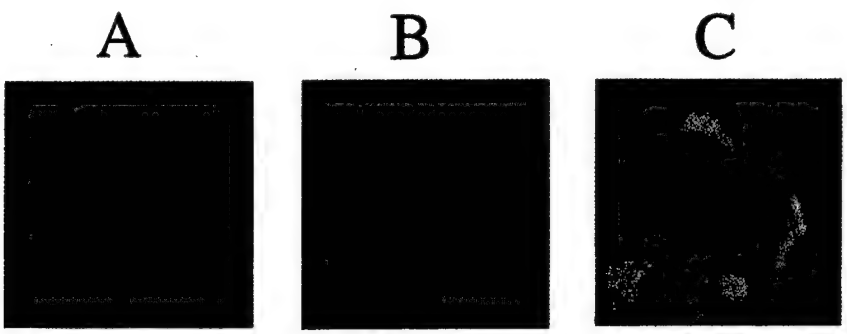

FIGURE 3: 12-LOX colocalization with keratin by laser cofocal immunofluoresence images. Cells were fixed, permeabilized, and incubated first with anti-12-LOX (A) or anti-keratin (B) antibodies, then with FITC-conjugated AffiniPure goat anti-mouse IgG (A, green) or Rhodamine Red-X-conjugated AffiniPure goat anti-rabbit IgG (B, red). Merged image in C (yellow) superimposes image from the first two images. Yellow color indicates overlap between 12-LOX (green) and keratin (red).

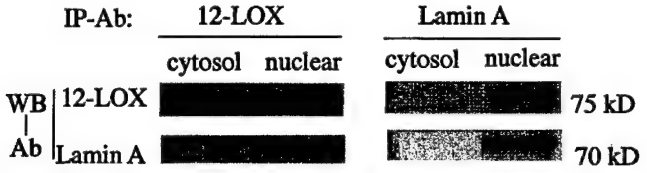

FIGURE 4: Interaction of 12-LOX and lamin A in A431 cells by immunoprecipitation assay: 12-LOX and lamin A coimmunoprecipitated from nuclear extracts of untransfected A431 cells. After the centrifugation at 25000*g*, the supernatants and pellets from 5 $\times$ 10^6 cells were designated as either subcellular fraction of cytosol or nuclear. The supernatnants and resuspended pellets were immunoprecipitated either with anti-12-LOX or anti-lamin A antibodies. After the samples were washed, precipitated pellets were resolved by SDS-PAGE and proteins were detected by immunoblotting with anti-lamin A or anti-12-LOX antibodies. Positions of 12-LOX and lamin A are indicated. The experiment was repeated three times. For each experiment, mouse or rabbit IgG and Sepharose 4B-conjugated protein G beads alone were used as controls.

co-immunoprecipitated 12-LOX with keratin in A431 cells and transfectants (Figure 2B). We also co-immunoprecipitated 12-LOX with lamin A using 12-LOX antibody and co-immunoprecipitated lamin A with 12-LOX using lamin A antibody (Figure 4). We were able to use immunofluorescent staining in A431 cells to show that 12-LOX co-localized with keratin in the cytoplasm, mostly around the cell nucleus forming a ring-like structure (in yellow), as seen in Figure 3. Combined, our results indicate that 12-LOX physically interacts with keratin in the cytoplasm and with lamin A in the nucleus of human tumor cells.

Our findings are consistent with a recent report that 12-LOX activity is detected predominantly in the particulate fractions in murine keratinocytes (*50*). These particulate fractions were found by ultrastructural analysis to contain mainly insoluble proteins such as keratin but not membrane structures (*50*). Taken together, these findings suggest that human keratin may be a novel regulator of 12-LOX activity by its effect on 12-LOX subcellular localization. The mechanism whereby keratin may affect the subcellular localization of 12-LOX is unknown. However, there are studies suggesting that intermediate filaments participate in intracellular trafficking of proteins to the plasma membrane. For example, it has been demonstrated that intermediate filaments associate and facilitate the transport of single vesicles and lipoprotein droplets in CHO, adipose and steroidogenic cells (*51*−*52*). Another study has shown that 5-LOX binding to certain cytoskeletal proteins including α-actin and that actin may mediate compartmentalization and translocation of 5-LOX in myeloid cells (*53*). Interestingly, we recently observed that the translocation of 12-LOX from cytosol to membrane upon stimulation in A431 cells was blocked after disrupting the keratin component of intermediate filaments (data not shown). It is tempting to speculate that keratin may be similarly involved in the transport of 12-LOX from the cytoplasm to a membrane-bound site. Hagmann et al. (*41*) have demonstrated 12-LOX activity in isolated nuclei, and our laboratory has demonstrated that, upon stimulation, 12-LOX associates with membrane structures and that this association results in an increase in 12-LOX activity (*36, 41*). We are currently attempting to further characterize the interaction between keratin and 12-LOX.

In addition to keratin, we demonstrated that 12-LOX associates with lamin A, phosphoprotein C8FW, and integrin β4 subunit by yeast two-hybrid screen. Like type II keratin K5, lamin A is also an intermediate filament protein and has been identified as a component of the nuclear lamin A, a meshwork of intermediate filaments on the inner surface of nuclear membranes. The association of 12-LOX with lamin A is consistent with the finding of 12-LOX activity in isolated nuclei, as mentioned above. Since keratin and lamin A both are components of cytoskeletal intermediate filaments, we hypothesize that keratin and/or lamin A may contribute to the regulated trafficking of 12-LOX. As will be described elsewhere, we also have shown by coimmunoprecipitation and confocal immunofluorescent colocalization that the β4 integrin interacts specifically with 12-LOX in A431 and CHO cells and that this interaction increases enzymatic activity of 12-LOX with increased 12(S)-HETE production (Tang et al., unpublished observation). When the same experiment was performed and probed with antibodies to 5-LOX or 15-LOX no association between the β4 integrin and 5-LOX or 15-LOX was observed (data not shown) demonstrating the specificity of 12-LOX interaction with the β4 integrin. The β4 integrin is expressed on carcinoma cells and is linked to tumor cell motility and invasion (*54*). Another 12-LOX interactor as determined by yeast two-hybrid analysis is the phosphoprotein C8FW. The human full-length has not been sequenced and no antibody is available. Therefore, we have not yet verified its interaction with 12-LOX in human cancer cells. A similar protein, called C5FW, has been cloned from dog thyroid cells and shares 95% amino acid identity with its human counterpart. These novel proteins can be phosphorylated after mitogenic stimulation, and meanwhile, they themselves can function as a kinase (*18*). It will be interesting to further characterize the

interaction between 12-LOX and these other proteins and how they may contribute to 12-LOX regulation.

In summary, we have isolated four 12-LOX interacting proteins: type II keratin K5, Lamin A, cytoplasmic domain of β4 integrin, and phosphoprotein C8FW. Thus far we have verified that three of these (keratin, lamin A, and β4 integrin) are bona fide 12-LOX binding proteins in human cancer cells. We further demonstrated 12-LOX and keratin physically interact and colocalize around the nuclear membrane. Further characterization of the individual interaction between 12-LOX and each of these four proteins will provide insights into the regulation of 12-LOX activity. Ultimately, a clearer understanding of 12-LOX regulation may permit therapeutic intervention in tumor progression and metastasis.

ACKNOWLEDGMENT

We thank Dr. Sam Brooks, Dr. John Crissman, Dr. Rafael Fridman, Dr. Mohit Trikha, and Dr. William Repaskey for helpful discussions. We thank Ms. Mary Bolin, Mr. Koloinin Mikhail, and Mr. Yinlong Cai for technical help.

REFERENCES

1. Funk, C. D. (1993) *Prog. Nuc. Acid. Res. Mol. Biol. 45*, 67−98.
2. Takahashi, Y., Ueda, Y., and Yamamoto, S. (1988) *Arch. Biochem. Biophys. 266*, 613−621.
3. Hansbrough, J. R., Takahashi, Y., Ueda, N., Yamamoto, S., and Holtman, M. J. (1990) *J. Biol. Chem. 265*, 1771−1776.
4. Funk, C. D., Funk, L. B., Fitzgerald, G. A., and Samuelsson, B. (1992) *Proc. Natl. Acad. Sci. U.S.A. 89*, 3962−3966.
5. Romano, M., Chen, X. S., Takahashi, Y., Yamamoto, S., Funk, C. D., and Serhan, C. N. (1993) *Biochem J. 296* (Pt 1), 127−133.
6. Funk, C. D., Furchi, L., and Fitzgerald, G. A. (1990) *Adv. Prostaglandin, Thromboxane, Leukotriene Res. 21*, 33−36.
7. Honn, K. V., Tang, D. G., Gao, X., Butovich, I. A., Liu, B., Timar, J., and Hagmann, W. (1994) *Cancer Metastasis Rev. 13*, 365−396.
8. Nie, D., Hillman, G. G., Geddes, T., Tang, K., Pierson, C., Grignon, D. J., and Honn, K. V. (1998) *Cancer Res. 58*, 4047−4051.
9. Filep, J. G., Zouki, C., Petasis, N. A., Hachicha, M., and Serhan, C. N. (1999) *Blood 94*, 4132−4142.
10. Hachicha, M., Pouliot, M., Petasis, N. A., and Serhan, C. N. (1999) *J. Exp. Med. 189*, 1923−1031.
11. Maddox, J. F., Colgan, S. P., Clish, C. B., Petasis, N. A., Fokin, V. V., and Serhan, C. N. (1998) *FASEB J. 12*, 487−494.
12. Gao, X., Grignon, D. J., Chbihi, T., Zacharek, A., Chen, Y. Q., Sakr, W., Portor, A. T., Crissman, J. D., Pontes, J. E., Powell, I. J., and Honn, K. V. (1995) *Urology 46*, 227−237.
13. Onoda, J. M., Kantak, S. S., Piechocki, M. P., Awad, W., Chea, R., Liu, B., and Honn, K. V. (1994) *Radiat. Res. 140*, 410−418.
14. Baba, A., Sakuma, S., Okamoto, H., Inoue, T., and Iwata, H. (1989) *J. Biol. Chem. 264*, 15790−15795.
15. Ozeki, Y., Nagamura, Y., Ito, H., Unemi, F., Kimura, Y., Igawa, T., Kambayashi, Ji., Takahashi, Y., and Yoshimoto, T. (1999) *Br. J. Pharmacol. 128*, 1699−1704.
16. Dixon, R. A., Diehl, R. E., Opas, E., Rands, E., Vickers, P. J., Evans, J. F., and Miller, D. K. (1990) *Nature 343*, 282−284.
17. Provost, P., Samuelsson, B., and Radmark, O. (1999) *Proc. Natl. Acad. Sci. U.S.A. 96*, 1881−1885.
18. Wilkin, F., Suarez-Huerta, N., Robaye, B., Peetermans, J., Libert, F., Dumont, J. E., and Maenhaut, C. (1997) *Eur. J. Biochem. 248*, 660−668.
19. Kolonin, M. G., and Finley, R. L., Jr. (1998) *Proc. Natl. Acad. Sci. U.S.A. 95*, 14266−14271.
20. Estojak, J., Brent, R., and Golemis, E. A. (1995) *Mol. Cell, Biol. 15*, 5820−5829.
21. Finley, R. L., Jr., and Brent, R. (1994) *Proc. Natl. Acad. Sci. U.S.A. 91*, 12980−12984.
22. Guthrie, C., and Fink, G. R. (1991) *In methods in enzymology*, Academic Press, Inc., Boston, MA.
23. Ausubel, F. M., Brent, R., Kingston, R. E., Moore, D. D., Seidman, J. G., and Struhl, K. (1987−1997) *Current protocols in molecular biology* (Chapter 13), Greene and Wiley-Interscience, New York.
24. Gietz, D., St. Jean, A., Woods, R. A., and Schiestl, R. H. (1992) *Nucleic Acids Res. 20*, 1425.
25. Gyuris, J., Golemis, E., Chertkov, H., and Brent, R. (1993) *Cell 75*, 791−803.
26. Paroush, Z., Finley, R. L., Jr., Kidd, T., Wainwright, S. M., Ingham, P. W., Brent, R., and Ish-Horowicz, D. (1994) *Cell 79*, 805−815.
27. Brook, T. G., McNish, R. W., and Peter-Golden, M. (1995) *J. Biol. Chem. 270*, 21652−21658.
28. Finley, R. L., Jr., and Brent, R. (1995) *In Gene probes: A Practical Approach* (Hames, B. D., and Glover, D. M., Eds.) pp 169−203, Oxford University Press. Oxford, UK.
29. Golemis, E. A., Serebriiskii, I., Finley Jr., R. L, Kolonin, M. G., Gyuris, J., and Brent, R. *Current Protocols in Molecular Biology*, Unit 20.1., and *Current Protocols in Protein Science*, Unit 19.1, John Wiley & Sons, Inc., New York.
30. Abmayr, S. M., and Workman, J. L. (1996) *Current Protocols in Molecular Biology*, Unit 12.1, John Wiley & Sons, Inc., New York.
31. Sloane, B. F., Moin, K., Sameni, M., Tait, L, R., Rozhin, J., and Ziegler, G. (1994) *J. Cell. Sci. 107*, 373−384.
32. Willingham, M. C., and Pastan, I. (1990) *Biotechniques 8*, 320−324.
33. Hagmann, W., Gao, X., Timar, J., Chen, Y. Q., Strohmaier, A. R., Fahrenkop, C., Kagawa, D., Lee, M., Zacharek, A., and Honn, K. V. (1996) *Exp. Cell Res. 228*, 197−205.
34. Takahashi, Y., Reddy, G. R., Ueda, N., Yamamoto, S., and Arase, S. (1993) *J. Biol. Chem. 268*, 16443−16448.
35. Yamamoto, S. (1992) *Biochem Biophys Acta 11*, 117−131.
36. Baba, A., Sakuma, S., Okamoto, H., Inoue, T., and Iwata., H. (1989) *J. Biol. Chem. 264*, 15790−15795.
37. Chang, W. C., Ning, C. C., Lin, M. T., and Huang, J. D. (1992) *J. Biol. Chem. 267*, 3657−3666.
38. Chang, W. C., Liu, Y. W., Ning, C. C., Suzuki, H., Yoshimoto, T., and Yamamoto, S. (1993) *J. Biol. Chem. 268*, 18734−18739.
39. Liu, Y. W., Asaoka, Y., Suzuki, H., Yoshimoto, T., Yamamoto, S., and Chang, W. C. (1994) *J. Pharmacol. Exp. Ther. 271*, 567−573.
40. Liaw, Y. W., Liu, Y. W., Chen, B. K., and Chang, W. C. (1998) *Biochim. Biophys. Acta 1389*, 23−33.
41. Hagmann, W., Gao, X., Zacharek, A., Wojciechowski, L. A., and Honn, K. V. (1995) *Prostaglandins 49*, 49−62.
42. Hazelbag, H. M., Fleuren, G. J., v d Broek, L. J., Taminiau, A. H., and Hogendoorn, P. C. (1993) *Am. J. Surg. Pathol. 17*, 1225−33.
43. Katagata, Y., and Kondo, S. (1997) *FEBS Lett. 407*, 25−31.
44. Timar, J., Baza, V., Kimler, V., Haddad, M., Tang, D. G., Robertson, D., Tovari, J., Taylor, J. D., and Honn, K. V. (1995) *J. Cell. Science 108*, 2175−2186.
45. Chopra, H., Timar, J., Rong, X., Grossi, I. M., Hatfield, J. S., Fligiel, S. E., Finch, C. A., Taylor, J. D., and Honn, K. V. (1992) *Clin. Exp. Metastasis. 10*, 125−137.
46. Timar, J., Trikha, M., Szekeres, K., Bazaz, R., Tovari, J., Silletti, S. A., and Honn, K. V. (1996) *Cancer Res. 56*, 5071−5978.
47. Liu, B., Marnett, L. J., Chaudhary, A., Ji, C., Blair, I. A., Johnson, C. R., Diglio, C. A., and Honn, K. V. (1994) *Lab. Invest. 70*, 314−323.

48. Honn, K. V., Tang, D. G., Grossi, I., Duniec, Z. M., Timar, J., Renaud, c., Leithauser, M., Blair, I., Johnson, C. R., and Diglio, C. A. (1994) *Cancer Res. 54*, 565−574.
49. Chen, Y. Q., Duniec, Z. M., Liu, B., Hagmann, W., Gao, X., Shimoji, K., Marnett, L. J., Johnson, C. R., and Honn, K. V. (1994) *Cancer Res. 54*, 1574−1579.
50. Nakamura, M., Yamamoto, S., and Ishimura, K. (1997) *Cell Tissue Res. 288*, 327−334.
51. Trinczek, B., Ebneth, A., and Mandelkow, E. (1999) *J. Cell. Sci. 112*, 2355−2367.
52. Schweitzer, S. C., and Evans, R. M. (1998) *Subcell. Biochem. 31*, 437−462.
53. Lepley, R. A., and Fitzpatrick, F. A. (1994) *J. Biol. Chem. 269*, 24163−24168.
54. Shaw, L. M., Rabinovitz, I., Wang, H. F., Toker, A., and Mercurio, A. M. (1997) *Cell 91*, 949−960.

BI992664V

Biochemical and Biophysical Research Communications 267, 245–251 (2000)
doi:10.1006/bbrc.1999.1840, available online at http://www.idealibrary.com on IDEAL®

Thromboxane A_2 Regulation of Endothelial Cell Migration, Angiogenesis, and Tumor Metastasis

Daotai Nie,* Mario Lamberti,* Alex Zacharek,* Li Li,† Karoly Szekeres,* Keqin Tang,* YuChyu Chen,* and Kenneth V. Honn*,‡

Department of Radiation Oncology and ‡Department of Pathology, Wayne State University School of Medicine, Detroit, Michigan 48202; and †Biomide Corporation, 410 Life Science Building, 410 West Warren Avenue, Detroit, Michigan 48202

Received October 11, 1999

Prostaglandin endoperoxide H synthases and their arachidonate products have been implicated in modulating angiogenesis during tumor growth and chronic inflammation. Here we report the involvement of thromboxane A_2, a downstream metabolite of prostaglandin H synthase, in angiogenesis. A TXA_2 mimetic, U46619, stimulated endothelial cell migration. Angiogenic basic fibroblast growth factor (bFGF) or vascular endothelial growth factor (VEGF) increased TXA_2 synthesis in endothelial cells three- to fivefold. Inhibition of TXA_2 synthesis with furegrelate or CI reduced HUVEC migration stimulated by VEGF or bFGF. A TXA_2 receptor antagonist, SQ29,548, inhibited VEGF- or bFGF-stimulated endothelial cell migration. *In vivo,* CI inhibited bFGF-induced angiogenesis. Finally, development of lung metastasis in C57Bl/6J mice intravenously injected with Lewis lung carcinoma or B16a cells was significantly inhibited by thromboxane synthase inhibitors, CI or furegrelate sodium. Our data demonstrate the involvement of TXA_2 in angiogenesis and development of tumor metastasis. © 2000 Academic Press

Key Words: **thromboxane A_2 (TXA_2); angiogenesis; eicosanoid; endothelial cell; tumor metastasis.**

Angiogenesis, the formation of new capillary blood vessels, is a tightly regulated process involving endothelial cell proliferation, migration, and tube differentiation (1). Persistent angiogenesis underscores many pathological conditions in adults such as tumor growth and metastasis, diabetic retinopathy, and chronic inflammations (2). During angiogenesis, angiogenic factors such as VEGF and bFGF can prompt endothelial cells to exit quiescence and undergo various angiogenic responses such as proliferation, migration, and survival (3). An understanding of the signaling mechanism which underlies angiogenesis is important since it will provide potential therapeutic targets to inhibit or enhance angiogenesis.

One key aspect of cellular signaling involves mobilization of arachidonic acid and subsequent formation of bioactive eicosanoids through cyclooxygenase (COX), lipoxygenase (LOX), or P450 epoxygenase pathways. In a previous study of prostate cancer, we found that platelet-type 12-LOX stimulated angiogenesis and tumor growth (4). In addition to 12-LOX, it has been shown that COX-1 and COX-2 was up-regulated in endothelial and tumor cells during angiogenesis (5, 6) and that expression of COX was associated with angiogenesis by human gastric endothelial cells (7). Inhibition of COX activity by non-steroidal anti-inflammatory drugs (NSAIDs) have been shown to reduce angiogenesis and tumor growth (for review, ref. 8). Among the products of the cyclooxygenase pathway, PGE_1 and PGE_2 are reported to promote angiogenesis (9–11). In contrast, 15-deoxy-$\Delta^{12,14}$-PGJ_2, a product from PGD_2, induces endothelial cell apoptosis by activation of PPARγ (12) and inhibits angiogenesis (13). It seems, therefore, that the actual profile of the downstream COX metabolites, rather than the level of COX protein or activity, is more relevant in angiogenesis regulation.

The purpose of the present study is to examine the possible involvement of the downstream eicosanoid products of the COX pathway in angiogenesis. Here we report that TXA_2, an eicosanoid metabolite from the sequential activities of COX and thromboxane synthase, is an important mediator for angiogenesis. A TXA_2 mimetic, U46619, stimulated endothelial cell migration while a TXA_2 receptor antagonist, SQ29,548, inhibited endothelial cell migration in response to VEGF or bFGF. We also present evidence that inhibi-

Abbreviations used: COX, cyclooxygenase; TXA_2, thromboxane A_2; TXB_2, thromboxane B_2; PG, prostaglandin; PGI_2, prostacyclin; CI, carboxyheptal imidazole; bFGF, basic fibroblast growth factor; VEGF, vascular endothelial growth factor; RV-ECT, rat vascular endothelial cell-tube forming.

0006-291X/00 $35.00

tion of TXA_2 biosynthesis reduced VEGF- or bFGF-stimulated endothelial cell migration *in vitro* and bFGF-induced angiogenesis *in vivo*. Our data suggest a functional role for TXA_2 in angiogenesis and also implicate the modulation of TXA_2 production or function as a potential therapeutic target for diverse diseases in which vascular endothelial cells play an important role.

MATERIALS AND METHODS

Materials. Prostaglandin E_2, $PGF_{2\alpha}$, carbacyclin, arachidonic acid, and SQ29,548 were purchased from Cayman Chemical Co. (Ann Arbor, MI). U46619, carboxyheptal imidazole (CI), furegrelate sodium were purchased from Biomol (Plymouth Meeting, PA). Recombinant human VEGF-A was purchased from R&D (Minneapolis, MN). Recombinant human bFGF was purchased from Sigma (St. Louis, MO).

Endothelial cell culture. The cord-forming angiogenic endothelial cell line established from rat brain resistance vessels, RV-ECT, was obtained from Dr. Clement Diglio at the Department of Pathology, Wayne State University (Detroit, MI). RV-ECT cells were cultured in DMEM with 10% FBS. Human umbilical vein endothelial cells (HUVEC) and human dermal microvascular endothelial cells (HMVEC) were purchased from Clonetics (San Diego, CA) and multiplied in EGM-2 and used between passage 4 to 10.

Immunoblot analysis of thromboxane synthase expression. Semi-confluent confluent (70–80%) HUVEC, HMVEC, or RV-ECT endothelial cells were rinsed with ice-cold PBS, scraped into lysis buffer containing 20 mM Tris-HCl, pH 7.5, 2 mM EDTA, 0.5 mM EGTA, 0.5 mM PMSF, 0.5 mM leupeptin, 0.15 mM pepstatin A, 1 mM dithiothreitol and 1% NP-40. Protein concentration was measured using BCA protein assay kit (Pierce, Rockford, IL). Seventy-five micrograms of protein from each samples were loaded into a minigel for electrophoresis separation. The proteins in the gel were then transferred onto a PVDF membrane and processed for immunodetection using a thromboxane synthase polyclonal antibody (Cayman Chemical Co., Ann Arbor, MI). Horseradish peroxidase conjugated goat anti-rabbit IgG antibodies and enhanced chemiluminescent (ECL) reagent was purchased from Amersham (Arlington Heights, IL).

Thromboxane A_2 production. RV-ECT cells were grown to 80–90% confluency in DMEM supplemented with 10% FBS and then serum starved overnight in serum-free DMEM. Fresh serum-free DMEM with 1 μM arachidonic acid was added one hour prior to VEGF or bFGF treatment. Thromboxane synthase inhibitor CI was added to a final concentration of 20 μM 15 min prior to VEGF or bFGF treatment. Recombinant human VEGF or bFGF was added in a final concentration of 10 ng/ml. After 20 min of treatment, cells were washed in PBS once and harvested using cell scrapers. After centrifugation, the cell pellets were resuspended in ice-cold 100% ethanol and sonicated. An aliquot was saved for determination of protein level. The samples were purified using BAKERBOND spe Octadecyl (C18) columns (J.T. Baker, Phillipsburg, NJ) and TXB_2 levels were measured using EIA kit as per the manufacturer's instruction (Cayman Chemical, Ann Arbor, MI). Experiments were performed using two different types of endothelial cells, RV-ECT and HUVEC.

Endothelial cell migration assay. Endothelial cell migration assay was conducted using modified Boyden Chamber essentially as previously described (4). HUVE cells were harvested and resuspended in EBM-2 with 2% FBS at density of 5×10^5 cells per ml. Cells (0.5 ml) were placed in the upper chamber and migration was initiated by placing 1 ml of same media containing various treatments in the bottom chamber. After 12–18 h, the cells on the upper side of the membrane were removed by cotton swab and the membrane was cut out, fixed, stained, and mounted in Permount. Cells migrated were enumerated in a double blind approach. For stimulation of endothelial cell migration, usually VEGF (10 ng/ml) or bFGF (10 ng/ml) was placed in the lower chamber. The concentrations of test compounds were described in text. For each treatment, at least three chambers were used unless otherwise indicated.

Wound healing assay. A confluent monolayer of HUVE cell culture was wounded with a pipet tip and the media changed to EBM-2 with 2% FBS. For treatment, VEGF or bFGF was added at the final concentration of 10 ng/ml. SQ29,548 was added to the final concentration of 4 μM. The closure of the wound was monitored and recorded every 6 h.

Matrigel implantation assay for angiogenesis. The Matrigel implantation assay was performed as described by Ito *et al.* (14) with the following modifications. An aliquot (0.4 ml) of Matrigel (Becton Dickinson, Bedford, MA) alone or with test additives was injected s.c. into nude mice (4 mice/group). Mice were sacrificed 5 days after injection and dissected to expose the implants for recording using an SP SZ-4060 stereomicroscope (Olympus America, Melville, NY). The amount of blood retained in the Matrigel was further assessed by measuring the hemoglobin levels using Drabkin's reagent (Sigma Diagnostics, St. Louis, MO).

Tumor cell lines, in vivo maintenance, and isolation of cell subpopulations. The B16 amelanotic melanoma and Lewis lung carcinoma, were originally obtained from the Division of Cancer Treatment, National Institutes of Health (Frederick, MD), and passaged in male C57BL/6J syngeneic mice (15). Monodispersed cells were prepared by enzymatic (collagenase) dispersion, and cell populations were isolated by centrifugal elutriation (16). Isolated cells typically consisted of 100% dispersed cells, >95% tumor cells, with 90–95% viability, and no detectable cellular debris (17).

Experimental metastasis assay. Elutriated cells were re-suspended in MEM at 7.5×10^5 cells/ml, and maintained at 4°C. Five to 10 min prior to injection, the cell suspension was warmed to 25°C. Cells (3.75×10^4) were injected into the lateral tail vein of unanesthetized C57BL/6J male mice (8–9 weeks old). A minimum of 12 animals were used per experimental group. Three days post injection, when all cells had cleared the vasculature as previously described (18, 19), animals were administered thromboxane synthase inhibitors (p.o.) daily for 18 days, after which they were sacrificed by cervical dislocation. Lungs were removed and fixed for minimum of 24 h in Bouin's fixative, and visible tumor colonies were enumerated as described previously (20). *In vivo* experiments with the B16A cells were repeated three times and with 3LL subpopulations, four times with reproducible results.

RESULTS

Stimulation of Endothelial Cell Migration by TXA_2 Receptor Agonist U46619

It has been shown in a number of studies that COX-1 and COX-2 were up-regulated in both endothelial and tumor cells during angiogenesis (5, 6). In addition, both COX-1 and COX-2 inhibitors are reported to inhibit angiogenesis (5–7). Since the immediate product of COX-1 and COX-2 activities, PGH_2, is used as substrate for the biosynthesis of PGE_2, $PGF_{2\alpha}$, PGI_2, TXA_2, and other eicosanoids by downstream enzymes, we examined the effects of these eicosanoids from the COX pathway on endothelial cell migration. As shown in Fig. 1, at 300 nM, PGE_2 and $PGF_{2\alpha}$ had no significant

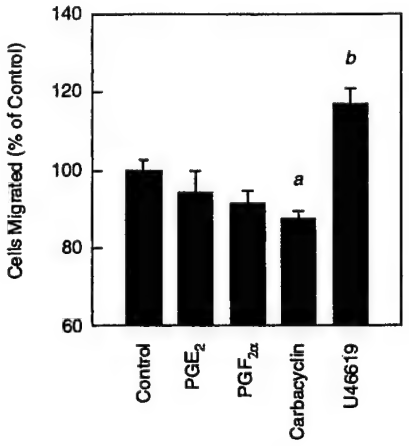

FIG. 1. Modulation of endothelial cell migration by major products of the COX pathway. Endothelial cell migration assay was conducted using modified Boyden Chamber. HUVE cells were harvested and resuspended in EBM-2 with 2% FBS at density of 5×10^5 cells/ml. Cells (0.5 ml) were placed in the upper chamber and migration was initiated by placing 1 ml of same media containing various treatments in the bottom chamber. After 12 h, the cells on the upper side of the membrane were removed by cotton swab and the membrane was cut out, fixed, stained, and mounted in Permount. Cells migrated were enumerated in a double blind approach. The concentrations of all testing compounds were 300 nM. Columns, average cell migration as compared to the basal control; bars, SE. a, $P = 0.002$; b, $P = 0.001$ (Student's t test).

effect on HUVEC migration. At the same concentration, carbacyclin, a PGI_2 stable analog inhibited cell migration while U46619, a TXA_2 receptor agonist, significantly stimulated HUVEC migration by ~20% ($P < 0.01$). The optimal dose for stimulation of endothelial cell migration by U46619 is approximately 300 nM. An increase in U46619 concentration to 3 μM or 30 μM was found to inhibit rather stimulate endothelial cell migration (data not shown), suggesting a biphasic response of the TXA_2 receptor, possibly due to receptor desensitization. The study suggests TXA_2 as a potential mediator of COX in the regulation of angiogenesis.

Stimulation of TXA_2 Production in Endothelial Cells by VEGF and bFGF and Its Involvement in Endothelial Cell Migration

When stimulated with xenoactive antibodies and complement, endothelial cells can release TXA_2 (21), suggesting the presence of thromboxane synthase in endothelial cells. To further confirm the expression of thromboxane synthase, we analyzed its expression in HUVE and HMVE cells by immunoblot analysis. As shown in Fig. 2A, both HMVE and HUVE cells express thromboxane synthase. In addition to endothelial cells of human origin, we also found that RV-ECT cells, an endothelial cell line originated from rat brain, express thromboxane synthase (data not shown).

To examine whether there is an increase in TXA_2 output during angiogenesis, we treated RV-ECT endothelial cells with bFGF or VEGF and measured the level of TXB_2, which is the stable product of TXA_2 after its rapid inactivation. As shown in Fig. 2B, when endothelial cells were treated by VEGF, the production of TXA_2 was increased by 3- to 4-fold. Pretreatment with a thromboxane synthase inhibitor, CI (20 μM), significantly reduced the TXA_2 biosynthesis. A similar increase in TXA_2 synthesis also was observed in RV-ECT cells when treated with bFGF (2.5-fold). We also studied the effect of VEGF or bFGF treatment on TXA_2 biosynthesis in HUVE cells and found that 20 min of VEGF or bFGF treatment increase the level of TXA_2 levels by 4.5- and 4.9-fold, respectively.

Next we examined the role of the increased synthesis of TXA_2 in VEGF- or bFGF-stimulated endothelial cell migration. As shown in Fig. 2C, both thromboxane synthase inhibitors, CI or furegrelate sodium, reduced

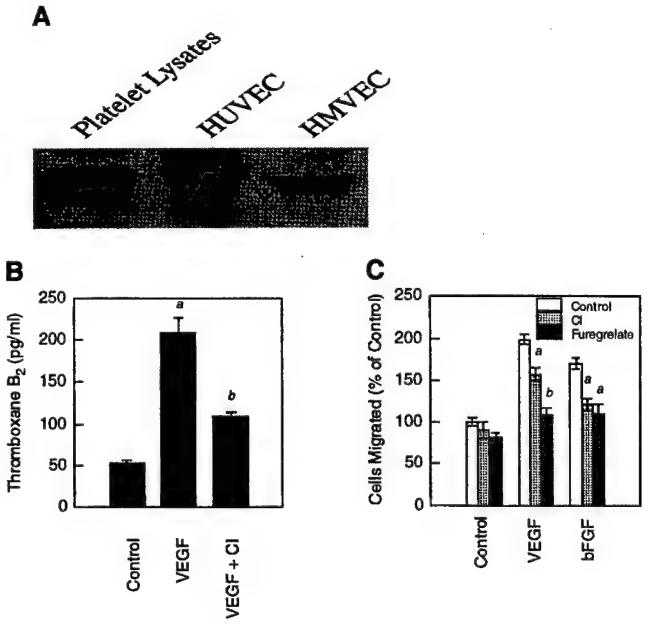

FIG. 2. Expression of thromboxane synthase, TXA_2 biosynthesis, and endothelial cell migration. (A) Western blot analysis of thromboxane synthase expression in various endothelial cells. Platelet lysates were used as the positive control. (B) Stimulation of TXA_2 biosynthesis by bFGF and VEGF. TXA_2 synthesis was measured by the levels of TXB_2 in RV-ECT endothelial cells after bFGF or VEGF treatment as described under Materials and Methods. A representative from three independent experiments is shown. Columns, average level of TXB_2 from triplicate samples; bars, SE. a, $P < 0.01$ when compared to the control; b, $P < 0.01$ when compared to VEGF-treated group (Student's t test). (C) inhibition of VEGF- or bFGF-stimulated endothelial cell migration by thromboxane synthase inhibitors. VEGF- or bFGF-stimulated endothelial cell migration assay was conducted as described under Materials and Methods. Columns, average cell migration as compared to the basal control; bars, SE. a, $P < 0.05$; b, $P < 0.01$ when compared to their respective control (within VEGF- or bFGF-treated group) (Student's t test).

endothelial cell migration stimulated by VEGF or bFGF, suggesting that the increased TXA_2 production is involved for VEGF- or bFGF-stimulated endothelial cell migration.

Inhibition of Endothelial Cell Migration by a TXA_2 Antagonist, SQ29,548

TXA_2 is synthesized within cells and exported immediately to the extracellular miliu. To study whether endogenously synthesized TXA_2 can stimulate endothelial cell migration in an autocrine manner, we next examined the effect of a TXA_2 receptor antagonist, SQ29,548 (22), on VEGF- or bFGF-stimulated wound healing of HUVEC monolayers, a process involving cell migration and proliferation. As shown in Fig. 3A, SQ29,548 inhibited VEGF- or bFGF-stimulated wound closure. SQ29,548 also attenuated endothelial cell migration stimulated by VEGF or bFGF (Fig. 3B). The data suggest that the involvement of TXA_2 in VEGF- or bFGF-stimulated endothelial cell migration, as described above, requires the activation of the TXA_2 receptor since SQ29,548 functions as an antagonist of the TXA_2 receptor.

Inhibition of Angiogenesis in Vivo by Thromboxane Synthase Inhibitor

The Matrigel implantation assay was used to study whether inhibition of TXA_2 synthesis compromises angiogenesis *in vivo*. As shown in the left panel of Fig. 4A, bFGF stimulated angiogenesis as evidenced by the penetration of blood vessels into and the accumulation of blood within the Matrigel plugs. Inclusion of CI in the gels significantly reduced angiogenesis (Fig. 4A, right panel) and reduced the accumulation of hemoglobin in the Matrigel plug (Fig. 4B), suggesting that inhibition of thromboxane synthesis compromised angiogenesis *in vivo*.

Inhibition of Tumor Metastasis by Thromboxane Synthase Inhibitors

Angiogenesis is required for the growth of any solid tumors including primary tumor and tumor metastasis (2). In order to demonstrate whether inhibition of TXA_2 biosynthesis can block the development of metastasis, we injected (tail vein) elutriated B16a or 3LL cells into C57Bl/6J mice and initiated oral administration with thromboxane synthase inhibitors three days post injection. As shown in Figs. 5A and 5B, oral administration of CI significantly reduced the number and the size of lung metastasis from B16a cells. Similar results were obtained with another thromboxane synthase inhibitor, furegrelate sodium. Both thromboxane synthase inhibitors also significantly inhibited the formation of lung metastasis from 3LL cells (Fig. 5B). Taken together, the data suggest that thromboxane synthase activity is required for development of tumor metastasis and that anti-angiogenic thromboxane synthase inhibitors are potential anti-metastatic agents.

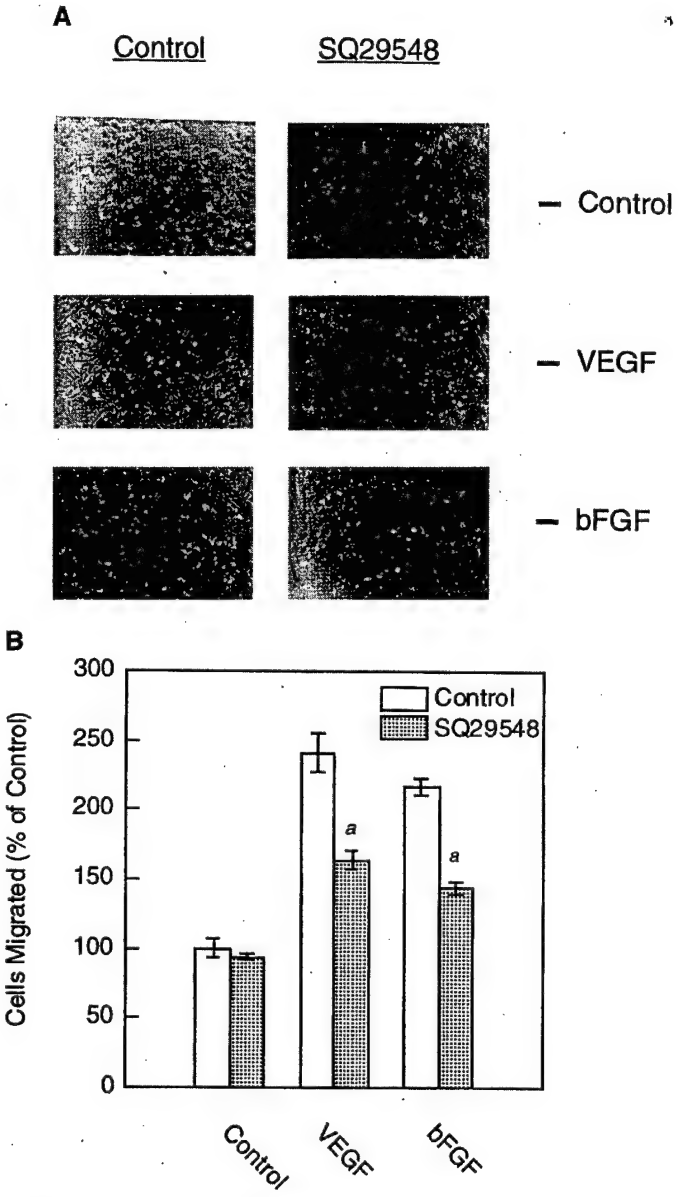

FIG. 3. Inhibition of VEGF- or bFGF-stimulated endothelial cell migration by SQ29,548, a TXA_2 receptor antagonist. (A) Effect of SQ29,548 on HUVEC monolayer wound healing. HUVEC culture monolayer was wounded with a pipet tip and changed into EBM-2 with 2% FBS. VEGF or bFGF was added at the final concentration of 10 ng/ml. SQ29,548 was added in the final concentration of 4 μM. Representatives from each group 36 hours after treatment are shown. (B) Inhibition of VEGF- or bFGF-stimulated endothelial cell migration by SQ29,548. The VEGF- or bFGF-stimulated endothelial cell migration assay was conducted as described under Materials and Methods. The concentration of SQ29,548 was 4 μM. Columns, average cell migration as compared to the basal control; bars, SE. a, $P < 0.05$ when compared to their respective controls (Student's t test).

DISCUSSION

In the present study, our data demonstrate that (i) among various major eicosanoid products from COX activity, the TXA_2 mimetic U46619 stimulates, while the PGI_2 analog carbacyclin reduces, endothelial cell migration, (ii) biosynthesis of TXA_2 is stimulated by bFGF or VEGF in endothelial cells, (iii) inhibition of endogenous TXA_2 synthesis reduced VEGF- or bFGF-stimulated endothelial cell migration, (iv) blocking TXA_2 function by SQ29,548 decreased VEGF- or bFGF-stimulated endothelial cell migration, (v) inhibition of thromboxane synthase activity by CI reduced bFGF-stimulated angiogenesis *in vivo,* and (vi) inhibition of thromboxane synthase activity by CI or furegrelate sodium reduced the development of experimental pulmonary metastasis from B16a or 3LL cells.

TXA_2 is a potent stimulator of platelet aggregation and smooth muscle constriction and is regarded as a mediator of myocardial infarction, atherosclerosis, and bronchial asthma (23). It is the main product of arachidonic acid metabolism via the COX pathway in platelets. The pro-angiogenic function of TXA_2 implicates the possible involvement of platelets in angiogenesis during tumor growth and metastasis. Indeed, platelets are intimately involved in tumor angiogenesis (24, 25) and platelet aggregation stimulates the release of VEGF (26). Clinically, 30–60% of advanced cancer patients possess platelet abnormalities, such as thrombocytosis and many other thromboembolic disorders. Also, activated platelets have been frequently associated with many malignant tumors (27). Pharmacologically, many anti-platelet agents, including thromboxane synthase inhibitors, have been shown to possess anti-metastatic effects (28). These original observations were believed to be due to the effect of thromboxane synthase inhibitors/receptor antagonists on platelet TXA_2 production. In the present study, thromboxane synthase inhibitors were administered 3 days post injection. This time interval between injection and treatment was chosen because of previous studies from our laboratory, which demonstrated that intravenously injected tumor cells attach to the endothelium, induce endothelial cell retraction, and extravasate from the vasculature into the lung parenchymal tissues within 24 hours post injection (18, 19). Therefore, any effect observed with these inhibitors could not be explained by inhibition of tumor/platelet/endothelial cell interactions or tumor cell extravasation. The inhibition of development of metastasis in the experiments presented here suggests that the thromboxane synthase inhibitors affected the ability of tumor cells to grow at the site of distant metastasis. One possible explanation could be a reduction in angiogenesis due to an inhibition of endothelial cell TXA_2 synthase.

Although it is generally accepted that TXA_2 is mainly produced by platelets, TXA_2 can also be synthesized by numerous cells in response to various physiological and pathological stimuli (23, 29). Synthesized TXA_2 is rapidly secreted from cells and acts as a local hormone in the immediate vicinity of its site of production. The human TXA_2 receptor (TP) is a typical G-protein coupled receptor with seven transmembrane segments (30). Activation of TP by TXA_2, or more stable synthetic agonists, evokes the activation of phospholipase C and a subsequent rise in the intracellular calcium ion concentration. Depending on cell type, TP activation will result in platelet aggregation (31), contraction of vascular smooth muscle cells (32) or release of prostacyclin from endothelial cells (33).

In this study, we found that putative angiogenic factors such as VEGF or bFGF can increase TXA_2 biosynthesis in endothelial cells and the increased TXA_2 biosynthesis mediates the stimulation of endothelial cell migration by VEGF or bFGF. The newly synthesized TXA_2 probably acts through its G protein-coupled receptor to modulate endothelial cell migration, since a TXA_2 receptor antagonist, SQ29,548, decreases VEGF- or bFGF-stimulated endothelial cell migration. The results suggest the activation of TXA_2 receptor is required for full stimulation of endothelial cell migration by VEGF or bFGF. However, it should be noted that neither thromboxane synthase inhibitors nor SQ29,548 are able to completely abolish the stimulation of endothelial cell migration by VEGF or bFGF, suggesting that VEGF or bFGF can activate multiple pathways, including TXA_2, to effect endothelial cell motility.

When included in bFGF-containing Matrigel implants, thromboxane synthase inhibitor CI inhibited bFGF-induced angiogenesis *in vivo.* Since CI can inhibit thromboxane synthase activity in proximal smooth muscle cells and platelets, as well as in endothelial cells, the exact contribution of TXA_2 synthesized by endothelial cells in angiogenesis remains to be defined. Nevertheless, the observed anti-angiogenic activity of a thromboxane synthase inhibitor, along with the recent observation that the TXA_2 receptor antagonist SQ29,548 inhibited corneal angiogenesis (34), suggests TXA_2 is an important factor in bFGF-induced angiogenesis *in vivo.*

It should be noted that although TXA_2 is involved in angiogenesis, we did not find that the activation of TXA_2 receptor by U46619 alone leads to *de novo* angiogenesis (Nie *et al.,* unpublished observation), suggesting TXA_2 must act in concert with other factors to promote angiogenesis. Indeed, angiogenesis is a complex process which involves extensive interplay between cell, extracellular matrix, and a plethora of angiogenic factors such as bFGF, VEGF, and angiogenin. For example, bFGF is a stronger endothelial cell mito-

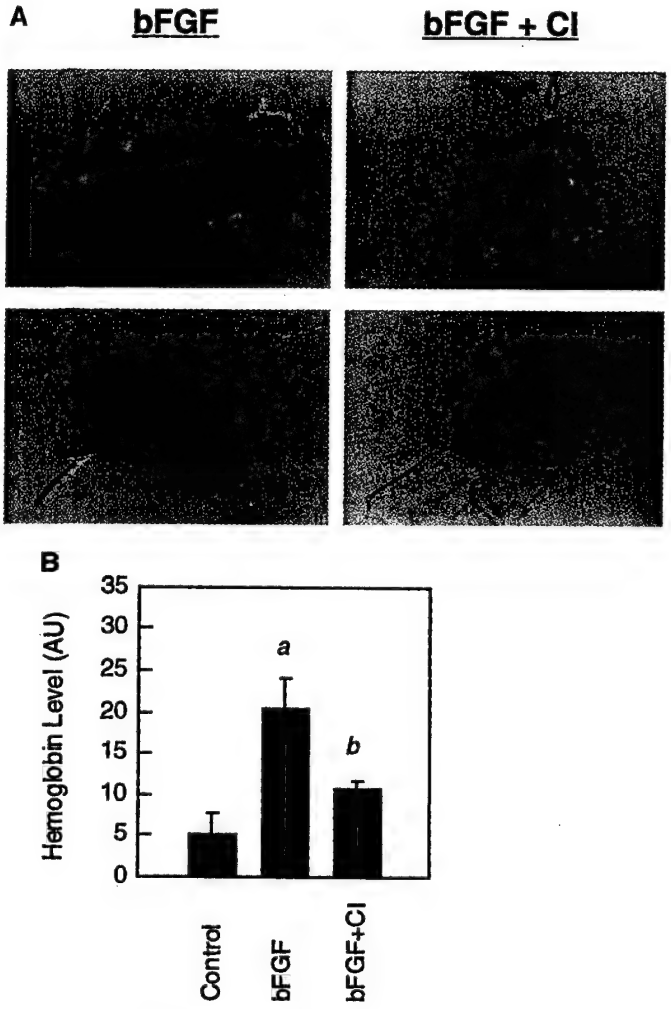

FIG. 4. Inhibition of bFGF-induced angiogenesis *in vivo* by a thromboxane synthase inhibitor, CI. Matrigel implantation assay for angiogenesis was conducted as described under Materials and Methods. (A) Matrigel implantation angiogenesis assay. Left panel: bFGF (5 μg/ml of Matrigel) *in situ;* Right panel: bFGF plus CI (2.5 mg/ml of Matrigel) *in situ.* (B) Hemoglobin levels in resected implants. The hemoglobin was measured by Drabkin's reagent. Columns, average hemoglobin levels (AU); bars, SE from quadruplicate samples. a, $P < 0.05$ when compared to the control; b, $P < 0.05$ when compared to the bFGF-treated group.

gen than VEGF while VEGF is stronger chemotactic stimulant than bFGF (35). For bFGF to induce angiogenesis, it stimulates VEGF expression in endothelial cells and together with VEGF, induces angiogenesis (36). Neutralization of VEGF function can block bFGF-induced angiogenesis, suggesting that different angiogenic factors must work together to induce angiogenesis (36). Currently, we are actively exploring the possible additive or synergistic interaction between TXA_2 and other angiogenic factors during angiogenesis.

In summary, here we identified TXA_2 as an important factor in angiogenesis. Modulation of the function of this eicosanoid presents a means to control angiogenesis in various diseases in which vascular endothelial cells play a prominent role. The identification of another lipid which regulates angiogenesis, in addition to 12(S)-HETE as described in our previous study of prostate cancer (4), provide a new paradigm that, in

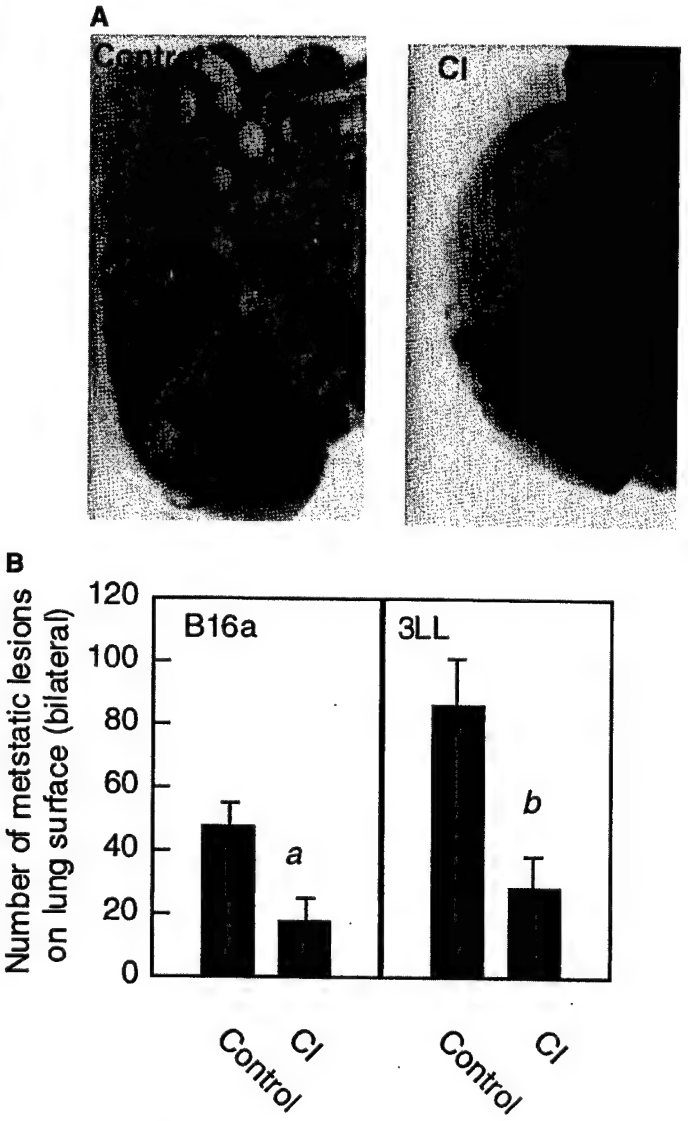

FIG. 5. Inhibition of development of experimental metastasis by thromboxane synthase inhibitor. Experimental metastasis study was conducted by injecting mice with 3.75×10^4 elutriated B16a or 3LL cells. Daily oral administration of CI was initiated 3 days post injection with the dose of 4 mg/kg mouse weight. After 18 days of treatment, mice were sacrificed and the number of metastatic lesions on lung surface was assessed as described under Materials and Methods. (A) Gross morphology of resected mouse lungs 21 days after tail vein injection of B16a cells. Left, a typical mouse lung in control group; right, a representative lung from the mice treated with CI for 18 days. (B) reduction of the formation of metastatic lesions by CI. Columns, average number of metastatic lesions per mouse lung (bilateral); Bars, S.E. from 12 samples. a and b, $P < 0.05$ when compared to their respective control.

addition to proteinaceous factors, angiogenesis is further regulated by small bioactive lipids such as 12(S)-HETE and TXA_2. Manipulation of the function or biosynthesis of these pro-angiogenic bioactive lipids provides a novel approach for development of anti-angiogenesis therapy for many diseases including cancer.

ACKNOWLEDGMENTS

This work was supported by NIH CA-29997, United States Army Research Program DAMD 17-98-1-8502, and an award from Cap CURE Foundation and Biomide Corporation (to K.V.H.). D.N. was supported by a fellowship from the Cancer Research Foundation of American. Special thanks are directed to Dr. Clement Diglio for providing RV-ECT endothelial cells.

REFERENCES

1. Hanahan, D., and Folkman, J. (1996) *Cell* **86,** 353–364.
2. Folkman, J. (1995) *in* The Molecular Basis of Cancer (Mendelsohn, T., Howley, P. M., Israel, M. A., and L. A. Liotta., Eds.), pp. 206–232, W.B. Saunders Co., Philadelphia, PA.
3. Pepper, M. S., Mandriota, S. J., Vassalli, J. D., Orci, L., and Montesano, R. (1996) *Curr. Top. Microbiol. Immunol.* **213,** 31–67.
4. Nie, D., Hillmanm G. G., Geddes, T., Tang, K., Pierson, C., Grignon, D. J., and Honn, K. V. (1998) *Cancer Res.* **58,** 4047.
5. Narko, K., Ristimaki, A., MacPhee, M., Smith, E., Haudenschild, C. C., and Hla, T. (1997) *J. Biol. Chem.* **272,** 21455–21460.
6. Tsujii, M., Kawano, S., Tsuji, S., Sawaoka, H., Hori, M., and DuBois, R. N. (1998) *Cell* **93,** 705–716.
7. Hull, M. A., Thomson, J. L., and Hawkey, C. J. (1999) *Gut* **45,** 529–536.
8. Peterson, H-I. (1983) *Invasion Metastasis* **3,** 151–159.
9. Benezra, D. (1978) *Am. J. Opthalmol* **86,** 455–461.
10. Ziche, M., Jones, J., and Gullino, P. M. (1982) *J. Natl. Cancer Inst.* **69,** 475–482.
11. Form, D. M., and Auerbach, R. (1983) *Proc. Soc. Exp. Biol. Med.* **172,** 214–218.
12. Bishop-Bailey, D., and Hla, T. (1999). *J. Biol. Chem.* **274,** 17042–17048.
13. Xin, X., Yang, S., Kowalski, J., and Gerritsen, M. E. (1999) *J. Biol. Chem.* **274,** 9116–9121.
14. Ito, Y., Iwamoto, Y., Tanaka, K., Okuyama, K., and Sugioka, Y. (1996) *Int. J. Cancer* **67,** 148.
15. Grossi, I. M., Fitzgerald, L. A., Umbarger, L. A., Nelson, K. K., Diglio, C. A., Taylor, J. D., and Honn, K. V. (1989) *Cancer Res.* **49,** 1029–1037.
16. Ryan, R. E., Crissman, J. D., Honn, K. V., and Sloane, B. F. (1985) *Cancer Res.* **45,** 3636–3641.
17. Onoda, J. M., Nelson, K. K., Grossi, I. M., Umbarger, L. A., Taylor, J. D., and Honn, K. V. (1988) *Proc. Soc. Exp. Biol. Med.* **187,** 250–5.
18. Crissman, J. D., Hatfield, J., Schaldenbrand, M., Sloane, B. F., and Honn, K. V. (1985) *Lab. Invest.* **53,** 470–478.
19. Crissman, J. D., Hatfield, J. S., Menter, D. G., Sloane, B., and Honn, K. V. (1988) *Cancer Res.* **48,** 4065–4072.
20. Honn, K. V. (1983) *Clin. Exp. Metastasis* **1,** 103–114.
21. Butos, M., Coffman, T. M., Saadi, S., and Platt, J. L. (1997) *J. Clin. Invest.* **100,** 1150–1158.
22. Ogletree, M. L., Harris, D. N., Greenberg, R., *et al.* (1985) *J. Pharmacol. Exp. Ther.* **234,** 435–441.
23. Negishi, M., Sugimoto, Y., and Ichikawa, A. (1995) *Biochim. Biophys. Acta* **1259,** 109–119.
24. Salgado, R., Vermeulen, P. B., Benoy, I., Weytjens, R., Huget, P., Van Marck, E., and Dirix, L. Y. (1999) *Br. J. Cancer* **80,** 892–897.
25. Pinedo, H. M., Verheul, H. M., D'Amato, R. J., and Folkman, J. (1998) *Lancet* **352,** 1775–1777.
26. Maloney, J. P., Silliman, C. C., Ambruso, D. R., Wang, J., Tuder, R. M., and Voelkel, N. F. (1998) *Am. J. Physiol.* **275,** H1054–1061.
27. Honn, K. V., Tang, D. G., and Crissman, J. D. (1992) *Cancer Metastasis Rev.* **11,** 325–351.
28. Honn, K. V., Cavanaugh, P., Evens, C., Taylor, J. D., and Sloane, B. F. (1982) *Science* **217,** 540–542.
29. Needleman, P., Turk, J., Jakschik, B. A., Morrison, A. R., and Lefkowith, J. B. (1986) *Annu. Rev. Biochem.* **55,** 69–102.
30. Hirata, M., Hayashi, Y., Ushikubi, F., Yokota, Y., Kageyama, R., Nakanishi, S., and Narumiya, S. (1991) *Nature* **349,** 617–620.
31. Needleman, P., Moncada, S., Bunting, S., Vane, J. R., Hamberg, M., and Samuelsson, B. (1976) *Nature* **261,** 558–560.
32. Ellis, E. F., Oelz, O., Roberts, L. J., Payne, N. A., Sweetman, B. J., Nies, A. S., and Oates, J. A. (1976) *Science* **193,** 1135–1137.
33. Hunt, J. A., Merritt, J. E., MacDermot, J., and Keen, M. (1992) *Biochem. Pharmacol.* **43,** 1747–1752.
34. Daniel, T. O., Liu, H., Morrow, J. D., Crews, B. W., and Marnett, L. J. (1999) *Cancer Res.* **59,** 4574–4577.
35. Kumar, R., Yoneda, J., Bucana, C. D., and Fidler, I. J. (1998) *Int. J. Oncol.* **12,** 749.
36. Seghezzi, G., Patel, S., Ren, C. J., Gualandris, A., Pintucci, G., Robbins, E. S., Shapiro, R. L., Galloway, A. C., Rifkin, D. B., and Mignatti, P. (1998) *J. Cell Biol.* **141,** 1659.

Eicosanoid regulation of angiogenesis: role of endothelial arachidonate 12-lipoxygenase

Daotai Nie, Keqin Tang, Clement Diglio, and Kenneth V. Honn

Angiogenesis, the formation of new capillaries from preexisting blood vessels, is a multistep, highly orchestrated process involving vessel sprouting, endothelial cell migration, proliferation, tube differentiation, and survival. Eicosanoids, arachidonic acid (AA)-derived metabolites, have potent biologic activities on vascular endothelial cells. Endothelial cells can synthesize various eicosanoids, including the 12-lipoxygenase (LOX) product 12(S)-hydroxyeicosatetraenoic acid (HETE). Here we demonstrate that endogenous 12-LOX is involved in endothelial cell angiogenic responses. First, the 12-LOX inhibitor, N-benzyl-N-hydroxy-5-phenylpentanamide (BHPP), reduced endothelial cell proliferation stimulated either by basic fibroblast growth factor (bFGF) or by vascular endothelial growth factor (VEGF). Second, 12-LOX inhibitors blocked VEGF-induced endothelial cell migration, and this blockage could be partially reversed by the addition of 12(S)-HETE. Third, pretreatment of an angiogenic endothelial cell line, RV-ECT, with BHPP significantly inhibited the formation of tubelike/cordlike structures within Matrigel. Fourth, overexpression of 12-LOX in the CD4 endothelial cell line significantly stimulated cell migration and tube differentiation. In agreement with the critical role of 12-LOX in endothelial cell angiogenic responses in vitro, the 12-LOX inhibitor BHPP significantly reduced bFGF-induced angiogenesis in vivo using a Matrigel implantation bioassay. These findings demonstrate that AA metabolism in endothelial cells, especially the 12-LOX pathway, plays a critical role in angiogenesis. (Blood. 2000;95:2304-2311)

Introduction

The formation of new capillaries from preexisting vessels, a process termed angiogenesis, is tightly regulated in physiologic processes such as embryonic development, wound repair, and hypertrophy of normal organs. In contrast, persistent unregulated angiogenesis underscores many pathologic conditions, such as tumor growth and metastasis, diabetic retinopathy, atherosclerosis, and chronic inflammation. Angiogenesis is a complex process involving an extensive interplay between cells, soluble factors, and extracellular matrix molecules that culminate in the proliferation, migration, and tube differentiation of endothelial cells.[1] A plethora of angiogenesis regulators such as vascular endothelial growth factor (VEGF) and basic fibroblast growth factor (bFGF) can elicit various angiogenic responses from endothelial cells.[2] An understanding of endothelial cell metabolism and the signaling that underlies angiogenesis is important because it provides potential therapeutic targets to inhibit or enhance angiogenesis.

12-lipoxygenases (12-LOX) are a family of isozymes that belong to the LOX superfamily. These enzymes catalyze the stereospecific oxygenation of arachidonic acid (AA) to form 12(S)-hydroperoxyeicosatetraenoic acid (HPETE) and 12(S)-hydroxyeicosatetraenoic acid (HETE). At least 3 types of 12-LOX have been well characterized: platelet-type, leukocyte-type, and epidermal 12-LOX.[3] Platelet-type 12-LOX exclusively uses AA released from glycerophospholipid pools to synthesize 12(S)-HPETE and 12(S)-HETE, whereas leukocyte-type 12-LOX can also synthesize 15(S)-HETE and 12(S)-HETE. In addition to leukocytes and platelets, the expression of 12-LOX isozymes has been detected in various types of cells, such as smooth muscle cells,[4] keratinocytes,[5] endothelial cells,[4,6] and tumor cells. Elevated 12-LOX activity has been implicated in hypertension,[7] vaso-occlusion in sickle cell disease,[8] inflammation,[9] thrombosis,[10] and mouse skin tumor development.[5] In human prostate carcinoma, the level of 12-LOX expression has been correlated with tumor stage.[11] Along this line, we recently demonstrated that the overexpression of platelet-type 12-LOX in human prostate cancer PC3 cells stimulated tumor growth by elaborating tumor angiogenesis.[12]

In endothelial cells, it has been shown that 12-LOX activity is required for serum- and bFGF-stimulated endothelial cell proliferation[13,14] and for minimally modified low-density lipoprotein-induced monocyte binding to endothelial cells.[15] It has been shown that 12(S)-HETE can directly stimulate endothelial cell mitogenesis,[13,16] migration,[12] and surface expression of $\alpha_v\beta_3$ integrin.[17-20] Because endothelial cell proliferation and migration and increased levels of surface $\alpha_v\beta_3$ integrin[21-23] are involved in angiogenesis, these observations prompted us to investigate the functional role of endothelial 12-LOX in angiogenesis. Here we report that endothelial 12-LOX activity is required for endothelial cell proliferation, migration, and tube differentiation in vitro and angiogenesis in vivo. This study suggests the importance of arachidonic acid metabolism in endothelial cell signaling as it relates to angiogenesis.

From the Departments of Radiation Oncology and Pathology, Wayne State University School of Medicine, and the Karmanos Cancer Institute, Detroit, MI.

Submitted June 2, 1999; accepted December 15, 1999.

Supported by National Institutes of Health grant CA-29997, United States Army Prostate Cancer Research Program DAMD 17-98-1-8502, the Harper Development Fund, a CaPCURE Foundation Award, and a Cancer Research Foundation of America Fellowship Award.

Reprints: Kenneth V. Honn, Department of Radiation Oncology, Wayne State University, 431 Chemistry Building, Detroit, Michigan 48202; e-mail: k.v.honn@wayne.edu.

The publication costs of this article were defrayed in part by page charge payment. Therefore, and solely to indicate this fact, this article is hereby marked "advertisement" in accordance with 18 U.S.C. section 1734.

Materials and methods

Inhibitors

BHPP, a 12-LOX inhibitor as previously described,[24] was a generous gift from Biomide (Grosse Pointe Farms, MI). The IC_{50} for BHPP to inhibit platelet-type 12-LOX activity in tumor cells is approximately 0.2 to 1 μmol/L, depending on cell type.[24,25] BHPP does not appreciably inhibit 5(S)-HETE or 15(S)-HETE synthesis in highly metastatic B16a cells.[25] Using recombinant enzymes, the IC_{50} of BHPP for the murine platelet-type 12-LOX is 0.8 μmol/L with arachidonic acid as a substrate. The rank of selectivity of BHPP for lipoxygenase inhibition is murine platelet-type 12-LOX > murine epidermis-type 12-LOX > human 5-LOX >> murine leukocyte 12-LOX >> rabbit 15-LOX-1 (Furstenberger G, personal communication). Because of its selectivity toward the platelet-type 12-LOX, BHPP was extensively used in the current study. Other inhibitors for AA metabolism—5-, 8-, 11-, and 14-eicosatetraynoic acid (ETYA), nordihydroguaiaretic acid (NDGA), 5-LOX-activating protein (FLAP) inhibitor MK886, and cyclooxygenase (COX) inhibitor indomethacin—were purchased from Calbiochem (San Diego, CA). Their sites of action are illustrated in Figure 1.

Cell culture

The cord-forming angiogenic endothelial cell line RV-ECT was isolated from the RV-EC cell line established from rat brain resistance vessels as previously described.[26] The mouse capillary endothelial cell line CD4 was originally established from mouse lung capillary blood vessels.[27] Both the RV-ECT and the CD4 cells were cultured in Dulbecco's modified Eagle's medium (DMEM) with 10% fetal bovine serum (FBS). Human umbilical vein endothelial cells (HUVEC) and human foreskin dermal microvascular endothelial cells (HMVEC) were purchased from Clonetics (San Diego, CA), multiplied in EGM-2, and used from passages 4 to 10.

Detection of 12-LOX expression by reverse transcription–polymerase chain reaction

Total RNA was isolated from semiconfluent (70% to 80%) endothelial cells using Tri-reagent (Molecular Research Center, Cincinnati, OH) according to the manufacturer's recommendations. After total RNA was isolated, it was further washed with 2 mol/L LiCl/5 mmol/L EDTA to reduce possible contamination from genomic DNA. Total RNA was reverse transcribed with oligo dT using Moloney murine leukemia virus reverse transcriptase (Life Technologies, Gaithersburg, MD). To detect the expression of platelet-type 12-LOX in human endothelial cells, nested polymerase chain reaction (PCR) was conducted using primers located in different exons of the human platelet-type 12-lipoxygenase to ensure the differentiation of PCR products from cDNA or genomic DNA as previously described.[11] The size of the first-round PCR product was approximately 590 bp and the second-round PCR approximately 190 bp. Negative controls with no reverse transcriptase added were also used to detect the possibility of false-positive signals. The PCR products were analyzed using 2% agarose gel.

To confirm further the expression of platelet-type 12-LOX in rat RV-ECT endothelial cells, primers were designed based on the partial sequence of rat platelet-type 12-LOX obtained from rat Walker 256 cells[24] because full-length rat platelet-type 12-LOX has not been cloned or sequenced. Total RNA was isolated using tri-reagent, and the cDNA sequence was synthesized using adapter primer according to the standard protocol from Gibco BRL's 3′ RACE kit (Rapid Amplification of cDNA Ends kit; #18,73-027; Life Technologies). Three different combinations of primers were used for nested PCR. The first combination yielded the final product of 111 bp with the first-round PCR primer set of AGACAATAGCAGCAGACT (1 U) and TAGACGGTTCCAGCTT (137 L) and the second-round primer set of TGACCTCCCTCCAAACAT (26 U) and CTCAGGGTATAAACA (119 L). The second combination yielded the final product of 62 bp using AGACAATAGCAGCAGACT (1 U) and CTCAGGGTATAAACA (119 L) as the first-round primer set and TGACCTCCCTCCAAACAT (26U) and TCAGCGTCCATTCTAAGT (70L) as the second PCR primer set. The expected product size of the third combination was 88 bp using CAGGAGACAATGCTTTTGGAC (LOS2) and GAACAACTCATCATCCTGCC (LO-AS2) as the first PCR primer set and AGACAATAGCAGCAGACT (1 U) and TCAGCGTCCATTCTAAGT (70 L) as the second primer ser. The final PCR products were analyzed using 2% agarose gel.

To study the expression of leukocyte-type 12-LOX in RV-ECT, the following pairs of primers were designed based on the leukocyte-type 12-LOX sequence characterized from rat brain and used for nested PCR: first-round PCR primers, GCCCAGGAGCCAAACGACAT (lower primer) and CATCTTCTGAGGGGACACTT (upper primer). The expected size of the first-round PCR product was 695 bp. The expected size of second-round PCR product was 342 bp using GCATTAGGAACCCAGTAGAA (lower primer) and ACCTATTGCTCATTGTGTCC (upper primer) as second-round PCR primers.

Immunoblot analysis of 12-LOX expression

Semiconfluent confluent (70% to 80%) HUVEC, HMVEC, RV-EC, RV-ECT, and CD4 endothelial cells were rinsed with ice-cold PBS, scraped into lysis buffer containing 20 mmol/L Tris-HCl, pH 7.5, 2 mmol/L EDTA, 0.5 mmol/L EGTA, 0.5 mmol/L phenylmethylsulfonyl fluoride, 0.5 mmol/L leupeptin, 0.15 mmol/L pepstatin A, 1 mmol/L dithiothreitol, and 1% NP-40. Protein concentration was measured using BCA protein assay kit (Pierce, Rockford, IL). Human platelet lysates (10-40 ng) or human epidermoid carcinoma A431 cell lysates (30 μg) were used for positive control. Cell lysates (80 μg) from each sample were loaded onto a minigel for electrophoresis separation. The proteins in the gel were then transferred onto a polyvinylidene difluoride membrane and processed for immunodetection using a rabbit polyclonal antibody to human platelet-type 12-LOX obtained from Oxford Biomedical Research (Oxford, MI). This antibody reacts strongly with platelet-type 12-LOX from various species, with slight cross-reactivity with 5-LOX and 15-LOX at higher concentrations. Horseradish peroxidase-conjugated goat antirabbit IgG antibodies and enhanced chemiluminescent reagent was purchased from Amersham (Arlington Heights, IL).

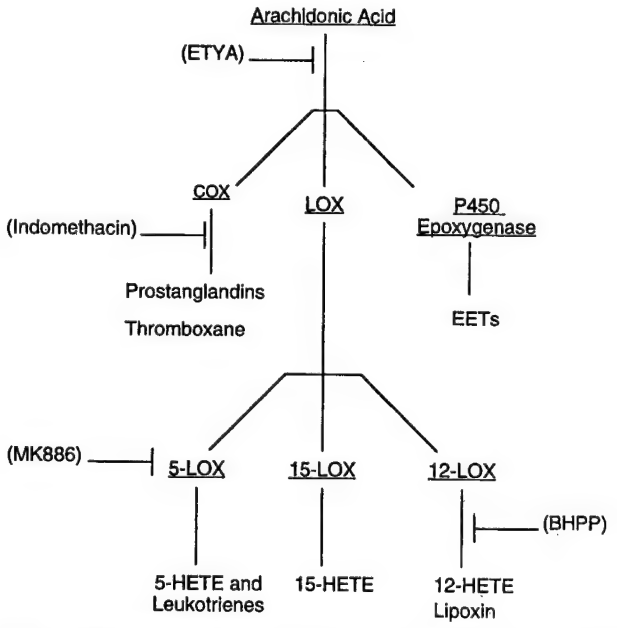

Figure 1. Scheme of AA metabolism. The AA released from phospholipids by PLA2 activity is metabolized by the COX pathways to various prostaglandins and thromboxanes (left), by the LOX pathways to various HETEs, leukotrienes, and lipoxins[42-44] (middle), and by P-450 epoxygenase to epoxyeicosatrienoic acids (right). The proposed site of action for the inhibitors used in this study is shown in parentheses.

Measurement of 12(S)-HETE levels by enzyme immunoassay

To measure 12(S)-HETE synthesis in cell culture, RV-ECT cells (4×10^6 cells) were plated and grown to 80% to 90% confluence in DMEM supplemented with 10% FBS and then serum starved overnight in serum-free DMEM. Fresh serum-free DMEM with 1 μmol/L arachidonic acid was added 1 hour before VEGF treatment. BHPP was added to a final concentration of 10 μmol/L 30 minutes before VEGF treatment. Recombinant human VEGF was added in a final concentration of 10 ng/mL. After 30 minutes of treatment, cells were washed in PBS once and harvested using cell scrapers. After centrifugation, the cell pellets were resuspended in cell lysis buffer and sonicated. Lipids were extracted from cell lysates by adding ethanol to a final concentration of 15%. After centrifugation at 375*g* for 10 minutes at 4°C, the supernatants were acidified to pH 3.5 with 3% formic acid and applied to BAKERBOND spe Octadecyl (C18) columns (J.T. Baker, Phillipsburg, NJ). After washing with ddH_2O, 15% ethanol, and petroleum ether, lipids were eluted with ethyl acetate and dried under N_2 gas, and 12(S)-HETE levels were measured using an EIA kit according to the manufacturer's instructions (Assay Designs, Ann Arbor, MI). To measure 12(S)-HETE levels in Matrigel (Becton Dickinson, Bedford, MA) implants, resected Matrigel plugs were homogenized in cell lysis buffer and processed for lipid extraction and 12(S)-HETE measurement.

Stable transfection of CD4 endothelial cells and characterization

Semiconfluent CD4 endothelial cells were transfected with a pcDNA 3.1 expression construct containing human platelet-type 12-lipoxygenase cDNA, which was a gift from Dr Colin Funk (University of Pennsylvania). Empty vector was used as a control. Transfection was performed using lipofectin reagent (Life Technologies). Transfectants were selected using 300 μg/mL geneticin (G418) in DMEM with 10% FBS. The expression of 12-LOX in CD4 transfectants was characterized by reverse transcription (RT)–PCR and Northern blot analysis for mRNA expression and by immunoblot for 12-LOX protein expression.

Endothelial cell proliferation assay

HUVEC cells were used to study the effects of 12-LOX inhibitors on endothelial cell proliferation. Cells were harvested by trypsinization, resuspended in EGM-2, and plated in a 96-well plate at 2000 cells per well. After overnight incubation, the media were changed to fresh EBM-2 with 1% FBS and treated with recombinant human VEGF-A or bFGF (R&D Systems, Minneapolis, MN) plus various amounts of BHPP. The concentrations of BHPP used were 0, 1, 10, and 50 μmol/L unless otherwise indicated. The final concentration of recombinant human VEGF and bFGF was 10 ng/mL. After 2 days, the plates were processed to quantitate the number of cells using an MTS cell proliferation assay kit (Promega, Madison, WI). The absorbance at 490 nm (A_{490}) indicated the relative number of cells.

The determination of the in vitro growth kinetics of CD4 12-LOX transfectants in culture was conducted essentially as previously described.[12] Basically, 2×10^3 cells were seeded onto 96-well culture plates in complete medium, and the number of viable cells at 48-hour intervals was assessed using an MTS cell proliferation assay kit. The A_{490} reading 2 to 3 hours after plating was used as a baseline. The number of cells was expressed as the percentage of increase from the A_{490} baseline.

Endothelial cell migration assay

RV-ECT endothelial cell migration assay was performed essentially as previously described.[12] VEGF (10 ng/mL), bFGF (10 ng/mL), or various other treatments were placed in the lower chamber. For each treatment, at least 3 chambers were used unless otherwise indicated. The migration assay for CD4 12-LOX transfectants was conducted in a similar way except that the number of cells seeded was 1×10^5 per chamber. The migrated cells were counted by a person unaware of the treatment regimen (blinded approach).

Endothelial cell tube/cord formation assay

Cord-forming RV-ECT cells or CD4 transfectants (1×10^5) were plated on a 24-well plate precoated with a thin layer of Matrigel (Becton Dickinson). After overnight incubation, BHPP was added. After 24 hours of treatment, the media were removed and the confluent monolayer was overlaid with 0.5 mL diluted Matrigel (Becton Dickinson; final concentration, 5 mg/mL). After solidifying at 37°C, 0.5 mL DMEM–10% FBS medium was carefully added without disturbing the gel. The formation of a tubelike structure was monitored microscopically every 6 hours and recorded.

Matrigel implantation assay for angiogenesis

The Matrigel (Becton Dickinson) implantation assay was performed as described by Ito et al[28] with the following modifications. Matrigel 0.4 mL premixed with bFGF (5 μg/ml) with and without BHPP (0.9 mg/ml) was injected subcutaneously into nude mice (4 mice/group). Mice were killed 5 days after injection and dissected to expose the implants for recording using an SP SZ-4060 stereomicroscope (Olympus America, Melville, NY). The amount of blood retained in the Matrigel was further assessed by measuring the hemoglobin levels using Drabkin's reagent (Sigma Diagnostics, St. Louis, MO).

Results

12-Lipoxygenase expression and activity in endothelial cells

Several studies have provided evidence that endothelial cells synthesize various lipoxygenase products such as 5(S)-HETE, 12(S)-HETE, and 15(S)-HETE.[16] The expression of platelet-type 12-LOX in HUVEC cells was previously detected by RT-PCR.[6] Using primers selective for platelet-type 12-LOX, the expression of 12-LOX mRNA was confirmed in HUVEC cells and also detected in microvascular endothelial cells, HMVEC (Figure 2A). In RV-ECT, an endothelial cell line derived from rat brain resistance microvessel, a faint band of PCR product was also present (Figure 2A). To further confirm the expression of platelet-type 12-LOX in RV-ECT cells, we designed 7 primers on the basis of the partial sequence obtained from rat Walker 256 cells.[24] The expression of platelet-type 12-LOX was detected by nested PCR using 3 different combinations of these 7 primers (Figure 2B). Interestingly, in addition to platelet-type 12-LOX, RV-ECT cells also expressed another isoform of 12-LOX that presumably was leukocyte-type as detected by using primers designed on the basis of the rat leukocyte-type 12-LOX sequence[29] (data not shown), suggesting that RV-ECT cells expressed both platelet- and leukocyte-type 12-LOX.

Immunoblot analysis using a rabbit polyclonal antibody against human platelet-type 12-LOX revealed that 12-LOX is also expressed in endothelial cells at the protein level. As shown in Figure 2C, primary cultures of HUVEC and HMVEC had the highest levels of 12-LOX expression, whereas CD4, an endothelial cell line derived from mouse pulmonary microvasculature,[27] had the lowest 12-LOX expression.

When RV-ECT cells were treated with VEGF for 30 minutes, a 5-fold increase in 12(S)-HETE biosynthesis was observed (Figure 2D). The increased 12-LOX activity was inhibited by pretreating RV-ECT cells with BHPP (10 μmol/L). Because BHPP is 20-fold more selective toward platelet-type 12-LOX than leukocyte-type 12-LOX, the results suggest that the increased 12(S)-HETE synthesis on VEGF treatment was probably caused by the increased activity of platelet-type 12-LOX.

It has been shown that arachidonic acid metabolism through the LOX pathways, especially the 12-LOX pathway, is involved in endothelial cell proliferation stimulated by serum or bFGF.[13,14] As

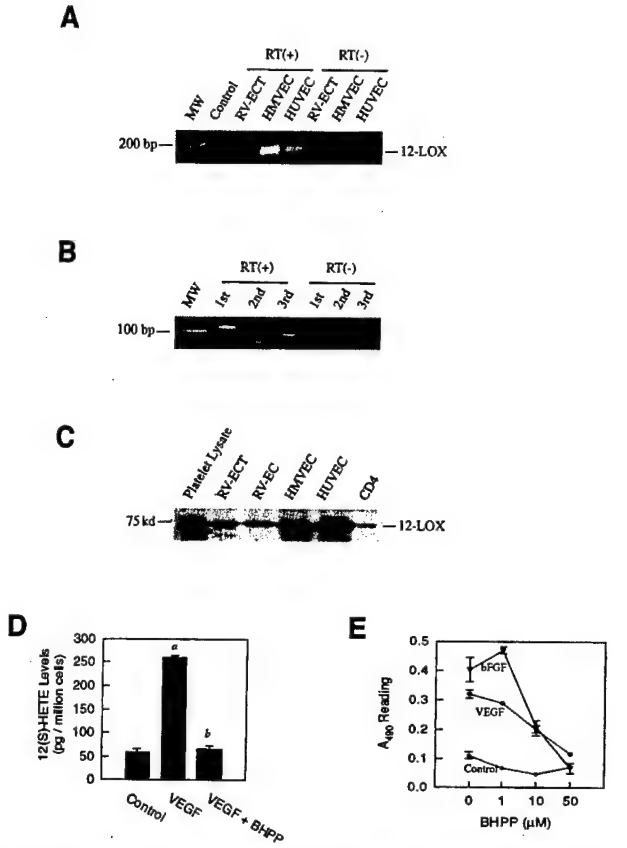

Figure 2. Expression of platelet-type 12-LOX in endothelial cells and its role in cell proliferation. (A) RT-PCR detection of 12-LOX expression in endothelial cells. Total RNA was isolated and processed for double-round RT-PCR using primers designed on the basis of human platelet-type 12-LOX sequence as described in "Materials and Methods." Control, no RNA present in PCR or RT reaction mixtures as controls for the quality of PCR; RT(−), no reverse transcriptase present in RT reaction mixtures as controls for the possible contamination of DNA in RNA samples; RT(+), reverse transcription present. (B) RT-PCR detection of platelet-type 12-LOX expression in RV-ECT cells. The primer combinations for 1st, 2nd, and 3rd are described in "Materials and methods." The target sizes of the final PCR product from 1st, 2nd, and 3rd primer combinations are 111 bp, 62 bp, and 88 bp, respectively. (C) Immunoblot analysis of 12-LOX expression in endothelial cells. The blot was probed with a rabbit polyclonal antibody to human platelet-type 12-LOX. (D) Inhibition of VEGF-stimulated 12-LOX activity by BHPP. Cell treatment and measurement of 12(S)-HETE are detailed in "Materials and methods." Columns, average levels of 12(S)-HETE per 1×10^6 cells (n = 3); bars, SE. a, $P < .01$ when compared with the unstimulated control; b, $P < .05$ when compared to the VEGF-stimulated cells. (E) Involvement of endothelial 12-LOX in bFGF- or VEGF-stimulated cell proliferation. HUVEC cells were plated in 96-well culture plates. Cell proliferation was stimulated with 10 ng/mL bFGF (open triangle) or 10 ng/mL VEGF (filled circle) in EBM-2 with 2% FBS. Cells with no bFGF or VEGF stimulation were used as controls (open circle). 48 hours after treatment with graded levels of BHPP, cell numbers were measured by an MTS method as described in "Materials and methods." Data point, mean from quadruplicate determination; bars, SE from quadruplicate of treatment.

shown in Figure 2E, inhibition of 12-LOX activity by BHPP significantly inhibited bFGF- or VEGF-stimulated HUVEC proliferation, suggesting that 12-LOX activity is required for the endothelial cell proliferative responses to bFGF or VEGF.

Involvement of endogenous 12-lipoxygenase in endothelial cell migration

Endothelial cell migration is a requisite step in angiogenesis. It has been shown that the activation of phospholipase A_2 is required for endothelial cell migration in response to bFGF.[30] To study whether AA released by phospholipase A_2 modulates endothelial cell migration, we selected the RV-ECT cell line, which can grow in DMEM–10% FBS without bFGF or VEGF supplementation,[26] for cell migration assay. First we examined the migratory response of RV-ECT cells toward exogenous AA, bFGF, and VEGF. As shown in Figure 3A, AA increased endothelial cell migration by 70% to 80%, a level comparable to that of bFGF but less than VEGF. This observation is consistent with the report that VEGF is a stronger chemotactic factor than bFGF.[31] Because mobilization of AA has been observed in endothelial cells on stimulation with angiogenic factors such as VEGF,[32] bFGF,[33] and angiogenin,[34] we studied the effect of various inhibitors of arachidonic acid metabolism on endothelial cell migration stimulated by VEGF. As shown in Figure 3B, ETYA, a promiscuous inhibitor for AA metabolism, inhibited VEGF-stimulated RV-ECT migration. NDGA, a general LOX inhibitor, also significantly reduced VEGF-stimulated RV-ECT migration. In contrast, indomethacin, a general COX inhibitor, had no effect. The results suggest that the LOX pathway, but not the COX pathway, of AA metabolism is involved in RV-ECT migration.

In the LOX pathways, AA can be used by 5-LOX to synthesize 5(S)-HETE and leukotrienes, by 12-LOX to synthesize mainly 12(S)-HETE, and by 15-LOX to synthesize15(S)-HETE. To delineate which pathway(s) is involved in endothelial cell migration, we first studied the effect of various types of HETEs on RV-ECT cell migration. As shown in Figure 3C, among the various types of HETEs tested, only 12(S)-HETE, but not 5(S)-HETE, 15(S)-HETE, or 12(R)-HETE, could stimulate endothelial cell migration. The stimulation of endothelial cell migration by 12(S)-HETE is consistent with previous observations.[12] To study whether the endogenous synthesis of 12(S)-HETE is involved in endothelial cell migration in response to VEGF, we examined the effect of BHPP on VEGF-stimulated endothelial cell migration. As shown in

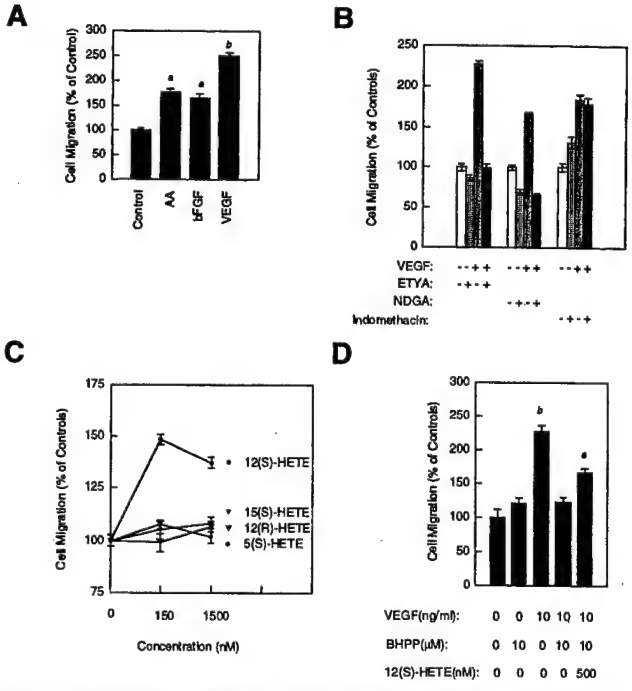

Figure 3. Arachidonate metabolites in endothelial cell migration. The migration assays were performed as described in "Materials and methods." (A) Stimulation of RV-ECT migration by arachidonic acid (1 μmol/L), bFGF (10 ng/ml), and VEGF (10 ng/ml). (B) VEGF-stimulated RV-ECT migration involves lipoxygenase-dependent arachidonic acid metabolism. Treatment: VEGF, 10 ng/mL; ETYA, 5 μmol/L; NDGA, 50 μmol/L; indomethacin, 50 μmol/L. −, absence of treatment (vehicle only); +, presence of treatment. (C) Differential effects on RV-ECT cell migration by various HETEs. (D) Modulation of RV-ECT cell migration by 12-LOX inhibitor BHPP and 12(S)-HETE. Columns, percentage of the average number of cells migrated when compared with the controls; bars, SE (a, $P < .05$; b, $P < 0.01$; Student's t test). All migration assays were repeated at least 4 times.

Figure 3D, BHPP inhibited VEGF-stimulated RV-ECT endothelial cell migration. Furthermore, exogenous 12(S)-HETE partially reversed the inhibitory effect of BHPP on RV-ECT migration (Figure 3D). We also tested the effect of an inhibitor of the 5-LOX pathway, ie, MK886, on VEGF-stimulated RV-ECT migration and did not observe any appreciable effects at a concentration of 10 μmol/L (data not shown). These results collectively suggest that 12-LOX activity and 12(S)-HETE are involved in endothelial cell migration.

Endothelial 12-lipoxygenase was involved in RV-ECT tube differentiation

Certain endothelial cell lines, under proper culture conditions, have the capacity to form tubelike structures. Confluent RV-ECT cells can spontaneously form cordlike structures under normal culture conditions.[26] Therefore, this cell line was chosen for the current study. When RV-ECT cells were cultured between 2 layers of Matrigel, the formation of cordlike structures was expedited, as manifested by the formation of numerous vacuoles within 4 to 5 hours and interconnected tubelike structures within 24 hours (Figures 4A, 4C). Pretreatment of RV-ECT cells with BHPP (10 μmol/L) significantly impaired their ability to form cordlike structures (Figures 4B, 4D), suggesting the potential involvement of 12-LOX in endothelial cell cordlike differentiation.

Endothelial cells that overexpress 12-LOX had increased motility and enhanced tubelike differentiation

To further explore the role of 12-LOX in endothelial cell migration and tubelike differentiation, we transfected CD4 endothelial cells with a pcDNA-12-LOX expression construct. The CD4 endothelial cell line was selected for 12-LOX overexpression study because of its low level of 12-LOX expression (Figure 2C). Stable transfectants were selected using G418, and the transfectant pools were characterized for the expression of 12-LOX mRNA by RT-PCR (Figure 5A) and Northern blot analysis (Figure 5B). The expression of 12-LOX was also increased in 12-LOX-transfected CD4 cells at protein levels as revealed by Western blot (Figure 5C). The growth rate of 12-LOX-transfected CD4 endothelial cells was similar to the mock transfectants (data not shown), suggesting that although 12-LOX is involved in bFGF- or VEGF-stimulated endothelial cell growth, the overexpression of 12-LOX in CD4 cells is not sufficient to stimulate endothelial cell proliferation. However, the overexpression of 12-LOX was able to stimulate CD4 endothelial cell migration (Figure 5D). Further, the increased motility in 12-LOX-transfected CD4 cells was inhibited by BHPP, suggesting that it is the increased 12-LOX activity in endothelial cells that enhances cell motility (Figure 5D).

When cultured within 2 layers of Matrigel, CD4 vector transfectants did not form tubelike structures (Figure 5E, left panel). In contrast, under identical conditions, CD4 12-LOX transfectants retracted and formed tubelike structures (Figure 5E, right panel). The results further suggest the involvement of 12-LOX in endothelial cell tube differentiation.

Inhibition of angiogenesis in vivo by 12-lipoxygenase inhibitor

The involvement of the 12-LOX pathway of arachidonic acid metabolism in endothelial cell proliferation, migration, and tube differentiation led us to study whether the inhibition of 12-LOX activity can compromise angiogenesis in vivo. Because the induction of angiogenesis in vivo by bFGF requires the angiogenic activities of VEGF,[35] we used bFGF premixed with Matrigel to induce angiogenesis. As shown in Figure 6A, bFGF induced

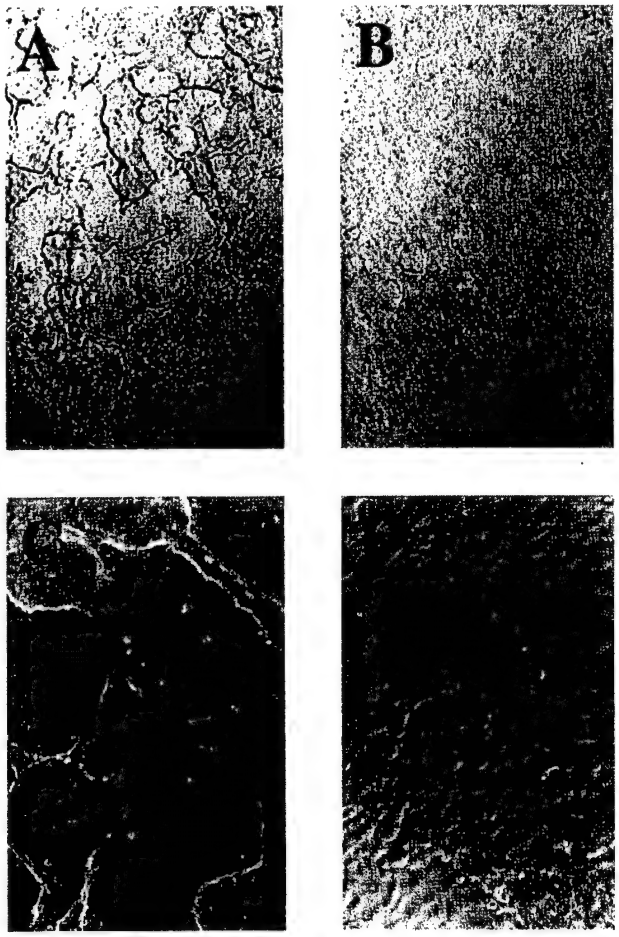

Figure 4. Involvement of 12-LOX in endothelial cell tubelike differentiation. The formation of cordlike structures by RV-ECT cells was facilitated by Matrigel as detailed in "Materials and methods." (A) RV-ECT treated with ethanol as control. Original magnification, ×40. (B) RV-ECT treated with 10 μmol/L BHPP. Original magnification, ×40. (C) RV-ECT treated with ethanol as control. Original magnification, ×100. (D) RV-ECT treated with 10 μmol/L BHPP. Original magnification, ×100. Shown here are typical observations from 4 independent studies on the tube-forming ability of RV-ECT and the effect of BHPP.

massive angiogenesis around and within the implant (upper panel, left). When dissected out, the implanted Matrigel retained a large volume of blood within the gel (upper panel, right). Matrigel implants without bFGF had little or no angiogenic activities in vivo (bottom panel). Inclusion of the 12-LOX inhibitor BHPP in the implants significantly reduced the ability of bFGF to induce angiogenesis (Figure 6A, middle panel), suggesting that 12-LOX is involved in angiogenesis in vivo. Figure 6B shows the hemoglobin levels in the dissected Matrigel. As shown in the Figure, BHPP significantly reduced the hemoglobin levels in Matrigel ($P < .05$), suggesting a reduction of angiogenesis. The reduction of angiogenesis was closely correlated with the levels of 12(S)-HETE in the Matrigel implants as shown in Figure 6C. Taken together, the data suggest a critical role of 12-LOX activity in angiogenesis in vivo.

Discussion

In this study we demonstrated that endothelial cells from different species (rat and human) and different organs (brain, umbilical cord, and foreskin) express platelet-type 12-LOX and elucidated its important role in endothelial cell responses to angiogenic stimuli.

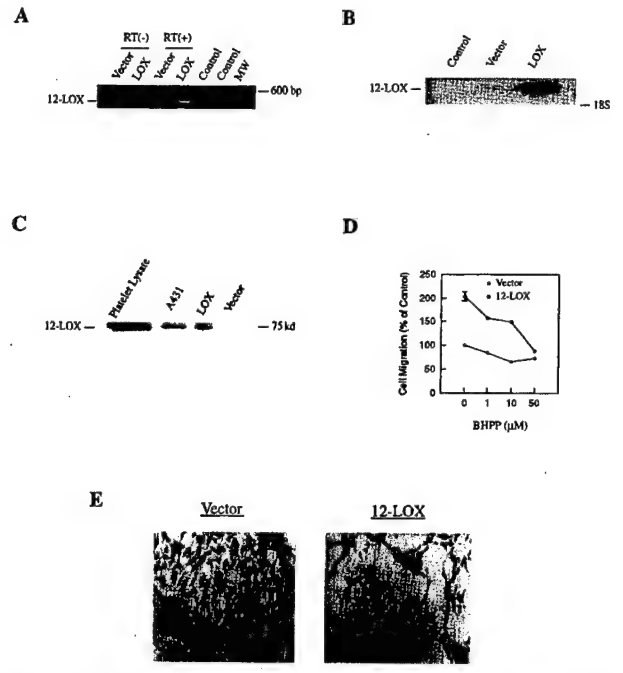

Figure 5. Stimulation of endothelial cell migration and tubelike differentiation by the overexpression of 12-LOX in endothelial cells. CD4 cells were transfected with a 12-LOX expression construct or an empty vector as a control. (A) Detection of 12-LOX mRNA expression by RT-PCR. Primers were the pair of the primers for the first round of PCR. The reaction was carried out for 30 cycles. Control, no RNA present in PCR or RT reaction mixtures as controls for the quality of PCR; RT(−), no reverse transcription present in RT reaction mixtures as controls for the possible contamination of DNA in RNA samples; RT(+), reverse transcription present. Vector, CD4 cells transfected with pcDNA 3.1; LOX, CD4 cells transfected with pcDNA construct with 12-LOX cDNA insert. (B) Northern blot analysis of 12-LOX mRNA levels. Control, loading buffer as the blank control. (C) Analysis of 12-LOX expression at the protein level by immunoblot. (D) Increased cell migration in CD4 12-LOX transfectants. The migration assay was performed as detailed in "Materials and methods" using CD4 cells transfected with pcDNA (open circle) or pcDNA 12-LOX construct (filled circle). Data point, mean from 30 fields counted; bars, SE. The migration assay was repeated for 3 times with similar results. (E) Increased formation of tubelike structures in CD4 12-LOX transfectants. Left panel, vector control; right panel, 12-LOX transfected CD4 cells.

Inhibition of 12-LOX activity by BHPP, a platelet-type selective inhibitor, attenuated the endothelial cell mitogenic and the migratory responses to the angiogenic factors bFGF and VEGF and the tubelike differentiation on Matrigel. Forced expression of 12-LOX in the CD4 endothelial cells stimulated cell migration and promoted tube differentiation. Inhibition of 12-LOX activity by BHPP significantly reduced angiogenesis in vivo. Our findings suggest that eicosanoids from the arachidonic acid metabolism through the 12-LOX pathway, ie 12(S)-HETE, are involved in modulating angiogenesis.

There are seemingly conflicting reports regarding the isozymes of 12-LOX expressed in endothelial cells as both leukocyte type 12-LOX[4] and platelet-type 12-LOX[6] are reported. In the current study, we demonstrated that platelet-type 12-LOX was expressed in HUVEC and HMVEC as well as in RV-ECT, an endothelial cell line originally isolated from rat brain resistance blood vessels.[26] RV-ECT cells also express another isoform of 12-LOX originally isolated from rat brain and close to leukocyte-type.[29] When RV-ECT cells were treated with VEGF, there was a 5-fold increase in 12(S)-HETE biosynthetic activity inhibitable by BHPP pretreatment. Because BHPP is much more selective toward platelet-type 12-LOX than leukocyte-type (Furstenberger G, personal communication), the results suggest that it is the platelet-type 12-LOX, not the leukocyte-type 12-LOX, that is activated in endothelial cells during angiogenic responses.

Arachidonic metabolites have been implicated in angiogenesis since the inhibition of arachidonic acid metabolism by α-guaiaconic acid (GR-12) attenuated endothelial cell migration, tube formation, and angiogenesis in vivo.[36] Cellular mobilization of AA is usually achieved by PLA_2 cleavage of phospholipids. The activation of PLA_2 and the subsequent mobilization of AA have been observed in endothelial cells in response to various extracellular cues such as angiogenin, bFGF, zinc, and phorbol ester.[33,34,37,38] As a potent angiogenic factor, bFGF stimulates the migration and proliferation of vascular endothelial cells. Abrogation of the release of AA in endothelial cells by the inhibition of PLA_2 activity inhibited bFGF-stimulated cell proliferation[14] and migration.[30] VEGF also can rapidly increase phosphorylation and activity of cytosolic PLA_2 and stimulate the release of AA in HUVEC.[32] In a recent study, it was shown that the inhibition of PLA_2 activity in granuloma by SB 203 347 significantly reduced angiogenesis,[39] suggesting that the activation of PLA_2 and the subsequent mobilization of AA and lysophospholipid are intrinsic steps during angiogenesis.

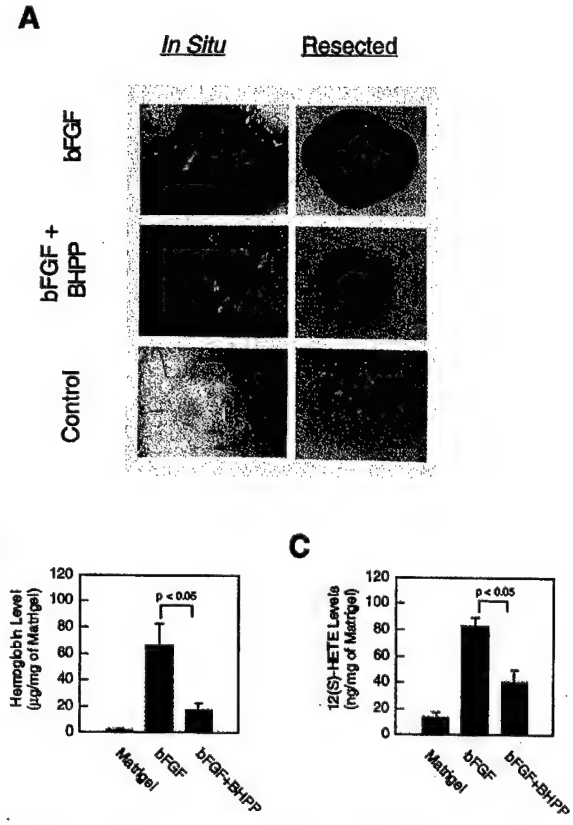

Figure 6. Attenuation of angiogenesis in vivo by 12-LOX inhibitors. Matrigel implantation assay for angiogenesis was performed as described in "Materials and methods" and repeated at least 3 times with similar results. (A) Matrigel implantation angiogenesis assay. Top panel: left, bFGF (5 μg/mL Matrigel) in situ; right, bFGF (5 μg/mL Matrigel) resected Matrigel. Middle panel: left, bFGF (5 μg/mL Matrigel) and BHPP (0.8 mg/mL Matrigel) in situ; right, bFGF (5 μg/mL Matrigel) and BHPP (0.8 mg/mL Matrigel) resected implant. Bottom panel: left, Matrigel alone in situ; right, resected Matrigel blank control. (B) Hemoglobin levels in resected implants. The hemoglobin was measured by Drabkin's reagent. Columns, hemoglobin levels normalized with protein concentrations. Bars, SE from quadruplicate samples. (C) 12(S)-HETE levels in resected implants. Lipids were extracted from the resected implants, and 12(S)-HETE levels were measured as described in "Materials and methods." Columns, average 12(S)-HETE levels normalized with protein concentrations. Bars, SE (n = 4 for Matrigel control; n = 3 for bFGF; n = 5 for bFGF plus BHPP).

The downstream events for released AA include the synthesis of various prostaglandins and thromboxanes through the COX pathway, various HETEs and lipoxins[42-44] through the LOX pathways, and various epoxyeicosatrienoic acids through cytochrome P-450 epoxygenase. In this study, we found that ETYA, a general inhibitor for arachidonic acid-derived metabolism, and NDGA, an agent that can inhibit LOX activity, inhibited endothelial cell migration stimulated by VEGF. On the other hand a general COX inhibitor, indomethacin, had no appreciable effect. In contrast, BHPP, which is a selective platelet-type 12-LOX inhibitor, blocked VEGF-stimulated endothelial cell migration. The involvement of 12-LOX and its AA metabolite in endothelial cell migration was further strengthened by the observations that exogenously added 12(S)-HETE directly stimulated RV-ECT migration and partially reversed the inhibitory effect of BHPP on cell migration. Finally, the overexpression of 12-LOX in CD4 endothelial cells significantly stimulated cell migration in a 12-LOX activity-dependent manner. The findings collectively suggest the role of endothelial 12-LOX and its AA metabolite, 12(S)-HETE, in endothelial cell migration.

In addition to its role in endothelial cell migration, we found that 12-LOX is involved in endothelial cell tube formation. Pretreatment of the RV-ECT cell line with BHPP significantly inhibited the formation of vessel-like structures within Matrigel. The second line of evidence is the observation that the overexpression of 12-LOX in CD4 endothelial cells promoted the formation of tubelike structures on Matrigel. Interestingly, it has been extensively documented that exogenous 12(S)-HETE can induce a reversible retraction of endothelial cell monolayers cultured on collagen by regulating PKC and $\alpha_V\beta_3$ integrin.[40,41] It remains to be determined, however, whether endothelial cell retraction is an early event of tube differentiation on matrix proteins such as collagens or Matrigel. Studies are under way to determine this potential relationship.

It has been reported that the 12-LOX pathway of AA metabolism is required in bFGF-stimulated endothelial cell proliferation.[14] We demonstrated that the inhibition of 12-LOX activity also compromised VEGF-stimulated endothelial cell proliferation. The role of 12-LOX in endothelial cell proliferation, together with the finding that 12-LOX is involved in endothelial cell migration and tube differentiation, implicate the mobilization of arachidonic acid and the generation of 12(S)-HETE through the 12-LOX pathway in endothelial cells as an early event in the intracellular cascade of angiogenic responses. Currently we are exploring the mechanism by which 12-LOX and 12(S)-HETE participate in the signaling events elicited by VEGF or bFGF in endothelial cells.

The involvement of 12-LOX in endothelial cell angiogenic responses in vitro is further corroborated by the observation that the 12-LOX inhibitor BHPP significantly reduced bFGF-stimulated angiogenesis in vivo. Because bFGF induces angiogenesis by modulating endothelial cell expression of VEGF, which in turn contributes to angiogenesis in an autocrine mechanism,[35] BHPP may have inhibited angiogenesis by attenuating endothelial cell angiogenic responses to bFGF and VEGF.

It should be noted that although platelet-type 12-LOX uses arachidonic acid to synthesize 12(S)-HETE almost exclusively, platelet-type 12-LOX has been shown to use leukotriene A_4 to synthesize lipoxin[42-44] and also 5(S)-HETE and 15(S)-HETE to form 5(S), 12(S)-DiHETE and 14(R), 15(S)-DiHETE, respectively.[45] It awaits further studies regarding whether other 12-LOX products, in addition to 12(S)-HETE, is angiogenic. In vivo, 12(S)-HETE is a prominent product of arachidonic acid metabolism through the LOX pathway in platelets. The pro-angiogenic function of 12(S)-HETE as delineated in the current study and in our previous reports[12,13] implicates the possible involvement of platelets in angiogenesis during tumor growth and metastasis. Indeed, platelets are intimately involved in tumor angiogenesis,[46,47] and platelet aggregation stimulates the release of VEGF.[48] Clinically, 30% to 60% of patients with advanced cancer have platelet abnormalities such as thrombocytosis and many other thromboembolic disorders. In addition, activated platelets have been frequently associated with many malignant tumors.[49] Obviously, the involvement of platelets adds to the complexity of tumor angiogenesis regulation.

In summary, our data suggest the important role of 12(S)-HETE generated by the 12-LOX pathway in angiogenesis and suggest the possibility of using 12-LOX inhibitors to treat angiogenic diseases such as tumor growth and arthritis. Studies are under way to evaluate the efficacy of 12-LOX inhibitors against solid tumor growth in vivo.

Acknowledgments

We thank Homan Kian, Yilong Cai, Alex Zacharek, and Kenny Hanna for their technical support and Dr Gerhard Furstenberger of Deutsches Krebsforschungszentrum (Germany) for sharing with us the unpublished data concerning the Ki of BHPP for various recombinant lipoxygenase enzymes.

References

1. Hanahan D. Signaling vascular morphogenesis and maintenance. Science. 1997;277:48.
2. Folkman J, Shing Y. Angiogenesis. J Biol Chem. 1992;267:10,931.
3. Funk CD, Keeney DS, Oliw EH, Boeglin WE, Brash AR. Functional expression and cellular localization of a mouse epidermal lipoxygenase. J Biol Chem. 1996;271:23,338.
4. Kim JA, Gu JL, Natarajan R, Berliner JA, Nadler JL. A leukocyte type of 12-lipoxygenase is expressed in human vascular and mononuclear cells: evidence for up-regulation by angiotensin II. Arterioscler Thromb Vasc Biol. 1995;15:942.
5. Krieg P, Kinzig A, Ress-Loschke M, et al. 12-Lipoxygenase isoenzymes in mouse skin tumor development. Mol Carcinog. 1995;14:118.
6. Funk C, Funk LB, FitzGerald GA, Samuelsson B. Characterization of human 12-lipoxygenase-genes. Proc Natl Acad Sci U S A. 1992;89:3962.
7. Sasaki M, Hori MT, Hino T, Golub MS, Tuck ML. Elevated 12-lipoxygenase activity in the spontaneously hypertensive rat. Am J Hypertens. 1997; 10:371.
8. Setty BN, Chen D, O'Neal P, Littrell JB, Grosman MH, Stuart MJ. Eicosanoids in sickle cell disease: potential relevance of 12(S)-hydroxy-5,8,10,14-eicosatetraenoic acid to the pathophysiology of vaso-occlusion. J Lab Clin Med. 1998;131:344.
9. Wang MM, Reynaud D, Pace-Asciak CR. In vivo stimulation of 12(S)-lipoxygenase in the rat skin by bradykinin and platelet activating factor: formation of 12(S)-HETE and hepoxilins, and actions on vascular permeability. Biochem Biophys Acta. 1999;1436:354.
10. Katoh A, Ikeda H, Murohara T, Haramaki N, Ito H, Imaizumi T. Platelet-derived 12-hydroxyeicosatetraenoic acid plays an important role in mediating carine coronary thrombosis by regulating platelet glycoprotein IIb/IIIa activation. Circulation. 1998; 98:2891.
11. Gao X, Grignon DJ, Chbihi T, et al. Elevated 12-lipoxygenase mRNA expression correlates with advanced stage and poor differentiation of human prostate cancer. Urology. 1995;46:227.
12. Nie D, Hillman GG, Geddes T, et al. Platelet-type 12-lipoxygenase in a human prostate carcinoma stimulates angiogenesis and tumor growth. Cancer Res. 1998;58:4047.

13. Tang DG, Renaud C, Stojakovic S, Diglio CA, Porter A, Honn KV. 12(S)-HETE is a mitogenic factor for microvascular endothelial cells: its potential role in angiogenesis. Biochem Biophys Res Commun. 1995;211:462.
14. Dethlefsen SM, Shepro D, D'Amore PA. Arachidonic acid metabolites in bFGF-, PDGF-, and serum-stimulated vascular cell growth. Exp Cell Res. 1994;212:262.
15. Honda HM, Leitinger N, Frankel M, et al. Induction of monocyte binding to endothelial cells by MM-LDL: role of lipoxygenase metabolites. Arterioscler Thromb Vasc Biol. 1999;19:680.
16. Setty BN, Graeber JE, Stuart MJ. The mitogenic effect of 15- and 12-hydroxyeicosatetraenoic acid on endothelial cells may be mediated via diacylglycerol kinase inhibition. J Biol Chem. 1987;262: 17,613.
17. Tang DG, Grossi IM, Chen YQ, Diglio CA, Honn KV. 12(S)-HETE promotes tumor-cell adhesion by increasing surface expression of $\alpha_v\beta_3$ integrins on ECs. Int J Cancer. 1993;54:102.
18. Tang DG, Chen YQ, Renaud C, Diglio CA, Honn KV. Protein kinase C-dependent effects of 12(S)-HETE on EC vitronectin receptor and fibronectin receptor. J Cell Biol. 1993;121:689.
19. Tang DG, Diglio CA, Honn KV. Activation of microvascular endothelium by 12(S)-HETE leads to enhanced tumor cell adhesion via upregulation of surface expression of a_vb_3 integrin: a post-transcriptional, PKC- and cytoskeleton-dependent process. Cancer Res. 1994;54:1119.
20. Tang DG, Chen YQ, Diglio CA, Honn KV. Transcriptional activation of EC integrin a_v by protein kinase C activator 12(S)-HETE. J Cell Sci. 1995; 108:2629.
21. Brooks PC, Clark RAF, Cheresh DA. Requirement of vascular integrin $\alpha_v\beta_3$ for angiogenesis. Science. 1994;264:569.
22. Brooks P, Montgomery A, Rosenfeld M, et al. Integrin $\alpha_v\beta_3$ antagonist promotes tumor regression by inducing apoptosis of angiogenic blood vessels. Cell. 1994;79:1157.
23. Brooks PC, Stromblad S, Klemke R, Visscher D, Sarkar FH, Cheresh DA. Antiintegrin $\alpha_v\beta_3$ blocks human breast cancer growth and angiogenesis in human skin. J Clin Invest. 1995;96:1815.
24. Chen YQ, Duniec ZM, Liu B, et al. Endogenous 12(S)-HETE production by tumor cells and its role in metastasis. Cancer Res. 1994;54:1574.
25. Liu B, Marnett LJ, Chaudhary A, et al. Biosynthesis of 12(S)-hydroxyeicosatetraenoic acid by B16 amelanotic melanoma cells is a determinant of their metastatic potential. Lab Invest. 1994;70: 314.
26. Diglio CA, Liu W, Grammas P, Giacomelli F, Wiener J. Isolation and characterization of cerebral resistance vessel endothelium in culture. Tissue Cell. 1993;25:833.
27. Liu B, Renaud C, Nelson K, et al. Protein-kinase-C inhibitor calphostin C reduces B16 amelanotic melanoma cell adhesion to endothelium and lung colonization. Int J Cancer. 1992;52:147.
28. Ito Y, Iwamoto Y, Tanaka K, Okuyama K, Sugioka Y. A quantitative assay using basement membrane extracts to study tumor angiogenesis in vivo. Int J Cancer. 1996;67:148.
29. Watanabe T, Medina JF, Haeggstrom JZ, Radmark O, Samuelsson B. Molecular cloning of a 12-lipoxygenase cDNA from rat brain. Eur J Biochem. 1993;212:605.
30. Sa G, Fox PL. Basic fibroblast growth factor-stimulated endothelial cell movement is mediated by a pertussis toxin-sensitive pathway regulating phospholipase A2 activity. J Biol Chem. 1994; 269:3219.
31. Kumar R, Yoneda J, Bucana CD, Fidler IJ. Regulation of distinct steps of angiogenesis by different angiogenic molecules. Int J Oncol. 1998;12:749.
32. Wheeler-Jones C, Abu-Ghazaleh R, Cospedal R, Houliston RA, Martin J, Zachary I. Vascular endothelial growth factor stimulates prostacyclin production and activation of cytosolic phospholipase A2 in endothelial cells via p42/p44 mitogen-activated protein kinase. FEBS Lett. 1997;420:28.
33. Fafeur V, Jiang ZP, Bohlen P. Signal transduction by bFGF, but not TGFβ1, involves arachidonic acid metabolism in endothelial cells. J Cell Physiol. 1991;149:277.
34. Bicknell R, Vallee BL. Angiogenin stimulates endothelial cell prostacyclin secretion by activation of phospholipase A2. Proc Natl Acad Sci U S A. 1989;163:902.
35. Seghezzi G, Patel S, Ren CJ, et al. Fibroblast growth factor-2 (FGF-2) induces vascular endothelial cells of forming capillaries: an autocrine mechanism contributing angiogenesis. J Cell Biol. 1998;141:1659.
36. Ito K, Abe T, Tomita M, et al. Anti-angiogenic activity of arachidonic acid metabolism inhibitors in angiogenesis model systems involving human microvascular endothelial cells and neovascularization in mice. Int J Cancer. 1993;55:660.
37. Kaji T, Miyamoto A, Yamamoto C, Fujiwara Y, Miyajima S, Koizumi F. Basic fibroblast growth factor-induced glycosaminoglycan production in cultured vascular endothelial cells results from enhanced protein synthesis mediated by the lipoxygenase pathway. Life Sci. 1997;60:873.
38. Patte C, Blanquet PR. Possible involvement of arachidonic acid metabolites in the synergistic action of endothelial mitogenesis by basic fibroblast growth factor and phorbol ester. Cell Mol Biol. 1992;38:429.
39. Jackson JR, Bolognese B, Mangar CA, Hubbard WC, Marshall LA, Winkler JD. The role of platelet activating factor and other lipid mediators in inflammatory angiogenesis. Biochim Biophys Acta. 1998;1392:145.
40. Tang DG, Diglio CA, Honn KV. 12(S)-HETE-induced microvascular endothelial cell retraction results from PKC-dependent rearrangement of cytoskeletal elements and $\alpha_v\beta_3$ integrins. Prostaglandins. 1993;45:249.
41. Honn KV, Tang DG, Grossi I, et al. Tumor cell-derived 12(S)-hydroxyeicosatetraenoic acid induces microvascular endothelial cell retraction. Cancer Res. 1994;54:565.
42. Romano M, Chen XS, Takahashi Y, Yamamoto S, Funk CD, Serhan CN. Lipoxin synthase activity of human platelet 12-lipoxygenase. Biochem J. 1993;296:127.
43. Sheppard KA, Greenberg SM, Funk CD, Romano M, Serhan CN. Lipoxin generation by human megakaryocyte-induced 12-lipoxygenase. Biochim Biophys Acta. 1992;1133:223.
44. Serhan CN, Sheppard KA. Lipoxin formation during human neutrophil-platelet interactions: evidence for the transformation of leukotriene A4 by platelet 12-lipoxygenase in vitro. J Clin Invest. 1990;85:772.
45. Dadaian M, Westlund P. Albumin modifies the metabolism of hydroxyeicosatetraenoic acids via 12-lipoxygenase in human platelets. J Lipid Res. 1999;40:940.
46. Salgado R, Vermeulen PB, Benoy I, et al. Platelet number and interleukin-6 correlate with VEGF but not with bFGF serum levels of advanced cancer patients. Br J Cancer. 1999;80:892.
47. Pinedo HM, Verheul HM, D'Amato RJ, Folkman J. Involvement of platelets in tumour angiogenesis? Lancet. 1998;352:1775.
48. Maloney JP, Silliman CC, Ambruso DR, Wang J, Tuder RM, Voelkel NF. In vitro release of vascular endothelial growth factor during platelet aggregation. Am J Physiol. 1998;275:H1054.
49. Honn KV, Tang DG, Crissman JD. Platelets and cancer metastasis: a causal relationship? Cancer Metastasis Rev. 1992;11:325.

[CANCER RESEARCH 58, 4047–4051, September 15, 1998]

Advances in Brief

Platelet-Type 12-Lipoxygenase in a Human Prostate Carcinoma Stimulates Angiogenesis and Tumor Growth[1]

Daotai Nie, Gilda G. Hillman, Timothy Geddes, Keqin Tang, Christopher Pierson, David J. Grignon, and Kenneth V. Honn[2]

Departments of Radiation Oncology [D. N., T. G., K. T., K. V. H.], Urology [G. G. H.], and Pathology [C. P., D. J. G., K. V. H.], Wayne State University School of Medicine, Detroit, Michigan 48202

Abstract

Previously, we found a positive correlation between the expression of platelet-type 12-lipoxygenase (12-LOX) and the progression of human prostate adenocarcinoma (PCa; Gao *et al.*, Urology, *46:* 227–237, 1995). To determine the role of 12-LOX in PCa progression, we generated stable 12-LOX-transfected PC3 cells, which synthesize high levels of 12-LOX protein and 12(*S*)-hydroxyeicosatetraenoic acid metabolite. *In vitro*, 12-LOX-transfected PC3 cells demonstrated a proliferation rate similar to neo controls. However, following s.c. injection into athymic nude mice, 12-LOX-transfected PC3 cells formed larger tumors than did the controls. Decreased necrosis and increased vascularization were observed in the tumors from 12-LOX-transfected PC3 cells. Both endothelial cell migration and Matrigel implantation assays indicate that 12-LOX-transfected PC3 cells were more angiogenic than their neo controls. These data indicate that 12-LOX stimulates human PCa tumor growth by a novel angiogenic mechanism.

Introduction

The growth and metastasis of solid tumors are dependent upon the ability of tumor cells to induce angiogenesis (1). Angiogenesis, the formation of new blood vessels from preexisting ones, involves endothelial cell proliferation, motility, and differentiation. Tumor cells can secrete a variety of angiogenic factors, such as basic fibroblast growth factor and vascular endothelial growth factor, to stimulate angiogenesis (2). Tumor cells also produce angiogenesis inhibitors such as thrombospondin and angiostatin to control angiogenesis (2). The balance between angiogenesis stimulators and inhibitors determines the angiogenicity of tumor cells (2). In human PCa,[3] the level of vascularization positively correlates with tumor stage (3–5). Inhibition of angiogenesis by linomide or TNP-470 potently inhibits PCa growth and metastasis by causing necrosis and apoptosis in tumors (6, 7). Although various potential angiogenesis factors have been identified in prostate cancer (8), it is still unclear by which process PCa cells become angiogenic. We have previously detected the expression of platelet-type 12-LOX in human PCa and demonstrated a correlation between 12-LOX mRNA expression and pathological stage (9). Platelet-type 12-LOX uses only arachidonic acid as substrate and forms 12(*S*)-HETE exclusively (10). Here, we have examined the function of 12-LOX on PCa tumor growth. Our data demonstrate that 12-LOX has no detectable effect on PCa cell growth *in vitro* but stimulates PCa tumor growth *in vivo*. This effect of 12-LOX on tumor growth is closely related to increased angiogenesis. Both *in vitro* and *in vivo* angiogenesis assays suggest that PCa cells expressing high levels of 12-LOX are more angiogenic than those expressing no or low levels of 12-LOX. Our results provide a novel function for platelet-type 12-LOX in PCa progression.

Materials and Methods

Cell Culture. Rat angiogenic endothelial cell line RV-ECT (a gift from Dr. Clement Diglio, Department of Pathology, Wayne State University) was maintained in DMEM with 10% FBS (11). The cells were used between passage numbers 29 and 34. The human prostate carcinoma cell line PC3 was originally purchased from American Type Culture Collection (Manassas, VA) and maintained in RPMI 1640 with 10% FBS. All culture reagents were purchased from Life Technologies, Inc.

Stable Transfection of PC3 Cells and Characterization. Passage 28 PC3 cells were cotransfected using a Lipofectin reagent (Life Technologies, Inc.) with a pCMV-platelet-type 12-LOX construct (a gift from Dr. Collin Funk, Center for Experimental Therapeutics, University of Pennsylvania; Ref. 10), and pCMV-*neo*, which encodes a neomycin-resistant protein. PC3 cells transfected with pCMV-*neo* were used as controls. Transfectants were selected using 1 mg/ml geneticin (G418) in RPMI with 10% FBS and then cloned using a limiting dilution method in 96-well plates. The cloned transfectants were propagated and characterized for 12-LOX mRNA expression by Northern blot and 12-LOX protein expression by Western blot. Human epidermoid carcinoma A431 cells that express 12-LOX (12) were used as a positive control. The probe used in Northern blot was the 12-LOX cDNA from pCMV 12-LOX construct. Rabbit 12-LOX polyclonal antibody used in Western blot was purchased from Oxford Biomedical Inc. (Oxford, MI). Actin antibody was from Amersham (Arlington Heights, IL). The synthesis of 12(*S*)-HETE by 12-LOX transfectants was determined using a RIA kit from Perspective Diagnostics (Cambridge, MA) according to the manufacturer's instructions.

***In Vitro* Proliferation Assay.** To study the growth kinetics of PC3 transfectants in culture, 2×10^3 cells per well were seeded in 96-well culture plate. The number of viable cells at intervals of 48 h was assessed using an MTS cell proliferation assay kit (Promega Corp, Madison, MI). The $A_{490\ nm}$ readings 2–3 h after plating were used as baselines. The number of cells was expressed as the percentage of increase from the $A_{490\ nm}$ baselines.

Animal Model and Histochemical Studies. A total of 4×10^6 12-LOX-transfected PC3 cells or neo control cells in 200 μl of HBSS were injected s.c. into the right flank of 4–6-week-old male BALB/c nude mice (obtained from University of South Florida, Tampa, FL). The resulting tumors were measured using a vernier caliper, and tumor volume was calculated using the formula: $(\text{width})^2 \times \text{length} \times 0.5$ (7). Six to 7 weeks after injection, mice were sacrificed, and the tumors were resected and photographed under an SP SZ-4060 stereomicroscope (Olympus America, Melville, NY). Tumors were fixed in 10% neutral buffered formalin and embedded in paraffin, and sections (5 μm) were prepared for histology staining. Sections were stained with H&E to examine the presence of necrosis. The assessment of tumor necrotic area was performed for a total of 10 HPFs per tumor using a double-blind approach.

CD31 staining was used to assess tumor vascularization. Immunohistochemical staining for CD31 (DAKO Corp.; dilution, 1:20) was performed

Received 5/20/98; accepted 7/30/98.

The costs of publication of this article were defrayed in part by the payment of page charges. This article must therefore be hereby marked *advertisement* in accordance with 18 U.S.C. Section 1734 solely to indicate this fact.

[1] This work was supported by NIH CA 29997, United States Army Prostate Cancer Research Program DAMD 17-98-1-8502, and the Harper Hospital Development Fund (to K. V. H.). D. N. was supported by a fellowship from the Cancer Research Foundation of American.

[2] To whom requests for reprints should be addressed, at Department of Radiation Oncology, 431 Chemistry Building, Wayne State University, Detroit, MI 48202. Phone: (313) 577-1018; Fax: (313) 577-0798.

[3] The abbreviations used are: PCa, prostate adenocarcinoma; 12-LOX, 12-lipoxygenase; 12(*S*)-HETE, 12(*S*)-hydroxyeicosatetraenoic acid; RV-ECT, rat vascular endothelial cells-tube forming; FBS, fetal bovine serum; HPF, high-power field.

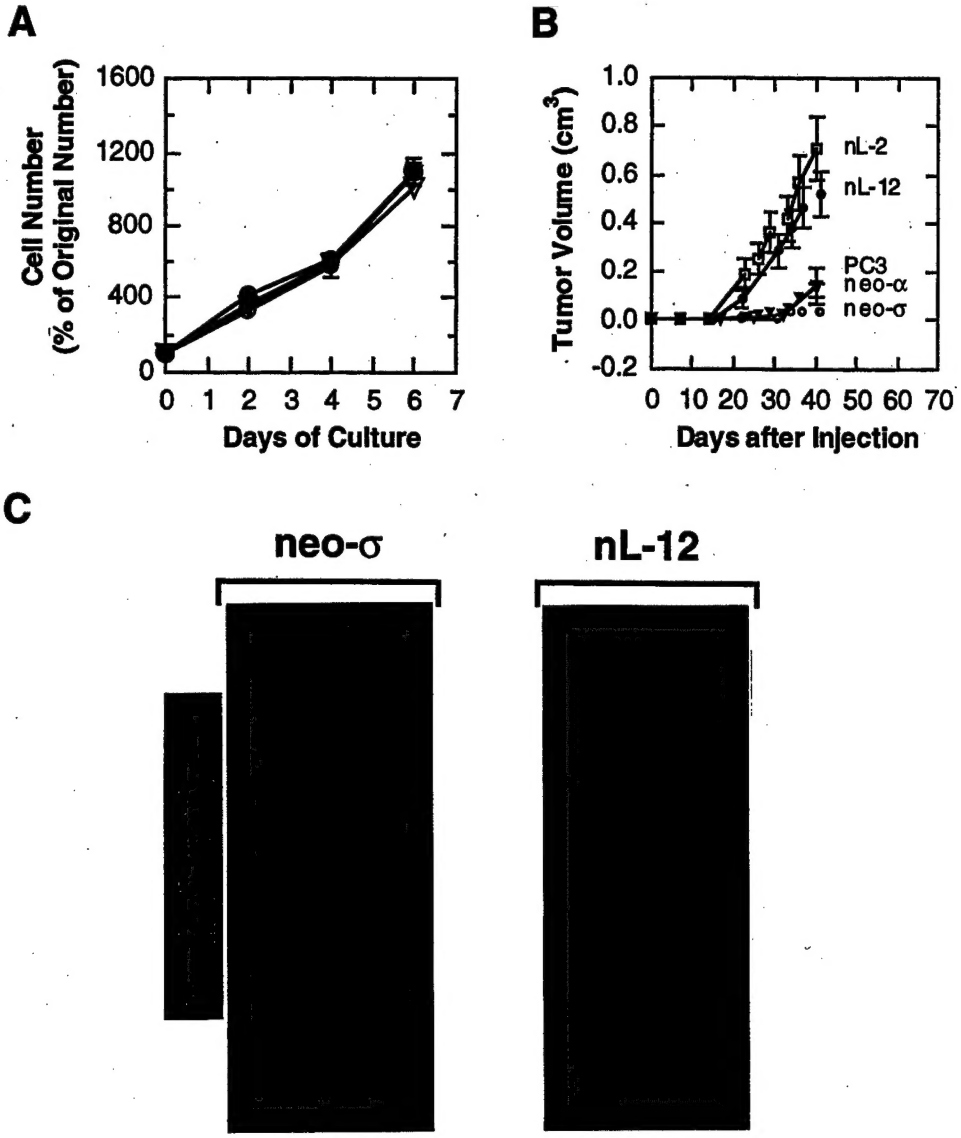

Fig. 2. 12-LOX transfectants have an *in vivo* but not *in vitro* growth advantage. *A*, growth kinetics of PC3 transfectants in culture. Cell proliferation of various transfectants was measured as described in "Materials and Methods." Shown here are the growth curves of PC3 wild type (○), neo-σ (●), nL-8 (▽), and nL-12 (▲). *Data points*, means of six determinations; *bars*, SE. Other clones such as nL-2 and neo-α also had similar growth kinetics (data not shown). *B*, growth kinetics of the tumors derived from 12-LOX transfectants and neo controls. *Data points*, mean volumes of eight tumors for nL-12 (●) and neo-σ (○), five tumors for nL-2 (□) and neo-α (▽), and six tumors for PC3 wild type (▼); *bars*, SE. *C*, mice with tumors from 12-LOX transfectants or from neo control. *Left*, three mice with tumors from neo-σ (*arrows*); *right*, three mice bearing tumors from 12-LOX-transfected PC3 cells (nL-12; *arrows*).

dependent. We found significant vascularization in tumors derived from 12-LOX-transfected PC3 cells, whereas the neo control tumors showed little vessel penetration (Fig. 3*A*). Immunostaining with CD31 antibody, which detects the presence of endothelial cells, showed that the vascular networks in tumors derived from nL-12 were sinusoidal in pattern and well developed in structure (Fig. 3*B*, *right*). In contrast, in neo control tumors, endothelial cells were present but were randomly distributed and did not form an organized vascular network (Fig. 3*B*, *left*). There were fewer vessels in neo-σ tumors than in nL-12, as suggested by microvessel density (Fig. 3*C*). The assessment of the vessel organization demonstrated that the majority of vessels in the tumors derived from 12-LOX-transfected PC3 cells were highly organized, whereas in those from neo-σ, they showed a disorganized to intermediate pattern (Fig. 3*D*). In tumors derived from nL-2 and nL-8, we also observed a similar increase in angiogenesis when compared to neo-α (data not shown).

Increased Angiogenicity of 12-LOX Transfectants. The increased angiogenesis in the tumors generated from 12-LOX-transfected PC3 cells raises the question of whether the observed increase in angiogenesis is the cause or a consequence of the increased tumor growth. To address this issue, we first assayed the conditioned culture medium of PC3 12-LOX-transfected PC3 cells or neo controls for their ability to stimulate endothelial cell migration. As shown in Fig. 4*A*, the medium from the 12-LOX-transfected PC3 cells induced more RV-ECT migration than did the medium from neo controls. Under similar assay conditions, 12(*S*)-HETE itself also stimulated RV-ECT migration at nanomolar levels (Fig. 4*B*). The increased angiogenicity of 12-LOX transfectants was confirmed by the Matrigel implantation assay. As shown in Fig. 4*C*, within 12 days, 12-LOX-transfected PC3 cells (nL-12) in Matrigel induced massive angiogenesis, indicated by the accumulation of blood in the gel, compared to the neo control (neo-σ). The results clearly illustrate that the 12-LOX-transfected PC3 cells are more angiogenic than their neo controls.

Discussion

Here, we found that the increased expression of 12-LOX in human PCa cells stimulates prostate tumor growth by enhancing their angiogenicity. The findings have significant bearing on the regulation of PCa progression because, in patients diagnosed with prostate carcinoma, some tumors are extremely malignant, with rapid progression, whereas others are localized and dormant for many years. Exploration of the mechanism underlying the transition from latent to rapidly growing PCa will provide useful information for PCa management.

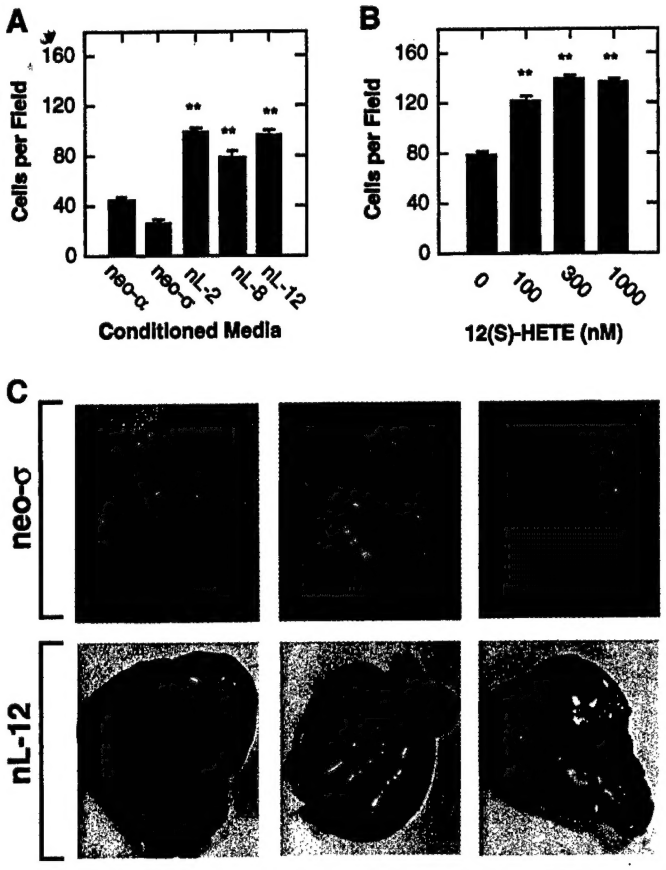

Fig. 4. Increased angiogenicity of 12-LOX-transfected PC3 cells. *A*, stimulation of endothelial cell migration by the conditioned medium from 12-LOX transfectants. The conditioned media were harvested after 24 h of culture and used for migration assay as described in "Materials and Methods." *Columns*, average numbers of cells migrated per field; *bars*, SE (**, $P < 0.01$ by Student's *t* test). *B*, 12(*S*)-HETE stimulates endothelial cell migration. The migration assay was performed essentially as described in *A* except that media with various levels of 12(*S*)-HETE, instead of the conditioned media, were placed into the lower chamber. *Columns*, means; *bars*, SE (**, $P < 0.01$ by Student's *t* test). *C*, induction of angiogenesis in Matrigel by 12-LOX transfectants. *Top*, three Matrigel implants premixed with 2×10^6 neo-σ cells. Note the vessel penetration into the gel was minimal, with little blood accumulated in the gel. *Bottom*, in contrast, the Matrigel premixed with 2×10^6 12-LOX transfectant (nL-12) demonstrates considerable blood accumulation.

One final point concerns the expression of 12-LOX during human PCa progression. If the effects of 12-LOX on PCa tumor growth and angiogenesis just described are of physiological significance, it should be expected that PCa cells express 12-LOX. This has, in fact, been observed *in vivo*, where the expression of 12-LOX has been positively correlated with tumor stage (9). The question of how 12-LOX expression is up-regulated in PCa cells is currently being explored.

Acknowledgments

Special thanks are directed to Dr. Clement Diglio for providing RV-ECT endothelial cells. We thank Dr. Mohit Trikha and Karoly Szekeres for helpful discussions. We acknowledge the excellent technical support from Homan Kian and Ning Wu.

References

1. Folkman, J., and Shing, Y. Angiogenesis. J. Biol. Chem., *267:* 10931–10934, 1992.
2. Hanahan, D., and Folkman, J. Patterns and emerging mechanisms of the angiogenic switch during tumorigenesis. Cell, *86:* 353–364, 1996.
3. Vartanian, R. K., and Weidner, N. EC proliferation in prostatic carcinoma and prostatic hyperplasia: correlation with Gleason's score, microvessel density, and epithelial cell proliferation. Lab. Invest., *73:* 844–850, 1995.
4. Wakui, S., Furusato, M., Itoh, T., Sasaki, H., Akiyama, A., Kinoshita, I., Asano, K., Tokuda, T., Aizawa, S., and Ushigome, S. Tumor angiogenesis in prostatic carcinoma with and without bone marrow metastasis: a morphometric study. J. Pathol., *168:* 257–262, 1992.
5. Weidner, N., Carroll, P. R., Flax, J., Blumenfeld, W., and Folkman, J. Tumor angiogenesis correlates with metastasis in invasive prostate carcinoma. Am. J. Pathol., *143:* 401–409, 1993.
6. Vukanovic, J., and Isaacs, J. T. Human prostatic cancer cells are sensitive to programed (apoptotic) death induced by the antiangiogenic agent linomide. Cancer Res., *55:* 3517–3520, 1995.
7. Yamaoka, M., Yamamoto, T., Ikeyama, S., Sudo, K., and Fujita, T. Angiogenesis inhibitor TNP-470 (AGM-1470) potently inhibits the tumor growth of hormone-independent human breast and prostate carcinoma cell lines. Cancer Res., *53:* 5233–5236, 1993.
8. Campbell, S. C. Advances in angiogenesis research: relevance to urological oncology. J. Urol., *158:* 1663–1674, 1997.
9. Gao, X., Grignon, D. J., Chbihi, T., Zacharek, A., Chen, Y. Q., Sakr, W., Porter, A. T., Crissman, J. D., Pontes, J. E., Powell, I. J., and Honn, K. V. Elevated 12-lipoxygenase mRNA expression correlates with advanced stage and poor differentiation of human prostate cancer. Urology, *46:* 227–237, 1995.
10. Funk, C. D., Furci, L., and FitzGerald, G. A. Molecular cloning, primary structure, and expression of the human platelet/erythroleukemia cell 12-lipoxygenase. Proc. Natl. Acad. Sci. USA, *87:* 5638–5642, 1990.
11. Diglio, C. A., Liu, W., Grammas, P., Giacomelli, F., and Wiener, J. Isolation and characterization of cerebral resistance vessel endothelium in culture. Tissue Cell, *25:* 833–846, 1993.
12. Hagmann, W., Gao, X., Timar, J., Chen, Y. Q., Strohmaier, A. R., Fahrenkopf, C., Kagawa, D., Lee, M., Zacharek, A., and Honn, K. V. 12-Lipoxygenase in A431 cells: genetic identity, modulation of expression, and intracellular localization. Exp. Cell Res., *228:* 197–205, 1996.
13. Ito, Y., Iwamoto, Y., Tanaka, K., Okuyama, K., and Sugioka, Y. A quantitative assay using basement membrane extracts to study tumor angiogenesis *in vivo*. Int. J. Cancer, *67:* 148–152, 1996.
14. Tang, D. G., Renaud, C., Stojakovic, S., Diglio, C. A., Porter, A., and Honn, K. V. 12(*S*)-HETE is a mitogenic factor for microvascular ECs: its potential role in angiogenesis. Biochem. Biophys. Res. Commun., *211:* 462–468, 1995.
15. Honn, K. V., Tang, D. G., Grossi, I., Duniec, Z. M., Timar, J., Renaud, C., Leithauser, M., Blair, I., Johnson, C. R., Diglio, C. A., Kimler, V. A., Taylor, J. D., and Marnett, L. J. Tumor cell-derived 12(*S*)-hydroxyeicosatetraenoic acid induces microvascular endothelial cell retraction. Cancer Res., *54:* 565–574, 1994.
16. Tang, D. G., Chen, Y. Q., Diglio, C. A., and Honn, K. V. Transcriptional activation of EC integrin α_v by protein kinase C activator 12(*S*)-HETE. J. Cell Sci., *108:* 2629–2644, 1995.
17. Brooks, P. C., Clark, R. A. F., and Cheresh, D. A. Requirement of vascular integrin $\alpha_v\beta_3$ for angiogenesis. Science (Washington DC), *264:* 569–571, 1994.
18. Brooks, P. C., Stromblad, S., Klemke, R., Visscher, D., Sarkar, F. H., and Cheresh, D. A. Antiintegrin $\alpha_v\beta_3$ blocks human breast cancer growth and angiogenesis in human skin. J. Clin. Invest., *96:* 1815–1822, 1995.
19. Kumar, R., Yoneda, J., Bucana, C. D., and Fidler, I. J. Regulation of distinct steps of angiogenesis by different angiogenic molecules. Int. J. Oncol., *12:* 749–757, 1998.